A Modelling Framework For Virtual Power Plants Under Uncertainty

by

James Ciaran Naughton

ORCID: https://orcid.org/0000-0002-4058-611X

Doctor of Philosophy

June 2022

Department of Electrical and Electronic Engineering
Faculty of Engineering and Information Technology

Submitted in total fulfilment for the jointly awarded
degree of Doctor of Philosophy at the
University of Melbourne
and the
University of Birmingham

Abstract

The increased integration of renewable energy sources (RES) and distributed energy resources (DER) into electrical networks is causing operational challenges. The reduction in conventional generators, which would traditional provide the reliability and security services for electrical networks, means that these services must now be supplied by other resources. Simultaneously, the intermittency of RES and the lack of visibility of DER means that in some cases these services are required more frequently to maintain a reliable electrical grid. If RES and DER are aggregated and properly controlled in a virtual power plant (VPP) they have the potential to provide network services as well as increase their profitability.

The operation of a VPP is a complex problem. While this problem has been examined by numerous authors, no operating framework has been previously proposed that includes consideration of: participation in multiple markets; provision of network and contractual services; modelling of network power flows and voltages; interactions between multiple energy vectors; uncertainty in operational forecasts and; tractability for short dispatch periods. These are key properties for a comprehensive framework that fully captures and unlocks the potential of a VPP. This thesis presents the design and application of a VPP operational framework that incorporates these six key properties. This optimisation-based framework is decomposed into three optimisations to integrate these properties in a tractable manner.

This framework is applied to various realistic case studies to prove the efficacy of the proposed approach. The application of this framework demonstrates that the combination of scenario-based optimisation and receding horizon control used is effective at mitigating the effects of uncertainty. The inclusion of short dispatch periods is shown to be key for revenue generation in markets with short dispatch windows. In addition, the application of this framework demonstrates the ability of a VPP to participate in multiple markets and services, and that doing so is essential for maximising VPP revenue. Moreover, the integration of hydrogen resources into the electrical grid provides flexibility that can be assigned to various markets and services. Furthermore, operating in multiple markets fundamentally changes the operational strategy of hydrogen resources, and can increase the amount of hydrogen that can be profitably generated. Additionally, the convex relaxation used for the dispatch of resources is sufficiently accurate to allow a VPP to maintain a network within allowable limits whilst maintaining problem tractability. Lastly, the framework is versatile enough to be utilised by other entities (such as a distribution system operator), or for different purposed (such as techno-economic analysis for business case assessments).

Declaration of Authorship

I declare that this thesis titled 'A Modelling Framework for Virtual Power Plants Under Uncertainty' and the work presented in it are my own. I confirm that:

- The thesis comprises only my original work towards the Doctor of Philosophy except where indicated in the preface;
- due acknowledgement has been made in the text to all other material used; and
- the thesis is fewer than 100,000 words in length, exclusive of tables, maps, bibliographies and appendices.

James Ciaran Naughton, June 2022

Preface

Parts of this thesis have been carried out in collaboration with Dr Han Wang (The University of Melbourne) and Dr Shariq Riaz (The University of Melbourne) as well as my supervisors Prof. Pierluigi Mancarella (The University of Melbourne), Prof. Xiao-Ping Zhang (The University of Birmingham), and my co-supervisor Prof. Michael Cantoni (The University of Melbourne). The list below identifies the chapters that include content from published works. The published works are listed, as well as the contributions from the authors.

Chapter 4

Section 4.2

1. **J. Naughton**, H. Wang, M. Cantoni, and P. Mancarella. "Co-optimizing Virtual Power Plant Services Under Uncertainty: A Robust Scheduling and Receding Horizon Dispatch Approach." *IEEE Transactions on Power Systems*, 36(5):3960–3972, 2021.

The first author contributed modeling, analysis of results, and writing the paper. The second author contributed writing and proofreading. The third and fourth author contributed supervision and proofreading.

Chapter 5

Section 5.2

2. **J. Naughton**, S. Riaz, M. Cantoni, and P. Mancarella, "Operational Flexibility from Integrated Electricity-Hydrogen Energy Hubs", *in progress*

The first author contributed modeling, analysis of results, and writing the paper. The second author contributed modeling, analysis of results, writing, and proofreading. The third and fourth author contributed supervision and proofreading.

Section 5.3

3. **J. Naughton**, H. Wang, S. Riaz, M. Cantoni, and P. Mancarella, "Optimization of Multi-Energy Virtual Power Plants for Providing Multiple Market and Local Network Services", *Electric Power Systems Research*, vol. 189, p. 106775, 2020

The first author contributed modeling, analysis of results, and writing the paper. The second and third author contributed analysis of results, writing, and proofreading. The fourth and fifth author contributed supervision and proofreading.

Chapter 6

4. **J. Naughton**, S. Riaz, M. Cantoni, X.P. Zhang, and P. Mancarella, "Business Case of a Value Stacking Renewables-Hydrogen Virtual Power Plant", *in progress*.

The first author contributed modeling, analysis of results, and writing the paper. The second author contributed modeling and proofreading. The third, fourth, and fifth authors contributed supervision and proofreading.

As per regulation of The University of Melbourne, it is hereby declared that I, James Ciaran Naughton, have contributed to the majority (at least 51%) of the content found in publications 1-4.

Dad,

Thank you for imbuing me with your love of maths and science,
and starting me on this long and winding road.

You are loved and missed.

Acknowledgements

I would like to thank my University of Melbourne supervisor Professor Pierluigi Mancarella for his guidance and support throughout my candidature. Your passion and drive on this subject have inspired me over the past four years.

I would also like to thank my University of Melbourne co-supervisor Professor Michael Cantoni for his invaluable instruction and assistance on the subjects of optimisation and control. I also greatly appreciated the support of Professor Xiao-Ping Zhang, my University of Birmingham supervisor, for welcoming me and supporting me during my time at the University of Birmingham.

Special thanks go to my friends and colleagues in the University of Melbourne Power and Energy Systems group including: Dillon, Han, Shariq, Carmen, Andrea, Sebastian, William, and Nando for the many discussions - work-related and otherwise.

My heart-felt gratitude goes out to my family and friends in the UK and Ireland - though you are far away, you are near to my heart. Especially Judith, Trevor, Michael and Naomi, thank you for always believing in me and encouraging me. My thanks also go out to Peter, for being a reminder of the importance of being passionate about the work we do.

Finally, I would like to thank my fiancé Shenae. Your unwavering love and support has bolstered me through ups and downs, and always helps me maintain perspective and remember what really matters in life.

Contents

List of Figures

List of Tables

Acroynms

AC	Alternating Current
AEMO	Australian Energy Market Operator
AEMC	Australian Energy Market Commission
BESS	Battery Energy Storage System
CAES	Compressed Air Energy Storage
CAPEX	Capital Expenditure
CCGT	Closed-Cycle Gas Turbine
CHP	Combined Heat and Power Plant
CVPP	Commercial Virtual Power Plant
DC	Direct Current
DER	Distributed Energy Resources
DMO	Distribution Market Operator
DNSP	Distribution Network Service Provider
DPP	Discounted Payback Period
DSO	Distribution System Operator
EAC	Equivalent Annual Cost
EB	Electric Boiler
EHP	Electric Heat Pump
EV	Electric Vehicle
FCAS	Frequency Control Ancillary Service
FFR	Fast Frequency Response
FOR	Feasible Operating Region
H_2	Hydrogen
HVAC	Heat, Ventilation and Air Conditioning
LAES	Liquid Air Energy Storage

LNS	Local Network Support
LP	Linear Program
MES	Multi-Energy System
MILP	Mixed Integer Linear Program
MINLP	Mixed Integer Non-Linear Program
MIP	Mixed-Integer Program
NEM	National Energy Market
NLP	Non-Linear Program
NPV	Net Present Value
NSP	Network Service Provider
O&M	Operation and Maintenance
OCGT	Open-Cycle Gas Turbine
OE	Operating Envelope
OLTC	On Load Tap Changer
OPEX	Operational Expenditure
OPF	Optimal Power Flow
PEM	Proton Exchange Membrane
p.u.	Per Unit
PV	Photovoltaic
RES	Renewable Energy Sources
SA	South Australia
SDP	Semi-Definite Program(ming)
SOCP	Second Order Cone Program(ming)
SOP	Soft Open Point
SRAS	System Restart Ancillary Service
TES	Thermal Energy Storage
TNSP	Transmission Network Service Provider
TVPP	Technical Virtual Power Plant
VCAS	Voltage Control Ancillary Service
VPP	Virtual Power Plant

Nomenclature

Indices and Sets

$k \in \Psi^{K}$	Set of resources
$k \in \Psi_{i}^{K}$	Set of resources located at node i
$k \in \Psi_{i,e}^{K}$	Set of resources located at node i operating in energy vector e
$k \in \Psi^{\text{Stor}}$	Set of energy storage resources
$(i,j) \in \Psi^{L}$	Set of lines
$i \in \Psi^{N}$	Set of nodes
$e \in \Psi^{\text{Non-elec}}$	Set of non-electrical energy vectors
$r \in \Psi^{\text{Raise}}$	Set of frequency raise services
$l \in \Psi^{\text{Lower}}$	Set of frequency lower services
$t \in [1:T]$	Set of time steps in the optimisation horizon
$s \in [1:S]$	Set of scenarios considered in the optimisation

Parameters

S^{HL}	Number of scenarios in high-level optimisation
S^{ML}	Number of scenarios in mid-level optimisation
S^{LL}	Number of scenarios in low-level optimisation
π_{s}^{HL}	Probability of high-level optimisation scenario s occurring
π_{s}^{ML}	Probability of mid-level optimisation scenario s occurring
π_{s}^{LL}	Probability of low-level optimisation scenario s occurring
Δt^{HL}	Length of high-level optimisation time step
Δt^{ML}	Length of mid-level optimisation time step
Δt^{LL}	Length of low-level optimisation time step
T^{HL}	Number of time steps in high-level optimisation
T^{ML}	Number of time steps in mid-level optimisation

T^{LL}	Number of time steps in low-level optimisation
$b_{ij,t}$	Susceptance of line (i,j) at time t
$g_{ij,t}$	Conductance of line (i,j) at time t
$r_{ij,t}$	Resistance of line (i,j) at time t
$x_{ij,t}$	Reactance of line (i,j) at time t
$y_{ij,t}$	Admittance of line (i,j) at time t
$z_{ij,t}$	Impedance of line (i,j) at time t
$\overline{S}_{ij}$	Apparent power limit of line (i,j)
$\overline{V}_{i,t}$	Maximum voltage magnitude limit of node i at time t
$\underline{V}_{i,t}$	Minimum voltage magnitude limit of node i at time t
$\overline{\theta}_i$	Maximum voltage angle limit of node i
$\underline{\theta}_i$	Minimum voltage angle limit of node i
$\tilde{\zeta}_{k,t}$	Binary commitment status of resource k at time t once the commitment schedule has been finalised (i.e., in mid-level and low-level optimisations)
H_k^g	Inertia constant of resource k
$\overline{S}_k$	Apparent power limit of resource k
$\overline{E}_k^{\mathrm{elec}}$	Electrical energy storage capacity of resource k
$\overline{E}_i^e$	Energy storage capacity of energy vector e at node i
$\overline{E}_i^{e,\mathrm{exp}}$	The maximum export limit of energy vector e at node i
$\underline{E}_i^{e,\mathrm{exp}}$	The minimum export limit of energy vector e at node i
$\xi_{k,s,t}$	Available fuel (if positive) / demanded load (if negative) of resource k for scenario s at time t
$\xi_{i,s,t}^e$	Availability / demand of energy vector e at node i for scenario s at time t
ν_k	Storage losses of resource k
ν_i^e	Storage losses of energy vector e at node i
x_k^{init}	Initial level of normalised electrical storage of resource k
$x_i^{e,\mathrm{init}}$	Initial level of normalised energy storage of energy vector e at node i
$P_k^{\mathrm{g,init}}$	Initial level of active power generation of resource k
$P_k^{\mathrm{d,init}}$	Initial level of active power demand of resource k
$U_{k,t}^{\mathrm{init}}$	Parameter ensuring minimum up time of resource k

	is enforced between optimisations
$D_{k,t}^{\text{init}}$	Parameter ensuring minimum down time of resource k is enforced between optimisations
X_k^{target}	Target level of normalised electrical stored energy of resource k at end of the optimisation
$X_i^{e,\text{target}}$	Target level of normalised stored energy of energy vector e at node i at the end of the optimisation
$\overline{P}_k^{\text{g}}$	Maximum active power generation limit of resource k
$\underline{P}_k^{\text{g}}$	Minimum active power generation limit of resource k
$\overline{P}_k^{\text{d}}$	Maximum active power demand limit of resource k
$\underline{P}_k^{\text{d}}$	Minimum active power demand limit of resource k
$\overline{Q}_k$	Maximum reactive power limit of resource k
$\underline{Q}_k$	Minimum reactive power limit of resource k
$\overline{\rho}_k$	Maximum ramp up limit of resource k
$\underline{\rho}_k$	Maximum ramp down limit of resource k
$\tan\left(\overline{\phi}_{k,t}\right)$	Upper limit of power factor for resource k
$\tan\left(\underline{\phi}_{k,t}\right)$	Lower limit of power factor for resource k
η_k^{g}	Generation electrical efficiency of resource k
η_k^{d}	Demand electrical efficiency of resource k
$\eta_k^{\text{g},e}$	Generation efficiency of resource k coupling energy vector e and electricity
$\eta_k^{\text{d},e}$	Demand efficiency of resource k coupling energy vector e and electricity
α_k	Allowable percentage curtailment of resource k in each time step
β_k	Allowable percentage curtailment of resource k across optimisation horizon
α_i^e	Allowable percentage curtailment of energy vector e at node i in each time step
β_i^e	Allowable percentage curtailment of energy vector e at node i across optimisation horizon
U_k	Minimum up time of resource k
D_k	Minimum down time of resource k
κ_k^{g}	Generation quadratic cost coefficient for resource k

κ_k^{d}	Demand quadratic cost coefficient for resource k
χ_k^{g}	Generation linear cost coefficient for resource k
χ_k^{d}	Demand linear cost coefficient for resource k
γ_k	Constant cost coefficient for resource k
$\lambda_k^{\mathrm{curt}}$	Price of curtailing resource k
$\lambda_i^{\mathrm{e,curt}}$	Price of curtailing energy vector e at node i
λ_k^{on}	Price of turning on resource k
λ_k^{off}	Price of turning off resource k
$\lambda_{s,t}^{e}$	Price of energy vector e for scenario s at time t
$\lambda_{s,t}^{\mathrm{I}}$	Price of inertia provision for scenario s at time t
$\lambda_{s,t}^{P}$	Price of wholesale energy for scenario s at time t
$\lambda_{s,t}^{Q}$	Price of reactive power for scenario s at time t
$\lambda_{s,t}^{l}$	Price of frequency lower service l for scenario s at time t
$\lambda_{s,t}^{r}$	Price of frequency raise service r for scenario s at time t
$\lambda_{ij}^{\mathrm{loss}}$	Price attributed to losses in line (i, j)
$\lambda_k^{\text{d-pen}}$	VPP defined penalty for deviating from demand reference level for resource k
$\lambda_k^{\text{g-pen}}$	VPP defined penalty for deviating from generation reference level for resource k
$\lambda_k^{\text{x-pen}}$	VPP defined penalty for deviating from electrical energy storage reference level for resource k
$\lambda_i^{\text{e-pen}}$	VPP defined penalty for deviating from non-electrical energy vector e storage reference level for resource k at node i
$\underline{P}_t^{l}$	Contractual level for provision of frequency lower service l at time t
$\underline{P}_t^{r}$	Contractual level for provision of frequency raise service r at time t
$\overline{Q}_t^{\mathrm{exp}}$	Maximum reactive power export limit at time t
$\underline{Q}_t^{\mathrm{exp}}$	Minimum reactive power export limit at time t
τ^r	Required response time for frequency raise service r
τ^l	Required response time for frequency lower service l
δ^r	Duration of frequency raise service r
δ^l	Duration of frequency lower service r

$\Phi_k^{r,\text{cntr}}$	Indicates the percentage of power injection of resource k that contractually needs to be covered by raise service r
$\Phi_k^{l,\text{cntr}}$	Indicates the percentage of power injection of resource k that contractually needs to be covered by raise service l
$\underline{I}_t$	Contractual level for provision on inertia at time t
$P_{k,t}^{\text{d-ref}}$	Low-level optimisation reference demand level for resource k at time t
$P_{k,t}^{\text{g-ref}}$	Low-level optimisation reference generation level for resource k at time t
$X_{k,t}^{\text{ref}}$	Low-level optimisation reference electrical normalised energy storage level for resource k at time t
$X_{i,t}^{\text{e-ref}}$	Low-level optimisation reference non-electrical normalised energy storage level for energy vector e at node i at time t

Variables

$c_s^{\text{tot}}(t)$	Total VPP cost for each scenario s at time t
$c_s^{\text{op}}(t)$	VPP operating cost for each scenario s at time t
$c_s^{\text{pen}}(t)$	Total penalty for low-level optimisation deviation from set points defined by mid-level optimisation for each scenario s at time t
$P_s^{\text{exp}}(t)$	Active power exported by VPP for scenario s at time t
$Q_s^{\text{exp}}(t)$	Reactive power exported by VPP for scenario s at time t
$E_{i,s}^{e,\text{exp}}(t)$	Energy vector e exported from node i for scenario s at time t
$x_{i,s}^{e}(t)$	Normalised energy storage level of energy vector e at node i for scenario s at time t
$V_{i,s}(t)$	Voltage magnitude at node i for scenario s at time t
$v_{i,s}(t)$	The square of the voltage magnitude at node i for scenario s at time t
$\theta_{i,s}(t)$	Voltage angle at node i for scenario s at time t
$\zeta_k(t)$	Binary committed status of resource k
$x_{k,s}(t)$	Normalized level of stored electrical energy of resource k for scenario s at time t
$P_{k,s}(t)$	Active power injection by resource k for scenario s at time t
$Q_{k,s}(t)$	Reactive power injection by resource k for scenario s at time t
$P_{k,s}^{g}(t)$	Active power generation by resource k for scenario s at time t

$P^{d}_{k,s}(t)$	Active power demand by resource k for scenario s at time t
$P^{l}_{k,s}(t)$	Provision of frequency lower service l by resource k for scenario s at time t
$P^{r}_{k,s}(t)$	Provision of frequency raise service r by resource k for scenario s at time t
$\omega_{k,s}(t)$	Curtailment of resource k, for scenario s at time t
$\omega^{e}_{i,s}(t)$	Curtailment of energy vector e at node i for scenario s at time t
$P_{ij,s}(t)$	Active power flow in line (i,j) for scenario s at time t
$P^{\text{Raise}}_{ij,s}(t)$	Active power flow in line (i,j) for scenario s at time t if raise services are called
$P^{\text{Lower}}_{ij,s}(t)$	Active power flow in line (i,j) for scenario s at time t if lower services are called
$Q_{ij,s}(t)$	Reactive power flow in line (i,j) for scenario s at time t
$\Lambda_{ij,s}(t)$	The square of the magnitude of current flow in line (i,j) for scenario s at time t

Chapter 1

Introduction

1.1 Challenges in Evolving Electrical Networks

Over the past decades, countries around the world have been recognising the human impact on climate change, and have resolved to lower their carbon and greenhouse gas emissions [1]. The energy sector (electricity, heat and transport) is the biggest contributor to world wide greenhouse gas emissions [2]. This is why the energy sector has been identified as an area where changes can be made to drastically reduce global greenhouse gas emissions. As the emissions within this sector come from a myriad of different operations (industry, road transport, aviation, agriculture, building energy use, etc.) there is no silver bullet for this problem. With that being said, one of the major methods that governments have been focusing on to help decarbonise the energy sector is the integration of renewable energy sources (RES) into electrical networks around the world. Of the 190 countries that have signed the Paris Agreement, 71% have quantified renewable energy targets [3]. The global capacity of RES was almost 2,800 GW in 2020, an increase on over 10% on the value in 2019 and showing no sign of slowing [4]. Two RES technologies that have been rising rapidly are wind and solar photovoltaic (PV) generation. Not only have these resources been introduced at transmission level on large scale but they have also become wide spread in distribution networks, through the introduction of rooftop solar PV.

Rooftop PVs are an example of distributed energy resources (DER) that have seen massive growth in recent years. More than 2.7 million households in Australia (approximately 21%) have rooftop PV, totalling more than 13.5 GW capacity [5]. The large uptake of rooftop PV in South Australia has led to two major issues that the Australian Energy Market Operator (AEMO) has identified [6].

1. Many distributed PV inverters disconnect in response to voltage disturbances. This could act to increase the size of the largest credible contingency in the region. The magnitudes of some reserve requirements are based on the size on the largest credible contingency, so this acts to increase the amount of reserve required.

2. Rooftop PV is reducing the minimum demand level of the South Australian network. This is reducing to such a level that South Australia may not be able to operate in islanded mode (disconnected from the wider grid) during times of high PV generation, as there would not be enough demand to balance the synchronous generation required to provide system inertia.

Rooftop PV are not the only DER that have seen growth in recent years. DER such as: combined heat and power plants (CHPs) [7], electric heat pumps (EHPs) [8], heating, ventilation and air condition (HVAC) systems [9], battery energy storage systems (BESS) [10], electrolysers and fuel cells [11], and electric vehicles (EVs) [12] have also become more widespread. In the past, distribution networks have been designed and operated based on the assumption of uni-directional power flow from transmission lines to a well defined passive load, generally following an expected daily load curve. However, in the middle of a sunny day distribution networks may now be exporting energy to the wider grid, as shown in Figure 1.1. This reverse power flow may results in issues in the distribution network such as line congestion, high nodal voltages and incorrect operation of protection systems [13]. Conversely, with the increase in EHPs, HVACs, and EVs, as well as the electrification of the transport and heating sectors, the average and peak load of the distribution network may also increase [14], and require network reinforcement. The coupling of these two phenomenon, along with the uncertainty and intermittency of large-scale RES generation, can lead to very fast changes in generation or load for which the system operator needs to compensate.

Due to the fact that electrical energy cannot be stored in the physical infrastructure of the network, the energy supply and demand in the system must be instantaneously

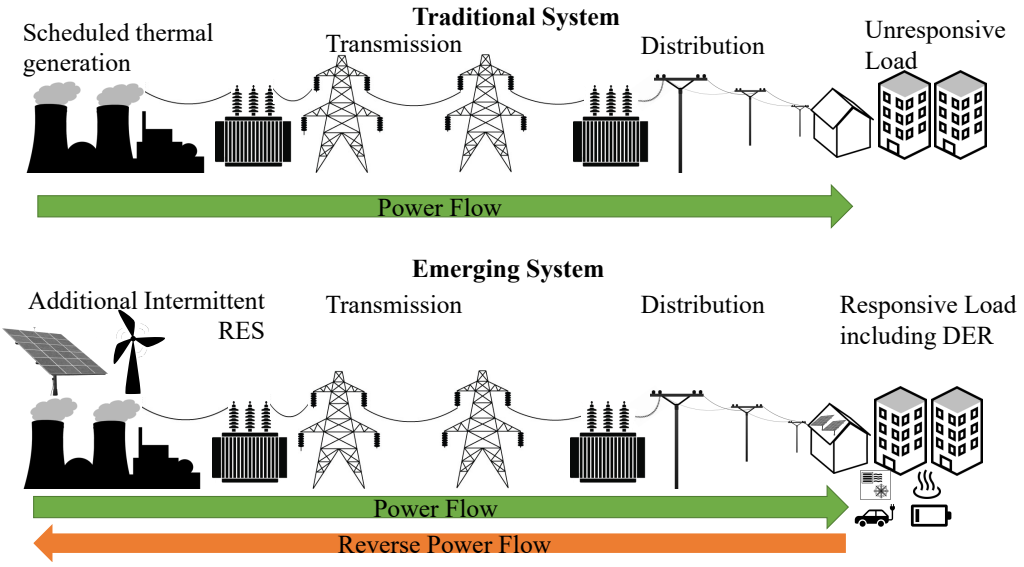

FIGURE 1.1: Illustration of traditional uni-directional system operation, and the new multi-directional power flow caused by DER

balanced at all times. If the generation and load are not perfectly balanced the system frequency will deviate from the nominal value (50 Hz in Australia). If the system operator fails to restore balance, it can lead to frequency deviations which can ultimately result in blackouts and system collapse. Therefore, having sufficient provision of network services is crucial to secure and reliable system operation. There are a number of markets and services that a system operator can utilise to raise or lower the system frequency and maintain generation/load balance in a network. Traditionally this system balancing was provided by the dispatchable synchronous thermal generators.

The widespread introduction of RES and DER is making the task of balancing the generation and load in the network a more difficult one. Once the RES have been built and start operating, they do not need to purchase fuel to be able to provide energy to the network. Therefore, they can bid into energy markets at a very low price, as they have an almost zero marginal cost (marginal cost is the change in total cost of production that comes from increasing production by one unit). In this way they undercut conventional thermal generators, which are then priced out of the market. As the amount of RES integrated into a network increases, this phenomenon becomes more prevalent [15]. Therefore, integration of RES increases the amount of intermittent generation whilst decreasing the amount of available scheduled generation. This can act to both increase the magnitude of balancing services that system operators need to procure [16], as well as reduce the number of resources operating in the market that can provide them. While

RES can reduce the amount of energy that they are generating (through curtailment), they have limited capability to increase their generation to provide balancing services. This can mean that even though thermal generators are being priced out of the energy market, other factors relating to network security and reliability may force operators to dispatch these resources instead of, or in addition to, RES [17].

With countries relying on RES to replace thermal generation to meet their greenhouse gas emission targets, this reliance on thermal generators to provide network services needs to be addressed. If electrical networks are still relying upon fossil fuel burning generators to supply essential services to the network, and if integration of RES and DER can lead to more of these services being required, just adding RES and DER will not necessarily lead to a lower carbon electricity grid.

The next section will outline the range of markets and network services that are present in Australia to maintain secure and reliable system operation.

1.2 Australian Electricity Market Structure and Services

While similar mechanisms and services are required in electrical networks around the world to address system balancing and security, the case studies that are utilised in this work are considered to operate within the Australian National Energy Market (NEM). Therefore, it is pertinent to provide a brief overview of how the NEM operates and what markets and services are utilised by the operator to maintain a stable and secure network.

1.2.1 Wholesale Energy Market

The NEM does not have a day-ahead energy market, as many other electrical systems do. The energy market is instead cleared at 5-minute intervals, with pre-dispatch prices for the day ahead being provided and updated every 5 minutes. Currently, the market settlement period is 30 minutes (meaning the average price and the average power supplied/demanded over a 30-minute period is used for payment). However, by the end of 2021 the energy market will have moved to 5-minute settlement [18]. This is the mechanism that the Australian Energy Market Operator (AEMO) uses to balance the

predicted demand and available supply in the network. However, if demand predictions are inaccurate, or there is an unexpected change in generation (i.e., a drop in RES generation, or a generator disconnects from the network) then AEMO has mechanisms for that maintaining system balance. These mechanisms are called frequency control ancillary services (FCAS).

1.2.2 Frequency Control Ancillary Services

There are eight FCAS markets in the NEM. These can be divided into four raise services (for increasing system frequency) and four lower services (for decreasing system frequency). Of the four raise FCAS markets, one is a regulation market and three are contingency markets. The raise regulation market is commonly provided by resources with automatic generator control that allows the AEMO to send control signals to the resources to maintain system frequency during normal system operation. The three contingency raise FCAS markets are used in the case of an event causing a large change in frequency in the network (if the frequency deviates above 50.15 Hz or below 49.85 Hz). These are classified based on their required response time as fast (6 seconds), slow (60 seconds) and delayed (5 minutes). The four lower FCAS markets are defined in the same way [19] (see Figure 1.2). These services are procured through a 5-minute market in a similar way to the wholesale energy market.

1.2.3 Voltage Control Ancillary Services

It is AEMO's responsibility to maintain system voltages at transmission network connection points in the electrical network within set tolerances. Voltage control ancillary services (VCAS) is one method that AEMO has to do this. When providing VCAS, resources generate or absorb reactive power to help control the local voltage [19]. It is generally more effective to address voltage management close to where it is required [20]. Therefore, the location of a resource is an important consideration for provision of this service. This service is currently procured by contracts with AEMO [21].

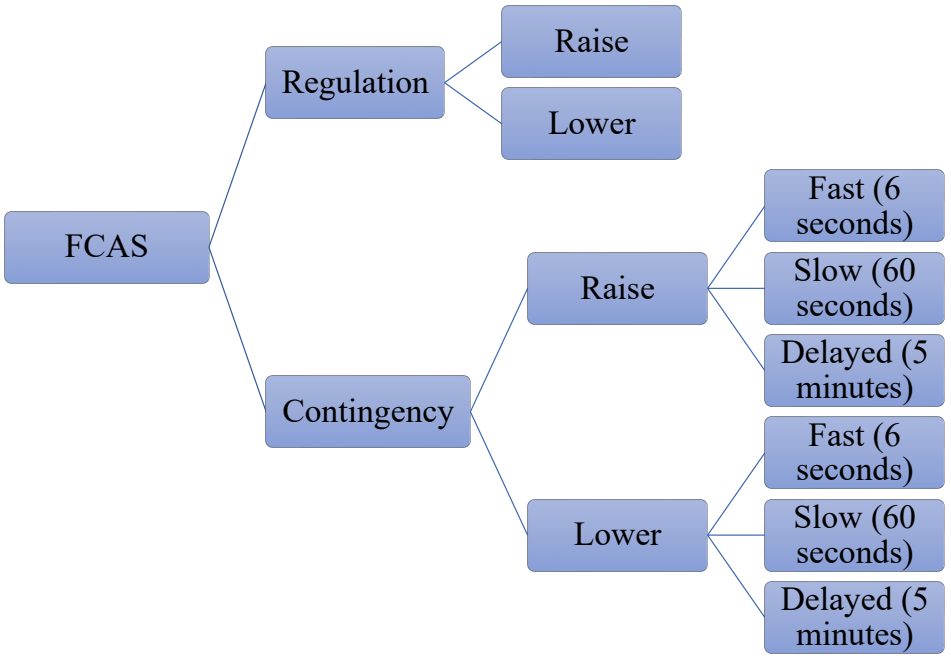

FIGURE 1.2: Illustration of the eight FCAS markets.

1.2.4 System Restart Ancillary Services

The system restart ancillary services (SRAS) are required to restart the electrical network after a partial or full black-out. This is traditionally provided by synchronous generator that can start-up and supply energy to the grid without an external source of supply [19]. This can then be used to energise an area of the network and restore power to more load, so that additional generators can be brought online. In recent years, research into utilising 'grid forming' inverters to provide SRAS has been of increasing interest [22]. The amount of SRAS that is required in each area of the network is calculated by AEMO and procured through contracts [23].

1.2.5 Fast Frequency Response

The reduction in synchronous generators in the NEM has lead to faster and more severe frequency deviations. The traditional FCAS markets may no longer be sufficient, and new faster mechanisms may be required. This is the role of fast frequency response (FFR). Within the context of the Australian electricity system, FFR is defined as '*... the delivery of a rapid active power increase or decrease by generation or load in a time frame of two seconds or less, to correct a supply-demand imbalance and assist in managing power system frequency*' [24]. It has been considered by the Australian

Energy Market Commission (AEMC) to impose a requirement on new RES to be able to provide FFR [25]. There has also been a request for an FFR ancillary service market to be included for the Australian electricity grid [24].

1.2.6 Inertia

System inertia used to be guaranteed through the prevalent use of synchronous thermal generators to generate electricity. Now, as more synchronous generators are being priced out of the market by RES, the amount of available inertia in the system has been dropping [26]. AEMC looked at making an inertia market in 2018, but decided against it at the time. However, a new inertia rule for transmission network service providers (TNSPs) was implemented that stated '*From 1 July 2018, TNSPs that are Inertia Service Providers will have an obligation to provide inertia network services if an inertia shortfall has been identified.*' [27]. So while there is currently no central market mechanism (although there may be one introduced in the future), TNSPs may need to procure inertia services to meet the requirements of this new rule.

1.3 Opportunities for RES and DER

Previously, maintaining system frequency entailed generators changing their output to match the load. With increasingly intermittent generation this becomes more difficult. However, the uptake in DER have led to the prospect of a responsive load as well as generation to maintain system balance. Demand response from industrial, commercial and domestic loads has been considered for helping maintain system balance [28]. Energy storage has also been used to provide ancillary services to the network, and have in fact proved much more effective at providing FCAS services that traditional thermal generation [29].

The negative effects that DER integration is having in distribution networks is leading to consideration of new methods of ensuring reliable distribution network operation through the coordinated operation of DER [30]. The increase in DER may be a cause of the problems that distribution networks are currently facing, but may also be a solution, and could possibly even facilitate provision of services to the wider network [31]. In the report where AEMO laid out the issues faced by increased rooftop PV integration [6],

it was also stated that having mechanisms for unlocking value from DER via two-way markets was crucial, with a backstop mechanism to provide instruction to DER directly. It is therefore apparent that new control methods, regulations and market structures are required that facilitate RES and DER in providing services to the network. Enabling this has a two-fold benefit. Firstly, if RES and DER can provide these services, then electrical networks become less reliant on thermal generation. Secondly, provision of such services can supply RES and DER operators with additional revenue streams, making further installations more economically attractive. This could help to accelerate the integration of these technologies, and hasten the arrival of a low carbon electrical network.

1.3.1 Electrical Flexibility

Electrical flexibility is a measure of a resource's ability to deviate its electrical operating point. This is the property of resources that can be leveraged to respond to market signals and provide services. In many cases it is specifically the active power operation of a resource that is examined with considering electrical flexibility. Electrical flexibility can be thought of as composed of two distinct types of flexibility - upward flexibility and downward flexibility. Upward flexibility is the ability of a resource to increase its net active power injection into the network. Downward flexibility is the ability of a resource to decrease its net active power injection into the network. To define the flexibility that a resource has at its disposal, two other parameters (apart from power magnitude) need to be defined: how quickly and for how long this flexibility can be provided.

Therefore, the metrics that can be used to measure the electrical flexibility of a resource are proposed in [32] as:

- Power ramp-rate capacity: How quickly can a resource alter its active power output.
- Power provision capacity: By what magnitude can a resource alter its active power output.
- Energy provision capacity: How long can a resource maintain an altered active power output.

Using these metrics, a resource's ability to take certain actions or provide services can be determined. There are many resources that can provide electrical flexibility, each with their own advantages and limitations. A selection of these will be further discussed in the following sections.

1.3.1.1 Energy Storage

Energy storage resources are those which can absorb energy from the grid, and store it to be injected back into the grid at a later time. Over recent years, BESS have come to the fore of energy storage investment, with 3 GW of BESS capacity installed worldwide in 2019 [10]. However, pumped hydro is still by far the most prevalent energy storage technology with over 1,300 GW of installed capacity [33], and other technologies such as compressed air energy storage (CAES) and liquid air energy storage (LAES) are all seeing increased interest over previous years. The ability of these resources to act as either a load or as a generator at any given time is a very attractive property, as it acts to dramatically increase the power provision capacity of these resources.

Many of these energy storage resources are also known to be highly responsive, with fast ramp rates. BESS are especially well known for this, with the ability to fully ramp up or down in under a second [29]. LAES can alter its active power output at a rate of 5% of P_n per second when acting as spinning generation, and 20% of P_n per minute otherwise [34] (where P_n is the nominal active power output of the resource). CAES has similar ramp-rate characteristics [35]. Pumped hydro storage can change from standstill to full output at a rate of $65-90\%$ of P_n per minute and from standstill to full load at a rate of $25-75\%$ of P_n per minute. If the turbine is operating in synchronous condenser mode, full power or load output can be achieved in under a minute [36].

These storage resources are now also achieve grid-scale power outputs, with LAES reaching 50 MW power [37], CAES can operate in the range of hundreds of MW [38], as can BESS [39]. Pumped-hydro can be sized into the GW range [40]. However, the limitation of energy storage resources usually comes from this energy provision capacity. For most of these resources, they can only operate at maximum power for at most hours before they run out of energy capacity, and this is a best case scenario. The energy provision capability of these storage resources is entirely dependent on the amount of stored energy at any given time. This may not be fully under the operators control,

for example pumped hydro stored energy can vary seasonally. Therefore, it is possible that a storage resource might not have any (or very little) energy provision capacity. This is why development of operational strategies for energy storage resources are very important to their successful utilisation of flexibility, and it has been seen that poor operational strategies of BESS can result in limited utility [41].

In general, energy storage resources are attractive for fast response, short duration services that are used to balance the system. This can be seen in Australia, where BESS and pumped hydro accounted for around 40% of the frequency control ancillary services (FCAS) market share in 2020 [15]. They also have the additional benefit that from an off state they can potentially provide either upwards or downwards flexibility, as required. However, long term balancing services or provision of energy is likely beyond these technologies due to the limited energy capacity. Effective management of stored energy is also essential to these resources being able to reliably provide services to the network.

1.3.1.2 Thermal Generators

The three major types are thermal generators that are found within power systems are coal fired generators, closed-cycle gas turbines (CCGTs) and open-cycle gas turbines (OCGTs). Coal-fired power plants have the slowest response of these with ramp rates of $1-3\%$ of P_n per minute, as well as having hours-long minimum up time and down time requirements [42]. CCGTs have a slightly faster ramp rate at $2-4\%$ of P_n per minute and OCGTs are the most responsive with $8-12\%$ of P_n per minute [43] and does not take hours to start from cold as with coal fired plants and CCGTs. This increase in response speed of OCGTs comes at the cost of reduced efficiency ($< 40\%$ compared to CCGT efficiency of $< 60\%$ [35]).

These technologies are mature and are widely implemented at grid-scale power. However, these resources can be limited not only by their maximum power output, but also by their minimum stable generation (the lowest amount of power they can provide while on and connected to the network). For thermal generators this can range from $20-50\%$ of P_n [43] which acts as an additional limit to the flexibility power provision capacity. Assuming a robust supply chain, the energy provision of these thermal generators can be considered as almost without limit. This is why coal-fired plants and CCGTs are

often used to address the base load of a system. Whilst they cannot quickly change their power output, they represent a significant amount of power, and have a very large energy capacity.

However, with the large increases in RES these coal and gas generators are supplying less and less of the energy demand in Australia. Due to their increased ramp-rate and low efficiency, OCGTs are often used as peaking power plants to address temporary high demand, as well as sometimes providing FCAS. However, in the past couple of years in Australia, the FCAS market share that gas generators hold has been diminishing in the face of the rising energy storage market share [15].

1.3.1.3 Renewable Energy Sources

Most RES utilised an inverter-based connection to grid, which can allow a RES to rapidly alter its power output in under a second [44]. While this provides RES with a great ability to provide downwards flexibility by curtailing generation, in order to be able to provide upwards flexibility a RES would need to operate below its maximum available generation. This could potentially involve curtailing a significant amount of energy. The power provision capability of a RES is uncontrolled and will vary with the availability of the source of energy being utilised. Similarly to having limited control over the power provision, RES also lack control over energy provision. There will be uncertainty over how long the RES will be able to maintain a set operating point, again due to the stochastic nature of the energy sources being utilised. So RES are best suited for providing fast response, short duration downwards flexibility services. However, inverter-based RES may be well positioned to provide reactive power flexibility, as inverters are extremely capable at altering their reactive power output [45].

1.3.1.4 Hydrogen Resources

The ability of RES to generate large amounts of 'green' energy has spurred investigation into how it might be used to help decarbonise sectors other than the electrical sector. While hydrogen has been hailed as a next-generation fuel for many years, due to advancements in technology maturity and reduction in capital cost, there is now significant interest and investment in hydrogen. Recently the concept of 'green hydrogen' (hydrogen

produced by an electrolyser utilising electrical energy from RES) has been considered to help decarbonise the gas networks, as well as transportation and agriculture sectors [46]. Specifically, there is increasing interest in the proton exchange membrane (PEM) electrolysers, which is replacing alkaline electrolysers as the favoured type due to lower footprint, high efficiency, and faster dynamic response time [47]. In fact, PEM electrolysers can respond to requests for flexibility within milliseconds, and can fully ramp up or down in under a second [48]. With PEM electrolysers now commercially available in the MW range [49], and assuming that there is a sufficient amount of hydrogen storage/export capability, PEM electrolysers have fast response times, large power ranges, and extended energy provision capacity making them a very flexible resource.

In addition, resources such as fuel cells and hydrogen-fuelled gas turbines can be used to convert hydrogen back into electricity to provide additional electrical flexibility. Both fuel cells and hydrogen OCGTs have fast ramp rates [50], but have energy provision capacity limited by the amount of stored hydrogen. Another drawback is that the round trip efficiency of converting electricity to hydrogen and back is low (around 30%) [51], so strong price signals would be required for this operation. The hydrogen created by these electrolysers can also be used to fuel hydrogen-based transportation, be synthesised into 'green' methanol [52], injected into gas networks [53], or converted in ammonia for the agriculture industry. Therefore, both the electrolyser's electrical flexibility, and the hydrogen that it creates are valuable to the decarbonisation effort.

Hydrogen has become an energy vector of interest in previous years in Australia, as can be seen in the number of electricity-hydrogen projects that are underway including the Hydrogen Superhub in Crystal Brook Energy Park in South Australia [54], the Denham Hydrogen Demonstration Plant [55] in Western Australia, and the ATCO Hydrogen Microgrid [56].

1.3.1.5 Heating Resources

The electrical and heating energy sectors are coupled through resources such as electric boilers (EBs), EHPs, HVAC and CHPs. CHPs can ramp at rates of 5-20% of P_n per minute and heating loads such as EB, EHP and HVAC can be shut down within a minute [35]. While the ramp rate of these resources is attractive, they likely have low power ratings meaning that the magnitude of flexibility each resource could provide

would be small. The energy capacity provision for these resources comes from thermal energy storage (TES), or the thermal energy that a building can inherently stored. The increase/decrease of building temperature can be seen as equivalent to charging/discharging storage [57]. This allows these heating and cooling resources to then provide electrical flexibility whilst satisfying their heating/cooling load [58]. However, there is associated uncertainty with how much equivalent energy capacity can be provide, and this would also vary over time. Therefore, these resources would be less suitable for provision of flexibility over an extended period.

1.3.2 Aggregated Flexibility - The Virtual Power Plant

The motivation behind aggregation is the idea that as a group, resources are better able to provide services and participate in markets. If there is a common goal of the aggregation of resources, implemented through an aggregator's control scheme, it allows them to appear to a network or market operator as a single resource [59]. This coordinated operation of DER is the method by which Gerard et al. [31] proposed DER could provide local services to a distribution network service provider (DNSP) (such as helping alleviate some of the distribution voltage and power flow issues mentioned earlier), as well as services to the wider network. An aggregator could go even further, and assist network operators by providing capacities services to postpone network reinforcement [60]. Aggregators could also allow DER to benefit from economies of scale, and are likely to have more complete information on which to act, reducing operational risk [61]. The rapid increase in DER penetration leads to a sharp growth in resources that are currently being under-utilised with regard to market participation and provision of services. Methods of resource co-ordination and aggregation are key to addressing the challenges outlined in Section 1.1, as well as maximising the value obtained from DER operation. A prominent method for resource aggregation seen throughout the literature is the virtual power plant (VPP) [59, 62].

A VPP can be thought of as a distributed power plant. A VPP can be comprised of a diverse set of resources (which can be loads, generation, or storage - controllable, or uncontrollable) with some form of central operating entity that acts as a intermediary between the resources and the network/market operator, as illustrated in Figure 1.3. The concept is that the network/market operator can view this VPP as a single entity

that can participate in markets and provide services, much like a conventional power plant [59]. As an example, the controlling entity of a VPP could be an aggregator, or an energy retailer. Therefore, another way to view a VPP is the fleet of resources which an aggregator controls. The VPP controller can submit bids to the market, and can then provide signals to the DER so that the operation of the VPP as a whole matches the bid submitted in the most efficient way possible. These VPPs have been identified as important tools in the future electricity network [6]. For example, there are seven VPP trials currently occurring in Australia [63]. The operators of these VPPs includes energy retailers, equipment manufacturers, equipment retailers, and energy generators. However, energy retailers are the most common operators of VPPs. Regulatory frameworks are also being developed to assist with the utilisation of these new entities, such as the AEMC looking to introduce a wholesale demand response mechanism that will allow consumers the provide demand response through aggregators [64]. The VPP operator may also be the owner of the resources, as is the case in Energy Locals VPP, where customers are offered discounted energy retail tariffs to allow the VPP operator to install DER at their home [65]. It should also be noted that just because a resource in operated as part of a VPP, does not mean that the VPP operator owns that resource. The VPP operator may pay the DER owner a set fee for access to their DER [66], or a $/kWh fee [67]. They may also provide incentives in the form of discounts off the purchase price of the DER [66]. The contractual arrangements between VPP operators and DER owners, and how DER profits are assigned to different stakeholders is outside the scope of this thesis.

The flexible resources outlined in the previous sections each have their own pros and cons - they may have a slow ramp, be of limited size, or lack long-lasting energy provision capacity. However, if a diverse group of resources are aggregated together into a VPP, the flexibility of the aggregator may not be limited in the same way. In fact it is highlighted in [32] that the flexibility of an aggregation of resources is greater than the sum of the flexibility of its individual resources. This means that a VPP would likely have the flexibility to provide a service that individual resources would not [63]. This is because multiple resources could operate together to provide a service and so be able to provide more flexibility, quicker and for longer than any individual resource. Aggregating resources across multiple energy vector to create a multi-energy VPP can provide economic and environmental improvements [68] and can provide greater flexibility to the

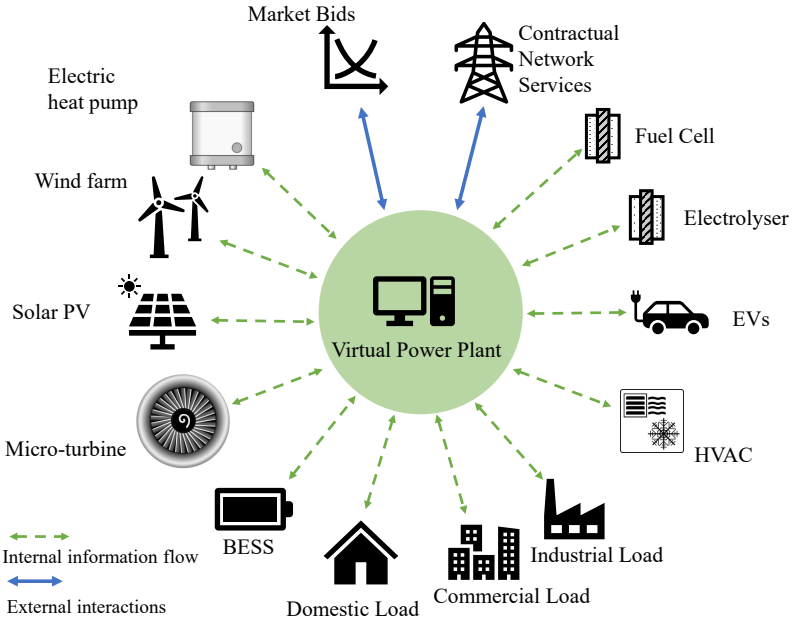

FIGURE 1.3: Overview of a VPP

electrical network [69].

A VPP operator cannot solely consider the active power outputs of its resources to provide electrical flexibility. The ability of a resource to change its reactive power operating point is also an important consideration, as this can be vital to providing network services [19]. The choice of active power operating point will have implications on the reactive power operating point due to resource's technical limitations and so these two aspects should be considered together. It has also been identified by Riaz and Mancarella [70] that the network in which a VPP exists can have a significant impact on the flexibility that a VPP can deliver without violating network constraints, and thus the electrical flexibility that a VPP can monetise.

While VPPs are an appealing prospect, challenges remain as to how this aggregation of resources is controlled, operated and interacts with other network entities to maximise revenue and utility to the network. This challenge of optimal operation and control of VPP is usually addressed through the formulation and solution of an optimisation problem.

1.4 Optimisation Theory

Optimisation theory is a wide-ranging area of research, and what is presented here will be only that which is sufficient for understanding the work reviewed and presented in this thesis, and heavily restricted to the context of optimal power flow (OPF). For readers unfamiliar with optimisation theory the following texts are recommended [71–74].

Classically, the aim of an optimisation is to minimise or maximise a given objective function by choosing values for a set of decision variables that are feasible in the sense that they do not violate a set of constraints. There are several categories of optimisation that will be mentioned in this work, and the following sections are to provide a reader with a cursory overview and introduction to nomenclature and definitions used throughout this work.

1.4.1 Linear Optimisation

In a linear optimisation (also know as a linear program (LP)) the objective function and all constraints of the optimisation are linear with regard to the decision variables. Linear optimisations are generally well understood, and there are algorithms which are very efficient at solving linear optimisations even at large scale, such as interior-point methods [75] used by commercial solvers. This makes them in general the most efficient optimisations to solve.

1.4.2 Convex Optimisation

In a convex optimisation, the objective function and all constraints of the optimisation are convex with regard to the decision variables. For a function to be convex, it must satisfy

$$f(\alpha y + (1-\alpha)z) \leq \alpha f(y) + (1-\alpha)f(z),\ \forall y, z \in \mathbb{R}^n \tag{1.1}$$

where $0 \leq \alpha \leq 1$. If a function does not satisfy this requirement, then it is non-convex. An example of a convex and non-convex function in two-dimensional space is shown in Figure 1.4.

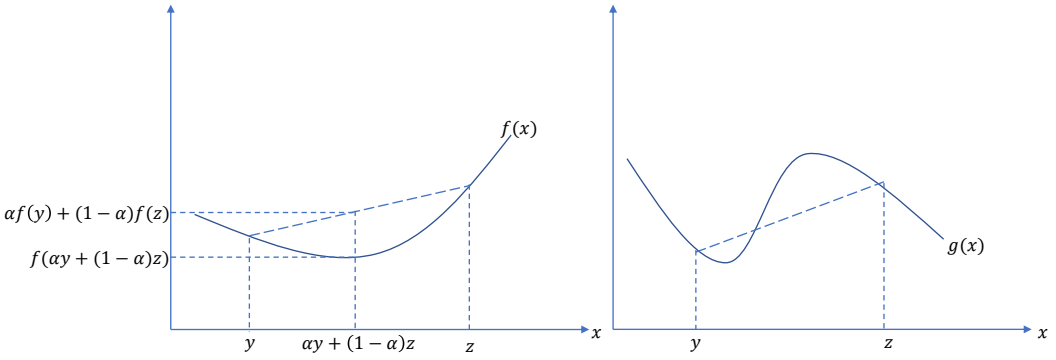

FIGURE 1.4: (Left) graph showing convex function $f(x)$. (Right) graph showing non-convex function $g(x)$.

The linear optimisation is a special case of a convex optimisation problem, as all linear functions are also convex. Convex optimisations can also generally be solved efficiently using interior points methods [72], although usually not as efficiently as LPs. An important characteristic of convex optimisation problems is the guarantee that local optimality (i.e., optimal over a feasible neighbourhood of the point) implies global optimality (optimal over the entire feasible set).

1.4.3 Non-Linear Optimisation

The term non-linear optimisation (also know as a non-linear program (NLP)) is used to describe problems that do not have the convexity properties to be classed as a convex optimisation. These optimisations are generally much harder to solve than convex optimisations, and solution algorithms may not find a global optimum, and may not converge to a feasible solution at all. There are a range of algorithms in use and under development to efficiently solve non-linear optimisations, such as particle swarm optimisation [76] and genetic algorithms [77].

1.4.4 Integer Variables

If a subset of the decision variables in an optimisation are integer variables, then the optimisation can be defined as a mixed-integer program (MIP). Integer variables generally represent on/off decisions, or yes/no decisions to take an action. They are also used in optimisations that consider indivisible units. The inclusion of these integer variables

makes an optimisation non-convex. However, methods have been developed to address this problem, such as the branch and bound [78], and cutting plane methods [79]. These involve iterative solving of relaxed versions of the MIP problem (these versions involve integer constraints being removed, or the value of integer variables being set). For this to be tractable, a solution to the relaxed problem must be achievable is an efficient manner. Generally mixed-integer linear programs (MILPs) can be solved most efficiently, because the linear relaxations can be solved most efficiently. Algorithms to efficiently solve mixed-integer convex and mixed-integer non-linear programs are an area of active research [80].

1.4.5 Uncertainty in Optimisations

When conducting an optimisation problem, there may be some optimisation parameters that are uncertain. This section will provide an overview of methods that can be used to incorporate these uncertain parameters into optimisations. The ideas on how to tackle a problem such as this falls within the topic of stochastic optimisation [81, 82]. There are a number of different approaches that have developed to address this issue of uncertainty, and a brief overview of the concepts of a selection of those is provided below.

1.4.5.1 Nominal Approach

The nominal approach is the simplest approach to consider uncertainty. By taking the expected value of the uncertain parameter this optimisation can be solved using conventional approaches to find the optimal solution. The simplicity of this approach comes at the cost of the robustness of the solution. Utilising this method provides no information about how the objective function with change with changing values of the uncertain parameter, or any guarantees that the solution is feasible as the value of the uncertain parameter changes.

1.4.5.2 Robust Approach

In its most basic form, the idea of a robust optimisation is that for all realisations of the uncertain parameter, the solution to the robust optimisation will be feasible. Whilst the exact value of the uncertain parameter may not be known, the set of values in which in

can fall may be known. In general, a robust optimisation is a problem with infinitely many constraints, which can lead it to be computationally intractable. However, knowledge of the properties of the uncertainty set allows tractable representations to be found in various cases [83]. In many cases where this approach is used in the OPF literature, a simple interval uncertainty is used [84–86]. The robust method of addressing uncertainty is likely to be the most conservative of the approaches considered here.

1.4.5.3 Chance-Constrained Approach

Instead of trying to find a solution to the objective, such that the constraints are satisfied for every possible realisation of the uncertain parameter (as with robust optimisations), chance-constrained optimisations instead try and ensure that the constraints are satisfied with a set probability. There does not exist a general solution method for chance constrained problems [87], making them difficult to solve. However, some special cases do exhibit favourable characteristic that make them easier to solve. If the problem does not fall into these special cases, then more complex methods are required to obtain a solution.

1.4.5.4 Scenario-based Approximation

Generally, chance-constrained optimisations are difficult to solve [88]. This has led to development of methods to be able to work with chance-constrained optimisations. One of these methods is the scenario-based approximation. A scenario-based optimisation creates a finite number of scenarios from the probability distribution that governs the uncertain parameter, and then solves the optimisation considering all these scenarios. This is an attractive proposition because, as detailed in [88], in general the robust approach and chance-constrained approach are very difficult to solve and can often be computationally intractable. The scenario-based approximation is generally much more tractable [89], and has the additional advantage that, if the number of scenarios is chosen properly, then the solution to the scenario-based approximation has a high probability of satisfying the chance-constraints [90]. The drawback of this approach is that a large number of scenarios may be required to provide useful probabilistic guarantees of chance-constraint satisfaction. A scenario-based approach to consider

uncertainty in VPP operational framework problems has been utilised in a number of works [91–94].

1.4.5.5 Receding Horizon Control

Receding horizon control (also known as model predictive control) is a form of feedback control [95]. A multi-period optimisation is solved over a prediction horizon, and then the first control action is implemented (i.e., the solution of the first time step is implemented). At the next time interval the optimisation is solved again, with the prediction horizon shifted one time step forward [96]. This control strategy does not necessarily explicitly consider uncertainty within the optimisation formulation. However, it allows a controller to defer decisions as long as possible, and to update them at every time step in light of updated information. Using this feedback mechanism has been shown to provide robustness to small disturbances (uncertainties) [97].

1.5 Aim and Scope of Thesis

This section will detail the aims and objectives of the research presented in this thesis, as well as the limits to the scope that have been set by the author.

1.5.1 Research Aims and Questions

A comprehensive operational framework that can be utilised by VPP operators (and aggregators more widely) to schedule and dispatch their resources is key to the integration of DER and RES into markets and service provision. Its use is also crucial for operators to be able to maximise the revenue and utility of their VPP, thereby attracting more investment into VPPs. The method by which a VPP can comprehensively determine its flexibility in multiple energy vectors and utilise this flexibility to participate in markets and provide services while considering uncertainty has not been well defined.

This thesis aims **to develop a comprehensive operational framework to allow a multi-energy VPP operator to utilise its operational flexibility while considering uncertainty.** Particularly, this thesis aims to answer the following key research questions:

1. To what extent can a VPP simultaneously participate in multiple markets and provide contractual network services, and what effect does this have on VPP profitability?

2. How effectively can the framework capture the flexibility inherent in the exchange of energy into different states, and how can it act to optimise this interaction?

3. In what way can the framework capture future uncertainties to allow the VPP to act in a feasible and near-optimal way whilst maintaining tractability of a problem with a 5-minute dispatch granularity and a 24-hour planning horizon?

4. In what ways can this operational framework be more widely used, other than for VPP operational scheduling and dispatch?

1.5.2 Objectives

To address these research aim and questions, the following objectives are defined:

1. Create a methodology for an optimisation-based VPP operational framework that schedules and dispatches resources within the VPP with the following attributes:

   (a) **Participation in multiple markets** - Considering all markets that the VPP has access to.

   (b) **Provision of network and contractual services** - Contractual agreements and services make up an important part of the electricity system operation.

   (c) **Modelling of network power flows and voltages** - To be able to provide some network services, and to have an understanding of the effects a VPP has on the local network state (and conversely how the state of the local network may effect the operation of a VPP) modelling the local network is essential.

   (d) **Interactions between multiple energy vectors** - As outlined above, the electrical network has become, and will continue to be, increasingly linked to other energy vectors. Being unable to consider this may severely limit application of operational frameworks in the future.

   (e) **Consideration of uncertainty** - Considering uncertainty in RES available generation and load demand is an important aspect to help aggregators to

ensure that they can deliver bids that they make. Considering uncertainty in market prices is also important to maximise aggregator revenue.

(f) **Tractable for use with short dispatch periods** - An aggregator should not be limited in their use of an operational optimisation tool because of the market structure in the country they are in. As market structures vary from country to country, it is important to consider how capable an optimisation tool is in markets with short dispatch periods (which would lead to a larger optimisation problem and are likely the most complex market structure for optimisations). Therefore, the framework should be able to consider 5-minute dispatch periods, and a 24-hour horizon.

2. Demonstrate the efficacy of all of the aspects of the proposed framework, and the potential additional benefits derived by a VPP operator utilising this framework for day-to-day operation through case studies.

3. Demonstrate that the proposed framework can be easily adapted in such a way as to be used by a non-VPP network entity, or for long-term techno-economic analysis.

1.5.3 Limits to Scope

This scope of the proposed operational framework is already very large by design, and the topic is complex and interwoven with other questions and challenges with respect to the future operation of electrical (and multi-energy) networks. Whilst the aim is to make the operational optimisation-based framework proposed in this work as comprehensive as possible, there are limits on the scope of this work in order to define the functionality of the framework.

1.5.3.1 Centralised Control

The control approaches of an aggregation of resources can be broadly split into centralised and decentralised approaches. A centralised approach features an single controlling entity (the aggregator) that has all the information, solves an optimisation problem and then issues control instructions to the resources. A decentralised approach has multiple decision makers who solve their sub-problems (potentially multiple times)

and interact with each other through some prescribed mechanism to converge on a solution to the problem as a whole. The main reasons provided for utilising decentralised optimisations are to allow the problem to scale more efficiently, and to address privacy concerns of the participating resources. While these are legitimate concerns, we shall show throughout this work that the centralised framework proposed maintains tractability when considering real world problems. Privacy issues are not considered in this work, as the aim of this work is to highlight the techno-economic impact of a comprehensive operational framework.

1.5.3.2 Energy Balance

The operation and modelling of electrical networks varies in scope and time scale from decades to microseconds. This is a change of fifteen orders of magnitude, and depending on which time scales are being examined, different considerations are required. This work focuses on the energy balancing in the network, and so deals with time scales of days to seconds. For this reason the very detailed modelling used for system dynamics and stability is not considered in this work, and a single-phase approximation of a balanced three-phase network is utilised.

1.5.3.3 Only Electricity Network Services

This work focuses on the myriad of services, markets and technical limitations that need to be considered for comprehensive operation in the electrical network. This is required do to the sensitivity of the electrical network to changes in state, and the requirement for instantaneous balancing of supply and demand. Many other energy vectors that have network infrastructures (i.e., gas, district heating) have an inbuilt buffer to these imbalances (i.e., through pipeline pressure, or water temperature). For this work to focus on the effects of multi-energy operation of the electrical network, these non-electrical energy vectors have their supply and demand balanced at each node, but their transportation networks are not modelled. Addition of energy flow modelling for non-electrical energy vectors could be a prospect for future work.

1.5.3.4 Price-Taker Market Participation

A 'price-taker' is an market entity that has no control of the price of goods/services (in this case the electricity market prices). This is usually because they have small transactions in the market. For the purposes of electrical market clearing, these entities would bid into the market at extreme low or high prices (depending on if they are selling or buying) to ensure that their bid is cleared through the market. A 'price-maker' is an entity that submits a price/power bids that the market operator will then use to clear the market. The resulting market clearing price will dictate how much power that entity buys or sell in the market. A 'price-maker' with a large market share could influence market price with its buying/selling power.

An aggregator is likely to have a relatively small capacity compared to the system as a whole. There is also a small likelihood that the aggregator would be setting the system marginal price. Therefore, for the purposes of highlighting the technical capabilities of and aggregator, and providing a reasonable estimate of aggregator revenues a price-taker approach has been used.

1.5.3.5 Communication Infrastructure

It is assumed that an aggregator utilising this operating framework will be able to establish the communications infrastructure required to support its operation. It is not considered that this framework has overly complex communication requirements, and the fact that there are currently VPP trials occurring indicates that the required communication infrastructure isn't overly onerous. As such, this infrastructure is outside the scope of this work.

1.6 Contributions

In general, the issue with previously proposed operational frameworks is that they fail to consider at least one major component of the overall problem identified in Section 1.5, which can limit their utility or cause them to miss vital opportunities/limitations. This will be further considered, and this research gap identified in Chapter 2.

A methodology for the proposed optimisation-based operational framework that addresses the six key attributes outlined in Section 1.5 is proposed in Chapter 3. This methodology is an innovative combination of three linked optimisations that operate over a range of time scales, from day-ahead to 5-minute intervals utilising scenario-based and receding horizon optimisations to address uncertainty. The detail with which the electrical network is considered varies across the framework to balance accuracy and tractability. Specifically, the framework couples a scenario-based optimisation for day-ahead resource scheduling, with linearised power flows, and two receding horizon optimisations for close-to-real-time dispatch, with a more accurate second order cone (SOC) relaxation of the power flows. A wide range of markets and contractual services can be considered, as can the coupling of multiple energy vectors.

In order to demonstrate the efficacy of the framework at allowing a VPP operator to provide multiple services and participate in multiple markets a case study VPP system is proposed in Chapter 4. This case study utilises the proposed framework to co-optimise a VPP's provision of multiple market (e.g., energy, reserve), system (e.g., FFR, inertia, VCAS), and local network (e.g., voltage support) services with the aim of maximising its revenue. The tractability of the proposed approach, operating within local network constraints, while accommodating the uncertain nature of market prices, local demand, and renewable output is shown. The results from this real Australian case study demonstrate how the proposed framework enables effective deployment of VPP flexibility to maximise its multi-service value stack, within an uncertain operating environment, and within technical limits.

Another case study is proposed in Chapter 4 to show how this framework can be utilised by different entities within the network, and how the different methods by which these entities might be able to interact to facilitate provision of local network support (maintaining voltages and power flows in a network within acceptable limits). This considers concepts of fairness in how this local network support is obtained, and the impact of different DER control methodologies on the provision of local network support. The ability to accurately model the voltages and power flows in the network and their dependence on both active and reactive power is a key property of the proposed framework that is utilised in this case study.

The flexibility that can be unlocked by a VPP operator utilising this framework with a

set of multi-energy resources is considered in Chapter 5. A case study uses multi-energy flexibility maps to illustrate the VPP's flexibility and to conduct *post hoc* analysis of its operation. The proposed multi-stage operational framework ensures time-varying multi-energy flexibility is optimally deployed in multiple downward and upward energy and reserve markets, and for the provision of inertia, FFR, VCAS, and local network support, while robustly hedging against uncertainty. The case study demonstrates the unique flexibility features of multi-energy hubs in promoting new business cases. In an additional case study, the use of the proposed framework enables optimised participation in multiple energy and ancillary service markets, while alleviating local network constraints. The case study deploys an electricity-hydrogen VPP demonstrating the efficacy of the proposed framework. The results highlight the tight interaction between local network support and system-level market participation, and how provision of local voltage and VCAS can enhance the VPP's ability to maximise its market revenues.

Finally, the utility of the proposed framework is further presented by applying it to a techno-economic assessment of an electric-hydrogen VPP to establish a business case using both net present value and discounted payback period metrics to assess economic viability. This techno-economic assessment considers multiple VPP configurations and the effect of participating in multiple markets and services on a VPP's economic viability. Energy, hydrogen and six FCAS markets are considered. Contractual FFR, VCAS, and SRAS services, as well as contracts with RES to purchase curtailed energy, are included. Sensitivity analysis to market prices is conducted, including 8 years of past energy and FCAS pricing. The ability of a VPP operator to leverage its multi-energy flexibility to participate in multiple markets and provision of multiple services is key to establishing an economically viable business case, identifying the benefit of utilising the proposed framework.

1.7 Overview of Thesis

This thesis aims to propose a comprehensive operational framework for VPPs that considers: multiple markets and services, multiple energy vectors, modelling of electrical power flow, methods to mitigate the impacts of uncertainty, and tractability across different market structures. In Chapter 2 the current literature in this area will be reviewed, and a research gap will be established which the work in this thesis aims to fill.

In Chapter 3 the formulation and operation of the framework will be provided in detail. Chapter 4 will present two case studies that illustrate the efficacy of the framework in providing multiple services, and how the framework can also accommodated multiple actors in a system. Chapter 5 proposes two case studies for a multi-energy electric-hydrogen VPP. These studies will demonstrate how the framework allows the VPP to harness its multi-energy flexibility to provide services and generate additional revenue. Chapter 6 highlights the versatility of the framework by utilising it to conduct a business case assessment of a proposed electric-hydrogen VPP. By conducting techno-economic analysis over long time scales, the framework is able to estimate the revenue that the VPP could generate with different market portfolios. Coupled with investment analysis, this chapter considers under what conditions these possible multi-energy VPPs would be a economically attractive prospect.

1.8 Overall Findings

The framework has the capability to consider participation in multiple market and provision of multiple services. This framework allows a VPP to simultaneously participate in markets and contractual services by assigning flexibility to each. Additionally, multi-market participation is key to long-term VPP profitability.

A multi-energy node formulation enables the framework to capture the flexibility available in the interchange between energy vectors. Through case studies it is demonstrated that multi-energy interactions are an effective source of flexibility for participation in markets and provision of services. In the case of coupling electricity and hydrogen, the consideration of both multi-energy flexibility and multi-market participation is important as it can fundamentally change the operation of multi-energy resources. It also increases the amount of hydrogen that can be profitably generated.

The combination of decomposing the framework into three optimisations with the utilisation of scenario-based optimisation and receding horizon control allows the framework to capture uncertainty in a tractable way, without being overly conservative. Being tractable for short time intervals, coupled with receding horizon control is important for maintaining VPP profitability in a market with short bidding windows.

The adaptable nature of the framework allows it to be used in a range of settings and by a range of entities. It is shown how a distribution system operator could use this framework to allocate network capacity to DER in the network. It is also shown that the framework could be used for long-term techno-economic evaluations for business case assessments.

Overall, the comprehensive optimisation-based operational framework to allow a multi-energy VPP operator to utilise its operational flexibility to participate in multiple markets and services while considering uncertainty proposed in this thesis is effective.

Chapter 2

Literature Review on Existing Virtual Power Plant Operational Frameworks

2.1 Introduction

VPPs have been identified as a potential method of utilising the inherent flexibility of RES and DER. Effectively utilising this flexibility could allow these resources to participate in markets and provide services to the network which were previously provided by fossil fuel thermal generators. However, the question remains as to how a VPP operator can optimally assign control instructions to its constituent resources to maximise the VPP's utility/revenue. In Chapter 1 Section 1.5 six attributes were outlined that are considered to be highly important in a comprehensive VPP operational framework:

1. Consideration of multiple markets.
2. Consideration of other network and contractual services.
3. Consideration of network power flows and voltages.
4. Consideration of multiple energy vectors.
5. Consideration of uncertainty.

6. Tractable for use with short dispatch periods.

In this chapter, previous proposed approaches to formulating VPP operational frameworks will be discussed in relation to these key attributes, and research gaps will be identified.

2.2 Virtual Power Plant

The concept of a VPP was introduced in [98] as a 'Virtual Utility', but the term 'Virtual Power Plant' was proposed in 2003 [99]. It wasn't long before optimisations for VPP operation were being examined. In 2004 an optimisation was proposed to minimise the operating costs of aggregated electricity generators, heat generators, co-generation plants, and thermal energy storage (TES) [100]. While this work was innovative in its consideration of multiple energy vectors, the electrical model was basic - considering only energy balance between generation, load and the grid. The framework proposed in [101] also focused on the interaction between heat and electricity. The authors considered how aggregated demand response from heating/cooling loads from a variety of consumer types can be used to minimize demand over a control window. This highlighted the ability of TES in buildings to be used as a form of energy storage to shift demand. However, this work was focused on the viability of the concept of providing demand response from thermal loads, and so there is little commercial consideration, and no network model.

2.3 Commercial and Technical Capabilities

The concepts of a Commercial VPP (CVPP) and a Technical VPP (TVPP) are provided in [102] as the following:

- A CVPP is '*... a representation of a portfolio of DER that can be used to participate in energy markets in the same manner as a transmission-connected generating plant.*'.

- A TVPP on the other hand '*... provides visibility of DER to the system operator(s), it allows DER to contribute to system management activities and facilitates use of DER capacity, providing system balancing at the lowest cost.*'.

Both [100, 101] would be considered CVPPs. As would [103], where a VPP demand response method is proposed. However, the work only considers load control, and the control of the VPP operator in this approach is limited. The operator selects a load profile for each load from a set of predetermined profiles submitted by the consumer to minimise VPP cost. The predetermined profiles are ranked in order of preference, and the VPP operator pays the consumer for selecting a profile other than the preferred one. Only active power balance was considered, with no other power flow considerations.

An example of a TVPP can be found in [104]. This work considers how aggregated control of PV inverters can be used to provide local network support by ensuring local voltages are maintained inside set limits while minimising network losses and power curtailment. A semi-definite programming (SDP) convex relaxation of the power flow equations is utilised to capture the influences of active and reactive power on system voltages with a high level of accuracy whilst maintaining the tractability of the optimisation. The work concluded that PV inverters were able to provide local network support, and utilising both active and reactive power control was the most effective way of doing so. This highlights the importance of using convex relaxations rather than linear approximations to better capture reactive power and network voltage interactions. A drawback of this work is that it only considers PV, and does not consider any commercial interactions. Therefore, it is unclear what the financial implications are of providing such a service.

There is obvious utility in a VPP (and an operational framework) that can be used for both commercial and technical purposes. This is why many operational frameworks proposed in this area consider in some form both commercial and technical operation of a VPP. This being said, the level of detail that is used to examine the commercial and technical aspects of VPP operation varies considerably.

2.4 Network and Power Flow Modelling

There have been attempts made to develop a VPP operational framework that can consider technical aspects of VPP operation without explicitly modelling the power flows in the network. One example is in [105], which considers a VPP consisting of distributed energy storage that participates in energy and system balancing markets. A service to a distribution system operator (DSO) is also considered by ensuring net power flow at the grid connection point is below the transformer apparent power limit. The VPP achieves provision of this service, however the network and power flows are not considered. Therefore, the application of this framework is limited to the context where all VPP resources are located at the transformer bus, which is deemed unlikely. However, what this work does highlight is that a VPP is capable of participating in multiple markets, and there is definite benefit in doing so.

There are many other works that also take a similar approach and propose a VPP operational framework that can provide technical services without explicitly considering power flows [93, 94, 106–109]. These usually require direction from a system operator, or basic energy balance is used to provide the service. As will be discussed in later sections, this omission in modelling power flows is usually because these works are focused on implementing another of the framework attributes outlined in the Section 2.1.

The importance of explicit consideration of network constraints and power flow modelling is highlighted in [70]. It is shown that the network may have a noticeable effect on a VPP's feasible operating region. This reduces the magnitude with which a VPP can participate in markets and provide services. Inclusion of power flow equations in modelling is then crucial, both to optimise the operation of a VPP within the context of this constrained environment, but also to be able to provide additional network services that may lead to additional revenue.

In [110], it is considered how a VPP can act commercially whilst providing technical services (voltage support in the local network). However, this is achieved through a network controller determining the reactive power operating point (and by extension allowable power factor range) of the resources in the VPP. The VPP optimisation takes these as an input whilst acting to minimise operating costs. So while this approach does consider both the technical and commercial capabilities of a VPP, they are not integrated

into an optimisation. This could limit both the technical and commercial operations of the VPP, and provides no insight into how the two are linked. A paper which combines both the technical and commercial aspects of VPP operation into a single optimisation can be found in [111]. An SDP convex relaxation of the power flow equations is used to yield a convex optimisation. This optimisation maximises VPP revenue in the wholesale energy market while ensuring the network operates within allowable limits. This allows the authors to investigate the effect of DER placement and different control schemes on VPP revenue. The authors determined that a centralized co-operative control scheme vastly outperforms a non-cooperative scheme, even if it is centrally controlled. Also highlighted in [111] is the importance of accurate network modelling to be able to capture phenomena such as losses, or renewable energy curtailment. However, the proposed framework in [111] does not include many of the other aspects needed for a comprehensive framework such as multiple markets/services, multiple energy vectors or consideration of uncertainty.

2.5 Participation in Multiple Markets and Services

One of the aims of utilising a VPP structure is to attempt to obtain the maximum revenue for the constituent resources. Very often this is not simply confined to the ability to participate in a single market or provide a single service. The importance of DER and RES being able to provide a range of network services was discussed in Chapter 1. If this aggregation approach is to be implemented in the real world, it must be economically viable. It is shown in the literature reviewed in this section that the economic benefits of forming/participating in a VPP are highly dependent on multi-market participation. For example, [106] shows that a diverse set of resources (including PV, battery energy storage system (BESS), gas generator and flexible load) can be controlled in a VPP to participate in a wide range of markets and provide contractual services. This work demonstrates that co-optimisation of different markets and services results in higher revenues which can effect the economic viability of DER installations. The flexibility available to the VPP operator is also visualised and quantified. However, power flows and network constraints are not considered, with the exception of constraints on total power imported/export by the VPP. So while [106] provides a thorough examination

of the economic aspects of VPPs, it overlooks some of the network-based technical considerations and uncertainty in the optimisation.

While the authors of [112] do not consider as wide a range of markets and services as in [106], they do consider network constraints and power flows. The authors propose a VPP operating framework formulated as a deterministic unit commitment problem that participates in the wholesale energy and spinning reserve markets. In this work the AC power flow equations are used to yield a mixed-integer non-linear program (MINLP). The results of implementing this proposed framework are show in [113] and again reinforces the notion of increased revenue being associated with effective multi-market participation. However, it is noted that a relatively small problem (384 decision variables) takes over 35 minutes to solve. Therefore, it is unlikely that this approach would be suitable for inclusion of further complicating considerations such as additional markets/services, multiple energy vectors, or uncertainty. A similar issue can be seen in [114] in which a VPP operational framework is proposed that conducts a day-ahead dispatch considering participation in multiple markets and using AC power flow equations to ensure network constraints are not violated. A second stage real-time balancing optimisation is then used, which dispatches some of the reserves that the VPP allocated in the first stage to match the first stage bid. This locks the VPP into decisions made at the day-ahead level, and due to the non-linear nature of the optimisation, it is unlikely to be able to be utilised at more regular time intervals. For this reason it is not suitable for networks with closer to real time markets, such as the NEM in Australia. While this approach does consider uncertainty in wind generation, it mitigates this through allocating reserve from dispatchable generation equal to the expected wind generation. This is both conservative, and may not be feasible in VPPs with a large share of RES. However, [114] does recognise the importance of uncertainty on VPP operation. A fact that [100, 101, 103–106, 110–113] overlook.

2.6 Operating VPPs Considering Uncertainty

When operating a VPP, operational decisions need to be made ahead of time. Whether this is 5 minutes ahead, or a day ahead, the VPP is optimising its operation with assumptions of what will occur in the future. These uncertainties can manifest in demanded

load, available RES generation, market prices, requesting of services, resource availability, etc.. The magnitude of these uncertainties, or probability of their occurrences, can vary depending on how far in the future the VPP is making decisions. In general, the closer to the time of operation the decisions are being made, the less uncertainty there is in the VPP operator's knowledge. This fact is leveraged in [115] by utilising receding horizon control. To assist with tractability the authors formulate a single optimisation with a variable time step length. The optimisation has 5-minute time steps close to the current time, and time steps of increasing size further in the future until 60 minute time steps are considered. This optimisation in total has a 24-hour horizon, which recedes every 5 minutes, at which point the problem is re-optimised. However, network constraints and power flows are not considered in the optimisation. Instead an iterative approach is taken where a solution is obtained and checked using load flow analysis to determine if any lines are overloaded. If they are, a new constraint is added with power injection sensitivity coefficients for those overloaded branches, and the optimisation is re-run. This method of considering network constraints limits the provision of services that can be optimised, and does not consider system voltages. This work is also very much focused on implementation with synchronous generation at transmission level, and so may not be suitable for VPPs located in distribution networks, or those containing RES and DER.

A framework that also utilises a receding horizon approach but is suitable for distribution systems is proposed in [116]. The framework presented is a dual horizon scheduling framework, where a day-ahead schedule is determined and a receding horizon operational dispatch is used to match the VPP output with the day-ahead schedule. This framework allocates a level of reserve dependent on the forecast RES and load that the receding horizon optimisation can utilise to ensure that the operational dispatch can match the day-ahead bid. The effectiveness of a receding horizon approach to operational dispatch is verified in this work. However, issues were found with the use of allocating reserve as the sole method to try and mitigate uncertainty in RES and load, specifically when a BESS was utilised. These issues were due to the BESS having access to a limited amount of stored energy and being unable to provide reserve across a whole day. This indicates that more rigorous methods of mitigating uncertainty should be considered. [116] accurately models the power flows in the network by utilising the AC power flow equations, leading to a non-linear optimisation. This could lead to intractability if

considering more complex operation with multiple markets/services, energy vectors or larger systems.

2.6.1 Chance-Constrained Optimisation

In general, the mathematically rigorous methods of considering uncertainty in VPP operation fall into three categories. The first of which are chance-constrained optimisations. Chance-constrained optimisations are the least common approach found in the literature. This is because, unless the problem is formulated in a specific way which yields desirable attributes, chance-constrained optimisations can be difficult to solve. In [117] a chance-constrained optimisation coupled with a scenario-based optimisation is utilised to address uncertainty in load, wind power generation and real time energy prices. The chance-constrained optimisation is used for resource scheduling to keep the loss of load probability below a set value. The optimisation does not model power flows, which allows the uncertain values of load and wind power to be confined to the right hand side of the chance constraints. This allows a deterministic optimisation to be formulated. A real time scenario-based optimisation is then used to maximise VPP revenue across all realisations of uncertainty considered. While this method acts to effectively reduce loss of load probability, if the optimisation considered power flow constraints and other complicating features, the chance constraints would no longer have the property that allows them to be easily converted into deterministic constraints. This can be seen in [118], where even the inclusion of sensitivity coefficients to provide a linear approximation of the relationship between bus active power injection and active power flow results in a more complex chance-constrained problem that requires iterative solutions. This requirement can then lead to tractability issues.

2.6.2 Scenario-based Optimisation

The second of the mathematically rigorous methods of considering uncertainty in VPP operation is the scenario-based approach. The scenario-based approach is popular in the literature, both because it is intuitive in its formulation, and flexible in its application. This approach can also be used as a method to solve chance-constrained optimisations with a set probability [90]. The greatest issue with scenario-based optimisation is the

fact that in general a large number of scenarios are required to capture the underlying uncertainty in the system [88], potentially rendering the optimisation intractable. Many authors utilise scenario-reduction techniques as a method to combat this, however by doing so they lose the associated probabilistic guarantees of chance-constraint satisfaction.

In [93], a diverse set of resources being optimised while considering uncertainty in wind speed, solar irradiance, load demand and resource failure is proposed. Monte Carlo simulations are used to generate 10,000 scenarios. A scenario-reduction technique is then used to reduce these to 10 scenarios to make the optimisation tractable. The optimisation conducts a power balance economic dispatch using forecasts of wind, PV and load and minimises the cost of providing balancing services in the scenarios considered. It is shown that conducting the stochastic scheduling provides a significant improvement on the operating cost of the VPP compared the a deterministic solution. However, network and power flows are not considered. Another work that utilises a scenario-based approach is [94]. In this work a two-stage optimisation is proposed where the first stage provides a medium-term contract, and the second stage aims to minimise imbalance and provide reserve. This work also uses a conditional value-at-risk term in the cost function to reduce the volatility of the expected profit across scenarios. Empirical multi-variate scenario generation tools are used to try and keep the number of scenarios required as small as possible while capturing uncertainty. This work also does not consider network or power flows and the consideration of medium-term contracts makes the problem non-linear. Another two stage optimisation is proposed in [108] with both a day-ahead and a close-to-real-time optimisation. The day-ahead optimisation takes a scenario-based approach utilising forecast scenarios for RES generation. The close-to-real-time optimisation utilises a receding horizon approach with no scenarios. This work also considers the nodal balancing of thermal loads through the use of co-generation plants and thermal storage. The economic considerations of this work are limited to the wholesale energy market, where the close-to-real-time optimisation is being used to reduce penalties for deviation from day-ahead bids. Power flow and voltages are not considered in either optimisation. However, for the close-to-real-time optimisation, a provision is considered where a DSO validates the bids of the VPP and if required provides instructions to the VPP to change its output. These instructions are issued through sensitivity coefficients which the DSO would acquire through formulation of the

Jacobian matrix of the network. However, the DSO is only considering active power flow, and there is no provision in the framework to consider reactive power flow which would be highly useful in providing local network support as shown in [104]. The lack of power flow consideration in [93, 94, 108] is a major drawback in these works.

A linear approximation of the power flow equations is utilised in [119], where the authors propose a two-stage risk constrained stochastic optimisation to provide a day-ahead schedule for a VPP. This optimisation utilises a scenario-based approach and the conditional value-at-risk metric to capture risk. Uncertainty in load, RES generation, pricing, as well as an uncertainty in the response rate of reserve calls made by the VPP are considered. K-means classification is used to reduce the number of scenarios to a tractable number. This work considers both the energy market and reserve markets, and shows that the more options a VPP is given to utilise its flexibility, the more revenue it can obtain. Although this work does not consider multi-energy systems, or operation of the VPP closer to real time, it presents a framework for day-ahead scheduling of a VPP that finds a balance between tractability and robustness. Although, the linear approximation used in [119] may not be sufficient to accurately provide some network services, or precisely identify network constraints. This method of considering uncertainty and risk results in the VPP reducing the use of its flexible resources when it is acting in a risk-adverse manner. The ability to alter the operation of flexible resources with short notice (i.e., through a receding horizon approach) would potentially provide a less conservative option to reduce risk.

A more detailed network modelling approach is presented in [120], where the authors use the non-convex AC power flow equations to accurately capture power flows and voltages within the network. However, this means that the scheduling problem proposed is an MINLP which is, in general, a type of problem that is difficult to solve. The framework considers only a wholesale energy market, but also puts reserve requirement constraints on the VPP. The point estimate method proposed in this work to consider uncertainty requires deterministic versions of the MINLP to be solved many times. This means that this approach is unlikely to be tractable if it was required to considered shorter time steps than 1 hour, or if the optimisation became more complex through introduction of multiple services or energy vectors. Another framework that models power flows through the use of the AC power flow equations to create a MINLP is found in [121]. Monte Carlo simulations are proposed to conduct multiple deterministic versions of

the scheduling optimisation to consider uncertainty (similar to the process proposed in [120]). Further to the work in [120], the authors of [121] propose a second optimisation that conducts a receding horizon close-to-real-time dispatch (1 minute time step, 5 minute horizon) of VPP resources to match the day-ahead bids. This close-to-real-time dispatch utilises online forecasts of the uncertain variables to conduct a deterministic optimisation. One drawback of [121] is that it only considers participation in the energy markets. Another drawback is that even with a small case study (8 resources, 10 node network) the computation times of the scheduling optimisation is 4 hours (utilising parallel computing), and the dispatch optimisation solves in 10 seconds. Increasing the complexity of the optimisation through multiple services, multiple energy vectors or larger systems could result in intractability.

2.6.3 Robust Optimisation

The last of the widely used methods for considering uncertainty in VPP operation is robust optimisation. The authors of [109] detail an integrated stochastic adaptive robust optimisation for VPP operation. This utilises robust optimisation techniques to consider the uncertainty of wind power generation, and utilises scenarios to model the uncertainty in market pricing. The results of this optimisation are that, as the uncertainty budget of this cardinality constrained robust optimisation increases, the conventional power plant is scheduled more and the revenue of the VPP decreases. The combination of robust and scenario-based techniques requires the decomposition of the whole optimisation problem into a master problem and sub-problem which are iteratively solved. However, this sub-problem contains large numbers of integer variables, which can lead to long computation times. The relatively small problem considered in [109] results in around a 30 minute computation time, and this only considers energy balance, not network power flow equations. It also only considers participation in energy markets. Therefore, a larger or more complex optimisation may prove intractable using this method.

A two-level stochastic scheduling optimisation for a VPP considering uncertainty in wind and solar generation is detailed in [122]. The day-ahead scheduling phase is conducted with a cardinality constrained robust formulation. At the hour-ahead stage it is assumed that the value of the stochastic variables for that time period are known, and BESS and demand response are used to minimise system operating costs. This approach considers

how uncertainty changes as forecast length increases, but assumes hour-ahead wind and PV generation are known quantities, which may be unlikely. The results of [122] demonstrate that a more robust formulation results in decreased VPP revenue due to increased use of conventional thermal generation. However, when additional flexibility is added to the VPP (in the form of BESS and demand response) that VPP revenue increases. The major limitation of this work is that no network constraints or power flows are considered. A robust optimisation based VPP operational framework where power flow equations are considered in proposed in [123] where another two-stage operational framework is proposed. This framework utilises robust optimisation to determine VPP bids in the day-ahead and real time markets. Interestingly, when an out of sample analysis was conducted with two different levels of conservatism, each performed better on separate days with no clear indication as to which would provide more revenue long term. This highlights that with the volatility of real time prices compared with day-ahead prices, it may be difficult for a VPP operator to optimally choose the level of conservatism to use in such an optimisation. Whilst power flow equations are utilised in [123], they are the DC power flow equations. This limits the applicability of the framework when considering distribution networks, or providing network services. The framework also only considers operation in energy markets (day-ahead and real time).

One of the key attributes detailed in Section 2.1 that has been missing from the previous approaches that consider uncertainty is the inclusion of multiple energy vectors. In [85], the authors propose a robust scheduling model for a multi-energy VPP that considers power-to-gas operation, including methanation. The optimisation aims to maximise profit considering electricity and gas wholesale markets, as well as minimising the conditional value-at-risk of the VPP. However, the method used to optimise this multi-objective optimisation requires a three step algorithm utilising a payoff table, fuzzy linearisation and rough weight calculations. While this may be applicable for a mixed-integer linear program (MILP) with only energy balancing considerations, for a more comprehensive model with power flows and multiple services this multi-objective optimisation will become more challenging and potentially intractable. Another multi-energy VPP operational framework utilising robust optimisation is propose in [124]. Specifically, this adjustable robust optimisation is for the operation of an electricity-heat multi-energy VPP. This VPP is assumed to operate as a load only - it cannot sell

power to the grid. This framework aims to minimise the cost to the VPP of purchasing energy and operating resources while providing upwards and downwards reserve. Uncertainty in the call time and magnitude of reserve services throughout the day is considered. This approach lacks network modelling and provision of services, limiting its utility. However, this work highlights again the additional flexibility (and associated cost savings) available from considering the operation of multi-energy resources, and multi-energy storage (such as building thermal inertia).

2.7 Multiple Energy Vectors

The ability to incorporate multiple energy vectors into the previously considered operation frameworks has been lacking, with a few notable exceptions [85, 100, 101, 108, 124]. However, these papers and other works [68, 69] have identified the technical and economic benefits of multi-energy integration. This is again re-affirmed in [125], where an electricity and heat multi-energy VPP operating framework is proposed. In this operating framework, the objective is to minimize the cost of buying electricity and gas. While this operating framework lacks a number of the attributes defined for a comprehensive framework (power flow modeling, multiple services, and uncertainty), it does illustrate the benefits of aggregating multi-energy resources, and the value of having highly flexible resources in an aggregation. A more comprehensive operational framework for a multi-energy, multi-service aggregator is formulated in [107]. This work also considers heat and electricity energy vectors. But, further to [125], the framework in [107] also considers energy, reserve, reliability, and gas markets. Uncertainty is addressed in this framework through scenario-based optimisation. This multi-market/service consideration allows the authors to identify that there are possible conflicts that arise between reserve and energy markets in certain pricing situations. This highlights the importance of considering these multiple markets holistically, so as to effectively maximize revenue. Still, the proposed approach in [107] does not model power flows and network constraints and so only conducts energy balance for electricity and heat. This limits its utility for considering other network related services, or identifying how networks may limit operation. A heat and electricity VPP operational framework that does consider power flows is formulated in [58] and shows that electrical and thermal energy vectors can be effectively co-optimised. However, the only power flows considered were active power

flows and the formulation is wholly dependent on the VPP being part of a radial network, so that power flow could be calculated as the summation of power injection from downstream nodes. As such, the network modelling in this work is of limited utility.

Traditionally the interest in multi-energy systems has been focused on the coupling between electricity and heat, as has been seen in much of the previously reviewed work that considered multiple energy vectors [58, 100, 101, 107, 124, 125]. However in recent years there has been increasing interest in the coupling of electricity and hydrogen, as hydrogen has been identified as an important fuel source for the future [46, 47, 126]. A VPP operational framework that considers this electricity and hydrogen coupling can be found in [127]. In this work the authors demonstrate how inclusion of an alkaline electrolyser into a VPP can expand its feasible operating region, both in terms of electricity and heat operation. In the case study it can be seen that the expanded feasible operating region is key to optimal VPP operation. Because this work focuses on the detailed modelling of the alkaline electrolyser, it does not model power flows or consider markets other than energy markets. A more comprehensive framework for an electricity-hydrogen aggregation is proposed in [128]. This operational framework for a distributed set of hydrogen refuelling stations operates in the electricity energy market while setting dynamic hydrogen pricing and providing capacity-based demand response. This capacity-based demand response is achieved by setting a minimum level of stored hydrogen so the refuelling stations can operator without generating new hydrogen for a set period. This framework considers the AC power flow equations to ensure that the DER operation does not violate any of the network constraints and the case study shows that the electrolysers are able to operate under these constraints. It also demonstrated that by participating in an additional market (the capacity-based demand reserve) the hydrogen refuelling stations were able to sell hydrogen at a lower price whilst maintaining a set profit level. This illustrates that electrolysers providing services and participating in markets could be key to reducing the market price of hydrogen. A disadvantage of this framework is that is employs a non-linear optimisation, which has associated issues with tractability. The case study in [128] considers a 1 hour time step and a 3 hour horizon. Therefore, this method is unlikely to be tractable for day-ahead consideration, or with inclusion of other markets/services.

Paper	**Multiple Markets**	**Network Services**	**Power Flow**	**Multi-Energy**	**Uncertainty**	**Tractable**
[100, 101]				✓		✓
[103]						✓
[104, 111]		✓	✓			✓
[105, 106]	✓	✓				✓
[110]			✓	✓		✓
[112]	✓	✓	✓			
[114, 121]	✓	✓	✓		✓	
[115]	✓	✓			✓	✓
[116]		✓	✓		✓	✓
[93, 117]	✓				✓	✓
[118, 119]	✓		✓		✓	
[94, 109]	✓				✓	
[108]		✓		✓	✓	✓
[120]		✓	✓		✓	
[122]		✓			✓	✓
[123]			✓		✓	✓
[85]	✓			✓	✓	✓
[107, 124]	✓	✓		✓	✓	
[125]	✓			✓		✓
[58]	✓		✓	✓		✓
[127]				✓		✓
[128]	✓	✓	✓	✓		

TABLE 2.1: Summary of literature

2.8 Summary of Gaps in the Literature

The range of previous works that have been reviewed in this chapter have been condensed into Table 2.1. This shows which of the six key attributes each of the previously proposed frameworks contain. Based on this, the key gaps in the literature can be summarised as follows:

- A significant number of the previous frameworks that consider uncertainty also appear to have tractability issues if operated at shorter time scales. The frameworks that don't suffer from this malady usually forgo modelling of power flow constraints. Some of those that do model power flow constraints use some form of linear approximation. However, these may not be accurate enough to provide reliable network services, or fully capture network constraints. In general, tractability issues seem to coincide with detailed power flow modelling. The use of convex relaxations of the power flow equations is not often seen in the previous

literature, but has strong potential of providing a compromise between accuracy and tractability. None of the frameworks reviewed consider uncertainty rigorously and include detailed power flow equations whilst remaining tractable.

- There are relatively few works that couple multiple energy vectors with uncertainty, or with the use of power flow equations. There are none that couple all three. One of the key advantages of multi-energy operation is the technical flexibility that can be provided from the non-electrical energy vector to the electricity network. Without consideration of the power flow equations alongside the coupling of multiple energy vectors, operational frameworks are not able to capture this technical flexibility. Such additional flexibility can also be used to help mitigate uncertainty. However these phenomena are rarely addressed.

- There are many works that do not consider multiple markets and contractual services. Without including these, a VPP operator will not be unlocking the full revenue potential of the VPP. Also, without considering a full complement of markets and services, an operator may be unaware of interactions between them that may hinder VPP operation. For example, providing network support may constrict a VPP's feasible operating region, limiting its revenue generating potential. If a VPP operator were to provide such a service, having an operational framework that can capture this interaction would help in pricing such a service. In the proposed works, the frameworks with an extensive consideration of markets and services forgo power flow modelling. This is a gap that the framework in this work aims to address.

- It is clear from examination of Table 2.1 that none of the frameworks in previous literature address all of the six key attributes. In fact, previous works have at most four of the six identified important attributes. Without consideration of all of these key attributes VPP operators could be:

  - forgoing additional revenue opportunities;
  - overestimating their operational envelope;
  - finding themselves unable to deliver their bids and faced with large penalty payments; or
  - locked into operating strategies which are not reflective of the real world markets due to the limited capability of their operating framework.

The framework proposed in this work aims to address all six of the key attributes in Table 2.1. In the next chapter, the formulations and methodology of the proposed framework will be presented in detail.

Chapter 3

Methodology: An Operational Framework for Virtual Power Plants

3.1 Introduction

As detailed in the previous chapters, a comprehensive VPP operational framework may be very advantageous for both the VPP operator and the electrical system operator. Allowing a VPP to provide critical network services, and participate in multiple markets through the use of multi-energy flexibility while considering uncertainty could help generate additional revenue for the VPP. This additional revenue is reflective of the additional value the VPP would bring to the network. However, it was uncovered in Chapter 2 that a comprehensive framework (one that can encompass multiple markets, network services, and models electrical power flows, multi-energy interactions, and uncertainty whilst remaining tractable for short bidding windows) is yet to be proposed and is complex in concept and implementation.

In this chapter, a brief summary of the concepts of the optimal power flow (OPF) problem is provided in Section 3.2. Following this the contributions of the chapter are shown. An overview of the operation of the proposed optimisation-based VPP operational framework is presented in Section 3.3, while the methods used to mitigate the effects of uncertainty are conveyed in Section 3.4. Finally, the formulation of the

innovate operational framework and its implementation are discussed in Sections 3.6 - 3.8.

3.2 Optimal Power Flow

The aim of an OPF problem is to minimise a given objective function (usually operating costs, or network losses) by making decisions on the operation of resources in the network, whilst adhering to all of the limitations that exist in an electrical network. These include (among many others):

- The physical laws that govern electrical power flow such as Kirchoff's current and voltage laws, and Ohms law.
- The operational constraints that govern the capabilities of resources in the network to turn on and off, and maintain and change power outputs (both active and reactive).
- The technical constraints of the network such as voltage limits, and thermal limits of lines and transformers.

The OPF formulations that are examined and utilised in this work require an assumption that the system that they are modelling is in a steady-state and is a balanced three-phase system. This allows a single-phase formulation to be used, and is a very common assumption throughout the literature when considering energy balancing in networks [129–133]. This is because balanced three-phase operation is an aim of grid operators, as it reduces grid power losses. Therefore, it is an acceptable approximation of real-world operation in three-phase networks. OPF in unbalanced systems is an active area of research of its own [134–136]. While there are many different formulations and uses of OPF that can be found in the literature, they can usually be classified depending on how they model the physical laws of the electrical network (the power flow equations). This can dictate whether the optimisation to be solved is linear, convex, or non-linear. These different models of the power flow equations will be detailed in the following sections.

3.2.1 Notation

Within this thesis we consider the single phase representation of a balanced three-phase AC electrical network consisting of a set of nodes Ψ^N, and a set of lines Ψ^L. The line that connects node $i \in \Psi^N$ to node $j \in \Psi^N$ is denoted line $(i,j) \in \Psi^L$. This would also imply that $(j,i) \in \Psi^L$. Each line $(i,j) \in \Psi^L$ has a complex impedance $z_{ij} = r_{ij} + \mathbf{j}x_{ij}$ and complex admittance $y_{ij} = g_{ij} + \mathbf{j}b_{ij}$. Note that $z_{ij} = z_{ji}$ and $y_{ij} = y_{ji}$. The apparent power flowing from node i to node j is $S_{ij} = P_{ij} + \mathbf{j}Q_{ij}$. The voltage at node i is $V_i = |V_i|e^{j\theta}$ and I_{ij} the current flow from node i to node j, while I_{ij}^* is the complex conjugate of I_{ij}. The value of $\mathbf{j} = \sqrt{-1}$. Per unit quantities are used throughout this thesis.

3.2.2 Non-Linear Formulation

The full derivation of the power flow equations from first principles can be found in [137]. The non-linear AC single-phase power flow in a network can be represented by:

$$S_{ij} = V_i I_{ij}^*, \ \ \forall (i,j) \in \Psi^L \tag{3.1}$$

$$V_i - V_j = z_{ij} I_{ij}, \ \ \forall (i,j) \in \Psi^L \tag{3.2}$$

$$S_i = \sum_{j \in \mathcal{N}_i} S_{ij}, \ \ \forall i \in \Psi^N \tag{3.3}$$

$$S_{ij} + S_{ji} = z_{ij}|I_{ij}|^2, \ \ \forall (i,j) \in \Psi^L \tag{3.4}$$

where $\mathcal{N}_i = \{j|\ (i,j) \in \Psi^L\}$ is the neighbourhood of node i (i.e., nodes connected to i by a line from Ψ^L). Apparent power flow is defined in (3.1), Ohms law is enforced by (3.2), Kirchoff's current law is found in (3.3), where S_i is the apparent power injected at node i, and (3.4) represents line losses.

These equality constraints can be used with relevant upper and lower bounds on power, voltage, and current to determine a feasible set for an optimisation. By introducing an appropriate cost function (such as minimisation of power losses in the network or operating costs of generators) this is a non-linear OPF problem. Due to the non-linearity and non-convexity of the problem, since (3.1) and (3.4) are non-convex constraints, these optimisations can be difficult to solve [138].

3.2.3 Linear Formulation

Due to the fact that linear optimisations can generally be solved more efficiently than their non-linear counterparts, sometimes a linear approximation of the non-linear power flow equations is used. However, this increased computational efficiency comes at a price. Simplifying assumptions are required to arrive at a linear approximation of the non-linear equations, resulting in a loss of accuracy in the power flow equations.

3.2.3.1 DC OPF

The most widely used of these linear approximation is known as the DC OPF, which is used for example in transmission grid planning [139] and unit commitment problems [140] which involve integer variables.

Firstly, by substituting (3.2) into (3.1) in accordance with $S_{ij} = P_{ij} + \mathbf{j}Q_{ij}$, and separating the real and imaginary parts of the resulting equations it can be found that:

$$P_{ij} = g_{ij}|V_i|^2 - |V_i||V_j|\big(g_{ij}\cos(\theta_i - \theta_j) - b_{ij}\sin(\theta_i - \theta_j)\big), \quad \forall (i,j) \in \Psi^L \tag{3.5}$$

$$Q_{ij} = b_{ij}|V_i|^2 - |V_i||V_j|\big(g_{ij}\sin(\theta_i - \theta_j) + b_{ij}\cos(\theta_i - \theta_j)\big), \quad \forall (i,j) \in \Psi^L \tag{3.6}$$

In DC OPF, to be able to linearise (3.1)-(3.6) the following assumptions are made:

1. The voltage magnitude at each node is close to its nominal value, i.e., $|V_i| \approx 1$.
2. The change in voltage angle across a line is very small. Therefore it is assumed $\sin(\theta_i - \theta_j) \approx \theta_i - \theta_j$.
3. The conductance of a line (g_{ij}) is much smaller than the susceptance of a line (b_{ij}). Therefore, it is assumed $g_{ij} \approx 0$.
4. Reactive power injection/absorption at nodes and flow along lines can be neglected. So it is assumed $Q_{ij} \approx 0$.

With all of these assumptions in place, the approximate power flow in the network can then be described by

$$P_{ij} = \ b_{ij}(\theta_i - \theta_j), \quad \forall (i,j) \in \Psi^L \tag{3.7}$$

$$P_i = \sum_{j \in \mathcal{N}_i} P_{ij}, \quad \forall i \in \Psi^N. \tag{3.8}$$

$$P_{ij} + P_{ji} = 0, \quad \forall (i,j) \in \Psi^L \tag{3.9}$$

This simplified set of constraints (3.7) - (3.9) can then replace (3.1) - (3.4) and can be used in a linear optimisation problem. While these assumptions may be acceptable for transmission networks (for which they were originally designed), they are less applicable to distribution networks which have higher line resistances, losses and voltage drops.

3.2.3.2 Linear Formulation used in the Proposed Framework

While the DC OPF formulation effectively simplifies the optimisation problem, it is based on many simplifying assumptions. The ability to consider reactive power and voltage magnitude in the operational framework is important. Therefore, a linearisation is chosen that also captures these aspects of the network power flow. The linearisation chosen is reproduced from [131].

Under the simplifying assumptions:

1. $\cos(\theta_i - \theta_j) \approx 1$
2. $\sin(\theta_i - \theta_j) \approx \theta_i - \theta_j$
3. $g_{ij}|V_i|\left(|V_i| - |V_j|\right) \approx g_{ij}\left(|V_i| - |V_j|\right)$
4. $b_{ij}|V_i||V_j|\left(\theta_i - \theta_j\right) \approx b_{ij}\left(\theta_i - \theta_j\right)$

the active and reactive power flows in (3.5) and (3.6) become

$$P_{ij} = g_{ij}\left(|V_i| - |V_j|\right) - b_{ij}\left(\theta_i - \theta_j\right), \quad \forall (i,j) \in \Psi^L \tag{3.10}$$

$$Q_{ij} = -b_{ij}\left(|V_i| - |V_j|\right) - g_{ij}\left(\theta_i - \theta_j\right), \quad \forall (i,j) \in \Psi^L. \tag{3.11}$$

This is a much more detailed model of the power flow equations compared to the DC OPF, as this linearisation includes reactive power and voltage magnitude. Additionally, both active and reactive power flows are dependent on both voltage magnitude and angle. Therefore, this linearisation is more applicable to distribution networks than the

DC OPF. This linearisation creates a problem for which a solution is much easier to obtain than for its non-linear counterpart. The trade-off is that information is lost in this linearisation process. Another choice that is widely used outside of the linear and non-linear formulations involves convex relaxation of the power flow constraints. We can look to such convex formulations as a compromise between the linear and the non-linear formulations in terms of accuracy and computational efficiency.

3.2.4 Second Order Cone Convex Relaxation

As outlined in Section 1.4, convex optimisation problems have a number of useful attributes that can be leveraged by solver algorithms to obtain timely solutions. There has been much work done on the topic of convexifying the OPF problem [74, 129, 130, 141, 142]. There are two prominent methods used to convexify the power flow equations: semi-definite programming (SDP) [143, 144] and second-order cone programming (SOCP) [130, 145]. The SOCP approach has the advantage of generally being more computationally efficient [74], with well defined situations for when the relaxation is tight [142] (i.e., the solution to the convex relaxation is also the solution to the non-convex problem). SOCP is the convexification approach used in this work, and so it will be used here as an example of convexification of power flow equations.

The SOCP approach starts by considering the power flow equations (3.1) - (3.4). Through squaring both sides of (3.1) and (3.2), and separating real and imaginary components of (3.3) and (3.4) the following can be obtained.

$$P_i = \sum_{j \in \mathcal{N}_i} P_{ij}, \quad \forall i \in \Psi^N \tag{3.12}$$

$$Q_i = \sum_{j \in \mathcal{N}_i} Q_{ij}, \quad \forall i \in \Psi^N \tag{3.13}$$

$$P_{ij} + P_{ji} = r_{ij}\Lambda_{ij}, \quad \forall (i,j) \in \Psi^L \tag{3.14}$$

$$Q_{ij} + Q_{ji} = x_{ij}\Lambda_{ij}, \quad \forall (i,j) \in \Psi^L \tag{3.15}$$

$$v_j = v_i - 2(r_{ij}P_{ij} + x_{ij}Q_{ij}) + (r_{ij}^2 + x_{ij}^2)\Lambda_{ij}, \quad \forall (i,j) \in \Psi^L \tag{3.16}$$

$$\frac{P_{ij}^2 + Q_{ij}^2}{v_i} = \Lambda_{ij}, \quad \forall (i,j) \in \Psi^L \tag{3.17}$$

where $\Lambda_{ij} = |I_{ij}|^2$ and $v_i = |V_i|^2$.

By moving to the use of Λ_{ij} and v_i as decision variables, rather than I_{ij} and V_i, the OPF problem drops the explicit consideration of nodal voltage angle. This means that for networks with loops, the requirement that voltage angles around a loop sum to 0 (Kirchoff's voltage law) is not enforced. In radial networks this consideration is not required, as there are no loops, and so for the case of radial networks no information has been lost by this transformation.

The equality constraint (3.17) is not yet convex, so a relaxation is introduced by changing (3.17) to the inequality

$$\frac{P_{ij}^2 + Q_{ij}^2}{v_i} \leq \Lambda_{ij}, \quad \forall (i,j) \in \Psi^L. \tag{3.18}$$

This relaxed constraint can be equivalently written as the SOCP constraint

$$\left\| \begin{array}{c} 2P_{ij} \\ 2Q_{ij} \\ \Lambda_{ij} - v_i \end{array} \right\| \leq \Lambda_{ij} + v_i, \quad \forall (i,j) \in \Psi^L, \tag{3.19}$$

which is convex, and where

$$\left\| \begin{array}{c} a \\ b \end{array} \right\| = \sqrt{a^2 + b^2}$$

is the Euclidean norm. The set of constraints (3.12) - (3.16), and (3.19) make the SOCP relaxation of the non-linear system in Section 3.2.2. In a radial network, if the constraint (3.19) is binding, then this relaxation is tight (i.e., the solution to the relaxation is also a feasible solution in the associated non-linear problem) [142].

3.3 Framework Overview

The aim of the operational framework is to schedule and dispatch multi-energy VPP resources to maximise profit from simultaneous participation in multiple markets, whilst providing network services. This is to be achieved under uncertainty in market prices, demand at the nodes, and availability of renewable energy sources (RES). The operational framework should allow for the day-ahead scheduling of resources in the VPP

and also be able to accommodate electrical markets with bidding windows as short as 5 minutes (as in the National Electricity Market in Australia [18]).

The operational framework would therefore need to solve a problem that is a multi-period (e.g., to deal with storage resources), non-linear (e.g., to deal with power flow equations), stochastic (e.g., to deal with uncertainty) optimisation with integer variables (e.g., to deal with commitment status). Solving such a problem can be challenging, particularly from the perspective of scalability. Rather than trying to solve the entire problem in a single optimisation, a different approach is taken in this thesis. It is recognised that different aspects of the problem require different considerations. For example, the only part of the problem that requires the use of integer variables is for the scheduling of resources. If the scheduling and dispatch problems were separated, the dispatch problem would become a continuous optimisation, which is less computationally challenging.

In an effort to maintain tractability for large problems a divide-and-conquer approach is taken. The proposed approach involves three sequentially coordinated optimisation problems:

- *High-Level Optimisation:* An optimisation problem that is a scenario-based mixed integer linear program (MILP) for day-ahead unit commitment with 30-minute time-steps and a 24-hour prediction horizon.
- *Mid-Level Optimisation:* A second order cone (SOC) receding horizon optimisation problem for preliminary dispatch of the scheduled resources with 30-minute time-steps over a 24-hour prediction horizon. This horizon recedes every 30 minutes.
- *Low-Level Optimisation:* A SOC receding horizon optimisation problem for 5-minute dispatch with a 30-minute prediction horizon that recedes every 5 minutes.

By decomposing the operational framework into these three coordinated optimisation problems, many of the key challenging properties of the overall problem are mitigated. Since the use of integer variables is restricted to the scheduling problem, a linearisation of the network power flow constraints is used in the high-level optimisation to arrive at a tractable MILP problem. This isolation of the integer variables allows a more accurate convex relaxation of the power flow equations to be utilised in the mid-level and low-level optimisations. This assists with the VPP's ability to provide network services and

to accurately capture network constraints. By splitting the mid-level and the low-level optimisations, the framework avoids the necessity of having both a 5-minute time-step and a 24-hour planning horizon in the same optimisation. Having so many time steps in the optimisation could lead to scaling and tractability issues, and would likely negate the ability of the operational framework to utilise receding horizon control to mitigate uncertainty.

As mentioned above, the non-convex constraints associated with the AC power flow equations for the VPP network are approximated by linearisation (in the high-level optimisation) or convex relaxation (in the mid-level and low-level optimisations). The high-level problem is utilised to create a schedule for the resources for the day ahead. Due to the fact that the dispatch of resources is not set by the high-level optimisation, a very accurate representation of the power flow is not essential. The provision of services and consideration of network constraints are accurately captured by the mid-level and low-level optimisations. As such, for the high-level optimisation a linear approximation can be used, resulting in a MILP. The mid-level and low-level dispatch problems are continuous (as the values of all integer variables are set by the high-level optimisation). Therefore, when dispatching the resources in the mid-level and low-level problems a convex relaxation is used, specifically a SOC relaxation [146]. Additional considerations may be required for low voltage feeders, where balanced three-phase operation may not be fully achieved. The SOC relaxation replaces the current flow equality that relates power and voltage by an inequality. The phasor sum of voltages around a loop is also neglected (due to the use of squared values of voltage and current as decision variables as part of convexifying the constraints). As most distribution networks are radial, the lack of voltage angles will often not affect the optimisation solution. In fact, if there are no upper bound on loads, this relaxation is exact for radial networks [147]. While the lack of upper bounds on network loads is unlikely to be applicable in real world operation, methods are proposed in [142] for obtaining an exact solution to the AC OPF problem from the solution to the SOC problem for radial networks. It is also noted in [142] that for non-exact solutions, the difference between the SOC solution and the AC OPF solution are minor. Additionally, for meshed networks the VPP dispatch points could be used as a starting point of an AC load flow to obtain a more accurate solution or verify the SOC solution. SOC optimisations can generally be solved more efficiently than other convex relaxations of the power flow equations [74] which is an important

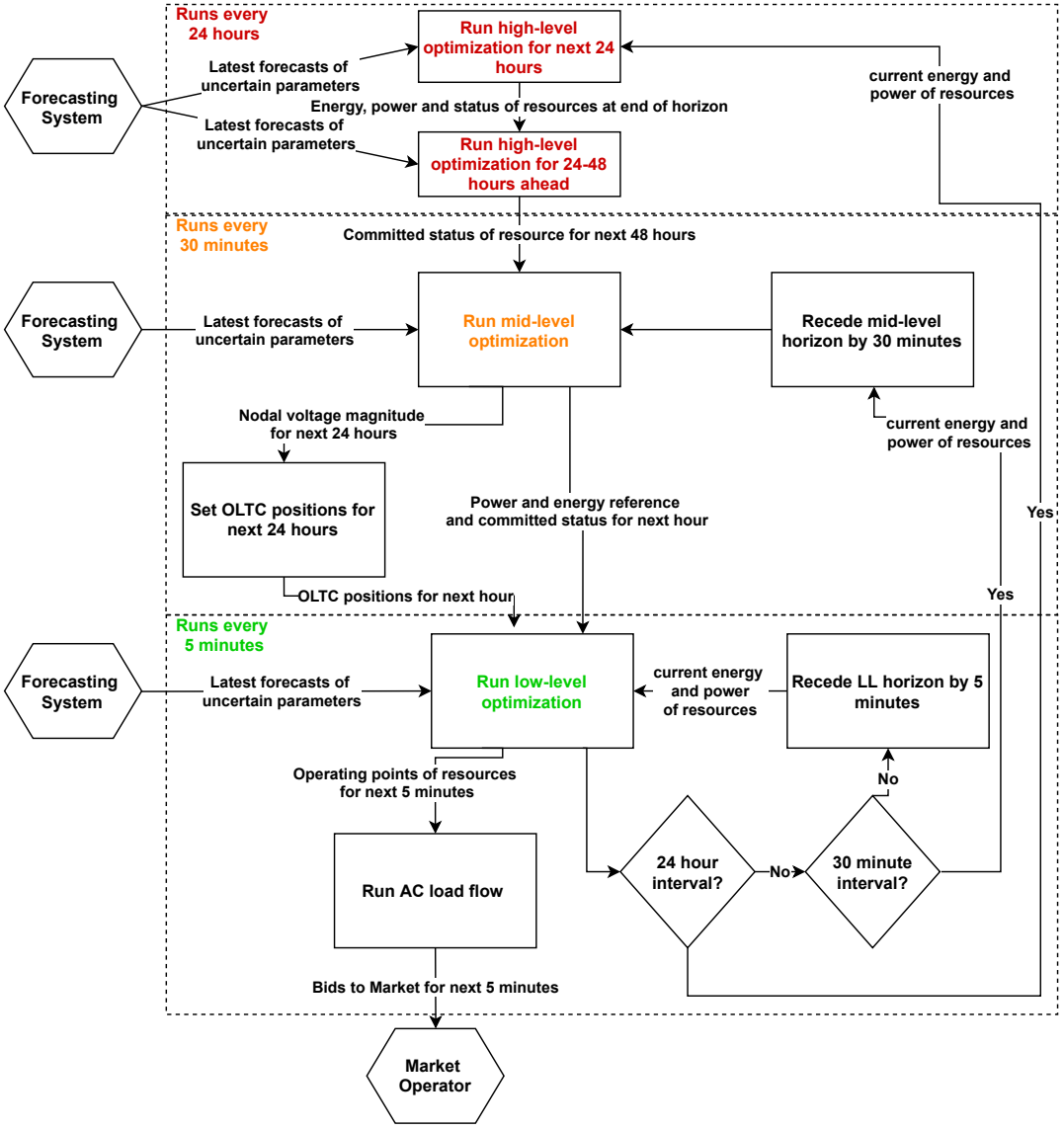

FIGURE 3.1: Example flowchart of VPP operation

consideration when coupled with the receding horizon approach of the mid-level and low-level optimisations. Considering the fact that DC power flow equations are often used for real world application of OPF, the use of the SOC power flow equation provides a significant increase in modelling accuracy, whilst maintaining problem tractability [142].

An overview of the proposed scheme operating in a near real-time market structure is illustrated in Figure 3.1. The committed status of resources for the next 48 hours (of which only the first 24 hours is binding) is determined by the high-level optimisation and then passed to the mid-level optimisation each day. The reason that the schedule given to the mid-level optimisation is for the next 48 hours rather than 24 hours is due

to the use of receding horizon control by the mid-level optimisation. As the horizon recedes by each 30-minute interval, its horizon extends past the end of the day for which the first 24-hour high-level optimisation has provided a schedule. Therefore, a schedule for the 24-48 hour period is required. However, this schedule is updated the next time that the high-level optimisation is run, so it is only a preliminary schedule (i.e., it is not binding).

The mid-level optimisation uses the unit commitment schedule and updated forecasts of the uncertain parameters to produce a preliminary dispatch for the coming 24 hours. The solution of the mid-level optimisation can also be used to determine if the position of on-load tap changers (OLTCs) in the network should be adjusted. The scheduling information, preliminary dispatch information, and OLTC positions for the next hour are then provided to the low-level optimisation.

The low-level optimisation is solved to obtain dispatch information for the next 30 minutes and the current operating status of the resources is run through an AC load flow to ensure accurate bids are provided to the market, and to provide a measure of the accuracy of the SOC relaxation. This is important, as the SOC relaxation may not be exact, which would mean that the power flow solution of the low-level optimisation would not be a feasible solution for AC power flow equations. By using the dispatch points determined by the low-level optimisation as an input to an AC load flow, the framework is able to determine the actual AC power flows in the network. If this solution violates network constraints, then this can be addressed in future optimisations by slightly tightening the upper and lower bounds of the network state variables in the SOC optimisation. The bids for the first 5 minutes are then provided to the market operator. This low-level optimisation is re-optimised every 5 minutes as the prediction horizon recedes. After each 30-minute period, the current operational points of the resources are provided to the mid-level optimisation and the mid-level problem is then re-run with a receded horizon. After each 24 hour period, the current operating point of each resource is provided to the high-level optimisation to create another unit commitment schedule.

The near real-time market structure assumed here is computationally onerous, which is why it has been used to illustrate the example operation of the framework. However, the framework is designed to be able to be flexibly applied to different market structures. For example, if there were a binding day-ahead market, then the high-level optimisations

and the first mid-level optimisation could be run to obtain the day-ahead market bid. And then subsequent mid-level and low-level optimisations can be used to match that bid while participating in the closer to real-time markets. If a day-ahead schedule is not required for resource operation, then the high-level optimisation could be omitted. Further, if the close to real-time markets are dispatched every 15 minutes, then the time step and horizon of the low-level optimisation can be updated accordingly without an increase in computational burden. These are just a few examples of ways that the operational framework can be tailored to specific market structures or VPP operator requirements. As the framework is designed to be tractable in the most onerous of conditions, it should also be tractable when adjusted in these ways, ensuring additional utility of the operational framework.

It should be noted that while the decomposition of the original problem into this three-tier methodology allows for solutions to be obtained in a tractable manner, there is no guarantee that these solutions will be the optimal solution of the original problem. To understand how sub-optimal the solution of this methodology is, it would need to be compared to the original multi-period, non-linear, stochastic, mixed-integer problem. As explained previously, this is a highly complex problem that will likely take a very long time to solve, if it converges to a solution at all. Therefore, this analysis has not been provided in this thesis. However, in Section 4.2.4.4 the solutions of this approach are compared with previously proposed solutions to provide an estimate of the additional benefit over the previous state of the art.

3.3.1 On Load Tap Changer Operation

The framework accommodates the modelling of OLTCs in the network. However, as inclusion of OLTC operation within the optimisations could lead to substantial increase in the complexity of the optimisation problems, it is proposed to update the OLTC settings via a heuristic strategy shown in Figure 3.2. For each OLTC, at each 30-minute time step (up to 24 hours ahead) the voltage magnitudes of all of the downstream nodes are considered. If any of these are within a set tolerance band of the maximum nodal voltage, the associated OLTC tapping ratio will be incremented one tap up. If any of these are within a set tolerance band of the minimum nodal voltage, the associated OLTC tapping ratio will be incremented one tap down. This heuristic method is conducted

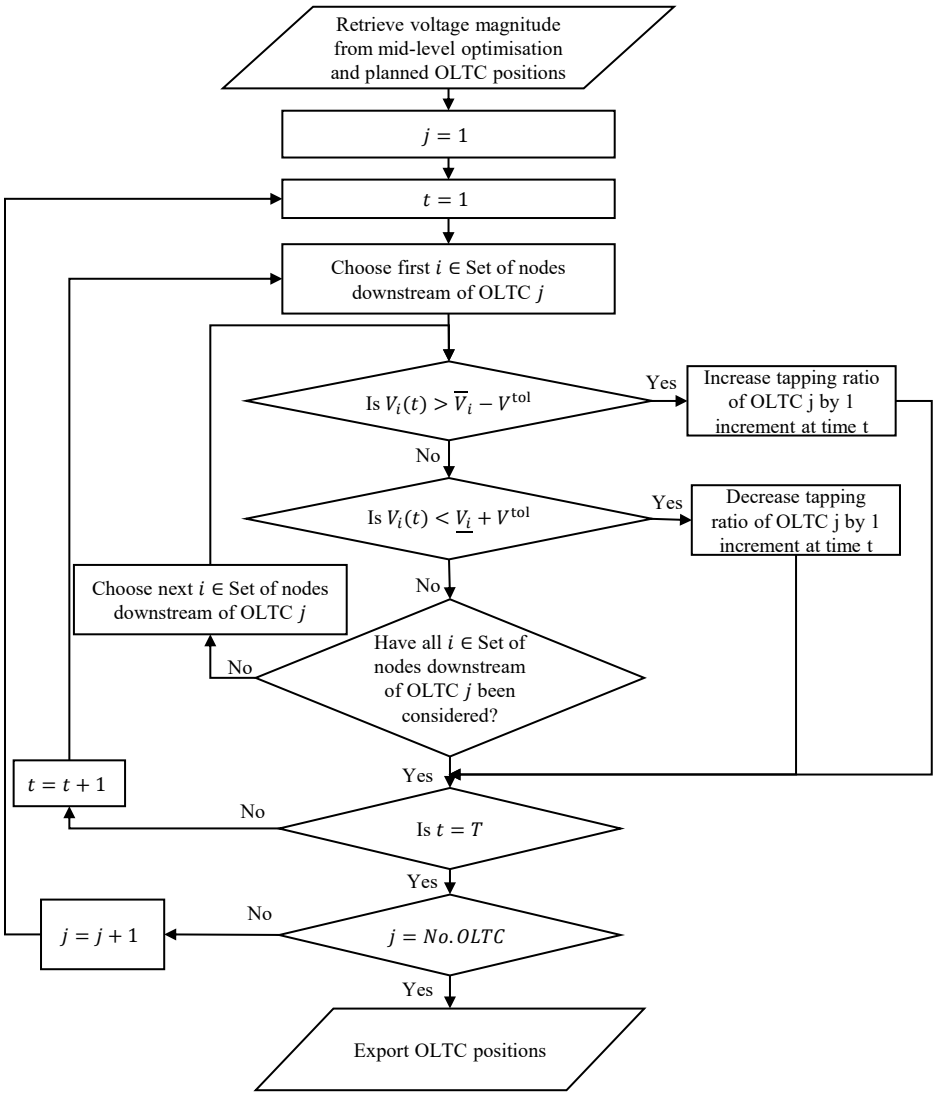

FIGURE 3.2: Flowchart for the heuristic method of assigning OLTC position

after each solution of the mid-level optimisation i.e., every 30 minutes. The OLTC positions obtained from this method are then used to determine the new per unit line impedance and nodal voltage limits downstream of the OLTCs. These values will be used in the optimisations until the completion of the next mid-level optimisation. This allows OLTC positions to be planned ahead of time, whilst providing the flexibility to alter their position throughout the day.

As noted in the previous paragraph, the additional integer variables in a MILP increases the computational complexity of the problem. In fact, theoretically the computational

complexity of finding the solution to a MILP scales exponentially (although the algorithms that obtain approximate solutions such as the branch-and-bound algorithm generally perform better). Therefore, when including additional integer variables, the addition modelling accuracy should be weighed against the potentially significant increase in computational complexity. For this reason, many resources/operations that occur in networks which require integer variables to model accurately are included in optimisations in a relaxed. Examples of this are on-load tap changers, which are often modelled as continuous rather than in steps to forgo integer variables, or as in the case of this framework, modelled in a heuristic sense. Switched capacitor banks are another example. However, these can be integrated into a unit commitment model by allocated commitment variables to the capacitor banks. Network reconfiguration problems are perhaps one of the most complex examples of using integer variables to model network operations. These are a sub-set of problems all of their own, and due to their complexity require their own approaches to solve tractably [148, 149], and so lie outside of the scope of this work.

3.4 Methods to Mitigate the Impact of Uncertainty

In principle, the high-level optimisation problem to be solved is a stochastic day-ahead unit commitment problem, with chance-constraints to reflect uncertainty in load and RES availability (market price uncertainty is confined to the objective function and so is not featured in chance-constraints). In general, chance-constrained optimisation problems are difficult to solve [87]. One approach is to employ a scenario-based approximation, in which the chance-constraints are replaced by a finite number of constraint realisations (i.e., scenarios), drawn from the underlying probability distributions of the uncertain parameters [88, 89, 150]. Therefore, the high-level optimisation is formulated as a scenario-based approximation of the stochastic unit commitment problem.

Generally, for scenario-based approximations a large number of scenarios is required for probabilistic guarantees of chance-constraint satisfaction [90], which can render the scenario-based problem intractable. This is usually dealt with by utilising some form of scenario-reduction technique such as forward scenario selection, backward scenario reduction [93], or K-means clustering [119]. Within the context of unit commitment with linearised power flow constraints, it is possible to exploit the problem structure

to construct a restriction that is a much smaller, and therefore tractable, optimisation problem to solve. In fact the restriction reduces the size of optimisation problem by a factor of S, where S is the number of scenarios. This is done by identifying which scenario is the most onerous for each inequality constraint, and creating a restriction with those constraints. This is possible, in part, because only a small subset of the variables in the problem are scenario independent (the committed status of the resources). Since it is a restriction, any solution it generates is feasible for all scenarios in the original approximation, with its associated guarantees regarding chance-constraint satisfaction. Details of this restriction can be found in Appendix A. It should be noted that, if the initial multi-scenario problem is not feasible, then this robust restriction will not yield a feasible solution. The author has not developed any proof with regard to the guarantee of obtaining a feasible solution from the robust restriction given a feasible solution to the multi-scenario problem. This could be a line of enquiry for future work. However, when used for the case studies in this thesis, there were no issues in obtaining feasible solutions. Reduced computational complexity might come at the price of a potentially conservative schedule arising from the restricted problem. This is investigated in later chapters through application of the framework in case studies. This provides a VPP operator which two choices of how to conducted the high-level scenario-based optimisation, depending on the robustness that they require - utilising a scenario-reduction technique, or the robust restriction proposed in Appendix A.

In the high-level optimisation, market price uncertainty is confined to the objective function (which is explicitly defined in Section 3.6). As the objective function is a function of a random variable, we must minimise the expected value (denoted by $\mathbb{E}[\cdot]$) of the objective function to be able to obtain a solution [82]. Directly computing the expected value of the cost function may not be possible, so instead this work utilises the sample average approximation of the expected value of the objective function [151] defined by

$$\mathbb{E}[f(x,\xi)] \approx \frac{1}{S}\sum_{s=1}^{S} f(x,\xi^s), \tag{3.20}$$

where ξ^s is the $s \in [1:S]$ realisation of the random variable ξ. This approach integrates well with the scenario-based approximation of the chance-constraints.

The receding horizon control based application of the mid-level and low-level optimisations is the main approach to mitigating the impact of uncertainty in these optimisations. It allows the VPP to update the dispatch regularly in response to changes in nodal demand, RES output, and market prices. However, with the aim of increasing the robustness of the solution obtained by the mid-level and low-level optimisations, both additionally consider three scenarios. They are formulated as an expected scenario, a scenario with higher generation/less load, and a scenario with less generation/higher load. This balances tractability and feasible outcomes that are to some extent insensitive to small perturbations in the uncertain parameters. How conservative the VPP operator wishes to be can be reflected in the choice of these scenarios.

In summary, the high-level optimisation delivers a single resource schedule over a 24 hour period which minimises the expected cost to the VPP whilst maintaining feasibility for all scenarios considered (or used in the creation of the robust restriction). This schedule is provided to the mid-level and low-level optimisations. The mid-level optimisation delivers a single storage operational trajectory across the prediction horizon and a single initial operating point for each resource for the first 30-minute time-step. These minimise the expected value of the cost functions across all scenarios considered. Subsequent 30-minute time-step actions are determined by repeatedly solving the mid-level problem in a receding horizon fashion. The preliminary dispatch and schedule for the next hour are provided to the low-level optimisation. The low-level optimisation delivers a single set of bids (only binding for the first 5-minute time-step of the corresponding prediction horizon) which minimises the expected value of the cost functions across all scenarios considered. This ensures bids can be robustly delivered, with re-optimisation every 5 minutes given updates of the system state. By combining a receding horizon approach and scenario-based approximation of the uncertainty a good trade off between optimality and robustness is achieved.

In the following sections, the detailed formulation of the high-level, mid-level, and low-level optimisation is provided.

3.5 Additional Notation

In addition to the notation defined in Section 3.2.1, the following notation is also proposed. The set of resources in the VPP is defined as Ψ^K. The set of resources at node i is $\Psi_i^K \subseteq \Psi^K$, and $\Psi_{i,e}^K \subseteq \Psi_i^K \subseteq \Psi^K$ is the set of resources at node i operating in non-electrical energy vector $e \in \Psi^{\text{Non-elec}}$. The notation for time-dependent decision variables is $a(t)$, whereas a time-dependent parameter is shown as a_t. The scenario dependence of a variable or parameter is denoted as a_s.

3.6 High-Level Optimisation

The aim of the high-level scenario-based MILP is to provide a schedule for the VPP resources for the day ahead, with 30-minute time steps.

3.6.1 Cost Function

The objective function for the high-level optimisation is:

$$\min \sum_{s=1}^{S^{\text{HL}}} \pi_s^{\text{HL}} \sum_{t=1}^{T^{\text{HL}}} c_s^{\text{tot,HL}}(t) \Delta t \tag{3.21}$$

where $c_s^{\text{tot,HL}}(t)$ is the total VPP cost for each scenario $s \in [1 : S^{\text{HL}}]$ for each time step $t \in [1 : T^{\text{HL}}]$ of length Δt, and is defined as:

$$\begin{aligned} c_s^{\text{tot,HL}}(t) = \; & \overbrace{c_s^{\text{op}}(t)}^{1} + \overbrace{\sum_{k \in \Psi^K} \left(\lambda_k^{\text{curt}} \omega_{k,s}(t)\right) + \sum_{e \in \Psi^{\text{Non-elec}}} \sum_{i \in \Psi^N} \left(\lambda_i^{e,\text{curt}} \omega_{i,s}^e(t)\right)}^{2} - \overbrace{\lambda_{s,t}^{\text{P}} P_s^{\text{exp}}(t)}^{3} - \overbrace{\lambda_{s,t}^{\text{Q}} Q_s^{\text{exp}}(t)}^{4} \\ & - \overbrace{\sum_{e \in \Psi^{\text{Non-elec}}} \left(\lambda_{s,t}^e \sum_{i \in \Psi^N} \frac{E_{i,s}^{e,\text{exp}}(t)}{\Delta t} \right)}^{5} - \overbrace{\sum_{r \in \Psi^{\text{Raise}}} \left(\lambda_{s,t}^r \left(\sum_{k \in \Psi^K} P_{k,s}^r(t) - \underline{P}_t^r \right) \right)}^{6} \\ & - \overbrace{\sum_{l \in \Psi^{\text{Lower}}} \left(\lambda_{s,t}^l \left(\sum_{k \in \Psi^K} P_{k,s}^l(t) - \underline{P}_t^l \right) \right)}^{7} - \overbrace{\lambda_{s,t}^{\text{I}} \left(\sum_{k \in \Psi^K} H_k^{\text{g}} \overline{S}_k \zeta_k(t) - \underline{I}_t \right)}^{8}. \end{aligned} \tag{3.22}$$

The first term in (3.22) is the operating cost of resources in the VPP and is defined further in (3.23). The second term in (3.22) is the cost associated with curtailing resources in the VPP. The other terms are negative as they are associated with revenue (negative cost). Term 3 and 4 are the revenue from exporting active power $P_s^{\text{exp}}(t)$ and reactive power $Q_s^{\text{exp}}(t)$ to the grid respectively. Term 5 is the revenue from exporting energy from non-electrical vectors $E_{i,s}^{e,\text{exp}}(t)$ in the set $e \in \Psi^{\text{Non-elec}}$. Term 6 is the revenue from all of the raise services in the set $r \in \Psi^{\text{Raise}}$. The power committed by each resource for each raise service is $P_{k,s}^{r}(t)$, and $\underline{P}^{r}(t)$ is the magnitude of each raise services that the VPP is contracted by other market entities to provide. Term 7 is the equivalent to term 6, but for lower services in the set $l \in \Psi^{\text{Lower}}$. Term 8 represents the revenue that the VPP can obtain from providing inertia, where $\lambda_{s,t}^{\text{I}}$ is the market price of inertia and $\underline{I}_t$ is the level of inertia the VPP is contractually obliged to provide. Note that this is referring to physical inertia provided by synchronous rotating machines. If the VPP does not contain these, then the VPP cannot provide inertia support through this framework.

The total operating cost of the resources within the VPP for each scenario $s \in [1 : S^{\text{HL}}]$ and for each time step $t \in [1 : T^{\text{HL}}]$ is upper bounded by $c_s^{\text{op}}(t)$:

$$c_s^{\text{op}}(t) \geq \sum_{k \in \Psi^K} \Big(\chi_k^{\text{g}} P_{k,s}^{\text{g}}(t) + \chi_k^{\text{d}} P_{k,s}^{\text{d}}(t) + \gamma_k \zeta_k(t) + \frac{\lambda_k^{\text{on}}}{\Delta t} \max\left(0, \zeta_k(t) - \zeta_k(t-1)\right) + \frac{\lambda_k^{\text{off}}}{\Delta t} \max\left(0, \zeta_k(t-1) - \zeta_k(t)\right) \Big). \quad (3.23)$$

In (3.23), χ_k^{g} and χ_k^{d} represent a linear cost coefficient associated with resource active power generation $P_{k,s}^{\text{g}}(t)$ and demand $P_{k,s}^{\text{d}}(t)$ respectively. There is a constant cost γ_k associated with resource k being on (encoded by the binary variable $\zeta_k(t)$). The last two terms in (3.23) are associated with the turn on/off costs of resource k respectively. In (3.23), an inequality rather than an equality is used to maintain the linearity of the problem which includes the two max terms. It can be seen that $\zeta_k(t)$ is not scenario-dependant. The high-level optimisation creates a single unit commitment schedule that is feasible across all scenarios, for use in the mid-level and low-level optimisations.

3.6.2 Power Flow Equations

This section deals with the equations that govern the flow of power in a network. These power flow equations are enforced for $s \in [1 : S^{\mathrm{HL}}]$ and $t \in [1 : T^{\mathrm{HL}}]$:

$$P_{ij,s}(t) = g_{ij,t}\left(V_{i,s}(t) - V_{j,s}(t)\right) - b_{ij,t}\left(\theta_{i,s}(t) - \theta_{j,s}(t)\right), \quad \forall (i,j) \in \Psi^L \tag{3.24}$$

$$Q_{ij,s}(t) = -b_{ij,t}\left(V_{i,s}(t) - V_{j,s}(t)\right) - g_{ij,t}\left(\theta_{i,s}(t) - \theta_{j,s}(t)\right), \quad \forall (i,j) \in \Psi^L \tag{3.25}$$

$$-\overline{S}_{ij} \leq P_{ij,s}(t) \leq \overline{S}_{ij}, \quad \forall (i,j) \in \Psi^L \tag{3.26}$$

$$-\overline{S}_{ij} \leq Q_{ij,s}(t) \leq \overline{S}_{ij}, \quad \forall (i,j) \in \Psi^L \tag{3.27}$$

$$P_{ij,s}(t) + Q_{ij,s}(t) \leq \sqrt{2}\,\overline{S}_{ij}, \quad \forall (i,j) \in \Psi^L \tag{3.28}$$

$$P_{ij,s}(t) - Q_{ij,s}(t) \leq \sqrt{2}\,\overline{S}_{ij}, \quad \forall (i,j) \in \Psi^L \tag{3.29}$$

$$-P_{ij,s}(t) + Q_{ij,s}(t) \leq \sqrt{2}\,\overline{S}_{ij}, \quad \forall (i,j) \in \Psi^L \tag{3.30}$$

$$-P_{ij,s}(t) - Q_{ij,s}(t) \leq \sqrt{2}\,\overline{S}_{ij}, \quad \forall (i,j) \in \Psi^L \tag{3.31}$$

$$P_{ij,s}(t) + P_{ji,s}(t) = 0, \quad \forall (i,j) \in \Psi^L \tag{3.32}$$

$$Q_{ij,s}(t) + Q_{ji,s}(t) = 0, \quad \forall (i,j) \in \Psi^L \tag{3.33}$$

$$\underline{V}_{i,t} \leq V_{i,s}(t) \leq \overline{V}_{i,t}, \quad \forall i \in \Psi^N \tag{3.34}$$

$$\underline{\theta}_i \leq \theta_{i,s}(t) \leq \overline{\theta}_i, \quad \forall i \in \Psi^N \tag{3.35}$$

$$\sum_{j \in \mathcal{N}_i} P_{ij,s}(t) = \sum_{k \in \Psi_i^K} P_{k,s}(t), \quad \forall i \in \Psi^N \tag{3.36}$$

$$\sum_{j \in \mathcal{N}_i} Q_{ij,s}(t) = \sum_{k \in \Psi_i^K} Q_{k,s}(t), \quad \forall i \in \Psi^N. \tag{3.37}$$

The high-level optimisation utilises a linear approximation of the power flow equations to yield a MILP formulation. This linearisation is detailed in (3.24) and (3.25), which was shown in [131] to adequately capture both voltage angle and magnitude in relation to active and reactive power. Additionally, the inclusion of reactive power makes this a superior linear approximation compared to the DC OPF, especially in distribution networks. Constraints (3.26) - (3.31) approximate the apparent power limits $\overline{S}_{ij}$ in the lines. Constraints (3.32) and (3.33) ensure that power flows through each line from

either direction are equal and opposite. Due to the linear approximation used for the high-level problem, line losses are neglected. The limits on voltage magnitude and angle are defined by (3.34) and (3.35). Constraint (3.36) ensures that the power flowing out of node i is the same as the net power injection of all resources connected to node i, designated by resources in the set Ψ_i^K. Constraint (3.37) provides a similar constraint for reactive power. Note that in the high-level optimisation the parameters $g_{ij,t}$, $b_{ij,t}$, $\overline{V}_{i,t}$ and $\underline{V}_{i,t}$ are time varying parameters. This is due to the use of OLTCs in the network. The tap positions of the OLTC may not be constant throughout the day, effecting the per unit voltage base in areas of the network.

3.6.3 Resource Modelling

In this section the electrical modelling of the resources in the VPP is presented. All of the following equations are enforced for $s \in [1 : S^{\mathrm{HL}}]$, $t \in [1 : T^{\mathrm{HL}}]$:

$$\overline{E}_k^{\mathrm{elec}} \left(x_{k,s}(t+1) - x_{k,s}(t)\right) = \left(\eta_k^{\mathrm{d}} P_{k,s}^{\mathrm{d}}(t) - \frac{P_{k,s}^{\mathrm{g}}(t)}{\eta_k^{\mathrm{g}}} + \xi_{k,s,t} - \omega_{k,s}(t) - \nu_k\right) \Delta t, \ \ \forall k \in \Psi^K \tag{3.38}$$

$$X_k^{\mathrm{target}} \leq x_{k,s}(T+1), \ \ \forall k \in \Psi^K \tag{3.39}$$

$$0 \leq x_{k,s}(t) \leq 1, \ \ \forall k \in \Psi^K \tag{3.40}$$

$$\zeta_k(t)\underline{P}_k^{\mathrm{g}} \leq P_{k,s}^{\mathrm{g}}(t) \leq \zeta_k(t)\overline{P}_k^{\mathrm{g}}, \ \ \forall k \in \Psi^K \tag{3.41}$$

$$\zeta_k(t)\underline{P}_k^{\mathrm{d}} \leq P_{k,s}^{\mathrm{d}}(t) \leq \zeta_k(t)\overline{P}_k^{\mathrm{d}}, \ \ \forall k \in \Psi^K \tag{3.42}$$

$$-\underline{P}_k^{\mathrm{g}}\left(1 - \zeta_k(t)\right) + \underline{\rho}_k \Delta t \leq P_{k,s}^{\mathrm{g}}(t) - P_{k,s}^{\mathrm{g}}(t-1) \leq \overline{\rho}_k \Delta t + \overline{P}_k^{\mathrm{g}}\left(1 - \zeta_k(t-1)\right), \ \ \forall k \in \Psi^K \tag{3.43}$$

$$-\underline{P}_k^{\mathrm{d}}\left(1 - \zeta_k(t)\right) + \underline{\rho}_k \Delta t \leq P_{k,s}^{\mathrm{d}}(t) - P_{k,s}^{\mathrm{d}}(t-1) \leq \overline{\rho}_k \Delta t + \overline{P}_k^{\mathrm{d}}\left(1 - \zeta_k(t-1)\right), \ \ \forall k \in \Psi^K \tag{3.44}$$

$$P_{k,s}(t) = P_{k,s}^{\mathrm{g}}(t) - P_{k,s}^{\mathrm{d}}(t), \ \ \forall k \in \Psi^K \tag{3.45}$$

$$0 \leq \left(\Phi_k^{\xi+} - \Phi_k^{\xi-}\right) \omega_{k,s}(t), \ \ \forall k \in \Psi^K \tag{3.46}$$

$$0 \leq \left(\Phi_k^{\xi+} - \Phi_k^{\xi-}\right) \left(\alpha_k \xi_{k,s,t} - \omega_{k,s}(t)\right), \ \ \forall k \in \Psi^K \tag{3.47}$$

$$0 \leq \left(\Phi_k^{\xi+} - \Phi_k^{\xi-}\right)\left(\beta_k \sum_{t=1}^{T} \xi_{k,s,t} - \sum_{t=1}^{T} \omega_{k,s}(t)\right), \quad \forall k \in \Psi^K \tag{3.48}$$

$$\omega_{k,s}(t) = 0, \quad \forall k \in \Psi^{\text{Stor}} \tag{3.49}$$

$$\zeta_k(t)\underline{Q}_k \leq Q_{k,s}(t) \leq \zeta_k(t)\overline{Q}_k, \quad \forall k \in \Psi^K \tag{3.50}$$

$$P_{k,s}(t)\tan(\underline{\phi}_{k,t}) \leq Q_{k,s}(t) \leq P_{k,s}(t)\tan(\overline{\phi}_{k,t}), \quad \forall k \in \Psi^K \tag{3.51}$$

$$\sum_{j=t}^{t+U_k-1} \zeta_k(j) \geq U_k\left(\zeta_k(t) - \zeta_k(t-1)\right), \quad \forall k \in \Psi^K \tag{3.52}$$

$$\sum_{j=t}^{t+D_k-1} \left(1 - \zeta_k(j)\right) \geq D_k\left(\zeta_k(t-1) - \zeta_k(t)\right), \quad \forall k \in \Psi^K. \tag{3.53}$$

In (3.38), $\overline{E}_k^{\text{elec}}$ is the electrical energy storage capacity of resource k, $x_{k,s}(t)$ is the normalised level of stored energy, $P_{k,s}^{\text{d}}(t)/P_{k,s}^{\text{g}}(t)$ are the active demand/generation of resource k with associated efficiencies $\eta_k^{\text{d}}/\eta_k^{\text{g}}$. The parameter $\xi_{k,s,t}$ encodes the magnitude of available generation of the corresponding resource if positive, and the magnitude of demanded active power if negative. The variable $\omega_{k,s}(t)$ is the amount of curtailed available generation if positive, and the amount of curtailed demand if negative. The storage losses of resource k is ν_k. The general operation of resources (assuming a constant efficiency) in the VPP can be modelled using (3.38) with supplementary constraints if required. Examples of how this can be applied to specific resources is provided in Appendix B.

Constraint (3.39) sets a minimum amount of stored energy that is required for each resource at the end of the optimisation horizon, and (3.40) sets the upper and low bounds for the normalised stored energy of each resource. The active power injection/absorption limits for each resource are constrained by (3.41) and (3.42). The ramp rates of the resources are governed by (3.43) and (3.44). The net power injection of each resources is defined in (3.45).

The magnitude of allowable curtailment of each resources is governed by (3.46) - (3.48). Constraint (3.46) ensures that the curtailment is positive if the resource is a generator, and negative if it is load. Constraint (3.47) sets a limit, α_k, on what percentage of supply/demand can be curtailed in each time period, and (3.48) limits the curtailment that occurs across the whole prediction horizon to β_k for each resource. Constraint (3.49) ensures the curtailment of storage resources is set to zero, as $\xi_{k,s,t}$ will also be

zero for storage resources. $\Phi_k^{\xi+}$ and $\Phi_k^{\xi-}$ are auxiliary parameters that are associated with the sign of $\xi_{k,s,t}$ such that:

$$\text{Generator}: \sum_{t=1}^{T^{\text{HL}}} \sum_{s=1}^{S^{\text{HL}}} \xi_{k,s,t} > 0 \implies \Phi_k^{\xi+} = 1,\ \Phi_k^{\xi-} = 0$$

$$\text{Load}: \sum_{t=1}^{T^{\text{HL}}} \sum_{s=1}^{S^{\text{HL}}} \xi_{k,s,t} < 0 \implies \Phi_k^{\xi+} = 0,\ \Phi_k^{\xi-} = 1$$

$$\text{Storage}: \sum_{t=1}^{T^{\text{HL}}} \sum_{s=1}^{S^{\text{HL}}} \xi_{k,s,t} = 0 \implies \Phi_k^{\xi+} = 0,\ \Phi_k^{\xi-} = 0$$

Because the sign of ξ_k is only dependent on the type of resource that k is (generator, load, storage), the values of $\Phi_k^{\xi+}$ and $\Phi_k^{\xi-}$ are known *a priori*.

The limits on resource reactive power injection is constrained by (3.50) and the limits on resource power factor is constrained by (3.51). The minimum up/down time for each resources is enforced by (3.52) and (3.53).

3.6.4 Service Provision

As well as modelling the operation of resources at their dispatch operating points, it must also be ensured that the resources can deliver the market bids and services if called upon. This is ensured by the constraints presented in this section. All constraints in this section are enforced for $s \in [1 : S^{\text{HL}}]$, $t \in [1 : T^{\text{HL}}]$:

$$0 \leq P_{k,s}^{r}(t) \leq \overline{\rho}_k \tau^r, \quad \forall r \in \Psi^{\text{Raise}}, \forall k \in \Psi^K \tag{3.54}$$

$$0 \leq P_{k,s}^{l}(t) \leq -\underline{\rho}_k \tau^l, \quad \forall l \in \Psi^{\text{Lower}}, \forall k \in \Psi^K \tag{3.55}$$

$$\zeta_k(t) \Phi_k^{\xi+} \overline{P}_k^{\text{g}} \geq \Phi_k^{\xi+} (P_{k,s}(t) + P_{k,s}^{r}(t)), \quad \forall r \in \Psi^{\text{Raise}}, \forall k \in \Psi^K \tag{3.56}$$

$$-\zeta_k(t) \Phi_k^{\xi-} \underline{P}_k^{\text{d}} \geq \Phi_k^{\xi-} (P_{k,s}(t) + P_{k,s}^{r}(t)), \quad \forall r \in \Psi^{\text{Raise}}, \forall k \in \Psi^K \tag{3.57}$$

$$\zeta_k(t) \Phi_k^{\xi+} \underline{P}_k^{\text{g}} \leq \Phi_k^{\xi+} (P_{k,s}(t) - P_{k,s}^{l}(t)), \quad \forall l \in \Psi^{\text{Lower}}, \forall k \in \Psi^K \tag{3.58}$$

$$-\zeta_k(t) \Phi_k^{\xi-} \overline{P}_k^{\text{d}} \leq \Phi_k^{\xi-} (P_{k,s}(t) - P_{k,s}^{l}(t)), \quad \forall l \in \Psi^{\text{Lower}}, \forall k \in \Psi^K \tag{3.59}$$

$$-\zeta_k(t) \overline{P}_k^{\text{d}} \leq (P_{k,s}(t) + P_{k,s}^{r}(t)) \leq \zeta_k(t) \overline{P}_k^{\text{g}}, \quad \forall r \in \Psi^{\text{Raise}}, \forall k \in \Psi^{\text{Stor}} \tag{3.60}$$

$$-\zeta_k(t) \overline{P}_k^{\text{d}} \leq (P_{k,s}(t) - P_{k,s}^{l}(t)) \leq \zeta_k(t) \overline{P}_k^{\text{g}}, \quad \forall l \in \Psi^{\text{Lower}}, \forall k \in \Psi^{\text{Stor}} \tag{3.61}$$

$$\Phi_k^{\xi+} P_{k,s}^r(t) \leq \Phi_k^{\xi+} \eta_k^{\mathrm{g}} \omega_{k,s}(t), \quad \forall r \in \Psi^{\mathrm{Raise}}, \forall k \in \Psi^K \tag{3.62}$$

$$-\Phi_k^{\xi+} P_k^l(t) \geq \Phi_k^{\xi+} \left(-\alpha_k \xi_{k,s,t} + \omega_{k,s}(t)\right) \eta_k^{\mathrm{g}}, \quad \forall l \in \Psi^{\mathrm{Lower}}, \forall k \in \Psi^K \tag{3.63}$$

$$\Phi_k^{\xi-} P_{k,s}^r(t) \leq \frac{\Phi_k^{\xi-}}{\eta_k^{\mathrm{d}}} \left(-\alpha_k \xi_{k,s,t} + \omega_{k,s}(t)\right), \quad \forall r \in \Psi^{\mathrm{Raise}}, \forall k \in \Psi^K \tag{3.64}$$

$$-\Phi_k^{\xi-} P_{k,s}^l(t) \geq \frac{\Phi_k^{\xi-}}{\eta_k^{\mathrm{d}}} \omega_{k,s}(t), \quad \forall l \in \Psi^{\mathrm{Lower}}, \forall k \in \Psi^K \tag{3.65}$$

$$\overline{E}_k^{\mathrm{elec}} x_{k,s}(t) \geq \sum_{r \in \Psi^{\mathrm{Raise}}} \left(\frac{1}{\eta_k^{\mathrm{g}}} \left(P_{k,s}(t) + P_{k,s}^r(t) \right) + \nu_k \right) \delta^r, \quad \forall k \in \Psi^{\mathrm{Stor}} \tag{3.66}$$

$$\overline{E}_k^{\mathrm{elec}} x_{k,s}(t+1) \geq \sum_{r \in \Psi^{\mathrm{Raise}}} \left(\frac{1}{\eta_k^{\mathrm{g}}} \left(P_{k,s}(t) + P_{k,s}^r(t) \right) + \nu_k \right) \delta^r, \quad \forall k \in \Psi^{\mathrm{Stor}} \tag{3.67}$$

$$\overline{E}_k^{\mathrm{elec}} \left(1 - x_{k,s}(t)\right) \geq \sum_{l \in \Psi^{\mathrm{Lower}}} \left(\eta_k^{\mathrm{d}} \left(P_{k,s}(t) - P_{k,s}^l(t) \right) - \nu_k \right) \delta^l, \quad \forall k \in \Psi^{\mathrm{Stor}} \tag{3.68}$$

$$\overline{E}_k^{\mathrm{elec}} \left(1 - x_{k,s}(t+1)\right) \geq \sum_{l \in \Psi^{\mathrm{Lower}}} \left(\eta_k^{\mathrm{d}} \left(P_{k,s}(t) - P_{k,s}^l(t) \right) - \nu_k \right) \delta^l, \quad \forall k \in \Psi^{\mathrm{Stor}} \tag{3.69}$$

$$\sum_{k \in \Psi^K} P_{k,s}^r(t) \geq \underline{P}_t^r + \sum_{k \in \Psi^K} \Phi_k^{r,\mathrm{cntr}} P_{k,s}(t), \quad \forall r \in \Psi^{\mathrm{Raise}} \tag{3.70}$$

$$\sum_{k \in \Psi^K} P_{k,s}^l(t) \geq \underline{P}_t^l + \sum_{k \in \Psi^K} \Phi_k^{l,\mathrm{cntr}} P_{k,s}(t), \quad \forall l \in \Psi^{\mathrm{Lower}} \tag{3.71}$$

$$\underline{Q}_t^{\mathrm{exp}} \leq Q_s^{\mathrm{exp}}(t) \leq \overline{Q}_t^{\mathrm{exp}} \tag{3.72}$$

$$\sum_{k \in \Psi^K} H_k^{\mathrm{g}} \overline{S}_k \zeta_k(t) \geq \underline{I}_t. \tag{3.73}$$

Constraints (3.54) and (3.55) encode raise services $P_{k,s}^r(t)$ and lower services $P_{k,s}^l(t)$ limits associated with the corresponding ramp rate limits $\overline{\rho}_k$ and $\underline{\rho}_k$, and the required response time for the raise/lower service τ^r/τ^l. The amount of reserve service that can be provided is also limited by the maximum generation/demand in (3.56) - (3.61). As well as being limited by the overall generation/demand limit of the resources, these raise/lower services are also constrained by the amount of curtailment that has occurred for the resource to operate at the current dispatch point, as well as the maximum allowable curtailment (3.62) - (3.65). If the resource is an energy storage resource (i.e., $k \in \Psi^{\mathrm{Stor}}$), then there must also be sufficient headroom, (3.66) and (3.67), and footroom, (3.68) and (3.69), to provide the raise/lower services respectively for their duration δ^r/δ^l. Because it is unknown if and when during the time period these services may be called, constraints are applied to both the stored energy at the start and the end of each time

step.

Additionally to market-based services, the VPP may want to create contracts with other market entities, or may be contractually obliged to provide certain services. These relationships are considered in (3.70) and (3.71) where the sum of the contingency raise/lower services must be greater than the sum of externally and internally contracted raise/lower services. In (3.70) and (3.71), $\Phi_k^{r,\text{cntr}}/\Phi_k^{l,\text{cntr}}$ allows the framework to consider contractual arrangements internally within the VPP. If raise or lower services need to be provided as a function of active power injection (this could be a reserve service such as the obligatory fast frequency response (FFR) for new generators that was considered in Australia[1] [25]. Or indeed a VPP operator could use this to internally schedule reserve to compensate for generation deviation from RES). If there is a requirement then this is encoded by $\Phi_k^{r,\text{cntr}}/\Phi_k^{l,\text{cntr}}$ which indicates the percentage of power injection that needs to be covered by raise/lower service r/l.

Constraint (3.72) imposes time-varying limits on the value of reactive power being exported to the grid. This grants the option for the VPP to provide contracted levels of reactive power to the grid, as well as/instead of reactive power being procured by way of a market structure. As inertia is not an active power service, it requires its own set of constraints. These are defined in (3.73) and ensure that at each time step the total VPP inertia is greater than the contractually required inertia. Note that this only considers inertia from synchronous machines, and is not considering 'synthetic inertia'.

3.6.5 Multi-Energy Node Formulation

Thus far, the modelling and constraints have been focused on the electrical operation of the VPP. However, one of the key aspects that needs to be considered in a comprehensive framework is multi-energy operation. Only the electrical network is modelled in this framework, and so the other energy vectors are considered by nodal balance only. These

[1] It is noted that in mid 2021, the Australian Energy Market Commission (AEMC) published a draft rule that suggests FFR is implemented in a market structure [152], rather than as an obligation to new generators. However, in the case studies presented in this thesis, FFR is considered as a obligatory service in line with [25] as an example of how the framework can consider contractual service arrangements. A strength of the framework is that it has the flexibility to be able to model either of these options.

multi-energy node constraints are enforced for $s \in [1 : S^{\mathrm{HL}}]$, $t \in [1 : T^{\mathrm{HL}}]$:

$$\overline{E}_i^e \left(x_{i,s}^e(t+1) - x_{i,s}^e(t)\right) = \left(\sum_{k \in \Psi_{i,e}^K} \left(\eta_k^{\mathrm{d},e} P_{k,s}^{\mathrm{d}}(t) - \frac{P_{k,s}^{\mathrm{g}}(t)}{\eta_k^{\mathrm{g},e}}\right) + \xi_{i,s,t}^e - \omega_{i,s}^e(t) - \nu_i^e\right) \Delta t - E_{i,s}^{e,\exp}(t), \quad \forall i \in \Psi^N, \forall e \in \Psi^{\text{Non-elec}} \tag{3.74}$$

$$X_i^{e,\text{target}} \leq x_{i,s}^e(T+1), \;\; \forall i \in \Psi^N, \forall e \in \Psi^{\text{Non-elec}} \tag{3.75}$$

$$0 \leq x_{i,s}^e(t) \leq 1, \;\; \forall i \in \Psi^N, \forall e \in \Psi^{\text{Non-elec}} \tag{3.76}$$

$$\underline{E}_i^{e,\exp} \leq E_{i,s}^{e,\exp}(t) \leq \overline{E}_i^{e,\exp}, \;\; \forall i \in \Psi^N, \forall e \in \Psi^{\text{Non-elec}} \tag{3.77}$$

$$0 \leq \left(\Phi_i^{e,\xi+} - \Phi_i^{e,\xi-}\right) \omega_{i,s}^e(t), \;\; \forall i \in \Psi^N, \forall e \in \Psi^{\text{Non-elec}} \tag{3.78}$$

$$0 \leq \left(\Phi_i^{e,\xi+} - \Phi_i^{e,\xi-}\right) \left(\alpha_i^e \xi_{i,s,t}^e - \omega_{i,s}^e(t)\right), \;\; \forall i \in \Psi^N, \forall e \in \Psi^{\text{Non-elec}} \tag{3.79}$$

$$0 \leq \left(\Phi_i^{e,\xi+} - \Phi_i^{e,\xi-}\right) \left(\beta_i^e \sum_{t=1}^{T} \xi_{i,s,t}^e - \sum_{t=1}^{T} \omega_{i,s}^e(t)\right), \;\; \forall i \in \Psi^N, \forall e \in \Psi^{\text{Non-elec}} \tag{3.80}$$

$$\overline{E}_i^e x_{i,s}^e(t) \geq \sum_{r \in \Psi^{\text{Raise}}} \left\{ \sum_{k \in \Psi_i^e} \left[\left(\frac{\Phi_k^{\xi+}}{\eta_k^{\mathrm{g},e}} + \Phi_k^{\xi-} \eta_k^{\mathrm{d},e} \right) \left(P_{k,s}(t) + P_{k,s}^r(t)\right) \right] - \left(\xi_{i,s,t}^e - \omega_{i,s}^e(t) - \nu_i^e - \frac{E_{i,s}^{e,\exp}(t)}{\Delta t} \right) \right\} \delta^r, \quad \forall i \in \Psi^N, \forall e \in \Psi^{\text{Non-elec}} \tag{3.81}$$

$$\overline{E}_i^e x_{i,s}^e(t+1) \geq \sum_{r \in \Psi^{\text{Raise}}} \left\{ \sum_{k \in \Psi_i^e} \left[\left(\frac{\Phi_k^{\xi+}}{\eta_k^{\mathrm{g},e}} + \Phi_k^{\xi-} \eta_k^{\mathrm{d},e} \right) \left(P_{k,s}(t) + P_{k,s}^r(t)\right) \right] - \left(\xi_{i,s,t}^e - \omega_{i,s}^e(t) - \nu_i^e - \frac{E_{i,s}^{e,\exp}(t)}{\Delta t} \right) \right\} \delta^r, \quad \forall i \in \Psi^N, \forall e \in \Psi^{\text{Non-elec}} \tag{3.82}$$

$$\overline{E}_i^e \left(1 - x_{i,s}^e(t)\right) \geq \sum_{l \in \Psi^{\text{Lower}}} \left\{ \sum_{k \in \Psi_i^e} \left[\left(\frac{\Phi_k^{\xi+}}{\eta_k^{\text{g},e}} + \Phi_k^{\xi-} \eta_k^{\text{d},e} \right) \left(P_{k,s}(t) - P_{k,s}^l(t) \right) \right] + \left(\xi_{i,s,t}^e - \omega_{i,s}^e(t) - \nu_i^e - \frac{E_{i,s}^{e,\text{exp}}(t)}{\Delta t} \right) \right\} \delta^l,$$

$$\forall i \in \Psi^N, \forall e \in \Psi^{\text{Non-elec}} \quad (3.83)$$

$$\overline{E}_i^e \left(1 - x_{i,s}^e(t+1)\right) \geq \sum_{l \in \Psi^{\text{Lower}}} \left\{ \sum_{k \in \Psi_i^e} \left[\left(\frac{\Phi_k^{\xi+}}{\eta_k^{\text{g},e}} + \Phi_k^{\xi-} \eta_k^{\text{d},e} \right) \left(P_{k,s}(t) - P_{k,s}^l(t) \right) \right] + \left(\xi_{i,s,t}^e - \omega_{i,s}^e(t) - \nu_i^e - \frac{E_{i,s}^{e,\text{exp}}(t)}{\Delta t} \right) \right\} \delta^l,$$

$$\forall i \in \Psi^N, \forall e \in \Psi^{\text{Non-elec}}. \quad (3.84)$$

The multi-energy node model is constrained by (3.74), which encodes how the stored energy of non-electrical vector e at node i ($x_{i,s}^e(t)$) changes over time. This constraint is applied for each node and for each non-electrical energy vector in the VPP. This is to account for the demand and generation of all resources located at node i that couple electricity with energy vector e (i.e., $k \in \Psi_i^e$). It also includes nodal energy demand/supply $\xi_{i,s,t}^e$ of energy vector e at node i, the curtailment of this demand/supply $\omega_{i,s}^e(t)$, and associated storage losses ν_i^e. Additionally to nodal demand, it can also be considered that the VPP may be able to buy or sell energy vector e at node i. The amount of energy vector e that is imported/exported at node i is expressed as $E_{i,s}^{e,\text{exp}}(t)$. Examples of how this is applied in conjunction with the resources model in (3.38) are provided in Appendix B.

The final levels of stored energy for all energy vectors are constrained by (3.75). The normalised levels of stored energy across energy vectors are constrained by (3.76) and the amount of energy that can be imported/exported is constrained in (3.77). The allowable curtailment of multi-energy demand at each node is governed by (3.78)-(3.80) where $\Phi_i^{e,\xi+}$ and $\Phi_i^{e,\xi-}$ are auxiliary parameters that are associated with the sign of $\xi_{i,s,t}^e$

such that.

$$\text{Supply of energy vector } e: \sum_{t=1}^{T^{\text{HL}}} \sum_{s=1}^{S^{\text{HL}}} \xi_{i,s,t}^{e} > 0 \implies \Phi_{i}^{e,\xi+} = 1,\ \Phi_{i}^{e,\xi-} = 0$$

$$\text{Demand of energy vector } e: \sum_{t=1}^{T^{\text{HL}}} \sum_{s=1}^{S^{\text{HL}}} \xi_{i,s,t}^{e} < 0 \implies \Phi_{i}^{e,\xi+} = 0,\ \Phi_{i}^{e,\xi-} = 1$$

Because the sign of $\xi_{i,s,t}^{e}$ is only dependent on the whether the node i has supply or demand of energy vector e (which is assumed to be set across the optimisation horizon), the values of $\Phi_{k}^{e,\xi+}$ and $\Phi_{k}^{e,\xi-}$ are known *a priori*.

It must also be ensured that there is sufficient headroom/footroom in any multi-energy storage at each node for the provision of the services that the mutli-energy resources at that node are participating in. This is enforced in (3.81) - (3.84) by considering the nodal energy demand, losses, and energy imported/exported. To ensure that the VPP can deliver the services at any point in the time step, the constraint is applied to both time step t and $t+1$.

3.6.6 Initialisation of Resources

The initial status of the resources also needs to be included in the optimisation for $s \in [1 : S^{\text{HL}}]$.

$$x_{k,s}(1) = x_{k}^{\text{init}},\ \ \forall k \in \Psi^{K} \tag{3.85}$$

$$x_{i,s}^{e}(1) = x_{i}^{e,\text{init}},\ \ \forall i \in \Psi^{N}, \forall e \in \Psi^{\text{Non-elec}} \tag{3.86}$$

$$P_{k,s}^{\text{g}}(0) = P_{k}^{\text{g,init}},\ \ \forall k \in \Psi^{K} \tag{3.87}$$

$$P_{k,s}^{\text{d}}(0) = P_{k}^{\text{d,init}},\ \ \forall k \in \Psi^{K} \tag{3.88}$$

$$U_{k,t}^{\text{init}} \zeta_{k}(t) = U_{k,t}^{\text{init}},\ \ \forall t \in [0 : U_{k} - 1], \forall k \in \Psi^{K} \tag{3.89}$$

$$D_{k,t}^{\text{init}} \zeta_{k}(t) = 0,\ \ \forall t \in [0 : D_{k} - 1], \forall k \in \Psi^{K} \tag{3.90}$$

The initial state of power and energy for each resource is defined in (3.85)-(3.88). Constraints (3.89) and (3.90) are used to set the value of $\zeta_{k}(0)$ as well as to ensure that the minimum up time and down time requirements of each resource are respected between optimisations. If $U_{k,t}^{\text{init}} = 1$, this will force $\zeta_{k}(t) = 1$. Similarly, if $D_{k,t}^{\text{init}} = 1$, this will force $\zeta_{k}(t) = 0$. If $U_{k,t}^{\text{init}} = 0$ and $D_{k,t}^{\text{init}} = 0$, then $\zeta_{k}(t)$ is unconstrained by (3.89) and (3.90).

3.6.7 High-Level Optimisation Full Formulation

Now that all of the constraints have been introduced, the high-level optimisation (where $\Delta t = \Delta t^{\mathrm{HL}}$) is:

$$\text{minimise (3.21)}$$

subject to:

$$\begin{gathered}(3.22)\text{ - }(3.84),\ \forall s \in [1 : S^{\mathrm{HL}}],\ t \in [1 : T^{\mathrm{HL}}] \\ \text{and } (3.85)\text{ - }(3.90),\ \forall s \in [1 : S^{\mathrm{HL}}].\end{gathered}$$

This high-level optimisation is a MILP and a representation of the problem size in terms of VPP parameters is given by:

Binary Variables $= T^{\mathrm{HL}}|\Psi^K|$,

Continuous Variables $=$

$$S^{\mathrm{HL}}T^{\mathrm{HL}}\left(4+|\Psi^K|(6+|\Psi^{\mathrm{Raise}}|+|\Psi^{\mathrm{Lower}}|)+2|\Psi^L|+|\Psi^N|\left(3|\Psi^{\text{Non-elec}}|+2\right)\right),$$

Constraints $=$

$$S^{\mathrm{HL}}\Bigg(|\Psi^K|\left(3+\sum_{k\in\Psi^K}(U_k+D_k)\right)+|\Psi^N||\Psi^{\text{Non-elec}}|+T^{\mathrm{HL}}\Bigg(5+12|\Psi^L|+$$

$$|\Psi^N|\left(6+13|\Psi^{\text{non-elec}}|\right)+5|\Psi^{\mathrm{Stor}}|+8|\Psi^K|\left(|\Psi^{\mathrm{Raise}}|+|\Psi^{\mathrm{Lower}}|\right)+|\Psi^{\mathrm{Raise}}|+|\Psi^{\mathrm{Lower}}|\Bigg)\Bigg).$$

It is clear that the number of constraints and variables increases proportionately to the number of scenarios considered. This is why the robust restriction in Appendix A is so effective at reducing the size of the problem - it reduces the number of constraints and variables by a factor of S^{HL}.

3.7 Mid-Level Optimisation

As the high-level optimisation sets the unit commitment schedule of the resources in the VPP, the mid-level optimisation contains no integer variables. This enables formulation

of the mid-level optimisation in terms of a more accurate SOC relaxation of the power flow equations. The more accurate modeling of power flows enables the VPP operator to better adhere to the network constraints, and reliably provide network services. The aim of the mid-level optimisation is to set a 24-hour ahead operational trajectory that maximises the VPP's ability to generate revenue while minimising its cost. The main time-coupling consideration that the mid-level optimisation must consider is the level of stored energy. Therefore, across each scenario, the level of stored energy for each resource and node at each time step is constrained to be the same.

3.7.1 Power Flow Equations

The main difference in formulations between the high-level optimisation and the mid-level optimisation is the use of the SOC relaxation of the power flow equations in the mid-level optimisation (the derivation of which is shown in Section 3.2.4). The following constraints are enforced for $s \in [1 : S^{\mathrm{ML}}]$, $t \in [1 : T^{\mathrm{ML}}]$:

$$\Lambda_{ij,s}(t) + v_{i,s}(t) \geq \left\| \begin{array}{c} 2P_{ij,s}(t) \\ 2Q_{ij,s}(t) \\ \Lambda_{ij,s}(t) - v_{i,s}(t) \end{array} \right\|, \quad \forall (i,j) \in \Psi^L \tag{3.91}$$

$$\underline{V}_{i,t}^2 \leq v_{i,s}(t) \leq \overline{V}_{i,t}^2, \quad \forall i \in \Psi^N \tag{3.92}$$

$$P_{ij,s}(t) + P_{ji,s}(t) = r_{ij,t}\Lambda_{ij,s}(t), \quad \forall (i,j) \in \Psi^L \tag{3.93}$$

$$Q_{ij,s}(t) + Q_{ji,s}(t) = x_{ij,t}\Lambda_{ij,s}(t), \quad \forall (i,j) \in \Psi^L \tag{3.94}$$

$$v_{j,s}(t) = v_{i,s}(t) - 2\left(r_{ij,t}P_{ij,s}(t) + x_{ij,t}Q_{ij,s}(t)\right) + \left(r_{ij,t}^2 + x_{ij,t}^2\right)\Lambda_{ij,s}(t), \quad \forall (i,j) \in \Psi^L \tag{3.95}$$

$$\overline{S}_{ij} \geq \left(P_{ij,s}(t)\right)^2 + \left(Q_{ij,s}(t)\right)^2, \quad \forall (i,j) \in \Psi^L \tag{3.96}$$

$$\overline{S}_{k} \geq \left(P_{k,s}(t)\right)^2 + \left(Q_{k,s}(t)\right)^2, \quad \forall k \in \Psi^K \tag{3.97}$$

Constraint (3.91) is the relaxed SOC constraint that relates the square of current magnitude $\Lambda_{ij,s}(t)$ and the square of voltage magnitude $v_{i,s}(t)$ to apparent power. The nodal voltage is constrained in (3.92), and the line losses are defined in (3.93) and (3.94). Line voltage drop is constrained by (3.95). The apparent power limits of lines and resources are constrained in (3.96) and (3.97) respectively.

3.7.2 Cost Function

The cost function for the mid-level optimisation is formulated as:

$$\min \sum_{s=1}^{S^{\mathrm{ML}}} \pi_s^{\mathrm{ML}} \sum_{t=1}^{T^{\mathrm{ML}}} c_s^{\mathrm{tot,ML}}(t) \Delta t, \tag{3.98}$$

$$\begin{aligned} c_s^{\mathrm{tot,ML}}(t) = \\ \overbrace{c_s^{\mathrm{op}}(t)}^{1} + \overbrace{\sum_{k \in \Psi^K} \left(\lambda_k^{\mathrm{curt}} \omega_{k,s}(t)\right) + \sum_{e \in \Psi^{\text{Non-elec}}} \sum_{i \in \Psi^N} \left(\lambda_i^{e,\mathrm{curt}} \omega_{i,s}^e(t)\right)}^{2} - \overbrace{\lambda_{s,t}^{\mathrm{P}} P_s^{\mathrm{exp}}(t)}^{3} - \overbrace{\lambda_{s,t}^{\mathrm{Q}} Q_s^{\mathrm{exp}}(t)}^{4} \\ - \overbrace{\sum_{e \in \Psi^{\text{Non-elec}}} \left(\lambda_{s,t}^e \sum_{i \in \Psi^N} \frac{E_{i,s}^{e,\mathrm{exp}}(t)}{\Delta t}\right)}^{5} - \overbrace{\sum_{r \in \Psi^{\mathrm{Raise}}} \left(\lambda_{s,t}^r \left(\sum_{k \in \Psi^K} P_{k,s}^r(t) - \underline{P}_t^r\right)\right)}^{6} \\ - \overbrace{\sum_{l \in \Psi^{\mathrm{Lower}}} \left(\lambda_{s,t}^l \left(\sum_{k \in \Psi^K} P_{k,s}^l(t) - \underline{P}_t^l\right)\right)}^{7} + \overbrace{\sum_{(i,j) \in \Psi^L} \lambda_{ij}^{\mathrm{loss}} \Lambda_{ij,s}(t)}^{8}. \end{aligned} \tag{3.99}$$

where $c_s^{\mathrm{tot,ML}}(t)$ is the total VPP cost for each scenario $s \in [1 : S^{\mathrm{ML}}]$ at each time step $t \in [1 : T^{\mathrm{ML}}]$.

The mid-level optimisation total VPP cost described in (3.99) is similar to the high-level equivalent described in (3.22). The difference is that the eighth term in (3.22) is dropped in (3.99) (as committed status of the resources is now fixed) and in its place is a term to penalise current flow (and by extension losses) in the network. This term helps to tighten the SOC relaxation by penalising excess current flowing in the network. Another difference is the formulation of $c_s^{\mathrm{op}}(t)$. The total operating cost of the resources within the VPP for each scenario $s \in [1 : S^{\mathrm{ML}}]$ at each time step $t \in [1 : T^{\mathrm{ML}}]$ is defined as:

$$\begin{aligned} c_s^{\mathrm{op}}(t) \geq \sum_{k \in \Psi^K} \Bigg(& \kappa_k^{\mathrm{g}} \left(P_{k,s}^{\mathrm{g}}(t)\right)^2 + \kappa_k^{\mathrm{d}} \left(P_{k,s}^{\mathrm{d}}(t)\right)^2 + \chi_k^{\mathrm{g}} P_{k,s}^{\mathrm{g}}(t) + \chi_k^{\mathrm{d}} P_{k,s}^{\mathrm{d}}(t) + \gamma_k \zeta_k(t) \\ & + \frac{\lambda_k^{\mathrm{on}}}{\Delta t} \max\left(0, \zeta_k(t) - \zeta_k(t-1)\right) + \frac{\lambda_k^{\mathrm{off}}}{\Delta t} \max\left(0, \zeta_k(t-1) - \zeta_k(t)\right) \Bigg), \end{aligned} \tag{3.100}$$

where κ_k^{g} and κ_k^{d} are the quadratic cost coefficients for generation and demand operation of resource k. This convex quadratic can represent some DER operating costs (such as OCGTs) more accurately than the linear version used in the high-level optimisation. It

should be noted that the turn on and turn off costs in (3.100) are constant as the unit commitment schedule has already been set. This is enforced for $t \in \left[1 : T^{\mathrm{ML}}\right]$ by

$$\zeta_k(t) = \tilde{\zeta}_{k,t}, \ \ \forall k \in \Psi^K. \tag{3.101}$$

3.7.3 Service Provision

When determining the active power based services that the VPP can provide, and modelling the network in more detail (as in the mid-level optimisations and low-level optimisations), it is important to ensure that provision of these services is possible within network constraints as well as resource technical constraints. The following constraints are enforced for $s \in [1 : S^{\mathrm{ML}}]$, $t \in [1 : T^{\mathrm{ML}}]$:

$$\overline{S}_k \geq \left(P_{k,s}(t) + \max_{r \in \Psi^{\mathrm{Raise}}} P^r_{k,s}(t)\right)^2 + \left(Q_{k,s}(t)\right)^2, \ \ \forall k \in \Psi^K \tag{3.102}$$

$$\overline{S}_k \geq \left(P_{k,s}(t) - \max_{l \in \Psi^{\mathrm{Lower}}} P^l_{k,s}(t)\right)^2 + \left(Q_{k,s}(t)\right)^2, \ \ \forall k \in \Psi^K \tag{3.103}$$

$$\sum_{j \in \mathcal{N}_i} P^{\mathrm{Raise}}_{ij,s}(t) = \sum_{k \in \Psi^K_i} \left(P_{k,s}(t) + \max_{r \in \Psi^{\mathrm{Raise}}} P^r_{k,s}(t)\right), \ \ \forall i \in \Psi^N \tag{3.104}$$

$$\sum_{j \in \mathcal{N}_i} P^{\mathrm{Lower}}_{ij,s}(t) = \sum_{k \in \Psi^K_i} \left(P_{k,s}(t) - \max_{l \in \Psi^{\mathrm{Lower}}} P^l_{k,s}(t)\right), \ \ \forall i \in \Psi^N \tag{3.105}$$

$$\overline{S}_{ij} \geq \left(P^{\mathrm{Raise}}_{ij,s}(t)\right)^2 + \left(Q_{ij,s}(t)\right)^2, \ \ \forall (i,j) \in \Psi^L \tag{3.106}$$

$$\overline{S}_{ij} \geq \left(P^{\mathrm{Lower}}_{ij,s}(t)\right)^2 + \left(Q_{ij,s}(t)\right)^2, \ \ \forall (i,j) \in \Psi^L. \tag{3.107}$$

Constraints (3.102) and (3.103) ensure that service provision does not violate the apparent power limit of the resources. Constraints (3.104) and (3.105) define the maximum power flows in each line when raise or lower services are called. Constraints (3.106) and (3.107) then ensure that these power flows do not exceed the apparent power limit of the lines. In this formulation, the power flow modelling for service provision is not extended to the modelling of network voltages when services are called. To do so would require tripling the number of SOC constraints used to model power flows. This in turn would increase the complexity of the optimisation. In most situations any voltage violations that occur during service provision (if the services are called) would be of short duration. That being said, if a specific application required the explicit consideration of network

voltages during provision of services, this can easily be implemented in the proposed framework by introduction of variables $v_{i,s}^{\text{Raise}}(t)$, $v_{i,s}^{\text{Lower}}(t)$, $\Lambda_{ij,s}^{\text{Raise}}(t)$ and $\Lambda_{ij,s}^{\text{Lower}}(t)$ and their associated versions of (3.91) - (3.95) as constraints.

3.7.4 Cross-Scenario Constraints

The resources operational results from the first 30-minute time step of the mid-level optimisation will be used by the low-level optimisation as an operational reference. Therefore, it should be the same across every scenario ((3.108)-(3.113)). Additionally, the stored energy level for each resource and node at each time step should be the same across all scenarios (3.114) and (3.115). This ensures that the VPP is well placed to be able to adjust its operation to account for future uncertainty.

$$P_{k,s_1}^{\text{d}}(1) = P_{k,s_2}^{\text{d}}(1), \;\; \forall k \in \Psi^K, \forall s_1, s_2 \in \left[1 : S^{\text{ML}}\right] \tag{3.108}$$

$$P_{k,s_1}^{\text{g}}(1) = P_{k,s_2}^{\text{g}}(1), \;\; \forall k \in \Psi^K, \forall s_1, s_2 \in \left[1 : S^{\text{ML}}\right] \tag{3.109}$$

$$P_{s_1}^{\text{exp}}(1) = P_{s_2}^{\text{exp}}(1), \;\; \forall s_1, s_2 \in \left[1 : S^{\text{ML}}\right] \tag{3.110}$$

$$Q_{s_1}^{\text{exp}}(1) = Q_{s_2}^{\text{exp}}(1), \;\; \forall s_1, s_2 \in \left[1 : S^{\text{ML}}\right] \tag{3.111}$$

$$P_{k,s_1}^{r}(1) = P_{k,s_2}^{r}(1), \;\; \forall k \in \Psi^K, \forall r \in \Psi^{\text{Raise}}, \forall s_1, s_2 \in \left[1 : S^{\text{ML}}\right] \tag{3.112}$$

$$P_{k,s_1}^{l}(1) = P_{k,s_2}^{l}(1), \;\; \forall k \in \Psi^K, \forall l \in \Psi^{\text{Lower}}, \forall s_1, s_2 \in \left[1 : S^{\text{ML}}\right] \tag{3.113}$$

$$x_{k,s_1}(t) = x_{k,s_2}(t), \;\; \forall k \in \Psi^K, t \in \left[1 : T^{\text{ML}}\right], \forall s_1, s_2 \in \left[1 : S^{\text{ML}}\right] \tag{3.114}$$

$$x_{i,s_1}^{e}(t) = x_{i,s_2}^{e}(t), \;\; \forall i \in \Psi^N, \forall e \in \Psi^E, t \in \left[1 : T^{\text{ML}}\right], \forall s_1, s_2 \in \left[1 : S^{\text{ML}}\right] \tag{3.115}$$

3.7.5 Mid-Level Optimisation Full Formulation

Now that all of the constraints for the mid-level optimisation (where $\Delta t = \Delta t^{\text{ML}}$) have been introduced it can be defined as:

minimise (3.98)

subject to:

(3.36)-(3.51), (3.54)-(3.72), (3.74)-(3.84), (3.99)-(3.107), $\forall t \in [1 : T^{\mathrm{ML}}]$, $s \in [1 : S^{\mathrm{ML}}]$, (3.85)-(3.88), $\forall s \in [1 : S^{\mathrm{ML}}]$, and (3.108)-(3.115).

This mid-level optimisation is a SOC optimisation and a representation of the problem size in terms of VPP parameters is given by:

$$\text{Continuous Variables} = S^{\mathrm{ML}} T^{\mathrm{ML}} \left(4 + 8|\Psi^K| + 5|\Psi^L| + |\Psi^N| \left(3|\Psi^{\text{Non-elec}}| + 1\right)\right),$$

$$\text{Constraints} = S^{\mathrm{ML}} T^{\mathrm{ML}} \Bigg(|\Psi^N| \left(6 + 13|\Psi^{\text{Non-elec}}|\right) + 5|\Psi^{\mathrm{Stor}}| + |\Psi^K| \left(25 + 8|\Psi^{\mathrm{Raise}}| + 8|\Psi^{\mathrm{Lower}}|\right) + |\Psi^{\mathrm{Raise}}| + |\Psi^{\mathrm{Lower}}| + 4 + 6|\Psi^L| \Bigg) + |\Psi^K| T^{\mathrm{ML}} + (S^{\mathrm{ML}} - 1) \Big(|\Psi^K|(2 + |\Psi^{\mathrm{Raise}}| + |\Psi^{\mathrm{Lower}}| + T^{\mathrm{ML}}) + 2 + |\Psi^N||\Psi^{\text{Non-elec}}| T^{\mathrm{ML}} \Big).$$

3.8 Low-Level Optimisation

The aim of the low-level optimisation is to adjust the close to real-time operation of the VPP in order to ensure service provision and satisfaction of contractual arrangements when faced with short term uncertainty. The low-level optimisation uses the preliminary dispatch from the mid-level optimisation (which has a full 24-hour horizon) as a reference for its operation. However, as the low-level optimisation horizon recedes, it has access to more accurate short-term forecasts than the mid-level optimisation. Therefore, the VPP can differ from the operation and market participation planned by the mid-level optimisation if there is sufficient financial incentive to do so, or if required to fulfill a contractual obligation. The low-level optimisation has a 5-minute time step and a 30-minute prediction horizon, so it is reliant on the reference dispatch from the mid-level optimisation to gauge how close it is operating to the longer term optimal dispatch (determined by the mid-level optimisation).

3.8.1 Cost Function

$$\min \sum_{s=1}^{S^{\mathrm{LL}}} \pi_s^{\mathrm{LL}} \sum_{t=1}^{T^{\mathrm{LL}}} \left(c_s^{\mathrm{tot,ML}}(t) + c_s^{\mathrm{pen}}(t)\right) \Delta t \tag{3.116}$$

The low-level optimisation objective function in (3.116) differs from the mid-level objective function with the inclusion of a penalty variable defined as

$$c_s^{\text{pen}}(t) \geq \sum_{k \in \Psi^K} \Bigg(\lambda_k^{\text{d-pen}} \left(P_{k,s}^{\text{d}}(t) - P_{k,t}^{\text{d-ref}} \right)^2 + \lambda_k^{\text{g-pen}} \left(P_{k,s}^{\text{g}}(t) - P_{k,t}^{\text{g-ref}} \right)^2 + \lambda_k^{\text{x-pen}} \left(x_{k,s}(t) - X_{k,t}^{\text{ref}} \right)^2 \Bigg) + \sum_{e \in \Psi^{\text{Non-elec}}} \sum_{i \in \Psi^N} \lambda_i^{\text{e-pen}} \left(x_{i,s}^e(t) - X_{i,t}^{\text{e-ref}} \right)^2. \quad (3.117)$$

This penalty function penalises the low-level optimisation for deviating from the reference resource demand level $P_{k,t}^{\text{d-ref}}$, reference resource generation level $P_{k,t}^{\text{g-ref}}$, reference resource electrical storage level $X_{k,t}^{\text{ref}}$, and reference nodal non-electrical storage level $X_{i,t}^{\text{e-ref}}$. These references are defined by the preliminary dispatch from the mid-level optimisation. The magnitude of this penalty for deviation from these reference points is set by $\lambda_k^{\text{d-pen}}/\lambda_k^{\text{g-pen}}/\lambda_k^{\text{x-pen}}/\lambda_i^{\text{e-pen}}$ respectively. The framework operator can choose the penalty values depending on how responsive to short-term uncertainty they wish to be.

3.8.2 Cross-Scenario Constraints

The low-level optimisation is concerned with feasible operation of the VPP, and the ability to fulfill the bids provided to the market. For this reason, the external interactions with markets must be the same across scenarios. This restriction is extended to all time steps considered by the low-level optimisation to help ensure that the planned operation of the VPP is feasible in all scenarios.

$$P_{s_1}^{\text{exp}}(t) = P_{s_2}^{\text{exp}}(t), \;\; t \in \left[1 : T^{\text{LL}}\right], \forall s_1, s_2 \in \left[1 : S^{\text{LL}}\right] \quad (3.118)$$

$$Q_{s_1}^{\text{exp}}(t) = Q_{s_2}^{\text{exp}}(t), \;\; t \in \left[1 : T^{\text{LL}}\right], \forall s_1, s_2 \in \left[1 : S^{\text{LL}}\right] \quad (3.119)$$

$$\sum_{k \in \Psi^K} P_{k,s_1}^r(t) = \sum_{k \in \Psi^K} P_{k,s_2}^r(t), \;\; t \in \left[1 : T^{\text{LL}}\right], \forall s_1, s_2 \in \left[1 : S^{\text{LL}}\right], \forall r \in \Psi^{\text{Raise}} \quad (3.120)$$

$$\sum_{k \in \Psi^K} P_{k,s_1}^l(t) = \sum_{k \in \Psi^K} P_{k,s_2}^l(t), \;\; t \in \left[1 : T^{\text{LL}}\right], \forall s_1, s_2 \in \left[1 : S^{\text{LL}}\right], \forall l \in \Psi^{\text{Lower}} \quad (3.121)$$

$$E_{i,s_1}^{e,\text{exp}}(t) = E_{i,s_2}^{e,\text{exp}}(t), \;\; \forall i \in \Psi^N, \forall e \in \Psi^E, t \in \left[1 : T^{\text{LL}}\right], \forall s_1, s_2 \in \left[1 : S^{\text{LL}}\right] \quad (3.122)$$

3.8.3 Full Formulation

Now that all of the constraints for the low-level optimisation (where $\Delta t = \Delta t^{\mathrm{LL}}$) have been introduced it can be defined as:

$$\text{minimise (3.116)}$$

subject to:

$$\begin{gathered}\text{(3.36)-(3.51), (3.54)-(3.72), (3.74)-(3.84), (3.99)-(3.107), (3.117) } \forall t \in [1 : T^{\mathrm{LL}}], \\ s \in [1 : S^{\mathrm{LL}}], \\ \text{(3.85) - (3.88) } \forall s \in [1 : S^{\mathrm{LL}}], \text{ and (3.118)-(3.122).}\end{gathered}$$

This low-level optimisation is a SOC optimisation and a representation of the problem size in terms of VPP parameters is given by:

$$\text{Continuous Variables} = S^{\mathrm{LL}} T^{\mathrm{LL}} \left(5 + 8|\Psi^K| + 5|\Psi^L| + |\Psi^N| \left(3|\Psi^{\text{Non-elec}}| + 1\right)\right),$$

$$\begin{aligned}\text{Constraints} = S^{\mathrm{LL}} T^{\mathrm{LL}} \Bigg(& |\Psi^N| \left(6 + 13|\Psi^{\text{Non-elec}}|\right) + 5|\Psi^{\text{Stor}}| + \\ & |\Psi^K| \left(25 + 8|\Psi^{\text{Raise}}| + 8|\Psi^{\text{Lower}}|\right) + |\Psi^{\text{Raise}}| + |\Psi^{\text{Lower}}| + 5 + 6|\Psi^L| \Bigg) + \\ & T^{\mathrm{LL}}(S^{\mathrm{LL}} - 1) \left(|\Psi^{\text{Raise}}| + |\Psi^{\text{Lower}}| + |\Psi^N||\Psi^{\text{Non-elec}}|\right) \Bigg) + |\Psi^K| T^{\mathrm{LL}}.\end{aligned}$$

3.9 Key Remarks

This chapter presents the formulation and operation of the comprehensive VPP operational framework proposed in this work. This framework consists of three linked optimisation problems to schedule and dispatch the resources in a multi-energy VPP. The high-level optimisation is a MILP that schedules the resources in 30-minute intervals over a 24-hour period, utilising a scenario-based approach to mitigate uncertainty. A single resource schedule is defined across all scenarios and provided to the mid-level optimisation. The mid-level optimisation is a convex optimisation (utilising the SOC

relaxation of the power flow equations) that provides a preliminary dispatch for resources in 30-minute intervals over a 24-hour period. The mid-level optimisation utilises receding horizon control to help mitigate uncertainty, coupled with limited inclusion of scenarios to increase the robustness of the solution. The energy storage trajectory in the VPP is the same across all mid-level scenarios. The results of the mid-level optimisation can then be used in a heuristic control strategy to adjust OLTC positions. The preliminary dispatch for the first hour is provided to the low-level optimisation. The low-level optimisation is a convex optimisation (utilising the SOC relaxation of the power flow equations) that dispatches VPP resources in 5-minute intervals over a 30-minute period. The low-level optimisation utilises receding horizon control to help mitigate uncertainty, coupled with limited inclusion of scenarios to increase the robustness of the solution. The low-level optimisation adjusts VPP operation from the preliminary dispatch provided by the mid-level optimisation in response to short-term uncertainty to ensure provision of services, and react to changes in market prices.

It is worth noting that the framework utilises various approximations and relaxations to model resources and network operations which may impact the optimality and/or feasibility of the solution when applied to the real-world network. These include the linear approximation of the power flow equations used in the high-level optimisation, the SOC relaxation used in the mid-level and low-level optimisations, and the heuristic OLTC operation. While the linear approximation of the power flow equations does come at the cost of accuracy, it is shown in [131] that this linear approximation vastly outperforms other common linear approximations. Additionally, this slight reduction in accuracy provides a significant reduction in computational complexity compared to the AC power flow equations. Under certain conditions the SOC relaxation can be exact, and when not exact the difference are often minor [142]. The heuristic approach to OLTC operation proposed in this framework ensure feasible solutions for OLTC positions. This is not the case with the continuous relaxation of the OLTC operation, which is an often-used approach. The continuous relaxation allows the OLTC tap to be in a position in-between the real-world step position. This can often lead to infeasible OLTC positions. There is then no guarantee that, when the tap is moved to the closest feasible position, the network constraints are respected. The benefit of the heuristic approach proposed is that the OLTC tap will always be located in a feasible position. This comes at the potential cost of sub-optimal positioning of OLTC taps. However, the receding horizon

approach used in their positioning should help reduce that sub-optimality.

This operational framework is designed to be applicable to, and tractable in, the most onerous market structures. This allows the framework to be easily adapted to other market structures, for example through the adjustment of:

- how the different optimisations interact;
- when in its operation the VPP provides bids to the market;
- addition or removal of markets, services, and energy vectors;
- time step length and prediction horizon adjustment.

It is also designed to easily model a variety of VPP configurations. Alterations to the objective function of the optimisation may also allow the framework to be used by different network entities. These adjustments and adaptations are discussed in Chapter 4.

In Chapter 4, it is shown how the framework can be effectively applied to a case study to demonstrate the ability of a VPP to participate in multiple markets. The efficacy of the framework's approach to mitigating the effects of uncertainty is also verified, and the importance of short-dispatch intervals in close-to-real-time market is highlighted. Also in Chapter 4, it is demonstrated how the framework can be easily adapted for use by different network entities, and to include different operating objectives and constraints.

In Chapter 5, electricity-hydrogen VPP case studies are provided to display how the framework can capture the additional flexibility available to multi-energy VPPs. It is also shown how this flexibility can directly translate into participation in markets and provision of services, including local network support. The effectiveness of the SOC relaxation in providing local network support will also be determined. The ability of hydrogen-based resources to simultaneously participate in markets will be further examined, and the impact on operational strategies will be illustrated.

In Chapter 6, the versatility of the proposed framework is further shown by its utilisation for a techno-economic assessment for VPP business cases. Different possible electricity-hydrogen VPPs are proposed, and their long-term economic viability is examined. The impact on revenue of considering multiple markets and services, as well as modelling of

network constraints will be examined in detail. These factors will also be examined as they relate to changes in hydrogen production.

Chapter 4

Provision of Grid Services and Market Participation from a VPP

4.1 Introduction

In this chapter, two studies are conducted to show the framework's ability to unlock VPP capabilities to provide services and participate in multiple markets. This chapter will also highlight the flexibility of the framework, and its ability to be easily tailored, for example to represent different network entities.

The first study co-optimizes a VPP's participation in wholesale energy, six frequency control ancillary service (FCAS) markets, and a reactive power market. Additionally, the VPP provides contractual fast frequency response (FFR), inertia, and local network services. The aim of this study is to highlight how effectively a VPP utilising the proposed operational framework can provide multiple contractual services and participate in multiple markets simultaneously, whilst considering uncertainty. To this end, this study will focus on the effect on VPP operation and revenue of introducing additional contractual services into the VPP portfolio. This case study also looks at the effectiveness of the framework's approach to mitigating uncertainty by comparing the proposed framework with one with perfect knowledge of the future. This would quantify the loss of revenue associated with future uncertainty. Comparison will also be drawn to the likely VPP revenue if a framework that could not operate in the short bidding windows

of the Australian market was utilised, as well as a framework that was not able to consider multiple markets. This highlights the necessity of consideration of short bidding windows. This study is based on the paper written by the author: *Co-optimizing Virtual Power Plant Services Under Uncertainty: A Robust Scheduling and Receding Horizon Dispatch Approach* [153].

The second study in this chapter considers a distribution system operator (DSO) that utilises the proposed framework to determine operating limits for the DER in the network that are controlled by VPPs. These operating limits ensure that DER operation does not violate network constraints. The VPPs in the network can then use the framework to optimise the operation of their DER within those limits. The aim of this study is to illustrate how the proposed operating framework can be utilised by different network entities (in this case a DSO and VPPs), and how these entities can interact. It also shows how the operating framework can be easily adapted to be suitable for modelling these new entities and interactions, including adapting objective functions and constraints. This study will also consider how different fairness paradigms implemented by the DSO impact VPP operation and revenue. Different network configurations are also studied to ascertain their impact on DER operating envelopes.

4.2 Study on VPP Participation in Multiple Markets and Services

In this study (based on the paper written by the author: *Co-optimizing Virtual Power Plant Services Under Uncertainty: A Robust Scheduling and Receding Horizon Dispatch Approach* [153]), the proposed framework is applied to a remote area of the South Australia (SA) network. This area has large potential for RES generation but is weakly connected to the grid, which may impede the export of electricity and cause voltage issues within the local network. Therefore, there is a benefit to providing local network support as well as storing excess energy via a battery energy storage system (BESS). This part of the network has a single connection point to the grid via a long transmission line. The VPP is comprised of the network and resources downstream of this grid connection point shown in Figure 4.1.

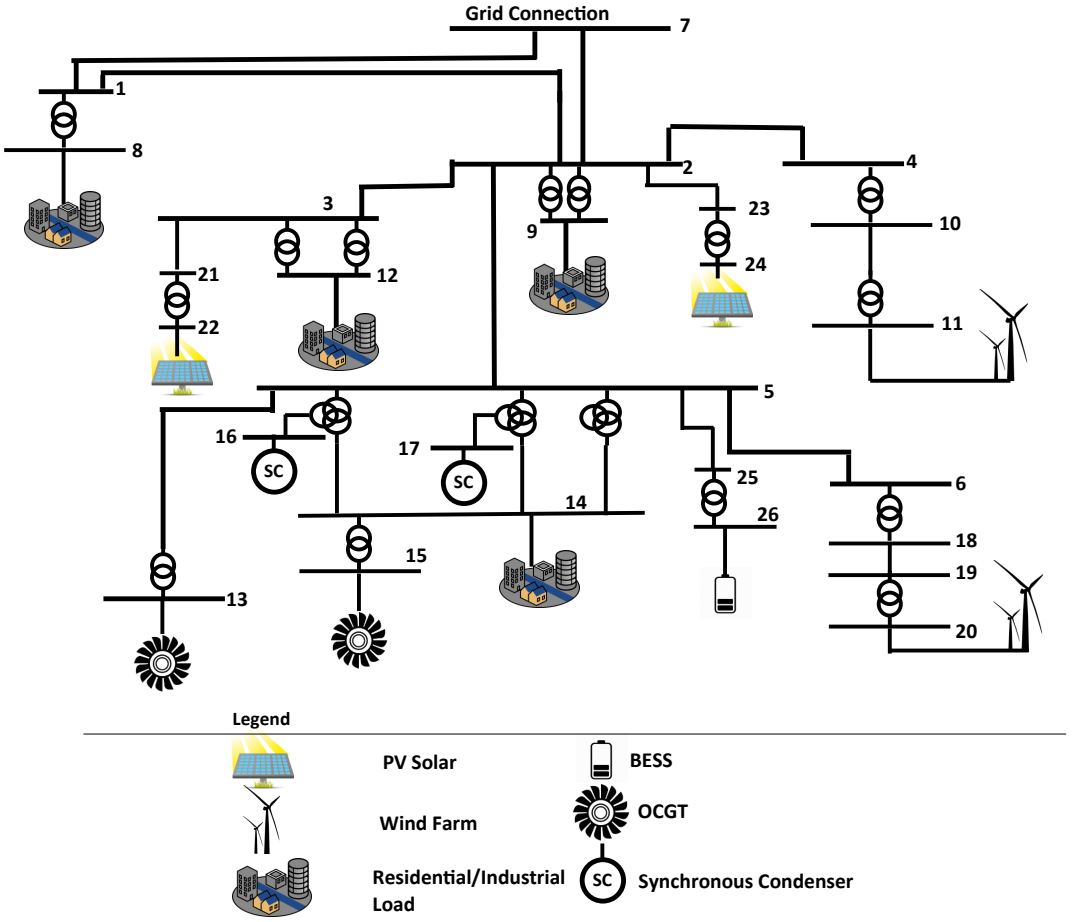

FIGURE 4.1: Single line diagram for VPP in study of VPP participation in multiple markets and services

The markets that are considered include a real-time wholesale energy and six contingency FCAS markets with different response times, namely, fast (6 second), slow (60 second), and delayed (5 minutes), and for raise/lower frequency [19]. Additionally, an upstream reactive power market is assumed to assist with reactive power circulating in transmission lines overnight. These markets are all cleared at 5-minute intervals, and participants are not required to provide bids before this time. Further, the VPP also provides FFR, inertia, and local network support which are assumed to be contracted on a specific basis in the absence of relevant markets.

A single line diagram of the network that is used as the VPP in the case study can be seen in Figure 4.1. This network contains the 132 kV, 66 kV, 33 kV, and 22 kV lines and nodes in the area (the per unit formulation allows the framework to easily consider the VPP operation across multiple voltage levels). The network downstream of load

Resource	**Size**	**Location**
Wind Farm 1	70 MW	Node 11
Wind Farm 2	66 MW	Node 20
Solar PV 1	30 MW	Node 22
Solar PV 2	30 MW	Node 24
OCGT 1	50 MW	Node 13
OCGT 2	23 MW	Node 15
Load 1	33 MW	Node 8
Load 2	23 MW	Node 9
Load 3	25 MW	Node 12
Load 4	66 MW	Node 14
Synchronous Condenser 1	20 MVar	Node 16
Synchronous Condenser 2	20 MVar	Node 17
BESS	30 MW / 100 MWh	Node 26

TABLE 4.1: VPP resources in study of VPP participation in multiple markets and services

substations at nodes 8, 9, 12, 14 is not modelled and is assumed to be operated by another entity. The VPP is only responsible for providing the required power to the load node for consumption downstream, and for maintaining the nodal voltage within acceptable limits. The resources within the VPP are detailed in Table 4.1. The curtailment of loads is considered to be fully controlled by the VPP operator at a cost of $500/MWh. The price of reactive power is set at -$1/MVarh between 22:00 and 05:00 and $0/MVarh otherwise. For the cases where there is a minimum inertia requirement it is set to 330 MWs. Inertia is available from Wind Farm 1 (which is assumed to be a type 2 wind farm, OCGTs 1&2, and Synchronous Condensers 1&2). As a part of the local network support provided by the VPP, the nodal voltages are maintained between 95%-105% of their nominal value and apparent power flows are maintained below line capacities. The BESS is assumed to start the day with 50 MWh stored energy and has an end-of-horizon target of the same. The FFR contract requires the BESS to be able to provide upwards reserve of a magnitude at least 50% of the current PV generation in the VPP.

4.2.1 Case Study Days

In this study three days are considered: 01 May 2016 (when energy prices were negative for a large portion of the day), 28 Aug 2016 (when there was a consistently high amount of available RES), and 31 Jan 2020 (when the SA network was islanded from the rest of the grid, causing a large fluctuation in energy and FCAS pricing). Historical prices

Case	Local Network Support	FFR	Inertia	Uncertainty
Case 1	✓	✓	✓	✓
Case 2		✓	✓	✓
Case 3	✓		✓	✓
Case 4	✓	✓		✓
Case 5	✓	✓	✓	

TABLE 4.2: Case descriptions for study of VPP participation in multiple markets and services

for the wholesale energy and FCAS markets, as well as wind farm generation data are taken from AEMO [154]. Substation load is based on data from SA Power Networks [155], the solar irradiances are from the Australian Bureau of Meteorology [156]. The studies to be conducted for each day are detailed in Table 4.2.

The prices for the wholesale energy and six FCAS markets for each of the three study days are shown in Figure 4.2. On 01 May 2016 the early morning has negative energy prices as well as elevated lower FCAS prices. The energy price increases throughout the day, and a spike in raise FCAS prices is seen in the early evening. On 28 August 2016 the energy price remains relatively low until the evening peak. The FCAS markets keep relatively consistent throughout the day, although the delayed lower FCAS does have an early morning price peak. By observing the logarithmic scale for 31 January 2020 it can be seen that the separation event had a significant impact on market prices. It can be seen that prices are within a normal range before the separation event, at approximately 13:25 hours. After this point, the wholesale energy market, and all of the FCAS markets see huge fluctuation in prices. For the wholesale energy market this includes both positive and negative prices of high magnitude. Moreover, this fluctuation in prices is not something that could have been foreseen in the scenarios generated to consider uncertainty before the separation event occurs. Therefore, it will be shown that the receding horizon control is key to the VPP being able to adjust its operation in response to new and evolving information.

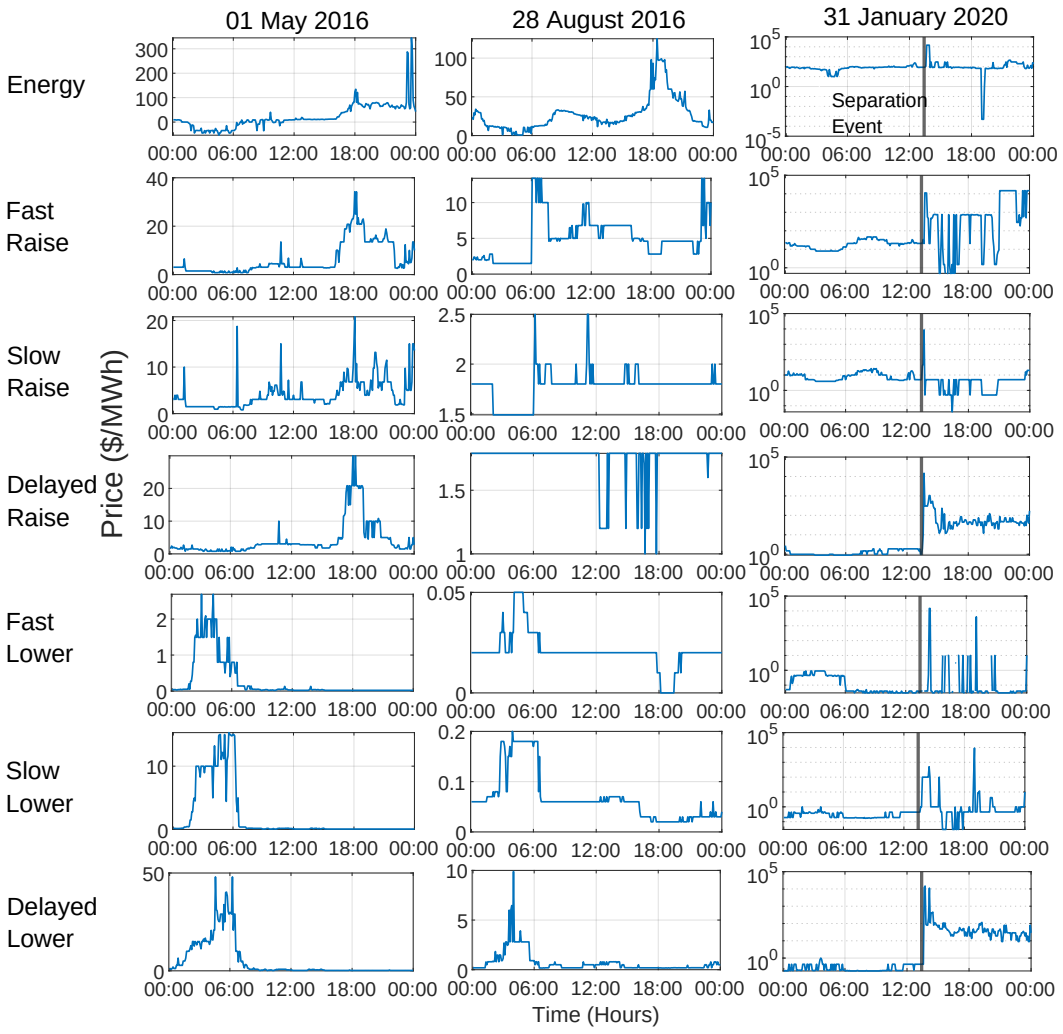

FIGURE 4.2: The wholesale energy and FCAS market prices for the three study days - (left) 01 May 2016, (center) 28 August 2016, (right) 31 January 2020

4.2.2 Uncertainty

Wind speed is modelled using Weibull distribution, described by

$$f(x|\lambda,k) = \frac{k}{\lambda}\left(\frac{x}{\lambda}\right)^{k-1} e^{(-x/\lambda)^k}, x \in [0,\infty), k,\lambda \in (0,\infty) \tag{4.1}$$

where k is the shape parameter and λ is the scale parameter, and solar irradiance is modelled using Beta distribution, described by

$$f(x|\alpha,\beta) = \frac{x^{\alpha-1}(1-x)^{\beta-1}}{\frac{\Gamma(\alpha)\Gamma(\beta)}{\Gamma(\alpha+\beta)}}, x \in [0,1], \alpha,\beta > 0, \tag{4.2}$$

where α and β are shape parameters, and Γ is the Gamma function defined as

$$\Gamma(x) = \int_0^\infty e^{-t} t^{x-1} dt. \tag{4.3}$$

A shape parameter value of $k = 3$ [157], and real-world values of mean and maximum wind speed were used to determine the scale parameter λ for the Weibull distribution. Shape parameter values of $\alpha = 4$, $\beta = 2$ [158], and real-world solar irradiance and clear sky irradiance were used for the Beta distribution. Uncertainty in load is modelled using a Gaussian distribution with a standard deviation calculated from historical load data. The market price scenarios are taken as the pre-dispatch prices provided by the market operator with a Gaussian distributed error [159]. The probability of a single realization of an uncertain variable is taken as the probability based on an interval of one percentile width centered at the chosen value. Assuming these uncertainties are independent events, multiplying the probability of each realization of uncertainty in each scenario provides the scenario probability. The variances of these distributions are reduced in a linear fashion from the last time-step to the first, to represent higher certainty closer to the present time. The high-level optimization considers 10,000 scenarios to capture the uncertainty in the system. The corresponding computationally tractable restriction described in Appendix A is then used to generate a resource schedule. Uncertainty at the mid-level and low-level is mitigated through the receding horizon approach. Each time the mid-level and low-level recede their horizons a new prediction for the market prices, load and renewable availability is generated based on the newest information. Additionally, a scenario with higher RES availability and lower load, and one with lower RES availability and higher load are also considered. This helps ensure the mid-level and low-level problems do not select highly sensitive solutions or operate too close to infeasible regions.

4.2.3 Computational Aspects

The VPP framework was implemented in MATLAB, using YALMIP [160] as a parser, and Gurobi [161] as a solver, utilising the University of Melbourne's Spartan High Performance Computing system [162]. The restricted formulation of the high-level optimization (for one problem with 24-hour horizon and 30-minute time-step) has 24,398

variables, 71,483 constraints and is solved in under 1 second. Running the original high-level problem with 1,000 scenarios takes approximately 15 hours to solve, which implies 10,000 scenarios would be intractable, justifying the need for the restricted problem. However, running the original high-level problem with 100 scenarios is solved in under 10 minutes. This shows that for this case study the high-level optimisation could be used in conjunction with scenario reduction techniques to arrive at a tractable problem without requiring the use of the robust restriction. The mid-level optimization (for one problem with 24-hour horizon and 30-minute time-step) contains 191,730 variables and 288,242 constraints. The mid-level optimization solution time is approximately 115 seconds. The low-level problem (for one problem with a 30-minute horizon and 5-minute time-step) contains 24,798 variables and 36,630 constraints and is solved in under 3 seconds. It is seen here that without reducing the size of the problem by splitting the low-level and mid-level optimizations, the problem would not be tractable for a 5-minute receding horizon.

4.2.4 Results

4.2.4.1 VPP Multi-Market Participation

One of the key aspects of the VPP is its ability to generate revenues via co-optimization in multiple markets simultaneously. For Case 1 - 01 May 2016, the VPP participation in the wholesale energy and six FCAS markets is shown in Figure 4.3. For the majority of the morning the wholesale energy prices are negative. However, the VPP does not completely curtail its RES generation. This allows the VPP to also participate in the lower FCAS markets, which in the early morning have elevated prices. Between 06:00 - 12:00 hours the energy price fluctuates between positive and negative, leading to the peaks and troughs in VPP wholesale energy participation. After 12:00 hours the energy prices turn positive, and the VPP stops curtailing its RES generation. This can be see in Figure 4.3 (middle) where the raise FCAS bids reduce to a more steady value. This is because the raise FCAS participation is now coming from the curtailable loads and the BESS, and not the RES generation. In the evening there is very little RES generation (hence the small lower FCAS participation in Figure 4.3 (bottom)). However, at the end of the day when the energy prices peak, the BESS discharges for maximum value.

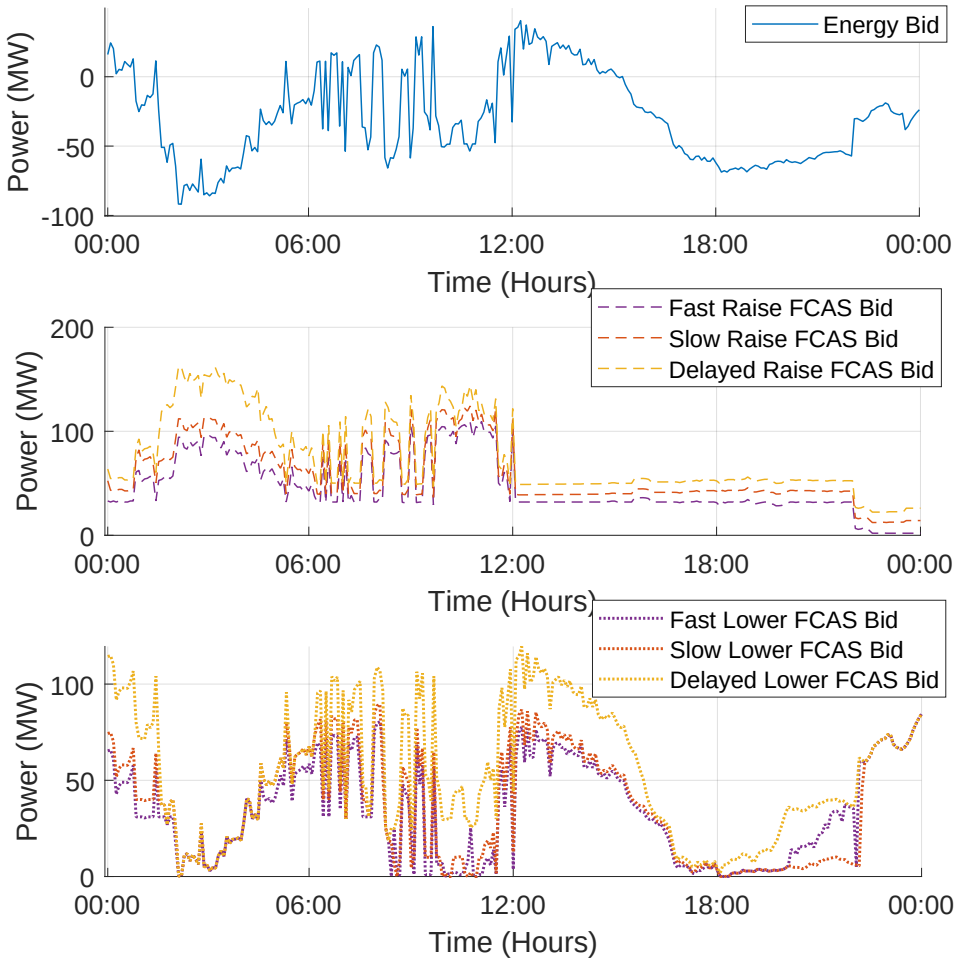

FIGURE 4.3: VPP participation in the energy and FCAS markets, for Case 1 - 01 May 2016. (Top) energy, (middle) raise FCAS, (bottom) lower FCAS.

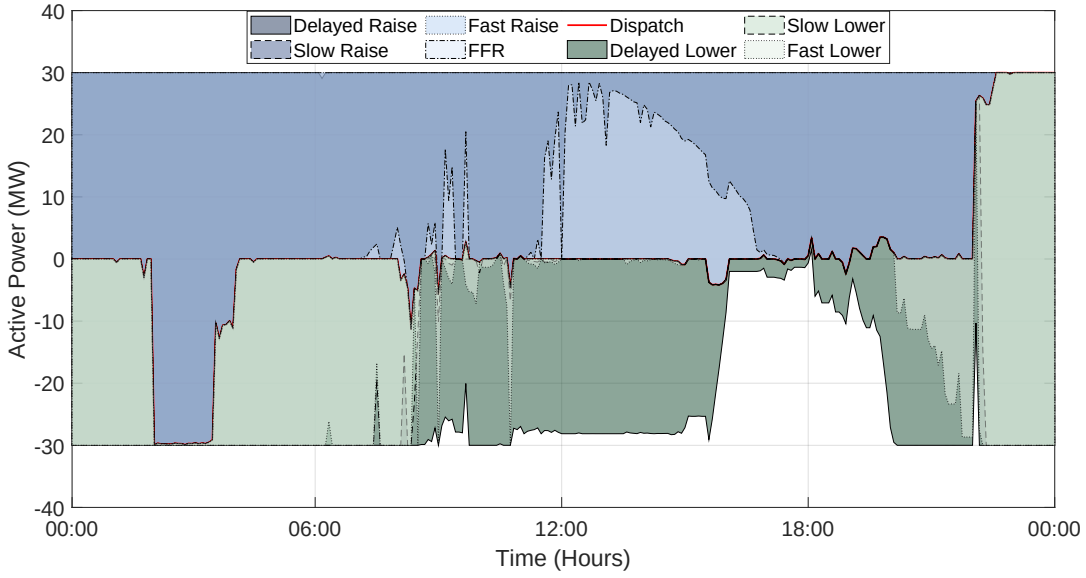

FIGURE 4.4: BESS bids in energy and FCAS markets for Case 1 - 01 May 16

The BESS is one of the most flexible resources in the VPP, and so its operation will be analysed further. Figure 4.4 shows the BESS dispatch points participation in FCAS markets and FFR for Case 1 on 01 May 2016. The BESS starts half-full of energy, so during the early portion of the day the BESS bids into the FCAS markets are not constrained by the energy headroom/footroom delivery requirements. Bids are constrained by the power of the BESS (for raise FCAS markets this is true through the entire day). During the morning negative price periods the BESS charges, but not fully, allowing it to still bid in the lower FCAS markets later in the day to generate revenue. The delayed lower FCAS market prices are greater than for slow or fast lower. So as the available headroom starts to constrain the BESS participation in the lower FCAS markets, the VPP prioritizes bids to the delayed lower market. The BESS reaches very close to full capacity in the evening (hence the reduction in lower FCAS market bids), before discharging during the peak energy price periods at the end of the day. The BESS power allocation for FFR matches the requirement from the PV in the system. The PV is curtailed for much of the morning (due to the negative energy prices), so the BESS does not need to provide FFR during that time.

4.2.4.2 Reactive Power Support

The price of the night time reactive power market to incentivise reactive power absorption is low compared to the other markets (a price of -$1/MVarh between 22:00 and 05:00). This means that any alteration that the VPP makes to its operation should not result in high operating costs or lost opportunity to generate revenue in other markets. However, the VPP can provide upstream reactive power support with limited effect on the VPP revenue in other markets. Figure 4.5 compares the VPP active and reactive power outputs for Case 1 on 28 Aug 2016 when participating in the reactive power market, and when it is not. Even this small price signal elicits a substantial change in VPP reactive power, highlighting the flexibility and effective co-optimization of the VPP. This service could easily be altered to be a contractual one by imposing a minimum value on the reactive power imported from the grid during this time, which is support by the operating framework as shown in constraint (3.72).

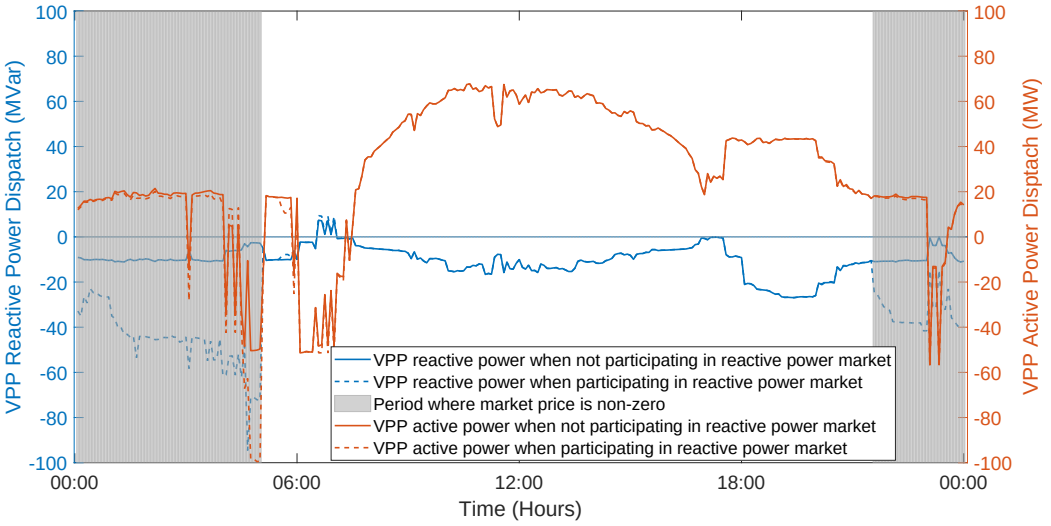

FIGURE 4.5: Changes in reactive power outputs when upstream support is requested for Case 1 - 28 Aug 16

4.2.4.3 Daily Revenue

Figure 4.6 shows the total daily revenue of the VPP for Case 1 in each of the three study days, as well as the revenue composition. It shows that the revenue composition and magnitude differ between days, further highlighting the importance of multi-market participation. On 01 May 2016, the VPP is a net importer of energy (approximately 700 MWh) and so the energy-related revenue is negative (VPP revenue from consumers of this energy is not considered in this analysis). However, the VPP still manages to obtain an overall positive revenue due to participation in FCAS markets. In contrast, for 28 Aug 2016 the revenue from the energy market makes up most of the revenue from the large amount of energy exported due to high availability of RES. Finally, for the 31 Jan 2020 (note the change in order of magnitude of the y axis in Figure 4.6) most of the revenue is coming from participation in the fast raise FCAS market. This comes mainly from the BESS and partial curtailment of inverter-based RES.

Table 4.3 contains the total revenue of each of the cases on each day. The importance of multi-market participation has already been shown in Figure 4.6. Table 4.3 shows how effectively the VPP can employ flexibility to provide contractual services with minimal impact in its revenue generation. It should be noted that no revenue has been attributed to the provision of the local network support, FFR or inertia services provided by the VPP, hence the lower revenue when these services are being provided. However, the reduction in market revenue for providing each of these three services is only less than 1%

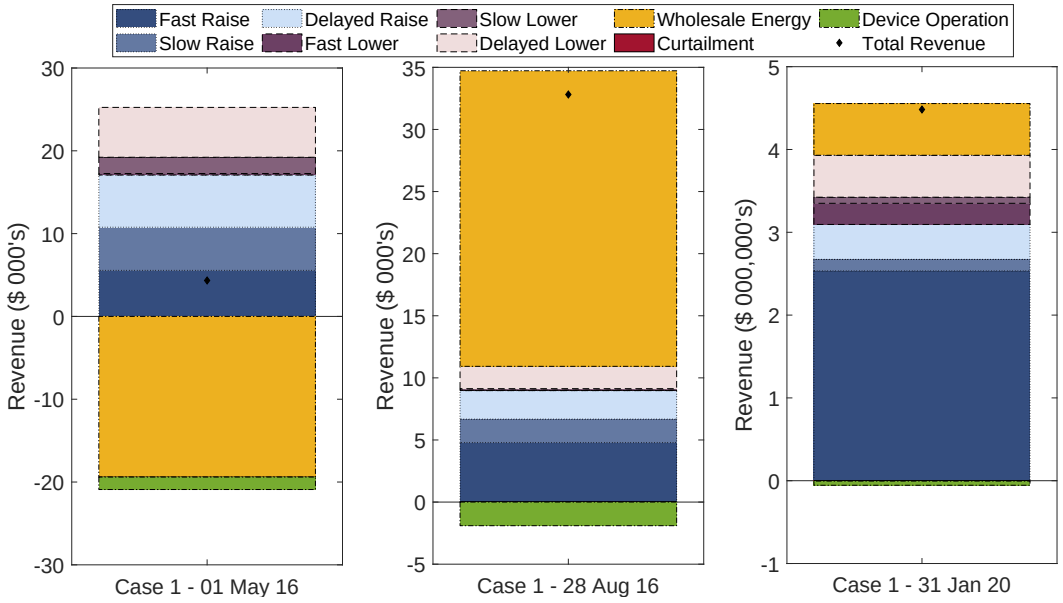

FIGURE 4.6: Comparison of total daily revenue for Case 1 across different days

Case	01 May 16	28 Aug 16	31 Jan 20
1	$4,339	$32,813	$4,482,907
2	$4,363	$33,020	$4,494,905
3	$4,339	$32,819	$4,579,243
4	$4,343	$32,827	$4,483,006
5	$4,931	$32,916	$5,057,684

TABLE 4.3: Daily revenue of case studies

of total revenue. The exception to this is providing FFR on 31 Jan 2020, which reduces VPP revenue by 2%. This slightly higher reduction in revenue is due to the opportunity costs associated with the BESS not being fully able to take advantage of the extreme market prices. This shows that the framework allows the VPP to effectively utilise its flexibility to provide multiple contractual and market services whilst maximising revenue. Whilst these contractual services have a limited cost impact, they can have a major benefit. Taking 01 May 2016 as an example, without local network support, the network voltages range from 0.9196–1.1208 p.u. (as shown in Figure 4.7) and exceeds voltage limits around 8% of the time.

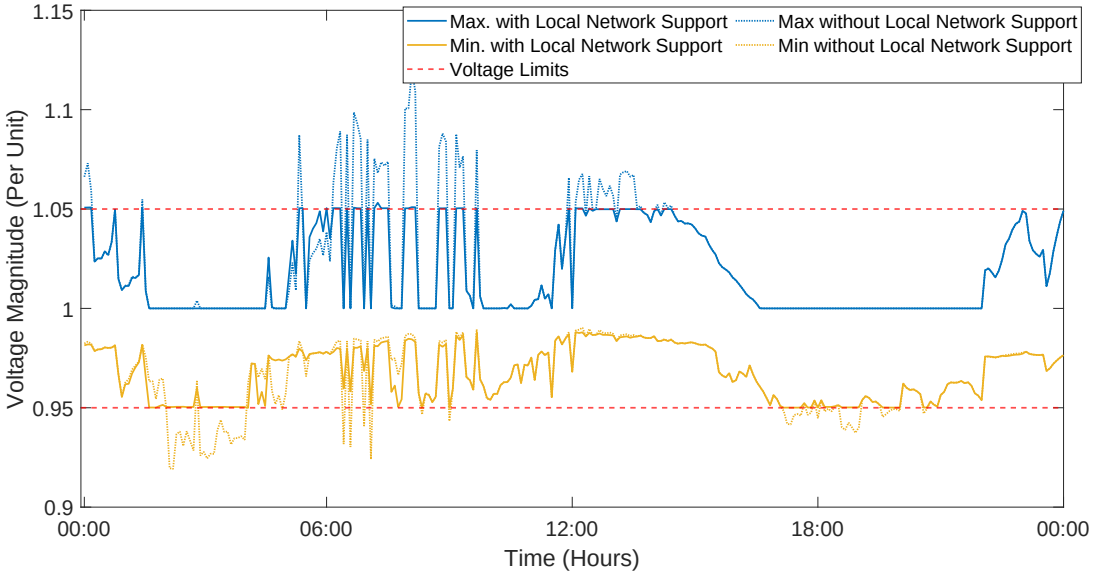

FIGURE 4.7: 01 May 2016 maximum and minimum network voltages throughout the day for Case 1 (with local network support) and Case 2 (without local network support).

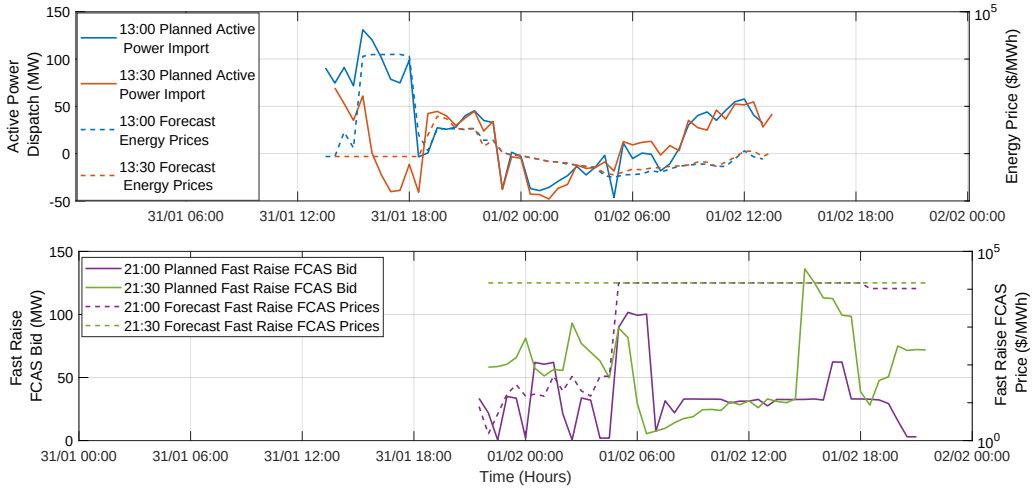

FIGURE 4.8: (Top) changes in wholesale energy price forecast and corresponding planned power import between 13:00 hours and 13:30 hours on Case 1 - 31 Jan 2020. (Bottom) changes to fast raise FCAS price forecast and corresponding planned bids between 21:00 hours and 21:30 hours on Case 1 - 31 Jan 2020.

4.2.4.4 Effects of Uncertainty

To verify the robustness of the high-level solutions the resource schedules were tested with an additional 10,000 realizations of uncertainty. These realizations were different to the ones used to generate the robust schedules. Nonetheless, feasibility was maintained in all cases as is expected.

The difference in revenue between Cases 1 and 5 (uncertainty vs perfect knowledge) for

28 Aug 2016, 31 Jan 2020, 01 May 2016 is 0.3%, 11%, 12% of total revenue respectively. The percentage difference for 01 May 16 is high because of the small revenue ($4,339) compared to the large cashflow (combined costs and revenues of $46,148). If the difference between Case 1 and Case 5 cashflows is considered for 01 May 16 then the difference is 1.3%. The revenue difference on 31 Jan 2020 is high because of an islanding event in SA which could not be predicted. The market price forecasts drastically changed after the islanding at 13:30 hours and continued to change for the rest of the day. Figure 4.8 gives just two examples of how quickly and drastically market price forecasts changed over 30-minute periods for 31 Jan 2020 (note the logarithmic scale for prices), and how the VPP changed operating strategies accordingly. These changes were of far greater magnitude than would be included in scenario generation. However, due to its flexibility and the receding horizon approach, the VPP could rapidly adjust its operation and still provide services and accrue a large revenue. As is shown in the next section, if an operational framework was used that didn't utilise short-term bidding windows to determine VPP dispatch, the impact on revenue would be even more significant.

4.2.4.5 Comparison of Results against previous frameworks

For the purpose of comparison, we have also adapted the framework proposed in this work to emulate the approaches to VPP operation proposed in previous works [108, 120, 121]. These previous works use binding day-ahead bids coupled with close-to-real time bid tracking, and do not consider multiple markets. To highlight the benefit derived from our framework, Table 4.4 shows the different revenues in Case 3 for the three study days. First, the proposed framework is applied with full flexibility. Second, day-ahead bids (in energy and FCAS) are set to be binding, and the low-level 5-minute receding horizon optimization is used to match those bids. Third, a further restriction is enforced by excluding participation in FCAS markets. Table 4.4 shows in all cases that the inclusion of a short-term bidding window and participation in multiple markets both greatly increased potential VPP revenue.

4.2.4.6 Accuracy of SOC Relaxation

By utilising a relaxation of the AC power flow constraints, the solution obtained by the optimization may be different than if the full AC power flow equations were used.

Framework	**Revenue($)**				
	Energy	**FCAS**	**Curtailment**	**Operating Cost**	**Total**
01 May 2016 Case 3					
Proposed Framework	-19,409	25,244	0	-1,496	**4,339**
Binding Day Ahead	-32,024	22,820	0	-2,377	**-11,581**
Binding Day Ahead No FCAS	-26,607	0	-1,259	-2,077	**-29,943**
28 Aug 2016 Case 3					
Proposed Framework	23,786	10,935	0	-1,902	**32,819**
Binding Day Ahead	-12,617	9,432	0	-910	**-4,095**
Binding Day Ahead No FCAS	-12,322	0	0	-373	**-12,695**
31 Jan 2020 Case 3					
Proposed Framework	639,660	3,993,834	-4,599	-49,652	**4,579,243**
Binding Day Ahead	-7,053	1,797,800	0	-22,645	**1,748,102**
Binding Day Ahead No FCAS	-8,504	0	0	-23,519	**-62,023**

TABLE 4.4: Revenue comparison against previous frameworks

As mentioned in Section 3.3, the dispatch points determined by the solution of the low-level optimisation can be used as an input to an AC load flow to determine the impact the SOC relaxation has on the exactness of the results. Taking Case 1 of 01 May 2016 as an example: the maximum error in nodal voltage magnitude caused by using the SOC relaxation is 0.003 p.u, with an average error of less than 0.0002 p.u; the maximum active power grid injection error is 0.28 MW, with an average error of 0.015 MW (for comparison the maximum active power grid injection is 91.88 MW); the maximum reactive power grid injection error is 0.55 MVar, with an average error of 0.043 MVar (for comparison the maximum reactive power grid injection is 12.79 MVar). The slight tightening of voltage and power flow constraints in the relaxed model would

help ensure that these limits are maintained in the real system. The maximum active power injection error is negligible compared to the maximum active power injection at 0.3%. The average reactive power injection error compare to the maximum reactive power injection is 0.34%. However, the maximum reactive power injection error is more noticeable when compared with maximum reactive power exchanged with the grid at 4.3%, which justifies the approach of running the final VPP dispatch through a full AC load flow conducted in MATPOWER [163] to ensure that an accurate bid can be provided to markets. While it is not part of the current framework, a possible future additional functionality could be an algorithm to automatically tighten the network voltage and power flow constraints and then re-run the low-level optimisation, iterating until the low-level optimisation provides a dispatch solution that is feasible in the AC load flow. This would avoid excessive tightening of network constraints during times when it was not required.

4.2.5 Summary of VPP Participation in Multiple Markets and Services

The framework that has been proposed in this work and applied in this study allows multi-service operational co-optimization and value stack maximisation of a VPP that participates in multiple markets and provides network and system services whilst considering uncertainty and local network constraints. The results of the case study show that the framework allows a VPP to flexibly and effectively alter its revenue maximisation strategy in response to different market prices and renewable availability. Participation in multiple markets could provide significant additional revenues, thus boosting the VPP's business case. The framework also allows a VPP to provide additional system and network services with limited impact on market revenue. Provision of local network support to prevent over-voltages in the local network and contribution to system operation via provision of FFR, inertia and upstream reactive power support facilitate system and network integration of DER and RES. The framework can successfully consider and adapt to uncertainty (both foreseeable and unforeseeable) through a combination of scenario-based robust optimization and receding horizon optimizations. The adopted SOC relaxation of the power flow equations allows a tractable formulation of a very complex problem. The resulting limited inaccuracy can be counter-acted through slight

tightening of network constraints, besides being practically checked via power flow analysis, as done here.

4.3 Study on Distribution System Operator & VPP Interactions

The second study in this chapter looks at how the proposed framework could be utilised by different entities in a network. In the first study, it is assumed that the VPP is directly responsible for maintaining the state of the network in which it is located within allowable limits. This is a useful assumption for determining how effectively the VPP can provide local network support, and the associated costs of such support. However, in the real world the VPP and distribution system operator (DSO) (the entity responsible for maintaining distribution network operation) are likely to be different entities. Therefore, it is pertinent to determine how the framework proposed in this thesis is able to be used in such a multi-entity setting.

This study will consider a DSO being responsible for ensuring that network limits are not violated by providing each active DER (a DER controlled by a VPP) in the network with operating limits. The VPPs in the network then optimises the operation of the DER (subject to the operating limits imposed by the DSO, and without direct modelling of the network constraints) to participate in electrical markets controlled by a distribution market operator (DMO). This process is illustrated in Figure 4.9. It should be noted that this is only one example of possible interactions between distribution network entities. This framework could easily be applied to other setups with different entities and interactions.

The main aspects of this multi-entity interaction that this study examines are:

1. How does the fairness paradigm employed by the DSO effect network export capabilities, and VPP revenue generation?
2. How does the method of DER control (only active power or active and reactive power) change the operating limits and best choice of fairness paradigm?
3. Can network flexibility (network owned and controlled assets) be used to assist in increasing the operational envelopes of the DER?

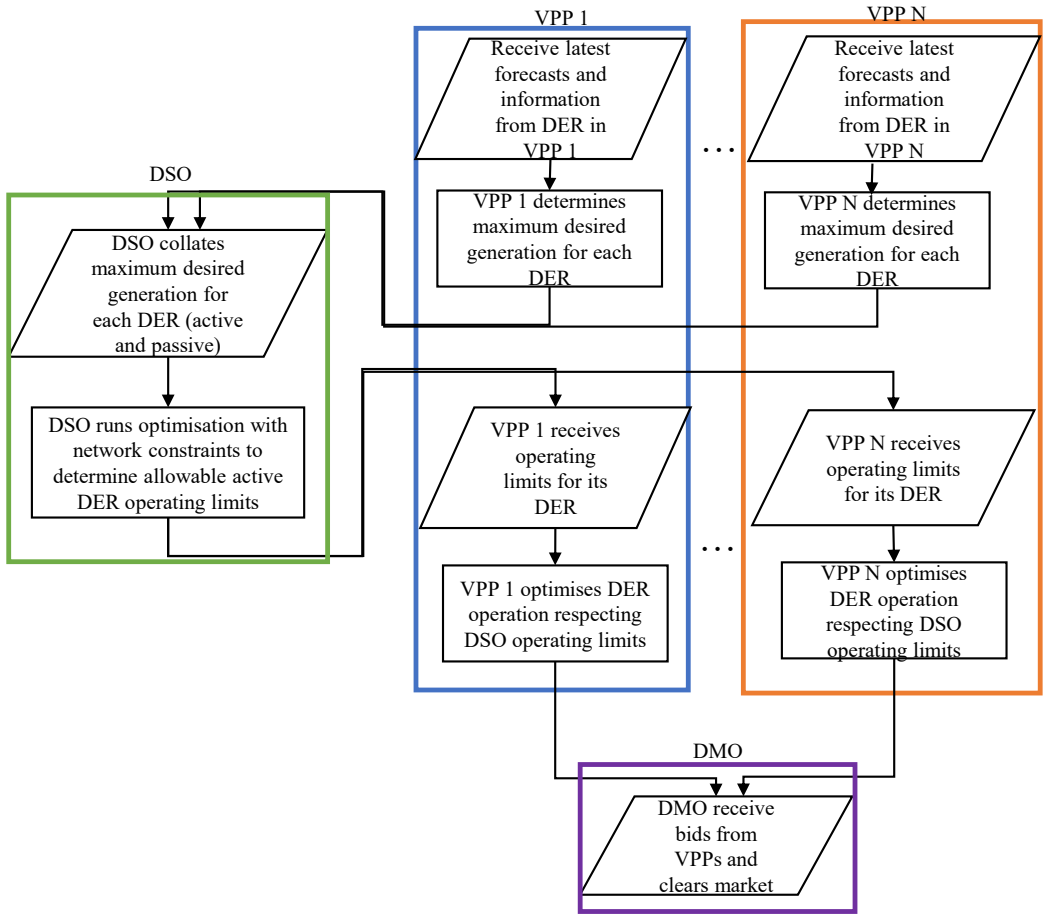

FIGURE 4.9: Flowchart to illustrate the proposed interaction between VPPs, DSO and DMO in a network

For purposes of clarity, when fairness is referred to in this chapter, it is applying to the method in which the available network capacity is being assigned by the DSO to each DER. The DSO does not consider which VPP the DER is part of when determining the fairness of its capacity allocation. Therefore, this is fairness from the perspective of the customer/DER owner. This chapter does not consider the economic fairness with which a VPP operator would redistribute profits to the DER (as there would likely be contracts in place between DER and the VPP operator as well as regulation to govern this), although the economic impacts on each VPP when these fairness paradigms are used is shown later in the chapter.

4.3.1 Fairness Paradigms

When a DSO is determining the operational limits of the active DER, the overall objective is likely to be to maximise the amount of active power that can be exported from the network whilst respecting network limits. This allows the greatest participation in electrical markets by DER within the distribution network. However, the DSO may also want to ensure that the restrictions that they are placing on the DER are in some way fair to the DER within the network. There are questions around what a fair method of defining operational limits would be, and how implementation of fairness effects the ability of the network to export power. There are many possible fairness paradigms that could be implemented, informed by DSO objectives and customer preferences. The aim of this case study with respect to fairness paradigms is to highlight the complexity involved in choice of fairness paradigm, especially in the context of overall economic efficiency of the distribution network. Therefore, in this study three fairness paradigms are considered:

1. **Maximum Power Export** - This has no concept of fairness, and instead chooses DER operational limits solely to maximise active power export. If the same value of power export has multiple solutions, the most efficient limits are chosen (those that also minimise losses in the network).

2. **Equal Export** - Using this method, the DSO ensures that all active DER in the network are allowed to inject the same amount of active power while aiming to maximise active power export.

3. **Proportional Curtailment** - Using this method, the DSO ensures that all active DER are curtailed at a level proportional to their maximum available generation while aiming to maximise active power export.

4.3.2 How the framework is applied

To illustrate how this interaction can be accomplished, and the effectiveness of the different concepts of fairness as well as the different control mechanisms, this study will consider a single time step optimisation only (i.e., $T = 1$). However, this can be readily expanded to multiple time steps. It is also assumed that none of the DER in this

distribution network require unit commitment modelling. Therefore, only the low-level optimisation of the framework is used in this study, (with the associated penalty function set to 0). This again highlights the flexibility of the operational framework allowing it to adapt to different modelling requirements. Uncertainty is also not considered in this study, so $S^{\mathrm{LL}} = 1$.

4.3.2.1 DSO Optimisation

For the DSO to be able to create the DER operational limits, it must receive from the DER the maximum power that it desires to generate in the specific time period $\hat{P}_{k,t}$. The DSO should also be advised by the VPPs operating in the network if their resources are using solely active power control, or active and reactive power control. The DSO can then use the low-level optimisation of the proposed framework with minimal alterations to be able to optimise the assignment of DER operational limits to maximise active power export. The objective function for the DSO is

$$\min \sum_{t=1}^{T} \left(-P^{\exp}(t) + \sum_{(i,j)\in\Psi^{L}} \lambda_{ij}^{\mathrm{loss}} \Lambda_{ij}(t) \right). \tag{4.4}$$

The loss term in the cost function acts to ensure that the most efficient choice of resources is utilised to maximise active power export. It also acts to tighten the SOC relaxation of the power flow equations to increase the accuracy of the modelling.

If the DSO is operating under the Maximum Power Export paradigm, there are no additional constraints. If the DSO is operating under the Equal Export paradigm, then the low-level optimisation would be supplemented with

$$P_k(t) = \tilde{P}_t, \quad k \in \Psi^{VPP}, \tag{4.5}$$

where $\tilde{P}(t)$ is the limit of power injection that each active resource can inject, and Ψ^{VPP} is the set of active DER in VPPs. This distinction is important for the DSO optimisation, as there are likely to be resources in the network that are not part of a VPP. These resources would not be participating in any electrical markets, but would also be unresponsive to DSO operational limits.

If the DSO is operating under the Proportional Curtailment paradigm the low-level optimisation would need to be supplemented with

$$\hat{P}_{k,t} - P_k(t) = \hat{P}_{k,t}\tilde{\omega}(t), \quad k \in \Psi^{VPP}, \tag{4.6}$$

$$\tilde{\omega}(t) \geq 0 \tag{4.7}$$

where $\tilde{\omega}(t)$ is the proportion of available active power $\hat{P}_{k,t}$ that each active resource must curtail.

4.3.2.2 Soft Open Points

A soft open point (SOP) is an electronic device that is positioned in the network at a point that would normally by open (disconnected), such as the ends of two feeders. This device is often two back-to-back voltage source converters [164]. Using a SOP links the active power flow through the SOP (defined by (4.8)), but allows the reactive power flow into and out of the SOP to be independent, limited only by the apparent power limit of the voltage source converters (as in (4.9) and (4.10)). This provides a network operator with a high degree of flexibility, allowing reactive power control at the end of feeders.

$$P^{\text{SOP,out}}(t) + \kappa^{\text{SOP}}(t)\left(\Lambda^{\text{SOP,out}}(t) + \Lambda^{\text{SOP,in}}(t)\right) = P^{\text{SOP,in}}(t) \tag{4.8}$$

$$(P^{\text{SOP,out}}(t))^2 + (Q^{\text{SOP,out}}(t))^2 \leq \overline{S}^{\text{SOP}} \tag{4.9}$$

$$(P^{\text{SOP,in}}(t))^2 + (Q^{\text{SOP,in}}(t))^2 \leq \overline{S}^{\text{SOP}} \tag{4.10}$$

In (4.8) - (4.10), $P^{\text{SOP,out}}(t)$ is the active power leaving the SOP, $P^{\text{SOP,in}}(t)$ is the active power entering the SOP, $\Lambda^{\text{SOP,out}}(t)/\Lambda^{\text{SOP,in}}(t)$ is the square of current flow out of / into the SOP respectively, and κ^{SOP} is the loss coefficient associated with current flow through the SOP. $Q^{\text{SOP,out}}(t)/Q^{\text{SOP,in}}(t)$ is the reactive power flow out of / into the SOP. The apparent power limit of the SOP is $\overline{S}^{\text{SOP}}$.

4.3.3 Distribution Network used in the study

The distribution network used in this study is shown in Figure 4.10 and is based on a real world 22 kV network. The DER in feeders A and B are a combination of PV and

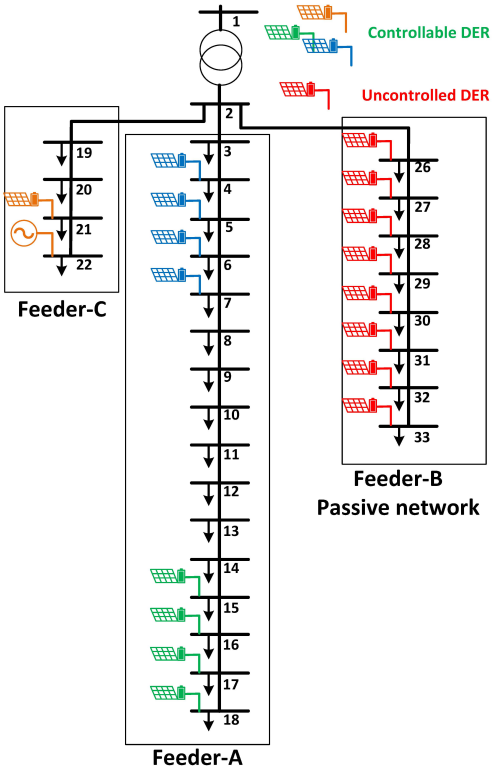

FIGURE 4.10: Distribution network used for study on DSO & VPP interactions containing controlled DER in feeder A and C, and uncontrolled DER in feeder B. The controlled DER are controlled by the three separate VPPs (denoted by the colours blue, green and orange)

BESS with a 0.25 MW inverter size and 0.02 MWh storage size. In feeder C the PV + BESS system is 0.5 MW / 0.02 MWh and there is also a 1 MW / 1.2 MVA diesel generator. These feeders are connected to the main grid via a 4 MVA transformer. To consider a worst case scenario, the load on each of the nodes is negligible (assuming that uncontrolled downstream rooftop PV is generating a sufficient amount of energy to cover the load requirement), and there is sufficient solar irradiance for each controllable PV to generate their rated power. It is also assumed that the DSO has a forecast of the operation of the uncontrolled DER. The DSO is responsible for maintaining power flow below line thermal limits, and nodal voltages within 95%-105% of nominal voltage. The controlled DER (the DER on feeders A and C) are divided into three different VPPs (Blue VPP, Green VPP and Orange VPP in Figure 4.10). To determine how network configuration and DSO controlled network flexibility effect DER operating limits, two variations on the network will also be considered. In Figure 4.11 the ends of feeder A and feeder B have been joined by a cable to create a looped network. In Figure 4.12 the ends of feeder A and feeder B are joined by an SOP.

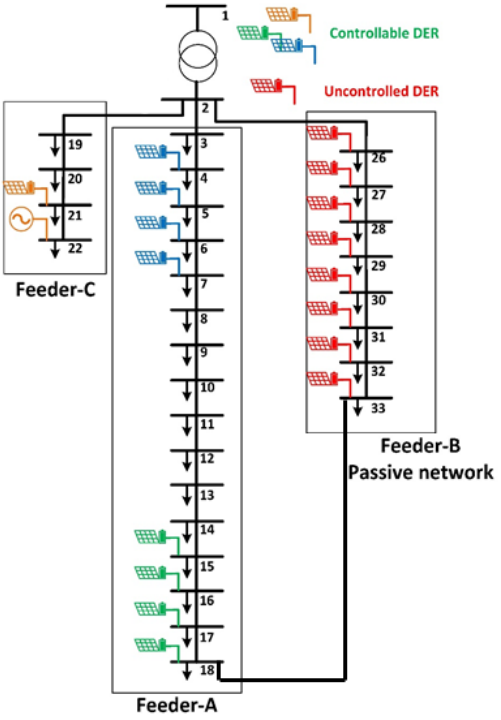

FIGURE 4.11: Distribution network with looped configuration used for study on DSO & VPP interactions containing controlled DER in feeder A and C, and uncontrolled DER in feeder B. The controlled DER are controlled by the three separate VPPs (denoted by the colours blue, green and orange)

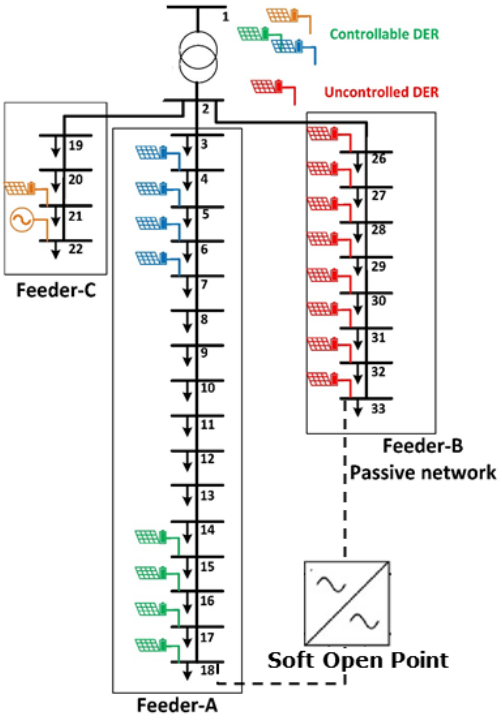

FIGURE 4.12: Distribution network with an SOP used for study on DSO & VPP interactions containing controlled DER in feeder A and C, and uncontrolled DER in feeder B. The controlled DER are controlled by the three separate VPPs (denoted by the colours blue, green and orange)

DER and Node Number	Rated Power	Maximum Export		Equal Dispatch		Proportional Curtailment	
	MW	MW	MVAr	MW	MVAr	MW	MVAr
PV+BESS - 4	0.25	0.25	0.00	0.12	0.00	0.09	0.00
PV+BESS - 5	0.25	0.21	0.00	0.12	0.00	0.09	0.00
PV+BESS - 6	0.25	0.00	0.00	0.12	0.00	0.09	0.00
PV+BESS - 7	0.25	0.00	0.00	0.12	0.00	0.09	0.00
PV+BESS - 15	0.25	0.00	0.00	0.12	0.00	0.09	0.00
PV+BESS - 16	0.25	0.00	0.00	0.12	0.00	0.09	0.00
PV+BESS - 17	0.25	0.00	0.00	0.12	0.00	0.09	0.00
PV+BESS - 18	0.25	0.00	0.00	0.12	0.00	0.09	0.00
PV+BESS - 21	0.50	0.50	0.00	0.12	0.00	0.17	0.00
Diesel Gen. - 22	1.00	0.24	0.00	0.12	0.00	0.35	0.00
Power from VPPs		**1.20**	**0.00**	**1.22**	**0.00**	**1.21**	**0.00**
Power Export to grid		**2.33**	**-0.06**	**2.34**	**-0.06**	**2.34**	**-0.06**

TABLE 4.5: DSO operational limits for DER with only active power control for each of the three fairness paradigms

4.3.4 Results - Radial Network

4.3.4.1 Active Power Control Only

Table 4.5 shows the DER operating limits set by the DSO for the controllable DER in the network, for each of the three fairness paradigms. These results are assuming active power control only, hence why the reactive power from the controllable DER is set to 0. In each of these cases, the amount of power that is exported to the grid is well below the 4 MW thermal limit of the grid connection transformer. This is because the power export of the DER is limited by the high voltage in the network. Specifically, the voltage at the end of feeder B (the uncontrolled feeder) is limiting the power export of the network. The power that is exported to the grid is also essentially the same in each of the three fairness paradigms[1]. It is apparent that for the Maximum Export paradigm DER close to the grid connection point are heavily favoured. This results in the majority of controllable DER not being permitted to generate at all.

[1]The Maximum Export value is actually marginally less than the other values (0.35% less). This is because, due to the lack of a fairness constraint, there are many possible solutions yielding similar results. This causes the progress that the solver makes close to optimally to be slow. Therefore, the solver terminates within a tolerance of the optimal solution.

DER and node Number	Rated Power	Maximum Export		Equal Dispatch		Proportional Curtailment	
	MW	MW	MVAr	MW	MVAr	MW	MVAr
PV+BESS - 4	0.25	0.18	-0.18	0.22	-0.11	0.17	-0.18
PV+BESS - 5	0.25	0.18	-0.18	0.22	-0.11	0.17	-0.18
PV+BESS - 6	0.25	0.18	-0.18	0.22	-0.11	0.17	-0.18
PV+BESS - 7	0.25	0.18	-0.18	0.22	-0.11	0.17	-0.18
PV+BESS - 15	0.25	0.18	-0.17	0.22	-0.11	0.17	-0.18
PV+BESS - 16	0.25	0.16	-0.17	0.22	-0.11	0.17	-0.16
PV+BESS - 17	0.25	0.01	0.00	0.22	-0.11	0.17	0.00
PV+BESS - 18	0.25	0.01	-0.01	0.22	-0.11	0.17	0.00
PV+BESS - 21	0.50	0.34	-0.36	0.22	-0.45	0.35	-0.36
Diesel Gen. - 22	1.00	1.00	-0.40	0.22	-0.18	0.69	-0.40
Power from VPPs		**2.42**	**-1.82**	**2.25**	**-1.51**	**2.43**	**-1.82**
Power Export to grid		**3.44**	**-1.95**	**3.26**	**-1.64**	**3.44**	**-1.95**

TABLE 4.6: DSO operational limits for DER with active and reactive power control for each of the three fairness paradigms

In both the Equal Dispatch and Proportional Curtailment paradigms, all of the controllable DER are able to operate in the network. The Equal Dispatch has slightly higher network losses due to the higher utilisation of the DER at the end of feeder A. The Proportional Curtailment results in curtailment of RES in favour of the diesel generator because of its larger size. This may be undesirable for a DSO, who may also want to include some form of emissions consideration in their fairness paradigm to avoid this.

4.3.4.2 Active and Reactive Power Control

In Table 4.6 it is assumed that the VPPs can control both the active and the reactive power of the DER. For the Maximum Export and Proportional Curtailment paradigms, the DSO operating limits are constrained both by the thermal limit of the grid connection transformer, and the system voltages. This is due to the high amount of reactive power that the DER are absorbing to try and mitigate high voltages in the network (specifically the voltages at the end of feeder B). This limits the capacity of the transformer to export active power. However, due to the control of reactive power, the amount of active power that can be exported to the grid is increased by almost 50% compared to the case with only active power control. By absorbing reactive power in feeders A and C the voltage at

node 2 can be reduced, which in turn reduces the voltage magnitude at the end of feeder B. Because the DER operating in feeder B are uncontrolled, the voltage drop in feeder B is also uncontrolled. However, by reducing the voltage at node 2, it can be ensured that the voltage at the end of feeder B (node 33) does not exceed the allowable limit. The reactive power value in Table 4.6 corresponds to the maximum reactive power operating point that the DER can be dispatched at. For most of the DER this is negative. For example for the DER at node 4 in the Maximum Export paradigm, the DER must absorb at least 0.18 MVAr of reactive power.

In general, for the Maximum Export paradigm, resources closer to the grid connection point are prioritised. Although, due to the reactive power control, more resources can be utilised than in the active power control case. The DER at nodes 4, 5, 6, 7, 15, and 21 are all operating at their maximum apparent power rating, injecting active power while absorbing reactive power. The diesel generator at node 22 is also operating absorbing the maximum reactive power that it can.

For the Equal Dispatch paradigm the small size of the DER inverters on feeder A leads to the larger resources on feeder C being limited in their ability to generate power. This in turn leads to a lower active power export capability than the other fairness paradigms. The Proportional Curtailment paradigm results in operational limits for DER as nodes 4, 5, 6, 7, 15, 16, and 21 that are almost identical to the Maximum Export paradigm. Where it differs is that the DER at the end of feeder A on nodes 17 and 18 are now allowed to operate. This comes at the cost of a more constrictive limit on the diesel generator in feeder C. This results in a slight increase in distribution network losses. This can be seen by the slightly larger power dispatch from VPPs in the Proportional Curtailment paradigm compared with the Maximum Export paradigm, but without an increase in power exported to the grid.

4.3.4.3 VPP Commercial Operation

The previous sections showed the DER operating limits that the DSO would assign under different fairness paradigms, and control strategies for the radial network. In this section the financial implications of the different operating limits are examined. As a baseline, the revenues of the VPPs are compared to the case where the network limits and all VPP operations are optimised in a single optimisation (as in the study on

VPP	Integrated Method	Maximum Export	Equal Dispatch	Proportional Curtailment
Active Power Dispatch				
Blue VPP	\$28.43	\$19.18	\$20.34	\$14.40
Green VPP	\$0.62	\$0.01	\$20.34	\$14.40
Orange VPP	\$20.83	\$23.24	\$6.31	\$10.66
Total	**\$49.88**	**\$42.42**	**\$46.99**	**\$39.47**
Active and Reactive Power Dispatch				
Blue VPP	\$35.32	\$29.37	\$37.42	\$28.88
Green VPP	\$35.53	\$15.25	\$37.42	\$28.88
Orange VPP	\$17.61	\$24.36	\$11.60	\$21.37
Total	**\$88.46**	**\$68.98**	**\$86.45**	**\$79.14**

TABLE 4.7: The total revenue that the VPPs in the radial distribution network can accrue given the DSO operational limits.

VPP participation in multiple markets and services in Section 4.2) without a fairness paradigm. It is assumed that the cost of operation of the PV+BESS DER is negligible. The cost of operation of the diesel generator is assumed to be \$380/MWh. In order to ensure that it is economically viable for the diesel generator to operate, the wholesale energy price is assumed to be \$500/MWh.

In Table 4.7 the revenue for each VPP, considering both control methods for each fairness paradigm are shown. For the active power control dispatch, even though the total power that the VPPs can export is similar, the revenue implications of the fairness paradigms are different. For both control strategies the Equal Dispatch paradigm is the closest to matching the revenue from the integrated method. This is because it minimises the use of the diesel generator in the network, which in turn reduces the operating costs of the DER in the network. So while the Equal Dispatch paradigm exports the least active power, it results in the highest total revenue in the network. However, this results in reduced revenue for the Orange VPP (which includes the diesel generator). The Proportional Curtailment paradigm most closely matches the revenues between the three VPPs, where the Orange VPP revenue is still less, but only 25% less as opposed to the nearly 70% less in the Equal Dispatch paradigm.

4.3.5 Results - Looped Network

Another important consideration is how the network configuration could impact the choice of fairness paradigm or effectiveness of a specific control strategy in unlocking

DER and node Number	Rated Power	Maximum Export		Equal Dispatch		Proportional Curtailment	
	MW	MW	MVAr	MW	MVAr	MW	MVAr
PV+BESS - 4	0.25	0.25	0.00	0.13	0.00	0.12	0.00
PV+BESS - 5	0.25	0.25	0.00	0.13	0.00	0.12	0.00
PV+BESS - 6	0.25	0.25	0.00	0.13	0.00	0.12	0.00
PV+BESS - 7	0.25	0.25	0.00	0.13	0.00	0.12	0.00
PV+BESS - 15	0.25	0.20	0.00	0.13	0.00	0.12	0.00
PV+BESS - 16	0.25	0.00	0.00	0.13	0.00	0.12	0.00
PV+BESS - 17	0.25	0.01	0.00	0.13	0.00	0.12	0.00
PV+BESS - 18	0.25	0.00	0.00	0.13	0.00	0.12	0.00
PV+BESS - 21	0.50	0.50	0.00	0.13	0.00	0.24	0.00
Diesel Gen. - 22	1.00	1.00	0.00	0.13	0.00	0.49	0.00
Power from VPPs		**2.72**	**0.00**	**1.34**	**0.00**	**1.70**	**0.00**
Power Export to grid		**3.77**	**-0.11**	**2.45**	**-0.07**	**2.80**	**-0.08**

TABLE 4.8: DSO operational limits for DER with active power control for each of the three fairness paradigms in a looped network

DER flexibility. This section studies the impact of feeder A and feeder B being connected in a loop (as in Figure 4.11), and what impact this has on the operating limits of the DER, the best choice of fairness paradigm, and VPP revenues.

4.3.5.1 Active Power Control

Comparing the operating limits for the radial network and the looped for active power control in Table 4.5 and Table 4.8, it can be seen that the loop in the network unlocks additional power export capability. This is due to the fact that the voltage magnitude at the end of feeder B is no longer solely determined by the voltage at node 2, but also by voltage at node 18. The loop allows some power from feeder B to be transferred to feeder A, reducing the voltage drop in feeder B. It can be seen that the Maximum Export paradigm results in priority being given to the resources closest to the grid connection point. This fairness paradigm is the one that benefits the most from the looped network in the active power control case - increasing power export by approximately 62%. The other fairness paradigms do not unlock as much power export capability as they required the DER at the end of feeder A to have generation capability. If the DER at the end of feeder A generate more than their operating limit in the Equal Dispatch or Proportional

DER and node Number	Rated Power	Maximum Export		Equal Dispatch		Proportional Curtailment	
	MW	MW	MVAr	MW	MVAr	MW	MVAr
PV+BESS - 4	0.25	0.25	0.00	0.14	0.08	0.12	0.08
PV+BESS - 5	0.25	0.25	0.00	0.14	-0.13	0.12	-0.12
PV+BESS - 6	0.25	0.25	0.01	0.14	0.05	0.12	0.05
PV+BESS - 7	0.25	0.25	0.01	0.14	0.08	0.12	0.08
PV+BESS - 15	0.25	0.21	0.02	0.14	0.02	0.12	0.02
PV+BESS - 16	0.25	0.00	-0.10	0.14	-0.13	0.12	-0.13
PV+BESS - 17	0.25	0.02	0.09	0.14	0.12	0.12	0.12
PV+BESS - 18	0.25	0.02	-0.08	0.14	-0.11	0.12	-0.11
PV+BESS - 21	0.50	0.50	0.00	0.14	0.25	0.25	0.33
Diesel Gen. - 22	1.00	1.00	0.15	0.14	0.00	0.50	0.01
Power from VPPs		**2.75**	**0.11**	**1.38**	**0.24**	**1.74**	**0.31**
Power Export to grid		**3.80**	**-0.01**	**2.49**	**0.17**	**2.84**	**0.23**

TABLE 4.9: DSO operational limits for DER with active and reactive power control for each of the three fairness paradigms in a looped network

Curtailment cases, then power will start to flow from feeder A to feeder B rather than the other way around. This would cause the voltage at the end of feeder A to exceed the voltage at the end of feeder B, which is the voltage that is constraining the DER operation. This is why the Equal Dispatch and Proportional Curtailment paradigms cannot export nearly as much as the Maximum Export paradigm.

4.3.5.2 Active and Reactive Power Control

What can be noted by comparing Table 4.8 and Table 4.9 is that the ability of VPPs to control the reactive power of their DER does not unlock a significant amount of extra power export capability in the looped network. This is because the direction of reactive power flow in the network can no longer be easily controlled by the injection/absorption of the DER. Therefore, it cannot be used as effectively to mitigate voltage drops. Because of this the Maximum Export paradigm unlocks substantially more export capability than the other two paradigms, which was not the case in the radial network. If the Maximum Export paradigm is utilised, then the looped network allows more power export than the radial network. But for the other two fairness paradigms, adding a loop to the network actually limits the active power export capability of the network. This is due to the

VPP	Integrated Method	Maximum Export	Equal Dispatch	Proportional Curtailment
Active Power Dispatch				
Blue VPP	\$41.67	\$41.67	\$22.35	\$20.25
Green VPP	\$9.58	\$8.97	\$22.35	\$20.25
Orange VPP	\$30.83	\$30.83	\$6.93	\$14.99
Total	**\$82.08**	**\$81.47**	**\$51.62**	**\$55.49**
Active and Reactive Power Dispatch				
Blue VPP	\$41.65	\$41.65	\$23.00	\$20.77
Green VPP	\$11.01	\$10.45	\$23.00	\$20.77
Orange VPP	\$30.83	\$30.83	\$7.13	\$15.37
Total	**\$83.50**	**\$82.94**	**\$53.14**	**\$56.91**

TABLE 4.10: The total revenue that the VPPs in the looped distribution network can accrue given the DSO operational limits.

effectiveness of reactive power control in a radial network, which is not duplicated in the looped network.

4.3.5.3 VPP Commercial Operation

For the looped network, the paradigm that allows the VPPs to most closely match the revenue from the integrated method is the Maximum Export paradigm. This is due to the large difference in the size of the operating limits that have been assigned to the DER in the Maximum Export paradigm compared to the other two. Even though it relies heavily on the more expensive diesel generator, this is outweighed by the additional export capability. The Proportional Curtailment paradigm is again the most effective at balancing revenue between VPPs. However, implementing this paradigm results in over a 30% reduction in revenue compared to the Integrated Method.

4.3.6 Results - Soft Open Point Network

A SOP is a network flexibility asset that a DSO could use to unlock additional flexibility in the network. To investigate how an SOP could impact the DSO assignment of DER operating limits, a 1 MVA SOP is placed between the end of feeder A and feeder B, as shown in Figure 4.12. The operation of this SOP is constrained by (4.8) - (4.10).

DER and node Number	**Rated Power**	**Maximum Export**		**Equal Dispatch**		**Proportional Curtailment**	
	MW	**MW**	**MVAr**	**MW**	**MVAr**	**MW**	**MVAr**
SOP In - 18	1.00	-0.09	0.12	-0.26	-0.30	-0.36	0.01
SOP Out - 33	1.00	0.07	-0.23	0.24	-0.33	0.34	-0.48
PV+BESS - 4	0.25	0.25	0.00	0.25	0.00	0.21	0.00
PV+BESS - 5	0.25	0.25	0.00	0.25	0.00	0.21	0.00
PV+BESS - 6	0.25	0.25	0.00	0.25	0.00	0.21	0.00
PV+BESS - 7	0.25	0.25	0.00	0.25	0.00	0.21	0.00
PV+BESS - 15	0.25	0.25	0.00	0.25	0.00	0.21	0.00
PV+BESS - 16	0.25	0.16	0.00	0.25	0.00	0.21	0.00
PV+BESS - 17	0.25	0.00	0.00	0.25	0.00	0.21	0.00
PV+BESS - 18	0.25	0.00	0.00	0.25	0.00	0.21	0.00
PV+BESS - 21	0.50	0.50	0.00	0.25	0.00	0.41	0.00
Diesel Gen. - 22	1.00	1.00	0.00	0.25	0.00	0.83	0.00
Power from VPPs		**2.91**	**0.00**	**2.50**	**0.00**	**2.90**	**0.00**
Power Export to grid		**3.92**	**-0.24**	**3.50**	**-0.76**	**3.88**	**-0.63**

TABLE 4.11: DSO operational limits for DER with active power control for each of the three fairness paradigms in a SOP network

4.3.6.1 Active Power Control

By looking at the results in Table 4.11 it can be seen that the SOP in the network is highly effective at unlocking DER flexibility. For both the Maximum Export and Proportional Curtailment paradigms the apparent power exchange to the grid is limited by the thermal line limit of the grid connection transformer as well as the network voltages. The ability to control reactive power injection/absorption at the end of the uncontrolled feeder B is key to unlocking DER export capability. For the Equal Dispatch paradigm in the SOP network, the two larger DER located at node 21 and 22 are limited by the size of the other DER (which are exporting their maximum active power capability). This indicates that this Equal Dispatch paradigm would also need to consider relaxing the limit on larger DER once the smaller DER have reached their maximum capacity.

DER and node Number	Rated Power	Maximum Export		Equal Dispatch		Proportional Curtailment	
	MW	MW	MVAr	MW	MVAr	MW	MVAr
SOP In - 18	1.00	-0.29	0.00	-0.26	-0.30	-0.52	0.00
SOP Out - 33	1.00	0.27	-0.45	0.24	-0.34	0.49	-0.67
PV+BESS - 4	0.25	0.25	0.02	0.25	0.00	0.21	0.12
PV+BESS - 5	0.25	0.25	0.02	0.25	0.00	0.21	0.03
PV+BESS - 6	0.25	0.25	0.02	0.25	0.00	0.21	0.00
PV+BESS - 7	0.25	0.25	0.02	0.25	0.00	0.21	0.01
PV+BESS - 15	0.25	0.14	0.01	0.25	0.00	0.21	0.00
PV+BESS - 16	0.25	0.02	0.00	0.25	0.00	0.21	0.00
PV+BESS - 17	0.25	0.08	0.00	0.25	0.00	0.21	0.00
PV+BESS - 18	0.25	0.20	0.00	0.25	0.00	0.21	0.00
PV+BESS - 21	0.50	0.50	0.02	0.25	0.08	0.42	0.26
Diesel Gen. - 22	1.00	1.00	0.44	0.25	0.00	0.85	0.37
Power from VPPs		**2.94**	**0.56**	**2.50**	**0.08**	**2.97**	**0.79**
Power Export to grid		**3.92**	**-0.04**	**3.50**	**-0.69**	**3.92**	**-0.05**

TABLE 4.12: DSO operational limits for DER with active and reactive power control for each of the three fairness paradigms in a SOP network

4.3.6.2 Active and Reactive Power Control

The ability to control DER reactive power output (results shown in Table 4.12) has an even more limited effect than in the looped network case. This is because both the Maximum Export paradigm and the Proportional Curtailment paradigm are constrained by the apparent power rating of the grid transformer. Additionally, the Equal Dispatch paradigm is constrained by the size of the DER in feeder A, meaning that additional active power cannot be sourced. This is why only in the Proportional Curtailment paradigm does reactive power control have an impact. In this case, it allows DER to reduce the reactive power exchange with the grid slightly, which unlocks additional capacity for active power exchange.

The relaxing of the Equal Dispatch paradigm once a DER's apparent power limit has been reached may not be straightforward if there are DER that can respond to reactive power control. For example, in Table 4.6 (radial network) the smaller DER are constrained by their apparent power limit due to the necessity of absorbing reactive

VPP	Integrated Method	Maximum Export	Equal Dispatch	Proportional Curtailment
Active Power Dispatch				
Blue	\$41.67	\$41.66	\$41.67	\$34.55
Green	\$41.67	\$17.03	\$41.67	\$34.55
Orange	\$24.53	\$30.75	\$12.92	\$25.54
Total	**\$107.86**	**\$89.45**	**\$96.25**	**\$94.64**
Active and Reactive Power Dispatch				
Blue	\$41.63	\$41.48	\$41.67	\$35.41
Green	\$41.66	\$18.36	\$41.67	\$35.41
Orange	\$25.12	\$30.67	\$12.92	\$26.01
Total	**\$108.40**	**\$90.51**	**\$96.25**	**\$96.83**

TABLE 4.13: The total revenue that the VPPs in the SOP distribution network can accrue given the DSO operational limits.

power. If the larger DER are then allowed to increase their active power export, this may lead the optimisation to reduce the active power export of the smaller DER so that they can provide additional reactive power absorption so that the larger DER can export more active power. This could then lead to the small DER resources being used as reactive power support so that the larger resources can export more active power. This would seem to contradict the Equal Dispatch paradigm unless provision of reactive power support was also monetized. Alternatively, the Equal Dispatch paradigm could be implemented such that the larger resources are only free to generate more if the smaller resources reach the upper limit of their active power export capability. However, this would result in the loss of reactive power compensation from smaller resources. In radial networks, this reactive power compensation is crucial to reduce high network voltages.

4.3.6.3 VPP Commercial Operation

By using the SOP, the DSO can unlock flexibility in the network. This results in minimal additional value from DERs responding to reactive power control. The Maximum Export paradigm relies heavily on the expensive diesel generator, which results in a slightly lower revenue than Equal Dispatch and Proportional Curtailment paradigms. These two paradigms result in very similar revenue, even though the power export capability from Proportional Curtailment is larger. This is again due to the expensive nature of the diesel generator. In this case the Proportional Curtailment paradigm has high revenue, and the most equal split of revenue across all of the fairness paradigms.

4.3.7 Summary of Study on Distribution System Operator & VPP Interactions

From the results of this study it can be seen that there is no clear solution as to which fairness paradigm is the most effective. Whilst the Maximum Export paradigm manages to export the most power in all cases, depending on the network and control strategy other 'fairer' paradigms can be employed to obtain similar power export capability (such as in the radial network). It is also noted that maximising the power export of the network doesn't necessarily maximise the revenue of the entities within the network as the DSO does not consider the operating costs of the DER. This is seen in the radial network where the Equal Dispatch paradigm exports the least power but allows the VPPs to accrue the highest revenue.

The effectiveness of reactive power control on expanding DER operating limits varies depending on the network structure. While highly effective in the radial network, there was little gained by employing it in the looped network. The same is true for the SOP network, although this is mostly because the DSO has access to a resource that uses reactive power control to unlock flexibility so that the DER do not need to.

In general, the Proportional Curtailment paradigm provided the most balanced distribution of revenues amongst the VPPs. The revenue was closely linked to the total size of the VPP. The Equal Dispatch paradigm favoured VPPs with many smaller DER rather than a smaller number of larger DER. How the DSO considers assigning operating limits once the maximum power of the smaller DER is reached should also be considered further to make this a more effective paradigm in a diverse network.

These operating limits set by a DSO can also be used to in conjunction with DER that are participating in multiple markets. For example, if the VPPs are also participating in FCAS markets, so long as the operating limits are not violated when the VPP is providing FCAS, then the network constraints will be satisfied.

This study shows that the proposed framework can be utilised by multiple entities in a network. It can easily be adjusted to their needs, whether that is by adjusting which optimisations are run, altering the objective function, or adding/removing some additional entity specific constraints.

4.4 Key Remarks

4.4.1 Study on VPP Participation in Multiple Markets and Services

This study is used to highlight the efficacy of the operational framework in its proposed configuration. The framework is utilised in this study to schedule and dispatch a VPP participating in wholesale energy, six FCAS and upstream reactive power markets and providing FFR, inertia, and local network support services. It is seen that multi-market participation is key to unlocking additional revenue for the VPP. The results also show that the framework allows the VPP to effectively provide services with limited impact on VPP revenue from other services. The method for mitigating uncertainty also allows the VPP to react to uncertainty in market prices, load and RES generation with only a small loss of revenue compared with perfect knowledge of the future. The choice of segmenting the overall problem into three optimisations to maintain tractability is shown to be a necessary measure in this work. It is also shown to be of great value as it allows the framework to utilise receding horizon control over 5-minute intervals in a tractable manner. This is shown to be highly valuable in the Australian market structure.

4.4.2 Study on Distribution System Operator & VPP Interactions

In this study it is highlighted that the proposed operational framework can be easily adapted to consider different network entities, and their interactions. The operational framework can be utilised by a DSO to set operational limits for DER in the network under numerous fairness paradigms and control strategies. It can also be used by the VPPs in the network to maximise their revenue while being restricted by the operational limits set by the DSO. Additionally, the operation of network flexibility devices such as the SOP is modelled. This study is used to illustrate the capability of the framework to consider this form of modelling and analysis, and so does not provide extensive analysis and conclusions. However, what is clear is that the most effective choice of fairness paradigm can be highly dependant on network configuration and DER control strategies. They can also be limited by the operation of the non-controlled DER in the network. Further investigation is warranted into more detailed fairness paradigms (including alterations to the Equal Dispatch paradigm so that it is not limited by the smallest DER, inclusion of a cost associated with DER emissions, etc.). It should also be considered how VPPs

may be able to manipulate different fairness paradigms (i.e., by misrepresenting their available power), and what controls would be required to mitigate this.

Chapter 5

Characterisation and Utilisation of Multi-Energy Flexibility from an Electricity-Hydrogen VPP

5.1 Introduction

This chapter focuses on the multi-energy functionally of the proposed operational framework. Specifically, the conversion of electricity to hydrogen (H_2) and *vice versa*, and how this is used to increase the flexibility of a VPP to provide grid services and participate in markets. Additional flexibility is available because there is now an additional degree of freedom over which to determine the operation of the VPP. The hydrogen energy vector is likely to be much less constrained than the electrical energy vector (e.g., there is no instantaneous balancing of load and generation required, and there is the ability to storage large amount of hydrogen over extended periods). Additionally, the resources that couple the hydrogen and electrical energy vectors can be highly flexible in their operation in both energy vectors (as mentioned in Section 1.3.1.4). The ability to participate in a hydrogen market is also unlocked by this multi-energy interaction. This is a key difference between hydrogen storage, and energy storage in batteries. A VPP operator does not need to convert the hydrogen back into electricity in order to monetize it. As the hydrogen itself has intrinsic value, a VPP operator has both the option of arbitrage, or direct sale of hydrogen. As these case studies contain hydrogen-based resources, the

framework is now considering the hydrogen energy vector in addition to the electrical energy vectors (i.e., $H_2 \in \Psi^{\text{Non-elec}}$).

The first study in this chapter focuses on the characterisation of multi-energy flexibility, and how this can translate into market participation and service provision. The operational framework proposed in this thesis is applied to an electricity-hydrogen VPP to produce a thorough flexibility assessment. This multi-energy flexibility is deployed for co-optimisation of several grid services and markets. Multi-energy flexibility maps are introduced to illustrate VPP flexibility and to conduct *post hoc* analysis of its operation. The proposed framework enables optimized deployment of time-varying multi-energy flexibility in multiple downward and upward energy and reserve markets, and for the provision of inertia, fast frequency response (FFR), reactive power, and local network services, while hedging against uncertainty. This study is based on a paper written by the author *Operational Flexibility from Integrated Electricity-Hydrogen Energy Hubs* that is currently under review.

The second case study focuses on the costs to the VPP of providing contractual services. The case study deploys the operational framework on a electricity-hydrogen VPP similar to that proposed in the first case study in this chapter. This case study considers 10 representative days throughout 2016 to provide an estimate of the cost to the VPP of providing contractual services - specifically local network support. The results highlight the tight interaction between local network support and system-level market participation, and how provision of local network support can enhance the VPP's flexibility to maximize its market revenues. This is particularly relevant in the context of distribution system operation and emerging DER marketplaces that are constrained by local network limits. This study is based on a paper by written the author *Optimization of Multi-Energy Virtual Power Plants for Providing Multiple Market and Local Network Services* [165].

5.2 Study on Multi-Energy Flexibility from Integrating Electricity & Hydrogen

This study (based on a paper written by the author *Operational Flexibility from Integrated Electricity-Hydrogen Energy Hubs* that is currently under review) focuses on

the characterisation and representation of the multi-energy flexibility of an electricity-hydrogen VPP. The main consideration is how multi-energy flexibility changes when providing FFR, participating in FCAS markets, and with varying prices for hydrogen. To support this, some additional definitions are provided in the next section.

5.2.1 Multi-Energy System Flexibility

Flexibility maps are used in this study to visualize the theoretical flexibility available to the VPP, as well as *post hoc* analysis of the VPP's use of flexibility, and how that flexibility is transferred between energy vectors. The multi-energy system (MES) flexibility can be defined as the technical ability of a system to regulate multiple energy vectors subject to operational constraints [69]. The key advantage of the MES is the ability to provide flexibility through internal rescheduling of the resources (i.e., without impacting input/output of other energy vectors) henceforth referred to as *internal flexibility*. MES can also deploy energy vector arbitrage (i.e., shifting energy consumption/generation from one energy vector to another) to provide flexibility to the electrical vector externally to the MES. Such flexibility is henceforth called *external flexibility*.

Let us define

$$\mathbf{F}^{+}(t) = \overline{\mathbf{P}}(t) - \mathbf{P}(t) \tag{5.1}$$

$$\mathbf{F}^{-}(t) = \mathbf{P}(t) - \underline{\mathbf{P}}(t) \tag{5.2}$$

$$\mathbf{F}(t) = \mathbf{F}^{+}(t) + \mathbf{F}^{-}(t) = \overline{\mathbf{P}}(t) - \underline{\mathbf{P}}(t). \tag{5.3}$$

In (5.1) - (5.3), $\mathbf{F}^{+}(t)$, $\mathbf{F}^{-}(t)$, and $\mathbf{F}(t)$ represent the upward, downward, and net flexibility available for time instance t respectively. The term $\mathbf{P}(t)$ is the collection of baseline active power operating points. The terms $\overline{\mathbf{P}}(t)$ and $\underline{\mathbf{P}}(t)$ represent the collection of resource maximum and minimum generation limits, respectively. The electrical flexibility is usually classified as upward and downward flexibility, where upward flexibility requires participants to inject power to the grid. This depends upon the operational head room of the MES as given by (5.1). By contrast, the downward flexibility requires participants to consume more power and depends upon the ability of the MES to reduce its power generation or increase its power consumption as given by (5.2). Therefore, upward/downward flexibility assessment always depends upon the baseline operation of

the MES. However, the net flexibility (described by (5.3)) of a fixed set of online resources remains constant, as $\overline{\mathbf{P}}(t)$ and $\underline{\mathbf{P}}(t)$ only vary when a resource is turned on or off.

Furthermore, both upward and downward flexibility can further be classified based on whether they are provided internally (i.e., by internal rescheduling of resources whilst maintaining operation in a secondary energy vector) or externally (i.e., through changing the VPP operation in a secondary energy vector) to MES as:

$$\mathbf{F}(t) = \mathbf{F}^{+,\text{int}}(t) + \mathbf{F}^{-,\text{int}}(t) + \mathbf{F}^{+,\text{ext}}(t) + \mathbf{F}^{-,\text{ext}}(t). \tag{5.4}$$

Differentiating between internal and external flexibility is important if there are constraints on the export/import of the secondary energy vector.

When using flexibility to provide services and participate in markets, the flexibility provision also needs to account for market specific requirements such as response time and call duration. Upward and downward flexibility considering these market requirements is explicitly encoded in the framework formulation in Section 3.7.3. This ensures that there is sufficient ramping capability, as well as power and energy headroom/footroom to provide the flexibility required for these services. Internal and external flexibility are not explicitly classified in the optimisation formulation. However, the way in which the optimisation utilises flexibility will result in the use of internal or external flexibility, depending on economic incentives and technical constraints.

5.2.2 Case Study Information

The case study considers the framework operating an electricity-hydrogen VPP. The VPP is based on a remote area of the South Australian electricity network augmented with solar PV and hydrogen-based technologies shown in Figure 5.1. The resources in the VPP are given in Table 5.1. The electrolyser, hydrogen-OCGT, fuel cell and hydrogen storage located at node 26 constitute a multi-energy node, shown in Figure 5.2.

It should be noted that, as the hydrogen-based resource are modelled using (3.74), they are modelled as having a constant efficiency. This is a simplifying assumption as part of the modelling to help ensure problem tractability. This assumption of constant efficiency

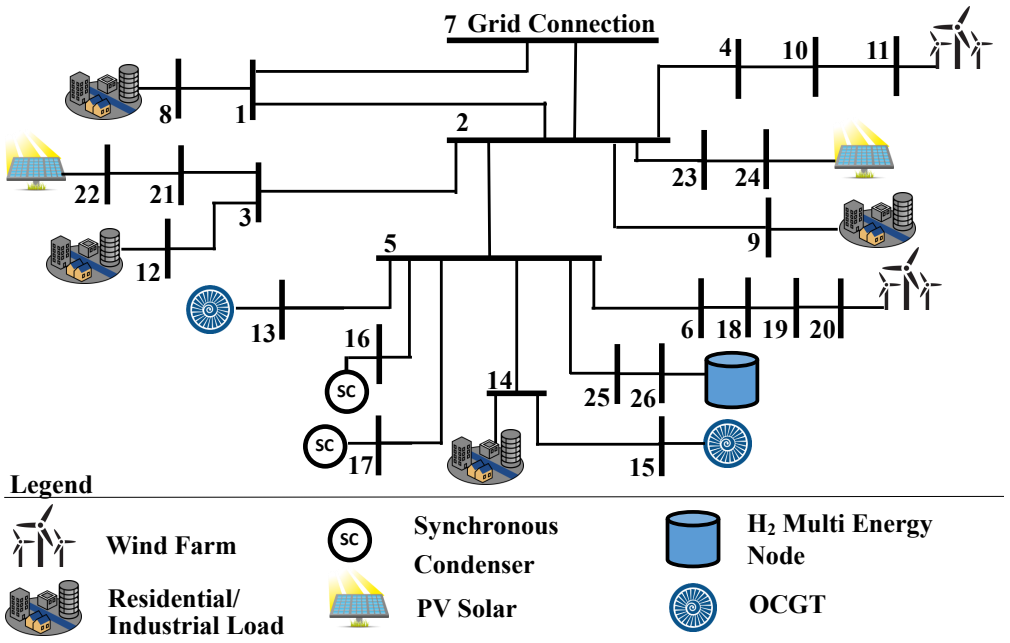

FIGURE 5.1: Single line diagram for multi-energy VPP in study on multi-energy flexibility from integrating electricity & hydrogen

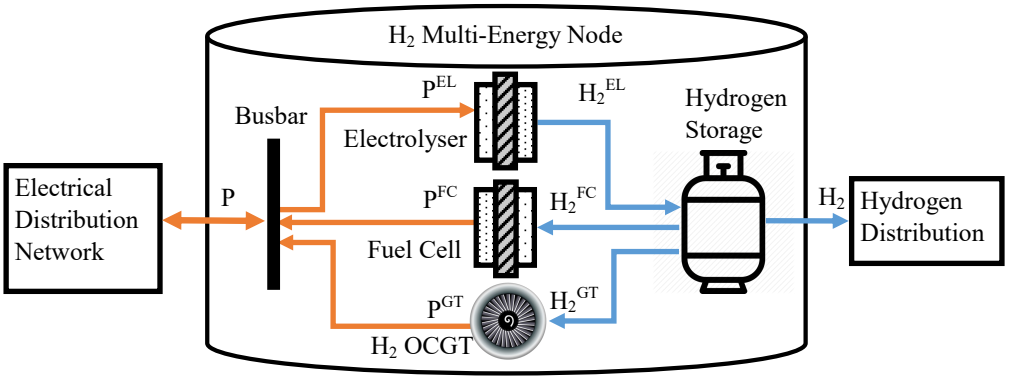

FIGURE 5.2: Formation of electricity-hydrogen multi-energy node in case study

during hydrogen production is seen in other literature [166]. However, electrolyser efficiency is impacted by variables such as temperature and current density [167]. As part of possible future work to increase the accuracy of the modelling of hydrogen generation, this constant efficiency could be exchanged for a piece-wise linear approximation. Inclusion of a standby operating mode [166] could also be included in future developments of the modelling framework.

The VPP participates in electricity and hydrogen energy markets, six FCAS markets,

Resource	**Size**	**Location**
Wind Farm 1	70 MW	Node 11
Wind Farm 2	66 MW	Node 20
Solar PV 1	30 MW	Node 22
Solar PV 2	30 MW	Node 24
OCGT 1	50 MW	Node 13
OCGT 2	23 MW	Node 15
Load 1	33 MW	Node 8
Load 2	23 MW	Node 9
Load 3	25 MW	Node 12
Load 4	66 MW	Node 14
Synchronous Condenser 1	20 MVar	Node 16
Synchronous Condenser 2	20 MVar	Node 17
Electrolyser	30 MW	Node 26
Hydrogen-OCGT	10 MW	Node 26
Hydrogen Fuel Cell	5 MW	Node 26
Hydrogen Storage	100 MWh	Node 26

TABLE 5.1: Resources in VPP for study on multi-energy flexibility from integrating electricity & hydrogen

and a reactive power market, whilst also providing local network support, FFR, inertia, and considering uncertainty over a 24-hour period. The six contingency FCAS markets have different response times, namely, fast (6 second), slow (60 second), and delayed (5 minutes), and for raise/lower frequency [19]. The local network support ensures that network voltages are maintained within allowable limits (95%-105% of nominal voltage), and ensures that thermal limits are not exceeded. FFR is provided by the electrolyser, which must be absorbing active power with a magnitude at least 50% of the PV generation in the VPP. If the FFR service is called, the electrolyser can reduce its active power absorption to provide a net increase in active power injection by the VPP. Upstream reactive power services are procured to help control transmission line voltages [21]. In this case study it is procured by a market-based mechanism, where reactive power absorption between 22:00-05:00 hours is requested to counteract the additional reactive power circulating in transmission lines overnight. This service is priced at \$1/MVArh. In Australia there is a new inertia rule that states "From 1 July 2018, TNSPs [Transmission Network Service Providers] that are Inertia Service Providers will have an obligation to provide inertia network services if an inertia shortfall has been identified" [27]. In this case study it is assumed that an Inertia Service Provider has entered into a contractual arrangement with the VPP to provide a minimum level of inertia of 330 MWs throughout the day. The price that consumers pay for their energy

is not considered in this case study, and so the VPP does not accrue any revenue from the consumers who are demanding the energy. The cost of curtailing load is set at \$500/MWh. The hydrogen storage starts the day with 50 MWh of stored hydrogen and must end the day with at least the same amount.

The historical data from 27 - 28 August 2016 is used for the case study. Prices for the wholesale energy and FCAS markets, as well as wind farm generation data are taken from AEMO [154]. Substation load is based on data from SA Power Networks [155], and the solar irradiances are from the Australian Bureau of Meteorology [156]. Uncertainty in wind speed is modelled using Weibull distribution, where a shape parameter value of $k = 2$ [157] and real-world values of mean and maximum wind speed are used. Uncertainty in solar irradiance is modelled by Beta distribution with shape parameter values of $\alpha = 4$, $\beta = 2$ [158] and real-world solar irradiance and clear sky irradiance are used for the distribution. Uncertainty in load is modelled using a Gaussian distribution with a standard deviation calculated from historical load data. The market price scenarios are taken as the dispatch prices provided by the market operator with a Gaussian distributed error [159]. 10,000 scenarios are considered to create the robust resource schedule via the robust restriction technique formalized in Appendix A. This reduces the size of the high-level problem solved and produces a robust schedule. The receding horizon dispatch optimisations each involve three scenarios: a "most likely", an "under-generation", and an "over-generation" scenario based on the same distributions detailed above. This helps to ensure solutions are still feasible under small constraint perturbations. These are updated considering the latest information each time the horizon recedes (at 30-minute intervals for the mid-level optimisation and 5-minute intervals for the low-level optimisation).

5.2.2.1 VPP service/market portfolios

This case study explores the techno-economic impact of the electricity-hydrogen VPP operating with different service/market portfolios. The VPP is participating in the wholesale energy market and providing local network support in all portfolios. However, the following considerations change between portfolios: i) FCAS participation, ii) FFR provision, and iii) hydrogen prices. The service/market portfolios considered in the case study are listed in Table 5.2, and named according to the following convention:

Portfolio Name	FCAS Provision	FFR Provision	Hydrogen Price
FCnFRn30	No	No	\$30/MWh
FCyFRn30	Yes	No	\$30/MWh
FCyFRy30	Yes	Yes	\$30/MWh
FCyFRn60	Yes	No	\$60/MWh
FCyFRy60	Yes	Yes	\$60/MWh
FCyFRn90	Yes	No	\$90/MWh
FCyFRy90	Yes	Yes	\$90/MWh

TABLE 5.2: Portfolio descriptions for the study on multi-energy flexibility from integrating electricity & hydrogen

- *FC* and *FR* indicates the FCAS and FFR services.
- *y/n* following *FC* and *FR* indicates whether VPP is participating in the particular service or not.
- Last two digits indicate hydrogen prices in \$/MWh.

For example, *FCyFRn30* represents a portfolio where the VPP is participating in FCAS markets but not providing FFR and considered hydrogen price at \$30/MWh. Moreover, the provision of reactive power to the upstream network is considered in all portfolios, except *FCnFRn30*.

5.2.2.2 Computation time

This case study contains 15 resources, 26 nodes, and 26 lines and is implemented in MATLAB with YALMIP as a parser and Gurobi as the solver. The robust restriction of the day-ahead unit commitment problem is solved in under 1 second. To show that the high-level optimisation is also suitable for use with scenario-reduction techniques, a 100-scenario optimisation was solved without the use of the robust restriction. This 100-scenario optimisation was solved in approximately 10 minutes. This is a significant number of scenarios when combined with scenario-reduction techniques, and a 10-minute solution time is acceptable for day-ahead scheduling purposes. The 30-minute receding horizon preliminary dispatch is solved on average in around 70 seconds. The 5-minute receding horizon dispatch optimisation is solved in 1-2 seconds.

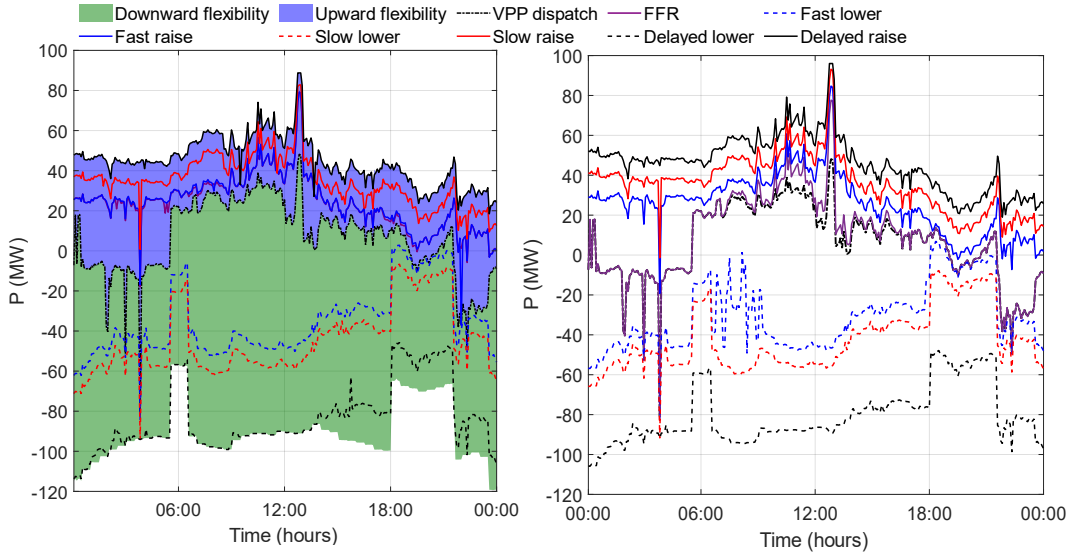

FIGURE 5.3: (Left) Available upwards/downwards flexibility and VPP participation potential for different services for *FCyFRy30*. (Right) Actual upwards and downwards flexibility committed for VPP participation for different markets and services in *FCyFRy30*.

5.2.3 Results

5.2.3.1 Operational Flexibility

From an operational perspective, the flexibility from a VPP can be divided into upward and downward flexibility depending upon the status of resources and baseline operation (i.e., dispatch) of the VPP. This can then be further quantified to calculate the VPP market participation potential and potential to provide services to the electrical grid. The flexibility potential of the VPP for *FCyFRy30* to bid into different markets is shown in Figure 5.3 (Left), whereas its actual commitment determined by the operational framework is shown in Figure 5.3 (Right). Mostly the VPP fully commits the available upwards and downward flexibility. A notable exception is FFR, which is only committed to match the required FFR provision for the PV within the VPP, as there is assumed to be no additional market for FFR. Another exception is fast lower FCAS participation between 06:00-09:00 hours. During this time the price of fast lower FCAS is intermittently \$0/MWh and so there is no incentive for the VPP to fully participate in the market.

In limited time periods the flexibility committed to participate in services is slightly greater than the available flexibility shown in Figure 5.3 (Left). This is because, for

this case study, the operational framework does not ensure voltage constraints are met in the event of FCAS being called, only that line thermal constraints are not breached. Rather, it only ensures VPP dispatch does not violate voltage constraints. If FCAS participation was called in times of these slight differences in flexibility it would entail a small, temporary violation of the local voltage constraints.

The VPP utilises its upward and downward flexibility to simultaneously participate in different services. The upward flexibility is used to provide FFR and raise FCAS services, while the downward flexibility is used to provide lower FCAS services. The periods of large reduction in downwards flexibility around 06:00 hours and after 18:00 hours are due to the electrolyser being turned off during those times. The peak in upwards flexibility just after 12:30 hours is from the electrolyser operating at a high load level to provide FFR for the PV. This illustrates the flexibility that is available from hydrogen-based resources (most visibly the electrolyser due to the size).

This flexibility also represents the extent to which the VPP can alter its operation throughout the day to responded to uncertainty. This is illustrated by the three dips in active power export in the early morning in Figure 5.3. In the pre-dispatch optimisation this operation did not occur because the VPP forecast did not predict the negative prices that occurred at these times. The VPP is using a large amount of the downward flexibility available to it to respond to this realisation of uncertain energy prices during these times.

For market-based flexibility services, such as FCAS, the VPP optimally assigns its flexibility across all markets, including energy markets (both electricity and hydrogen) to maximise its revenues. For contracted services the VPP reserves a portion of its flexibility to provide these services. For example, during the intervals with PV generation when the VPP is obligated to provide FFR. In the presence of the network constraints the flexibility from the VPP is a function of both active and reactive power. This is shown in Figure 5.4 for six representative time instances. Particularly for the time interval at 12:50 hours, where it is evident that the upward flexibility potential changes with increase/decrease of the reactive power export.

The upward flexibility provided by the VPP is chiefly through load curtailment and occasionally through headroom of the generators. The majority of the VPP's downward flexibility comes from the ability of generators to curtail their output. The large drop in

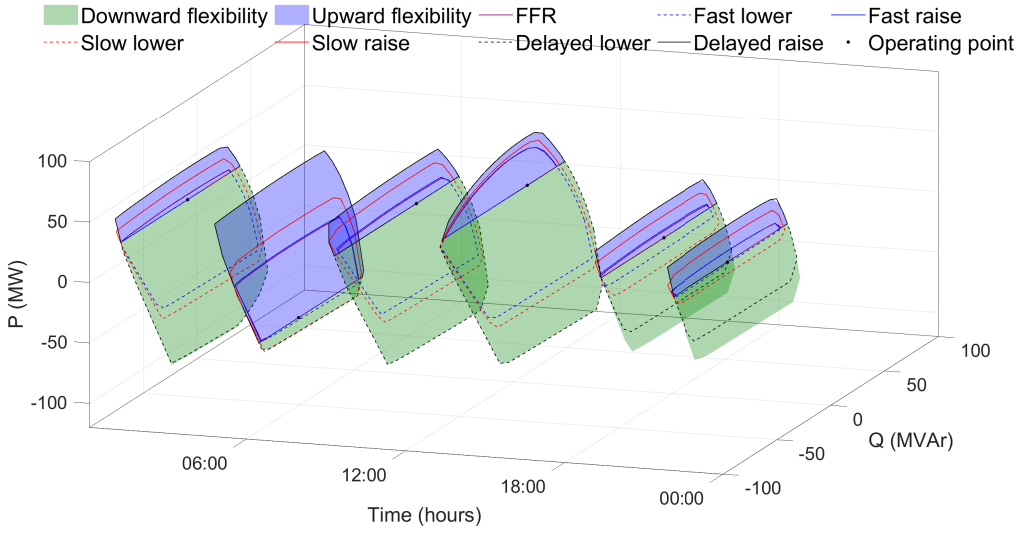

FIGURE 5.4: Dynamic active/reactive flexibility maps of the VPP for *FCyFRy30* at times 00:10 hours, 03:50 hours, 08:30 hours, 12:50 hours, 18:05 hours and 20:30 hours.

VPP dispatch at around 04:00 hours (due to the curtailment of wind energy in response to negative wholesale energy prices), results in a very small downward and a large upward flexibility potential, as illustrated in Figure 5.3. This is also shown in Figure 5.4, where VPP operation at 03:50 hours is close to the lower boundary of active power and therefore resulted in large upward flexibility potential. It is also clear from considering Figure 5.4 that the flexibility maps for 18:05 and 20:30 hours are of a smaller size than the previous ones. This is due to the electrolyser not being scheduled during these time periods. This reduction in net flexibility is as described in (5.3).

5.2.3.2 Multi-Energy Flexibility

The VPP couples electricity and hydrogen energy vectors as it includes an electrolyser, a hydrogen-OCGT and a fuel cell, and could also utilise network arbitrage flexibility (flexibility provision for one energy vector by leveraging flexibility of another energy vector [69, 168]). The individual characteristics of the three resources are shown in Figure 5.5 (left). The scale on the y-axis denotes the electrical active power converted to (negative) and from (positive) the hydrogen vector. The discontinuity in the resources P-H_2 characteristics is due to the minimum stable generation requirement of the resources and results in disjoint and non-convex operating envelopes as seen in Figure 5.5 (right). Therefore, the flexibility for MES is the ability of the system to modulate within the specific operating envelope.

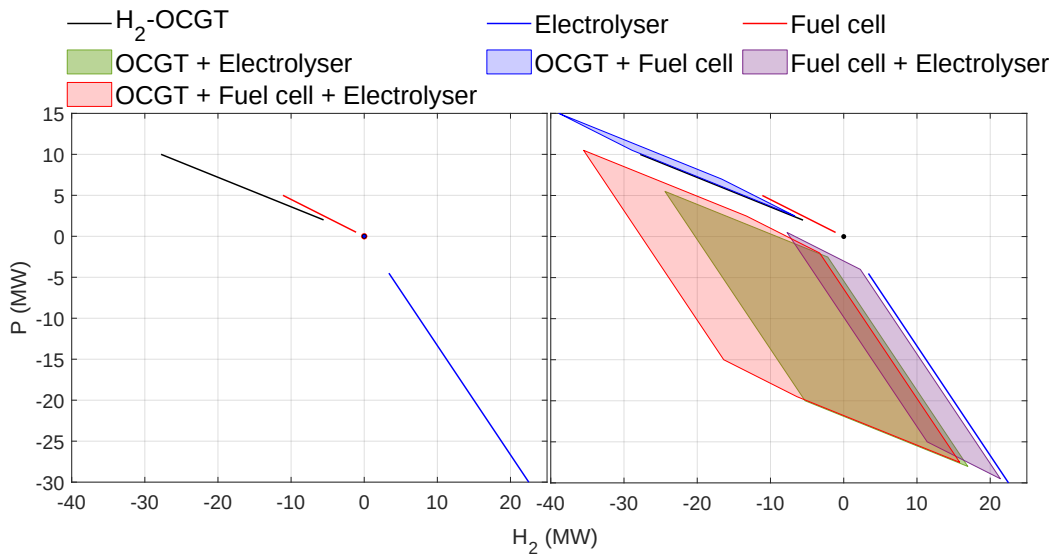

FIGURE 5.5: Individual characteristics of electricity-hydrogen coupling resources (left) and operating envelopes (right) formed by different combinations of electrolyser, fuel cell and hydrogen-OCGT, in bi-dimensional P-H_2 space.

These operating envelopes represent the aggregated dispatch points of the hydrogen-based resources and are determined here by the Minkowski summation of individual characteristics of the resources [69], as all of the hydrogen resources are located on the same node. Note that commitment variations of the hydrogen-based resources at node 26 could result in eight different combinations, and the relevant operating envelope for each interval is determined by the commitment decisions made by the high-level optimisation.

The operating envelopes are instrumental to understanding and quantifying the flexibility from energy vector interaction and applies both externally (e.g. arbitraging between electricity and hydrogen vectors) and internally (e.g. by modulating internal dispatch factors between resources). The net flexibility provided by hydrogen to the electrical vector (calculated by (5.3)) for different combinations of committed resources is mentioned in Table 5.3. In general, a larger difference between the maximum and minimum active power of the operating envelope represents higher energy vector arbitrage flexibility that can be provided to the electrical from the hydrogen vector. In case of only one online resource the flexibility can only be provided to the electrical side at the cost of hydrogen vector (i.e, externally to MES), and upward/downward flexibility vary as a linear function of active power operating point and is also linearly related to hydrogen consumption/generation. However, in the case of multiple committed resources, flexibility to the electrical vector can either be provided externally to MES or internally to

Committed Resources	**Flexibility (MW)**
None	0
Hydrogen-OCGT	8
Electrolyser	25.5
Fuel Cell	4.5
Hydrogen-OCGT & Electrolyser	33.5
Hydrogen-OCGT & Fuel Cell	12.5
Electrolyser & Fuel Cell	30
Hydrogen-OCGT, Electrolyser & Fuel Cell	38

TABLE 5.3: Flexibility available from hydrogen to electrical vector for various combination of online hydrogen resources.

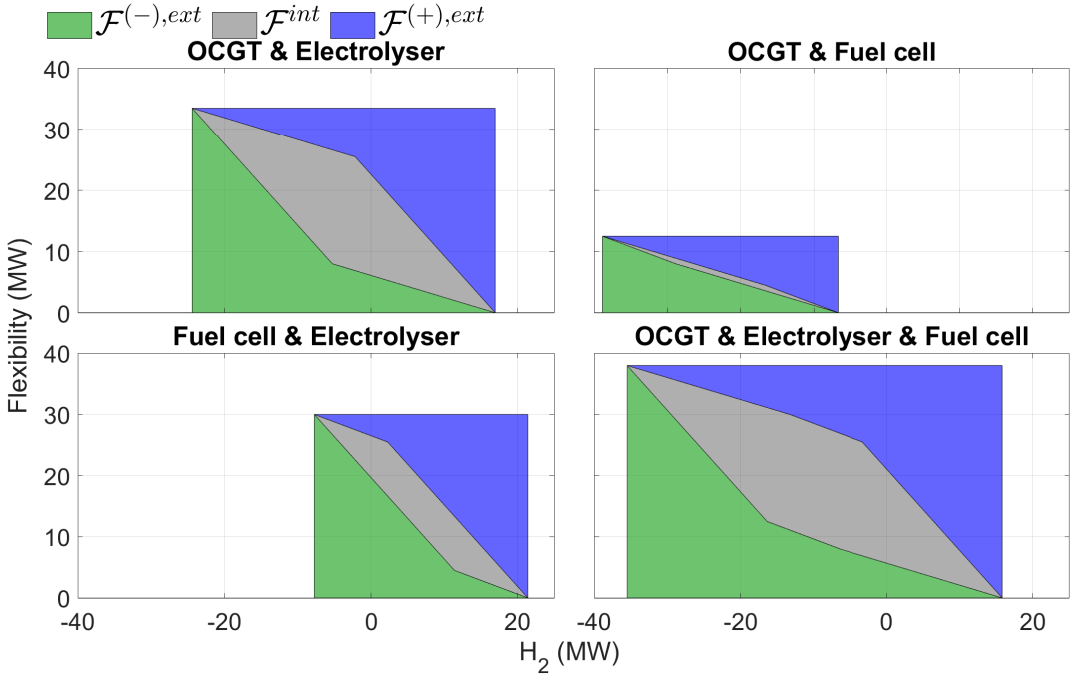

FIGURE 5.6: Internal and external flexibility potential of the VPP as a function of hydrogen consumption, for various combination of resources.

MES, that is by changing the internal dispatch factors of the resources in such a way that the aggregated hydrogen consumption remains the same.

The upward/downward external ($F^{+/-,ext}$) and internal flexibility (F^{int}) as a function of the hydrogen vector is shown in Figure 5.6. Note that the distribution of internal flexibility into upward and downward components is a function of the electrical vector operating point and cannot be defined by the hydrogen vector alone. Economically, it is more viable to provide flexibility to the electrical vector at the expense of the hydrogen

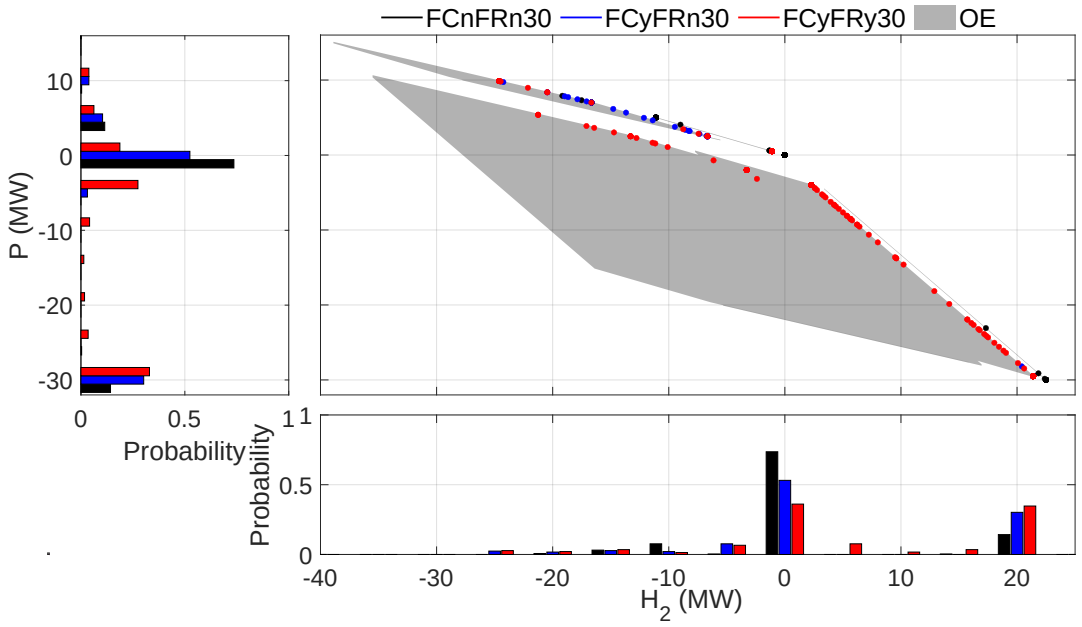

FIGURE 5.7: The aggregated dispatch points of hydrogen-based resources, against operating envelopes (OE) for *FCnFRn30*, *FCyFRn30*, and *FCyFRy30* along with the probability density functions for operation in (left) active power and (bottom) hydrogen vectors.

vector (flexibility external to MES), rather than through dispatch factor modulation (flexibility internal to MES) to minimize losses, and also because the hydrogen system is more flexible due to sufficient local storage and lack of network constraints. The commitment of the electrolyser with either hydrogen-OCGT or fuel cell results in higher losses, and therefore the electrolyser will be committed along with the OCGT or fuel cell only if there is sufficient financial incentive available from the various services and markets.

The aggregated operating points of the hydrogen resources in the P-H_2 bi-dimensional space for the study day are shown in Figure 5.7, for *FCnFRn30* (black), *FCyFRn30* (blue), and *FCyFRy30* (red). The time series upward/downward flexibility and aggregated operating point of the hydrogen resources is shown in Figure 5.8. In *FCnFRn30* (Figure 5.8 (top)), the operation of the hydrogen-based resources is solely governed by the electricity and hydrogen prices (as VPP is participating in energy markets only). Therefore, in this case there is no instance where the electrolyser is committed along with either hydrogen-OCGT or fuel cell, evident from the confinement of the black dots either to electrolyser or hydrogen-OCGT and fuel cell operating envelopes. In *FCyFRn30*, where the VPP is also providing FCAS along with participation in energy markets, the combination of electrolyser, hydrogen-OCGT and fuel cell is dispatched to maximise

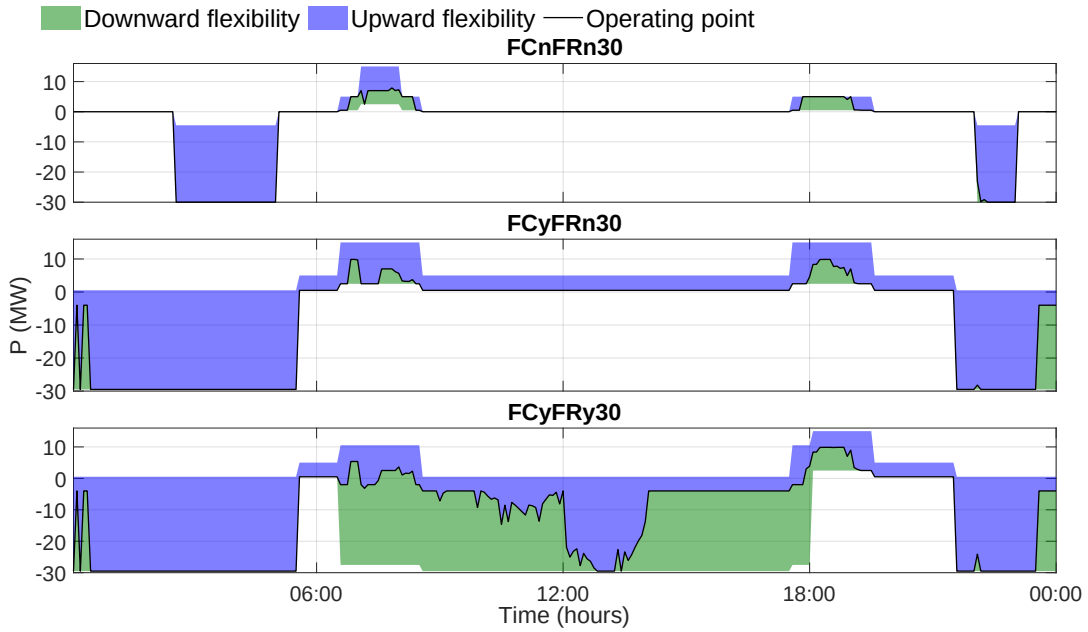

FIGURE 5.8: Upward flexibility and downward flexibility contribution from the hydrogen-based resources for (top) *FCnFRn30*, (middle) *FCyFRn30*, and (bottom) *FCyFRy30*.

revenue, based on prices of different markets, as shown by the probability histograms in Figure 5.7, and time series of Figure 5.8 (middle). This represents an increase in operational hours of the hydrogen-based resources. In *FCyFRy30*, the VPP is also providing FFR services. During intervals of high electricity price and PV generation the combination of hydrogen-OCGT and fuel cell is dispatched to generate revenues from the energy market and the electrolyser is online to fulfil FFR obligations, as represented by a few red operating points in the largest sub-region in Figure 5.7. The Figure 5.8 (bottom) and probability density function of Figure 5.7 also show a further increase in the activity of the hydrogen-based resources, represented by the shift in the peak of probability density functions towards negative values of active power and positive values of hydrogen.

Collectively from Figure 5.7 and Figure 5.8 it can be observed that there is a direct link between an increase in electrolyser operation and FFR provision. Moreover, VPP participation in FCAS (i.e *FCyFRn30* and *FCyFRy30*) results in the fuel cell being scheduled at the same time as the electrolyser and usually dispatched at minimum power to provide maximum upward flexibility. This indicates a greater associated value for upwards flexibility than the cost of hydrogen and the electrical inefficiency associated with the fuel cell and electrolyser operating at the same time. This phenomenon is not

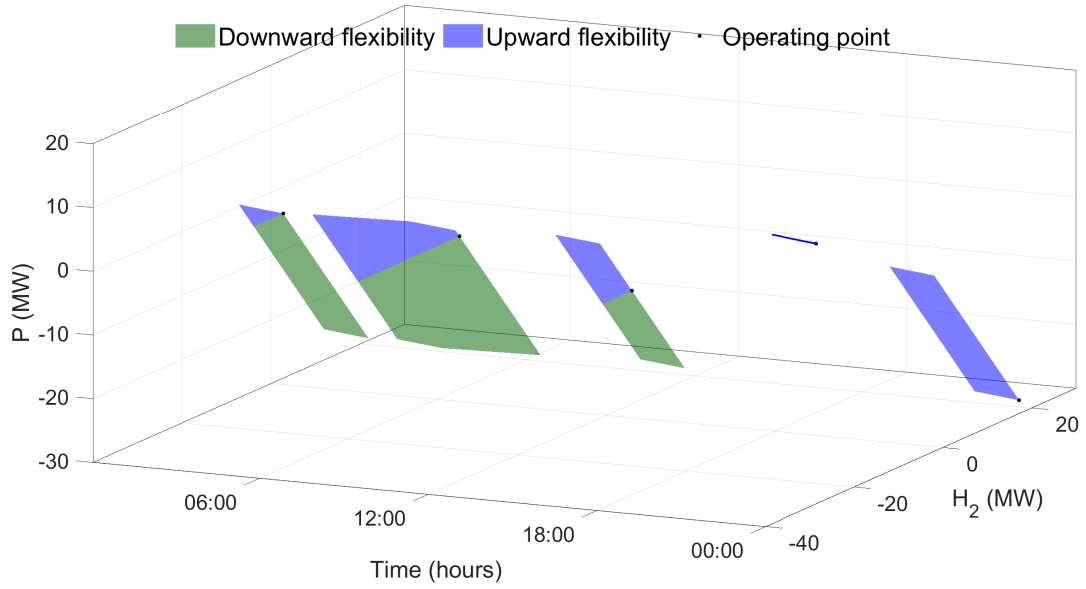

FIGURE 5.9: Flexibility maps in power and hydrogen vector space, of the hydrogen-based resources for *FCyFRy30* for time instances 00:10 hours, 07:10 hours, 11:20 hours, 19:40 hours and 23:20 hours

present in *FCnFRn30* where the VPP only participates in the energy market. This is due to the lack of financial incentives.

Each time interval represented in Figure 5.8 is representing the active power dimension of the corresponding operating envelope, seen in Figure 5.9 for five intervals. This again highlights that the net availability of multi-energy flexibility is controlled by the scheduling of resources. There is also clearly a large difference in available flexibility when multiple resources are scheduled concurrently (compare net flexibility at 07:10 hours vs net flexibility at 19:40 hours).

5.2.3.3 VPP Multi-Market Revenues

Beside energy and FCAS markets (considered for economic analysis in this section), the VPP can also participate and generate revenues from other non-market services, such as inertia provision, FFR, and local network support. The provision of these services will influence the operation of the VPP. Therefore, the economic analysis presented in this section should be considered alongside possible contractual service revenues. However, the aim of the economic analysis in this case study is not to provide a comprehensive assessment of VPP revenue for cost-benefit analysis or formation of business cases. The

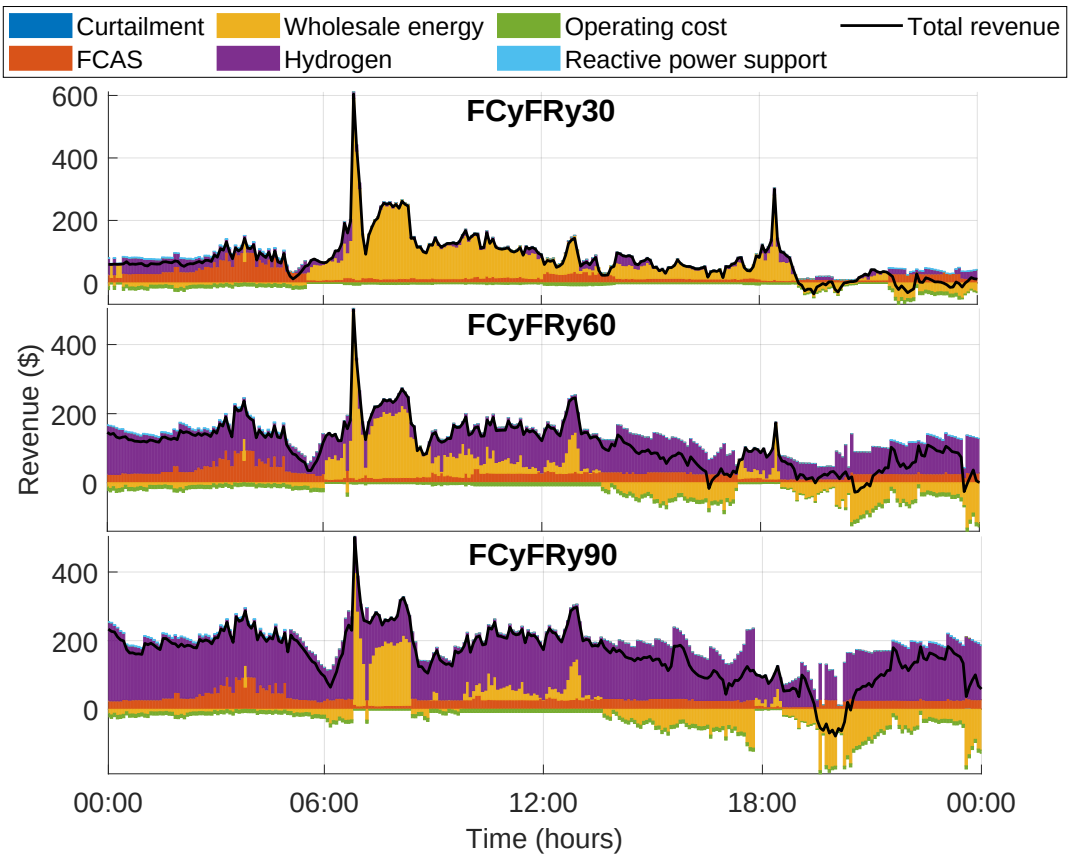

FIGURE 5.10: Revenue generation across case study days with differing hydrogen prices

aim of the economic assessment in this case study is to examine how the utilisation of VPP flexibility changes when exposed to different market/service portfolios and prices.

The different revenue generation strategies of the VPP with different hydrogen prices are shown in Figure 5.10. When hydrogen price is \$30/MWh there is very limited hydrogen revenue, as the average wholesale energy price for the case day is approximately \$40/MWh. Therefore, considering conversion losses it is not often economically viable to convert electricity to hydrogen to sell. Instead, if there is hydrogen being generated (for example by the electrolyser providing FFR) it is more likely to be converted back into electricity to provide electrical energy arbitrage. At a hydrogen price of \$60/MWh there is a marked increase in hydrogen production throughout the day as the hydrogen price is now sufficiently higher than the average wholesale energy price. There are large periods throughout the day when creating hydrogen to sell is economically viable. This is seen when comparing *FCyFRy30* to *FCyFRy60*. The latter now buys wholesale energy for much of the afternoon, where the former sells wholesale energy. When hydrogen is priced at \$90/MWh the VPP generates and sells even more hydrogen, importing large

amounts of energy in the latter half of the day to do so. The VPP operation is also less sensitive to the fluctuations in wholesale energy prices. This is because the high hydrogen price means that the change in electrical energy price required to economically justify conducting electricity-hydrogen-electricity arbitrage is very high. This can be seen by the reduced energy revenue peaks at 07:00 hours and 18:30 hours for *FCyFRy90*. It can also be seen that during the middle of the day in *FCyFRy60* and *FCyFRy90* the VPP is generating additional revenue from FCAS markets. As the hydrogen-based resources are scheduled more frequently in these cases, the net flexibility of the VPP is larger, and therefore it has greater capability to participate in these FCAS markets.

When hydrogen has a low value the VPP arbitrages electrical energy across time to sell electricity at its highest price at the cost of hydrogen production. When hydrogen value increases the VPP moves towards arbitraging electrical energy across energy vectors to sell hydrogen by actively buying electricity. This shows how the VPP is optimally arbitraging across multiple markets and energy vectors depending on the relative prices of the markets.

The impact of changing hydrogen prices, and provision of FCAS and FFR on the total daily revenue is shown in Figure 5.11. Access to more outlets for the VPP to monetise its flexibility (i.e. FCAS market and hydrogen market participation) leads to greater revenue. Comparing revenue from *FCnFRn30* and *FCyFRn30* shows that participation in FCAS markets also leads to an increase in hydrogen revenue. The additional revenue the electrolyser can accrue from FCAS while operational acts to effectively reduce the threshold energy price at which the VPP can profitably create hydrogen to sell. FCAS revenue is substantial across all cases and varies relatively little, highlighting the non-competitive relationship between FCAS and energy markets. The VPP avoids the need for costly load curtailment during the case studies, and the reactive power support price is very small compared to the other markets. Therefore, neither appear prominently in Figure 5.11. The provision of FFR reduces VPP overall revenue slightly, due to some VPP flexibility being reserved to provide that contractual service. However, it is again noted that the revenue that the VPP would accrue from contractual services, and from selling energy to consumers, has not been considered in this analysis. Increasing the hydrogen price reduces the amount of revenue the VPP generates from the wholesale energy markets, and eventually at a hydrogen price of \$90/MWh the VPP actually has a net loss in the wholesale energy market. This is due to the large amount of energy

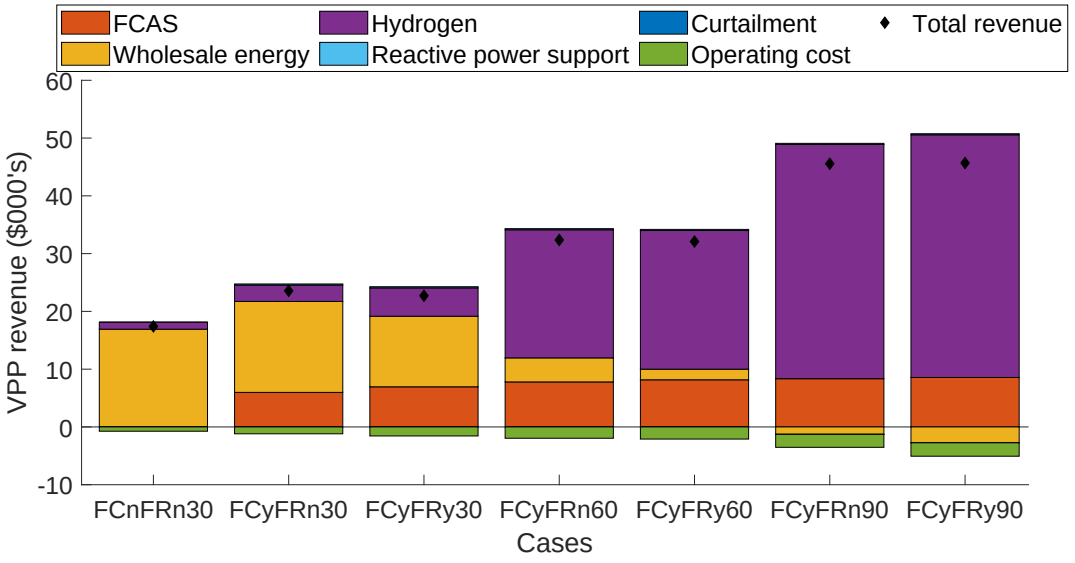

FIGURE 5.11: Total daily revenue of the VPP across cases

being procured to create hydrogen. It is apparent that the value obtained from selling hydrogen in this case vastly outweighs the loss in revenue from the wholesale energy market.

5.2.4 Summary of Study on Multi-Energy Flexibility from Integrating Electricity & Hydrogen

The multi-market VPP operational framework that is proposed in this work allows the multi-energy VPP in this case study to provide network services whilst participating in multiple markets to maximize VPP profit considering uncertainty. The increased flexibility from aggregating multi-energy DER into a VPP is shown through flexibility maps and allows DER to be used to effectively provide network services. Furthermore, this flexibility is considered across multiple time scales and can be optimally divided amongst multiple services and markets to maximise the revenue accrued by the VPP. Utilising multiple energy vectors allows a VPP to conduct inter-energy arbitrage as well as intra-energy arbitrage to unlock further flexibility. If there are multiple resources pairing energy vectors it is also possible to provide flexibility in one vector (electricity) without changing the net operation in the other vector (hydrogen). The VPP can manage multiple energy vectors; can effectively respond to changing price signals; and can prioritise energy vectors/markets depending on their value.

Resource	**Size**	**Location**
Wind Farm 1	70 MW	Node 11
Wind Farm 2	66 MW	Node 20
Solar PV 1	30 MW	Node 22
Solar PV 2	30 MW	Node 24
OCGT 1	50 MW	Node 13
OCGT 2	23 MW	Node 15
Load 1	33 MW	Node 8
Load 2	23 MW	Node 9
Load 3	25 MW	Node 12
Load 4	66 MW	Node 14
Capacitor Bank 1	20 MVar	Node 16
Capacitor Bank 2	20 MVar	Node 17
Electrolyser	30 MW	Node 26
Hydrogen-OCGT	10 MW	Node 26
Hydrogen Fuel Cell	5 MW	Node 26
Hydrogen Storage	100 MWh	Node 26

TABLE 5.4: Resources in service provision from multi-energy flexibility case study VPP

5.3 Study on Cost of Service Provision from Multi-Energy Flexibility

The first case study in this chapter establishes that multi-energy flexibility can be effectively used to participate in market and provide services. This second case study focuses on the costs to the VPP of providing services, specifically local network support. Additional to the methodology detailed in Chapter 3, this case study also considers capacitor banks in the VPP network. To account for the voltage dependence of the reactive power output of capacitor banks, (5.5) is included in the mid-level optimisation and low-level optimisation for capacitor bank modelling.

$$\zeta_{k,t}\underline{Q_k}v_{k,s}(t) \leq Q_{k,s}(t) \leq \zeta_{k,t}\overline{Q_k}v_{k,s}(t) \tag{5.5}$$

5.3.1 Case Study Information

This study considers an electricity-hydrogen VPP illustrated in Figure 5.12 (very similar to the VPP considered in the first case study in this chapter) with constituent resources as detailed in Table 5.4.

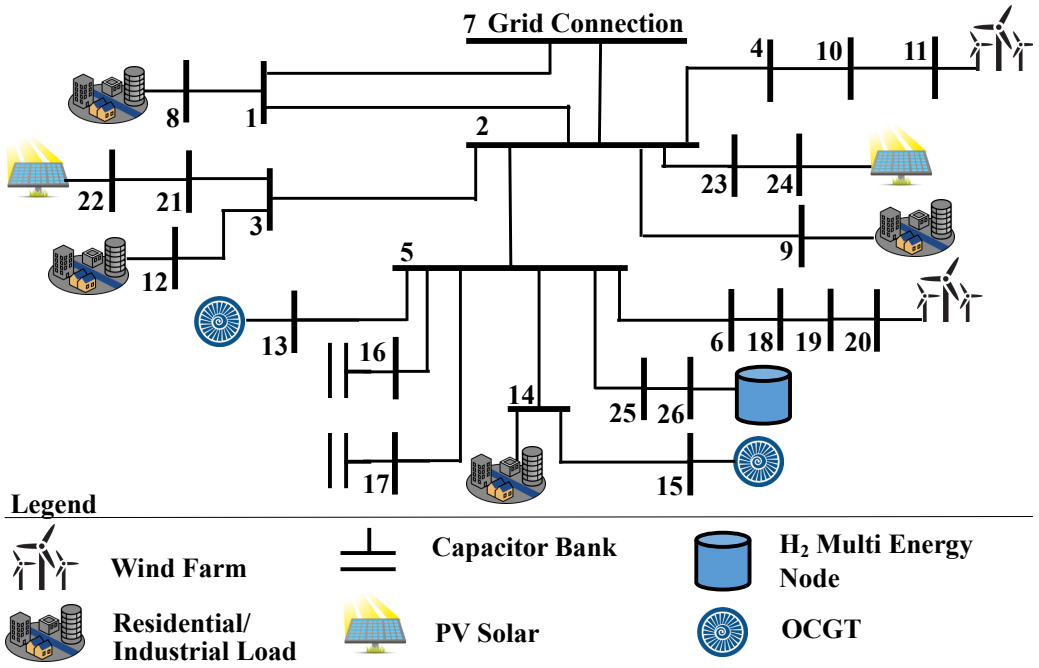

FIGURE 5.12: Single line diagram for multi-energy VPP in service provision from multi-energy flexibility case study

The VPP participates in wholesale energy, hydrogen, six FCAS markets, and an upstream reactive power market. This multi-market participation is key to determining an accurate value for the cost to the VPP of providing local network support. The VPP is providing local network support by ensuring that network voltages are maintained within allowable limits (95%-105% of nominal voltage), and ensuring that thermal limits are not exceeded. To assess the annual cost of providing local network constraint alleviation, the case study considers ten representative days for the year of 2016. These are a representative weekday and non-weekday for each season as well as a high-price and a low-price day. The dates, excess RES, and average wholesale energy price for each representative day is shown in Table 5.5. Historical prices for the wholesale energy and FCAS markets, as well as wind farm generation data are taken from AEMO [154]. Substation load is based on data from SA Power Networks [155], the solar irradiances are from the Australian Bureau of Meteorology [156]. It is assumed that hydrogen can be sold at \$30/MWh and that the cost of curtailing load is \$500/MWh. The hydrogen-based resources are located at node 26, and create the multi-energy node illustrated in Figure 5.2. The level of stored hydrogen is assumed to be 50 MWh at the start of the day, and must end the day with at least the same amount of stored energy.

Representative Days of 2016	**Date**	**Excess RES Generation (MWh)**	**Average Energy Price ($/MWh)**
Spring Weekday	23 November	-253	47.65
Spring Weekend	19 November	-296	37.46
Summer Weekday	23 December	-201	41.15
Summer Weekend	30 January	265	22.86
Autumn Weekday	21 March	-499	55.30
Autumn Weekend	20 March	-472	55.28
Winter Weekday	10 June	-138	53.81
Winter Weekend	18 June	-409	71.05
High Price Day	01 November	-285	84.93
Low Price Day	22 May	629	12.97

TABLE 5.5: The representative weekday and weekend day for each season as well as a high price day and a low price day. The amount of excess RES generation after VPP loads have been considered is also shown (a negative value infers there is more load than RES generation throughout the day). The average wholesale energy price for the day is also included.

5.3.1.1 Computation Time

This case study is implemented in MATLAB with YALMIP as a parser and Gurobi as the solver. For the considered case study the daily high-level optimisation considers eight scenarios and contains approximately 300,000 variables and approximately 755,000 constraints. Once posed, this optimisation is solved in 7-8 seconds. The mid-level optimisation considers three scenarios and contains approximately 200,000 variables and approximately 325,000 constraints. On average, the solver finds a solution to this problem in 90 seconds. The low-level optimisation considers three scenarios and contains approximately 25,000 variables and approximately 37,000 constraints and is solved and checked by AC load flow in under a second. It is worth noting that through all 480 mid-level optimisations that were conducted to model the 10 representative days, there was a single optimisation that failed to solve as Gurobi encountered a numerical issue. However, the receding horizon approach allows the framework to assign the VPP operating points from the previously solved optimisation for the current time step, and then conduct a new optimisation once the horizon recedes. This is an additional benefit of conducting the optimisations in a receding horizon fashion.

It is clear from the solution time for the high-level optimisation of 7-8 seconds that this

approach is suitable for larger networks than this current test network. There is also scope to increase the size of the problem, for example by reducing the time step length in the optimisation. However, care should be taken when considering these changes as doing so increases the number of integer variables in the MILP, increasing the computational complexity of the problem.

5.3.2 Results

5.3.2.1 Revenue Streams from Representative Seasonal Days

For the representative autumn weekday, the VPP contains 1.35 GWh of demand, and 1.08 GWh of renewable generation. The energy market has a peak of $328/MWh and an average price of $55.30/MWh. Figure 5.13 shows how the revenue/costs of the VPP change throughout the day for the representative autumn weekday, responding to changing market prices and load requirement/generation availability to maximise overall profit, whilst providing local network support. For most of the day there is less renewable generation than load, therefore the VPP must import energy from the grid or generate power from OCGTs. However, due to wholesale energy price spikes during the early morning, the VPP manages to reduce its energy import to reduce costs (and for a brief window export energy to generate revenue) by using the stored hydrogen to generate energy through the hydrogen-OCGT as well as by using a traditional thermal OCGT. The use of these operationally expensive OCGTs is the cause of the increased operating cost between 05:00-07:00 hours. In the middle of the day the VPP revenue is positive due to the PV providing excess energy to the VPP which is sold to the grid. The electrolyser is scheduled during low-price times in the morning and evening to generate hydrogen for the hydrogen-OCGT to use when it is scheduled during the morning and evening price peaks. It can also be seen that the VPP is consistently generating positive revenue from the FCAS markets throughout the day, albeit a relatively small amount.

Looking at the representative winter weekday revenue in Figure 5.14 as another example of VPP operation it can be seen that there is more variation in the participation and revenue from different markets. In the early part of the day, the VPP leverages the low wholesale energy prices to generate hydrogen. This is sold in the hydrogen market, as well as being used by the hydrogen-OCGT and fuel cell to generate electricity to respond

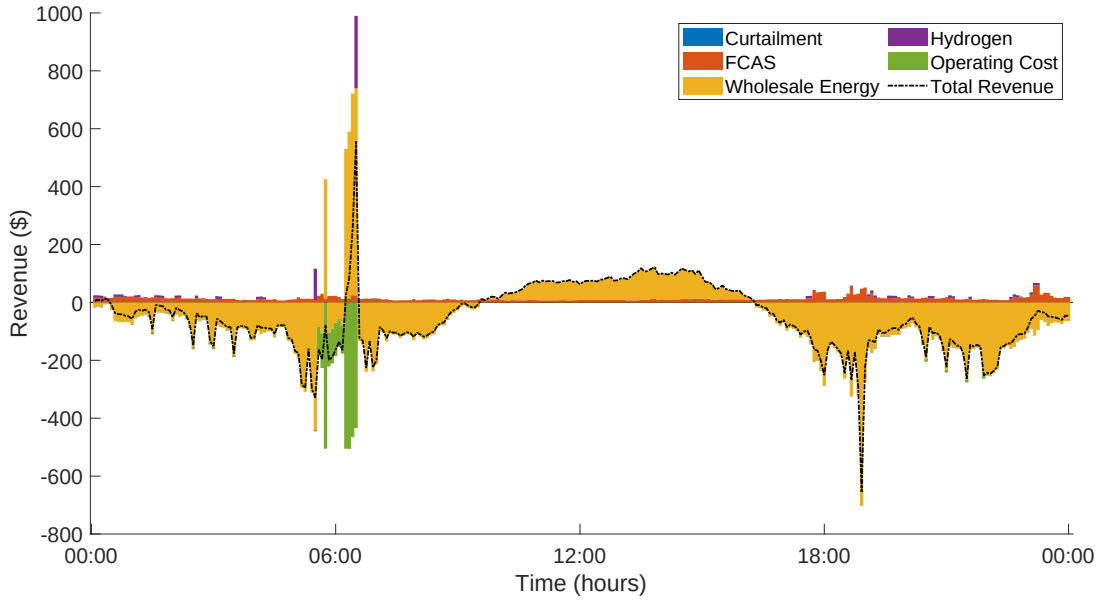

FIGURE 5.13: VPP revenue streams throughout representative autumn weekday

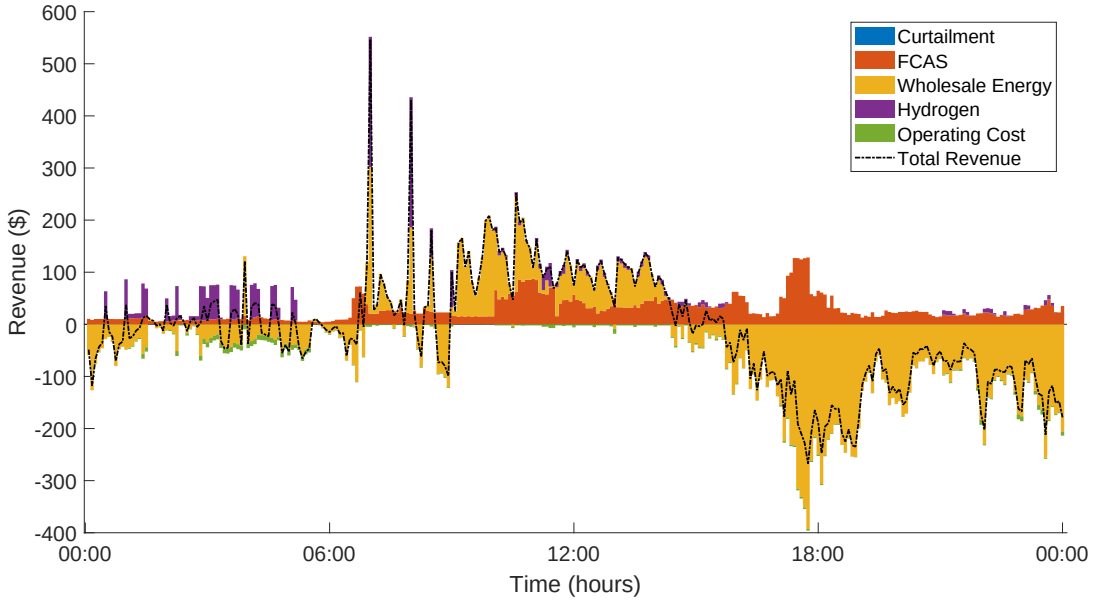

FIGURE 5.14: VPP revenue streams throughout representative winter weekday

to the spikes in wholesale energy price between 06:00 - 09:00 hours. However, unlike the representative autumn weekday, in this case the price spike is not large enough to warrant to dispatch of the traditional thermal OCGTs. In the evening the VPP does not have sufficient generation to cover all of the load it supplies. Therefore, it needs to buy energy from the grid. However, it does manage to generate significant profit from the FCAS markets during this time.

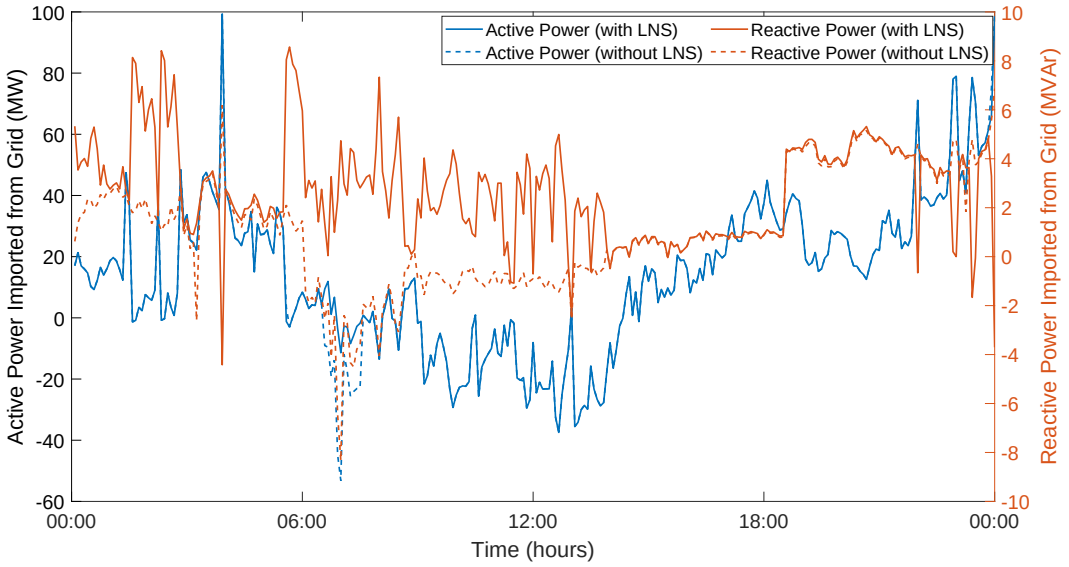

FIGURE 5.15: Active and reactive power imported by VPP on representative autumn weekday, with and without provision of local network support (LNS)

5.3.2.2 Provision of Local Network Support

Figure 5.15 shows the active and reactive power absorbed by the VPP from the grid on the representative autumn weekday when the VPP is providing local network support, and when it is not. The ability of the VPP to export active power is not hindered by the requirement to provide local network support, except for a couple of hours after 06:00 hours when the OCGTs are exporting. Apart from this, local network support can be provided solely by controlling the reactive power injection and absorption of the VPP resources. This can be seen in Figure 5.15 where the reactive power imported from the grid will often mirror the active power import when local network support is being provided.

Changing the VPP reactive power operating point to provide local network support can cause the active power operating point to move, and this could effect the capability of the VPP to participate in active power markets. Figure 5.16 shows the flexibility maps of the VPP (created using the method proposed in [70]) at various times during the representative autumn weekday. These maps show the feasible operating region (FOR) of the VPP at different times, as well as the magnitude of the possible active/reactive power bids that the VPP could offer to six contingency FCAS markets. In general, the provision of local network support has little or no effect on the active power set point of the VPP. As such it has minimal effect of the FCAS capability of the VPP. In

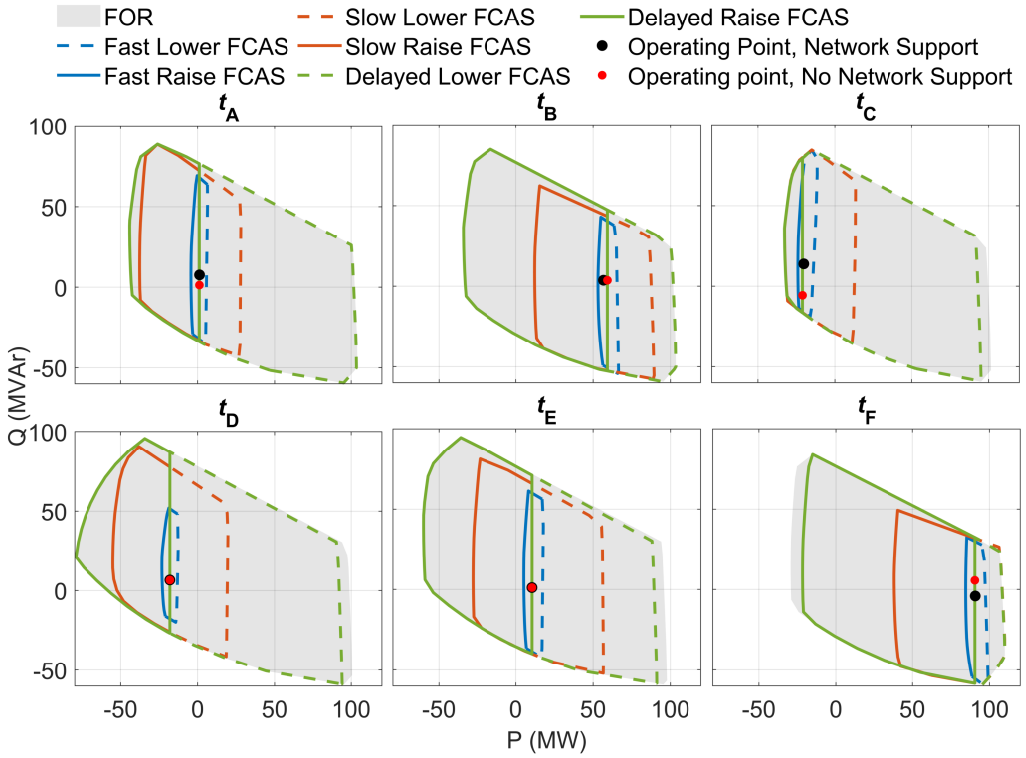

FIGURE 5.16: Flexibility maps for FORs of the VPP for representative autumn weekday for active and reactive power absorbed by the VPP. t_A to t_F are 00:20, 03:25, 06:10, 12:25, 16:35 and 21:50 hours respectively.

Local Network Support	Minimum Voltage (p.u.)	Maximum Voltage (p.u.)	Time Spent Outside Limits
Yes	0.9504	1.0543	0.99%
No	0.8797	1.1864	8.22%

TABLE 5.6: Minimum and maximum voltage magnitudes in the network for autumn weekday when local network support is provided and when it is not.

general it can be seen from Figure 5.16 that increasing generation of real/reactive power reduces the VPP's ability to generate reactive/real power. This is expected due to the overarching limits on apparent power flow/generation in conjunction with nodal voltage limitations. The largest change in operating point can be seen in Figure 5.16 t_C. This is around the time that the active power operating point of the VPP when providing local network support deviates from the active power operating point when it does not (shown in Figure 5.15).

The effectiveness of this local network support is evident from Table 5.6. It shows the range of local network voltages with and without local network support for the autumn weekday. These voltage ranges are also represented visually in Figure 5.17. It should be

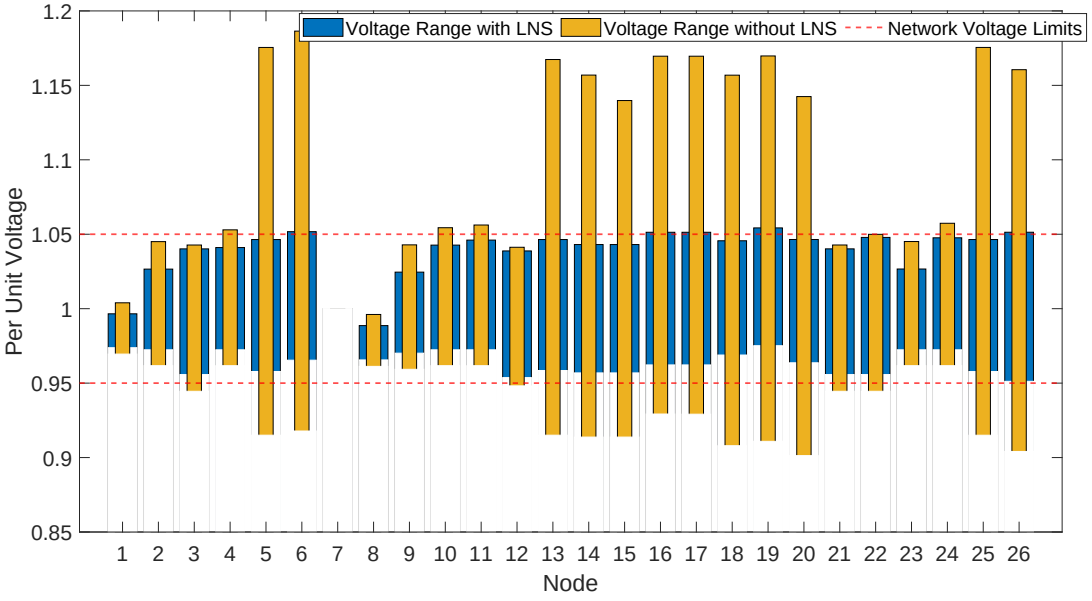

FIGURE 5.17: The voltage range of each node in the network for the representative autumn weekday when the VPP is providing local network support (LNS) and when it is not.

noted that these values are obtained from the non-convex AC load flow verification stage of the framework. The fact that when providing local network support the voltages can be slightly outside the set voltage limits highlights the slight loss of accuracy from using a relaxation of the power flow equations. However, these voltage violations are few, and very close to the limits. Therefore, this could be addressed by slightly tightening the limits in the convex optimisation to allow for this small inaccuracy. When local network support is not provided, the voltages have a much larger range of values and spend more time outside of the nominal voltage band. The system operator might therefore force the VPP to curtail its generation to maintain the network operation within allowable limits. So, this local network support can also be viewed as enlarging the operational envelope of the VPP to be able to provide more active power services without risk of curtailment by the system operator.

5.3.2.3 Cost of Provision of Local Network Support

The annual revenue from different operational aspects and the net revenue of the VPP with and without local network support is shown in Figure 5.18, where a negative amount of revenue represents cost. The annual net revenue is calculated as the revenue minus cost over a year. Over the course of the year, considering load and renewable generation

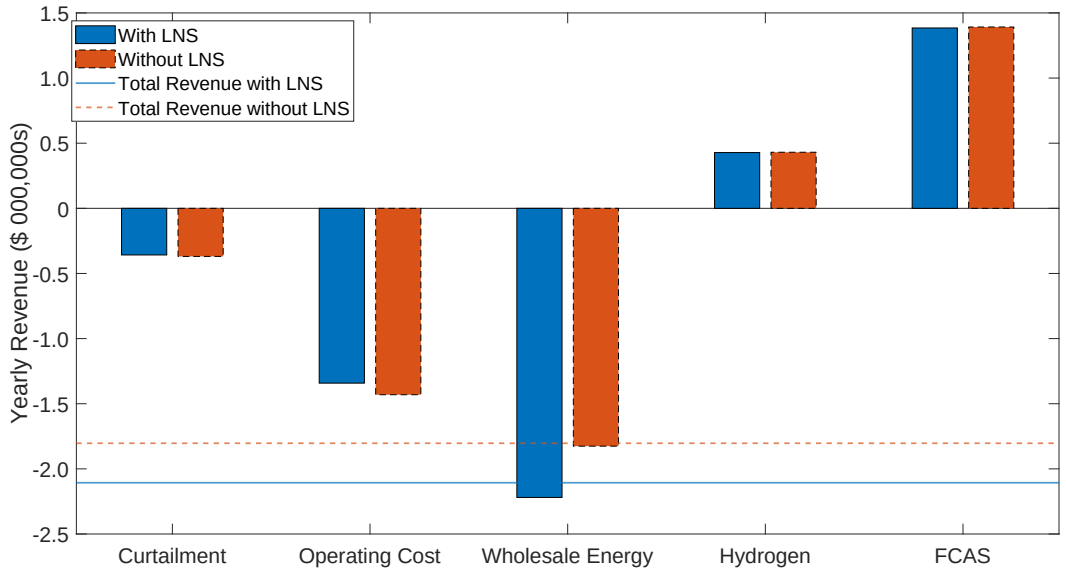

FIGURE 5.18: Estimate of the yearly VPP revenue broken into the different costs and revenue streams (without considering revenue for energy sold to energy retailers)

in the VPP, it would need to access an additional 50 GWh of energy (as revenue from selling energy to retailers downstream is not included in this graph), either by buying the energy from the grid or using its non-renewable generation. This is why the VPP has an annual net cost rather than an annual net revenue. When providing local network support, the net cost of the VPP increases by about $303,000 compared with the no local network support case. The main differences come from the wholesale energy market and device operation costs, while the differences in revenues from FCAS, hydrogen export and costs of load curtailments are minor. An increase in the costs of wholesale energy market and a decrease in device operation cost are observed when considering local network support. This is mainly because, in order to provide local network support, the active power export/import of VPP can be constrained, especially during the extreme high/low wholesale price periods (it is noted that 95% of the yearly revenue that is lost is from the High-Price day). As a result, there is a reduction in the revenue of exporting/importing electricity during extreme high/low price periods, when the VPP can obtain most revenues. Meanwhile, as less electricity is exported, there is also a reduction in the device operation costs. It should be noted that for the cases when the VPP does not provide local network support, forced curtailment by the network operator has not been considered. This occurrence could greatly reduce the revenue of the VPP when not providing local network support.

To provide a more comprehensive yearly revenue analysis it is assumed that the VPP has

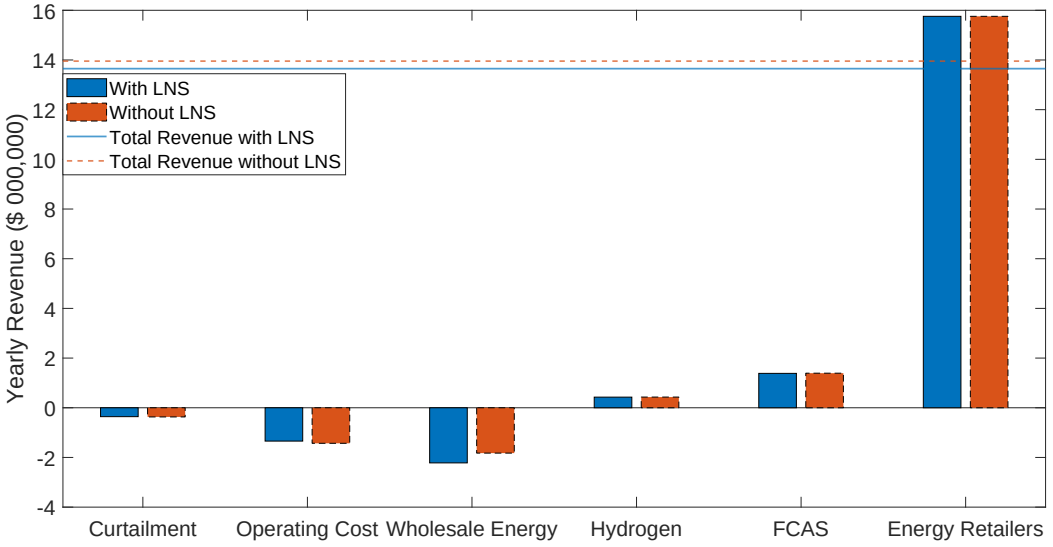

FIGURE 5.19: Estimate of the yearly VPP revenue broken into the different costs and revenue streams with consideration of revenue for energy sold to energy retailers

a contractual agreement with retailers downstream of the load substations to sell energy at a flat rate of $30/MWh (in the previous analysis no revenue from selling energy to the downstream consumer was considered). As can be seen in Figure 5.19 this has a massive impact of the yearly revenue of the VPP (although due to the contractual nature of the arrangement, this does not impact the optimisation results). In fact, this energy sold to energy retailers is worth over $15 million each year. This indicates that the VPP would be accruing revenue over the year. The absolute impact of providing local network support is still the same, costing the VPP about $303,000 a year. However, this is now a much lower percentage of VPP revenue, representation about 2.2% of VPP yearly revenue. The value from this assessment could be used by a VPP operator to inform the price they would associate with local network support contracts they may enter into.

The impact of considering energy sold to retailers on the value-stack of the VPP for each of the 10 representative days is shown in Figures 5.20 and 5.21. It can be seen that summing the revenue from selling energy to retailers and the cost of buying wholesale energy results in net revenue in all of the representative days. Additionally, the average wholesale price for 2016 was higher than $30/MWh, so the VPP could possibly generate even more revenue by increasing the price of the contract with retailers, reducing the percentage loss of providing local network support even further. However, this would not change the absolute cost of providing local network support. Figures 5.20 and 5.21 also

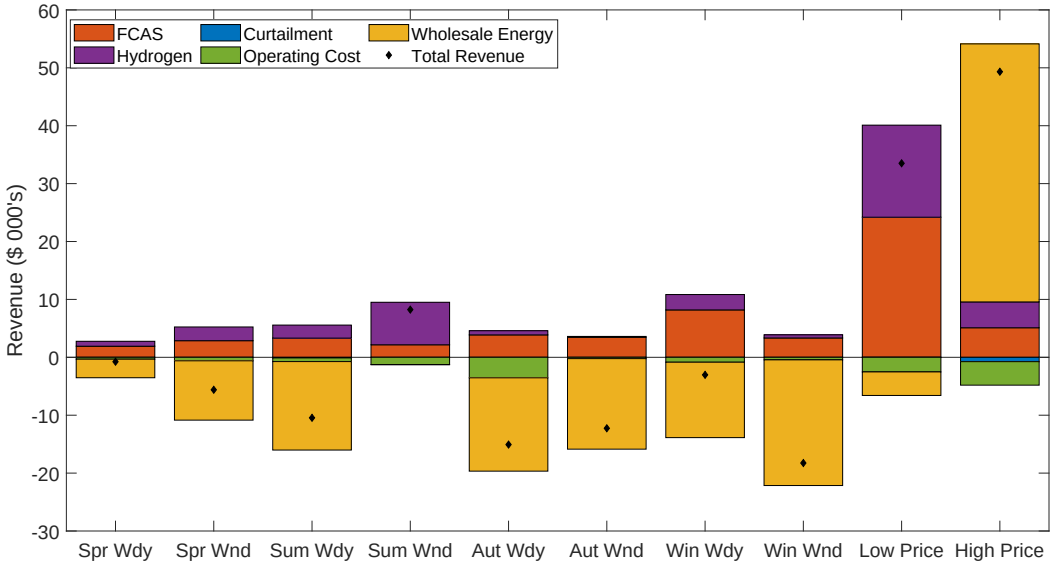

FIGURE 5.20: The total daily revenue of the VPP for each of the 10 representative days (without consideration of revenue from energy retailers)

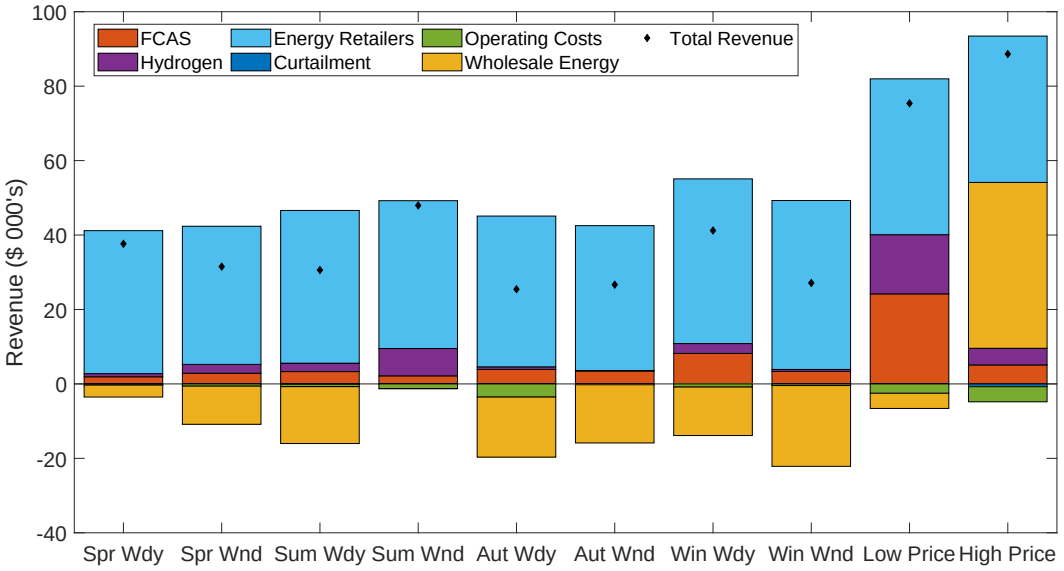

FIGURE 5.21: The total daily revenue of the VPP for each of the 10 representative days with consideration of revenue from energy retailers

highlight the importance of including multi-market participation when considering the associated cost of providing local network support, as on all of the days the additional markets play a significant role in determining VPP operation and revenue.

5.3.3 Summary of Study on Cost of Service Provision from Multi-Energy Flexibility

This case study demonstrates that for most of the time the VPP is able to provide local network support without altering its active power output. So, in most circumstances these services have limited impact on the VPP's participation in energy, FCAS, and hydrogen markets. However, during extreme pricing events the VPP operates close to the edge of its FOR and so may not be able to provide local network support without altering its active power output. Because of the active power curtailment in these extreme scenarios, there is a difference in the VPP revenue generation when the VPP is providing local network support and when it is not. However, when revenue from selling energy to downstream retailers is considered, this difference in revenue is relatively small. Overall, this case study clearly demonstrates the tight interaction between local network support and system-level market participation. VPP flexibility can be utilised to provide local network support while maximising its market revenues. This is particularly relevant in the context of distribution system operation and emerging DER marketplaces that are constrained by local network limits.

5.4 Key Remarks

5.4.1 Multi-Energy Flexibility from Integrating Electricity & Hydrogen

This case study considers an electricity-hydrogen VPP and characterises and quantifies the multi-energy flexibility available to the VPP. It is also shown how this flexibility can be assigned to specific markets and grid services. A clear link between available flexibility and scheduling of resources is drawn. It is seen that sufficient financial incentives can give rise to resources that create hydrogen and those that utilise hydrogen operating simultaneously. This would not be seen without multi-market participation, as it leads to reduced operating efficiency. However, it also leads to additional flexibility that can be used to provide grid services and participate in markets. It is also shown in the case study that the operating framework allows the VPP to effectively adjust its operating strategy in light of differing market/service portfolios to maximise its revenue.

5.4.2 Cost of Service Provision from Multi-Energy Flexibility

This case study also considers an electricity-hydrogen VPP. However, the focus of this case study is on the provision of local network support, and the cost to the VPP of providing such a service. Ten representative days throughout 2016 are considered to be able to estimate the yearly revenue of the VPP when it is providing local network support, and when it is not. Multiple markets are considered to help ensure that an accurate value of VPP revenue is considered. The results show that for the majority of the time the VPP can effectively provide local network support utilising reactive power control. In extreme scenarios, the VPP requires the use of active power curtailment to maintain network limits. This results in lost revenue for the VPP, around $303,000 per year. However, the VPP is extremely effective at providing this local network support, and without it the network operator would likely need to take action (such as forced curtailment) which could also reduce VPP revenue. Participating in multiple markets has a marked effect on VPP operating and revenue, and is therefore important when considering the cost of providing local network support.

Chapter 6

Techno-Economic Analysis of an Electricity-Hydrogen VPP

6.1 Introduction

In this chapter, a case study is examined to highlight how the proposed operational framework can be used for a techno-economic assessment to inform a business case for an electricity-hydrogen (H_2) VPP. Multiple markets and contractual services are considered for VPP participation to maximise its profits. Additionally, multiple possible VPP configurations (each containing a different set of resources) are considered. Required expenditure is calculated utilising current technology prices. This study of a VPP's placement in a renewable-rich, congested area of the Australian network shows that multi-market participation is crucial to the long-term economic viability of the electricity-hydrogen VPP. Daily optimisations are conducted for each day of a year to estimate VPP yearly revenue. Sensitivity to hydrogen prices and magnitude of contractual services is considered. The case study uses eight years of market data to investigate the VPP's sensitivity to changing electrical market prices, and to establish a more accurate figure for long term revenue. All configurations considered that participate in all available markets/services are found to be economically viable for a hydrogen price of \$3/kg.

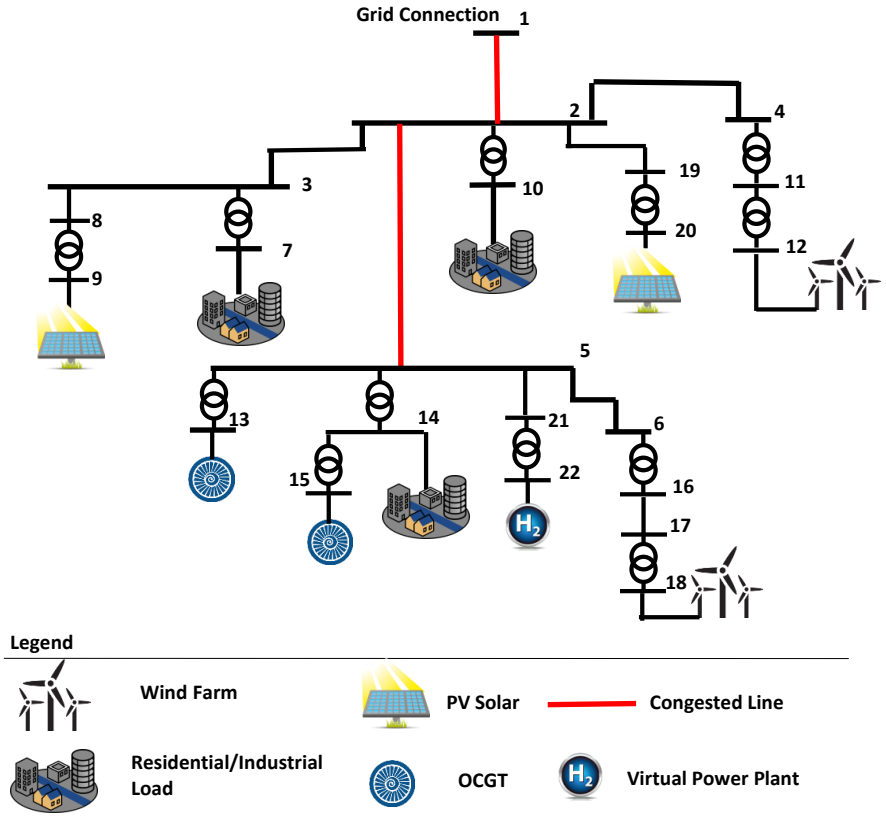

FIGURE 6.1: Diagram of the case study network and the position of the proposed VPP

6.2 Case Study Information

The VPP considered in this case study is different from the VPPs in the previous chapters insofar as all on the constituent resources of the VPP are located at the same node. In Figure 6.1 it can be seen that only the resources located at node 22 are part of the proposed VPP. It is assumed that all of the other generators are currently owned and operated by other entities. The lines running between nodes 1-2 and 2-5 have been identified as points of congestion that limit the export of RES in the area, leading to unwanted renewable curtailment. The case study will consider the techno-economic benefits of installing a VPP into the network. Possible resources to be included in the VPP are a battery energy storage system (BESS), proton exchange membrane (PEM) electrolyser, fuel cell, hydrogen-OCGT, and hydrogen storage.

6.2.1 How the Framework is Applied

While only the resources at node 22 are part of the proposed VPP, it is important to understand the interactions of the VPP with other network entities and the network itself. That is why the operational framework presented in this thesis should be used for this techno-economic analysis. In this case study, only the high-level optimisation will be used, and without considering uncertainty. This form of cost-benefit analysis to inform a business case does not necessarily require the full details of the operational model to provide an estimate of revenues. However, the ability to participate in multiple markets is an important inclusion as this will directly drive VPP revenue generation. As will be shown later in the case study, modelling the power flows in the network is also important due to the impact this can have on revenue generation, including unlocking access to provision of additional services. By considering all of the resources in the network in Figure 6.1 the proposed framework provides the likely operation of the other resources in the network. This is important, as this will have an impact of the state of the network and whether it is constrained. For this analysis it is assumed that the other resources in the network are solely participating in the wholesale energy market. This mean that by conducting the high-level optimisation, the other resources are essentially responding to market prices and generating when profitable (as could reasonably be expected from generators in a network). The revenues from the VPP at node 22 can then be determine *post hoc* from the results of the optimisation. The high-level optimisation is conducted for each day of the year to determine the estimated yearly revenue of the proposed configuration of the VPP.

6.2.2 Investment Costs of Flexible Resources

To be able to fully consider the profitability of the VPP, it is not sufficient to only consider the revenue that the VPP accrues from operating in markets. The investment over the lifetime of the resources including capital expenditure (CAPEX) and operational expenditure (OPEX) should be considered to determine how much revenue the VPP needs to obtain to balance these costs. Therefore, for the economic analysis of this case study it is assumed that the VPP operators will choose the resources for their VPP from

Resource	**Capital Investment**	**Fixed O&M**	**Lifetime**
BESS [169]	\$813/kW & \$543/kWh	\$10/kW/year	20 years
PEM Electrolyser [126, 170]	\$1,400/kW	\$54/kW/year	20 years
H_2 OCGT [170]	\$1,250/kW	\$12.6/kW/year	40 years
H_2 Fuel Cell [47]	\$2,109/kW	\$58/kW/year	20 years
H_2 Storage [47]	\$1,032/kg H_2/day	\$22/kg H_2/day	40 years

TABLE 6.1: The capital investment costs, fixed operation and maintenance (O&M) costs, and lifetime of each resource under consideration for inclusion in the VPP

those shown in Table 6.1. The table contains the capital investment and fixed operation and maintenance (O&M) costs of the resources under consideration in the VPP[1].

The equivalent annual cost (EAC) represents the annual cost of owning, operating and maintaining an asset. It is especially useful for comparing costs of assets with differing lifespans. The EAC is calculated using

$$EAC = \frac{CAPEX \times d}{1 - (1 + d)^{-n}} + OPEX, \tag{6.1}$$

where d is the discount rate (the interest that an entity could receive on its capital if it is left unspent) which in this case study is set at 7%, and where n is the lifetime of the asset in years. Using (6.1), the EAC can be calculated for the resources under consideration for the proposed VPP and can be found in Table 6.2. For this case study, the hydrogen storage capability is sized to be able to store 11,575 kg of hydrogen each day. This is the amount of hydrogen the electrolyser operating at 85% capacity factor would generate (this is the average capacity factor for a grid connected PEM electrolyser assumed in [47]). For this case study, the hydrogen is assumed to be stored at 150 bar (due to the stationary nature of the hydrogen system and to reduce compressor energy requirements). For 11,575 kg of hydrogen storage, this equates to 1,254 m^3 at 150 bar.

In total, seven different VPP configurations will be considered in this case study to determine how the choice of resources, and the interactions between resources, effects the economic viability of the VPP. The constituent resources and EAC for each of the seven proposed VPP configurations considered can be found in Table 6.3.

[1]Note that all costs and revenues in this study are in Australian Dollars.

Resource	Size	CAPEX	OPEX	EAC
BESS	30 MW/8 MWh	\$28.734M	\$300k/year	\$3.012M
PEM Electrolyser	30 MW	\$42.000M	\$1,620k/year	\$5.585M
H_2 OCGT	10 MW	\$12.500M	\$126k/year	\$1.064M
Fuel Cell	5 MW	\$10.545M	\$290k/year	\$1.285M
H_2 Storage	11,575 kg H_2/day	\$11.945M	\$255k/year	\$1.151M

TABLE 6.2: The capital expenditure (CAPEX), operational expenditure (OPEX), and equivalent annual cost (EAC) of each of the resources under consideration for inclusion in the VPP

Case	Resources	EAC
1	BESS only	\$3.012M
2	Electrolyser + H_2 storage	\$6.736M
3	Electrolyser + H_2 storage + fuel cell	\$8.021M
4	Electrolyser + H_2 storage + H_2 OCGT	\$7.800M
5	Electrolyser + H_2 storage + fuel cell + H_2 OCGT	\$9.085M
6	Electrolyser + H_2 storage + fuel cell + H_2 OCGT + BESS	\$12.097M
7	Electrolyser + H_2 storage + fuel cell + BESS	\$11.033M

TABLE 6.3: The seven VPP configurations that are under consideration in the case study, with the constituent resources and the total VPP equivalent annual cost (EAC)

6.2.3 Services and Markets

This section contains an overview of the markets/services that the VPP can participate in/provide during the case studies. The markets include wholesale energy, hydrogen, contingency frequency control ancillary service (FCAS), and voltage control ancillary services (VCAS). The services include contracts with RES to purchase their curtailed energy, fast frequency response (FFR), and System Restart Ancillary Services (SRAS). An overview of each of these markets and services is provided in the following sections.

6.2.3.1 Curtailed RES

Due to the remote location of this area of the network, and the high potential for RES, there are times when RES generation is curtailed due to line thermal limits being reached. In this work there is a contract that allows the VPP to purchase the energy that would otherwise be curtailed from RES for a price of \$30/MWh. This is sufficiently

low for the VPP to be able to generate hydrogen at a profit whilst providing RES with additional revenue. The VPP is positioned such that if line 2-5 is congested then the VPP can buy energy from the wind farm at node 18. If the line congestion is at line 1-2 then the VPP can buy energy from all of the RES in the network downstream of the grid connection point.

6.2.3.2 Wholesale Energy

The VPP participates in the wholesale energy market. While this market is priced and cleared every 5 minutes, currently market settlement is at 30 minute intervals. Therefore, the high-level optimisation with a time step of 30 minutes will provide a sufficient estimate of the VPP revenue from the wholesale energy market. The value that the VPP derives from the wholesale energy market can be found by considering the power injection/absorption of the VPP's constituent resources (not taking into account the energy that is coming from the contractual relationship with RES described above) and utilising the marginal loss factor associated with the VPP location in the network.

6.2.3.3 Hydrogen

The price of hydrogen is considered to be fixed across the duration of these studies. Fixed prices of \$2/kg and \$3/kg are considered to assess how hydrogen price affects VPP economic viability. These prices has been identified as the target price region for Australia to be able to compete with other exporting countries [47]. Transportation costs, and the trading mechanisms for hydrogen are not considered in this study.

6.2.3.4 Contingency Frequency Control Ancillary Services

Contingency FCAS services help the network cope with a sudden change in network load or generation (a contingency event). In Australia contingency FCAS is divided into two sets of services. Contingency raise FCAS services are used to raise the system frequency in the case of an event and are divided depending on the required response time into fast (6 seconds), slow (60 seconds) and delayed services (5 minutes). In addition, there are also fast, slow and delayed lower FCAS services with the same response time requirements that are used to lower the system frequency after a contingency. There are

then six contingency FCAS markets that the VPP can choose to participate in. While these markets are priced and cleared every 5 minutes, currently market settlement is at 30 minute intervals. Therefore, the high-level optimisation with a time step of 30 minutes will provide a sufficient estimate of the VPP revenue from the FCAS markets.

6.2.3.5 Fast Frequency Response

In this case study we define FFR as "*the delivery of a rapid active power increase or decrease by generation or load in a time-frame of two seconds or less*" [24] and it is assumed that the PV in the network have an obligation to provide FFR, as was proposed in [25]. Traditionally this would mean that the RES would need to install some form of storage (such as a BESS) to be able to provide such a service or contract the provision of FFR to a third party. This third party could be a curtailable load. In this case study it is considered that the two PV farms are newly connected RES, and as such are required to provide FFR. Two magnitudes of FFR are considered in this case study. One where the FFR provided must be 50% of the power generated by the PV farms, and the other where the FFR requirement is 33%. This is used to provide some sensitivity analysis to the magnitude of this contractual agreement. The yearly contract value for providing FFR is assumed to be a 50% of the EAC of procuring a battery suitable to provide FFR. This equates to $1,506,000/year.

6.2.3.6 Voltage Control Ancillary Services

AEMO maintains voltage levels across the transmission network within relevant limits. This can be done by absorbing or injecting reactive power into transmission network connection points [171]. High system voltages during periods of lower demand (i.e., overnight) are an emerging system issue which can be addressed by dispatching reactive power resources to absorb reactive power. From 2015 – 2019 AEMO had a contract for 800 MVAr absorbing reactive power VCAS with a network service provider (NSP) [21] worth approximately $10 million per year. The increase in converter-based DER provides NSPs an alternate avenue for sourcing reactive power absorption to provide VCAS. VCAS in this case study it is assumed to be a market structure, where the VPP injects/absorbs reactive power in response to price signals from an NSP or other entity.

In this case study the reactive power price signals are used to incentivise the absorption of reactive power between 22:00 hours – 05:00 hours at a fixed price of \$1/MVArh.

6.2.3.7 System Restart Ancillary Services

In the Australian system, the provision of black start services falls into the category of system restart ancillary services (SRAS). Each subsection of the Australian network is assessed on the magnitude of SRAS that it requires. For the South Australia (SA) system, this is 330 MW [23]. Each year AEMO publishes the costs of providing SRAS for each subsection [172]. By averaging the amount paid for this 330 MW of SRAS in SA over the past 7 years, the cost of procuring SRAS in SA can be estimated as \$10,300/MW/year. The 10 MW hydrogen-OCGT considered in this work has the capability to provide SRAS. Therefore, when it is part of the proposed VPP, it is assumed that the VPP has access to an additional \$103,000/year from provision of SRAS.

6.2.3.8 Service and Market Portfolios

There are 28 cases studies considered, utilising seven VPP configurations and four market/service portfolios as shown in Table 6.4. Past wind generation profiles, wholesale energy prices and FCAS prices are provided by AEMO [154]. Substation load is based on data from SA Power Networks [155], and the solar irradiances are from the Australian Bureau of Meteorology [156].

6.2.4 VPP Feasible Operating Region

A VPP can participate in markets and provide services by utilising its electrical flexibility – a measure of the capability of a VPP to deviate from a set dispatch point. Flexibility maps (created using the approach proposed in [69]) are a useful tool to illustrate VPP flexibility through feasible operating regions (FORs). The flexibility maps of each VPP configuration are shown in Figure 6.2, in reactive power-active power space and hydrogen-active power space. The discontinuities in the FORs represents the switching of resource with a minimum operating power requirements.

VPP Configuration	**Market/Service Portfolio**			
	Portfolio A: Energy + Curtailed RES + Hydrogen	**Portfolio B: Portfolio A + FCAS**	**Portfolio C: Portfolio B + FFR**	**Portfolio D: Portfolio C + VCAS + SRAS**
BESS	Case 1A	Case 1B	Case 1C	Case 1D
Electrolyser	Case 2A	Case 2B	Case 2C	Case 2D
Electrolyser + Fuel Cell	Case 3A	Case 3B	Case 3C	Case 3D
Electrolyser + H_2 OCGT	Case 4A	Case 4B	Case 4C	Case 4D
Electrolyser + fuel cell + H_2 OCGT	Case 5A	Case 5B	Case 5C	Case 5D
Electrolyser + fuel cell + H_2 OCGT + BESS	Case 6A	Case 6B	Case 6C	Case 6D
Electrolyser + fuel cell + BESS	Case 7A	Case 7B	Case 7C	Case 7D

TABLE 6.4: Naming of studies for different VPP configurations and market/service portfolios

Electrical flexibility can be considered as either upwards flexibility (the ability of a VPP increase its active power injection/consume less active power) or downwards flexibility (the ability of a VPP to decrease its active power injection/consume more active power). The amount of upwards and downwards flexibility that is available to the VPP at a specific time is dependent upon its dispatch point. For example, for the VPP in *Case 2* (the electrolyser) to provide 10 MW of upward flexibility (for example to provide FFR), it must be operating with an active power dispatch point no greater than -10 MW, forcing it to absorb power while providing the service. However, if the VPP in *Case 5* (electrolyser, fuel cell and hydrogen-OCGT) were providing that same 10 MW of upward flexibility, it would only need to have an active power dispatch less than 5 MW (assuming reactive power dispatch is 0 MVAr and all resources are on). Therefore, in *Case 5* the VPP still has the capability to either inject or absorb active power (to respond to market prices) while providing this level of FFR. As we will see from the results of this case study, this additional flexibility is translated into additional revenue

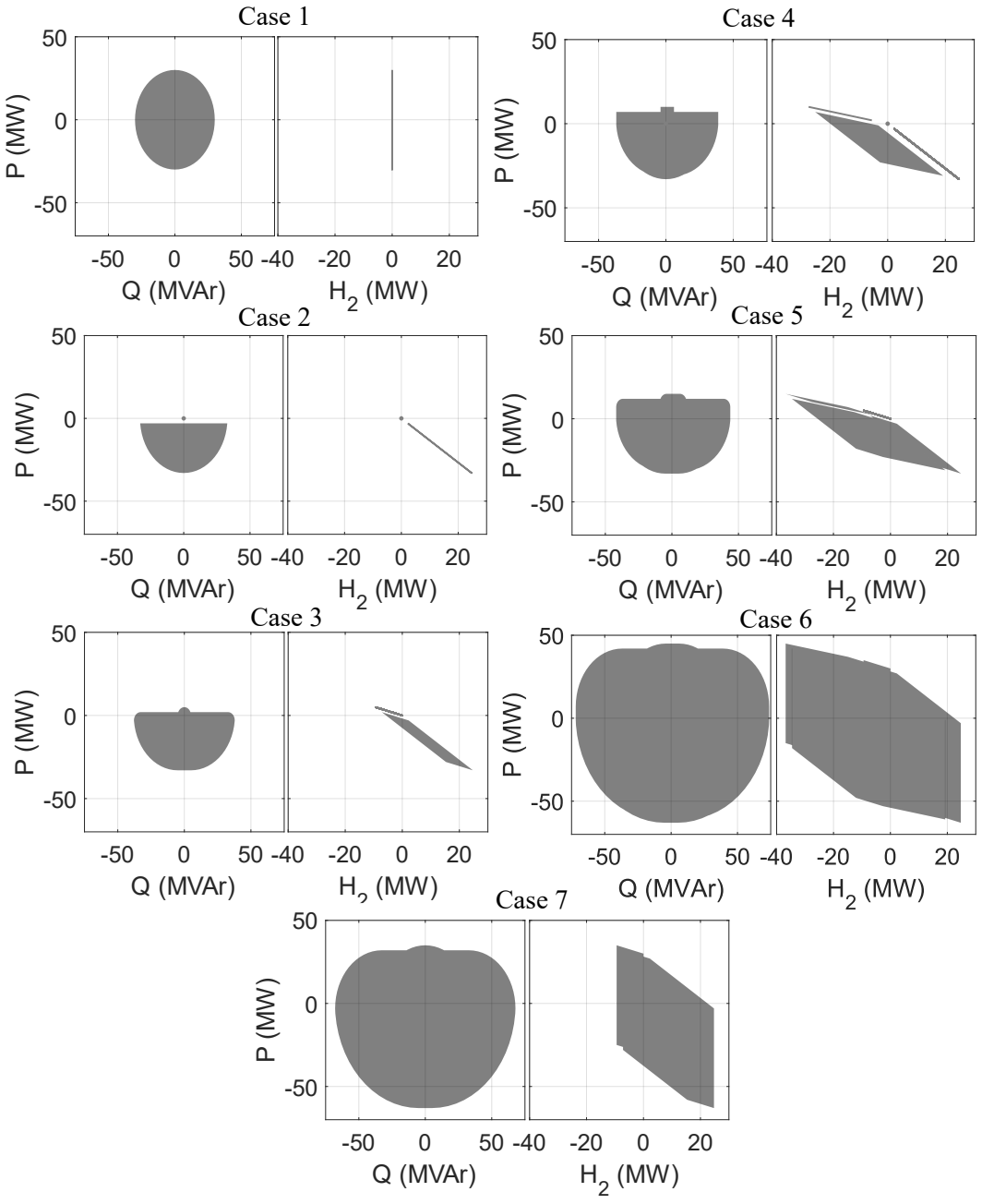

FIGURE 6.2: Reactive-active power (Q-P) and hydrogen-active power (H_2-P) flexibility maps showing the FORs of the seven proposed VPP configurations, where negative values indicate absorption/consumption and positive values indicate generation/injection

generation.

The VPP's upward and downward flexibility is dependent on the VPP's reactive power dispatch point as well as its active power dispatch. This highlights the importance of optimising VPP operation in all markets/services, considering both active and reactive

power, simultaneously. Making these decisions in a non-holistic manner may reduce the revenue accrued from multi-market participation.

It can be seen by looking at the flexibility maps for *Cases 1, 5* and *6* in Figure 6.2 that when resources are aggregated the resulting FOR is of greater size than the sum of the FOR of each individual resource. This aggregating of resources also dramatically increases the VPP flexibility in the hydrogen-active power space. This gives a VPP the ability to vary its hydrogen output whilst maintaining its active power dispatch point. In general, a VPP would want to maximize its hydrogen output for a set active power dispatch, as hydrogen can be monetised. However, if there existed strict constraints on the hydrogen infrastructure (storage size, export limits, etc.) the VPP could utilise its internal flexibility (by modulating internal dispatch factors) to be able to accommodate these constraints while minimising the effect that this would have on the VPP's electrical operation. These flexibility maps illustrate a clear benefit of resource aggregation, as flexibility is the means by which a VPP participates in markets/services, and by extension the means of accruing revenue.

6.3 Results

6.3.1 Benefits From Multi-Market Operation

Figure 6.3 and Figure 6.4 illustrate how the VPP revenue changes for the 28 cases with hydrogen price of \$2/kg or \$3/kg and FFR contract set at 50% or 33% of PV generation for 2016 and 2017 respectively. With the exception of contractual FFR, the addition of extra markets/services to the VPP portfolio always increases the revenue that the VPP can generate. In fact, without participating in multiple markets, none of the VPP configurations generate sufficient revenue in 2016 or 2017 to match their respective EAC, identifying multi-market portfolios as crucial to VPP economic viability.

The largest impact of multi-market participation can be seen when the VPPs add participation in the six contingency FCAS markets to their portfolio. In 2017 the FCAS prices are larger than in 2016, and the effect of this can be seen most prominently in VPPs containing a BESS (a resource with derives most of its value from FCAS).

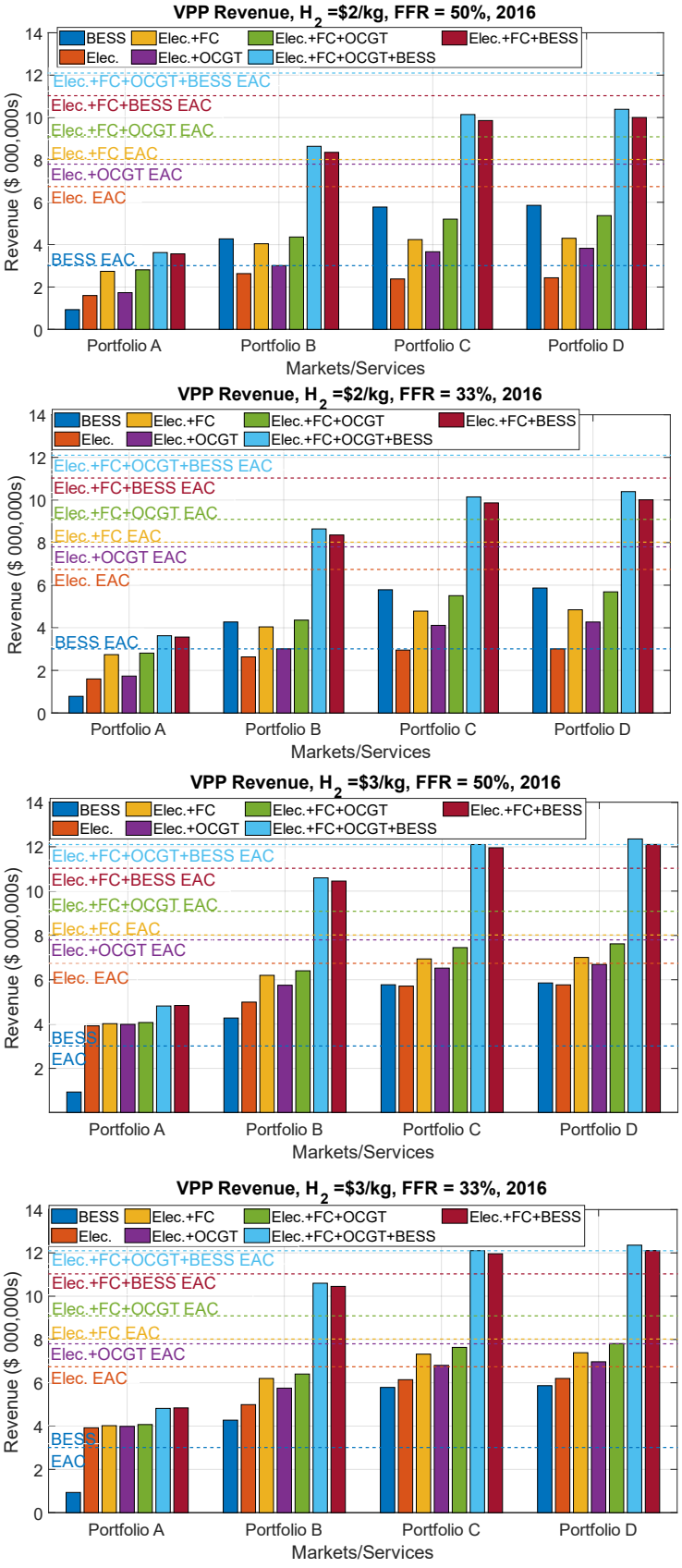

FIGURE 6.3: VPP revenues in 2016 for 50% and 33% contractual FFR provision and hydrogen prices of $2/kg or $3/kg.

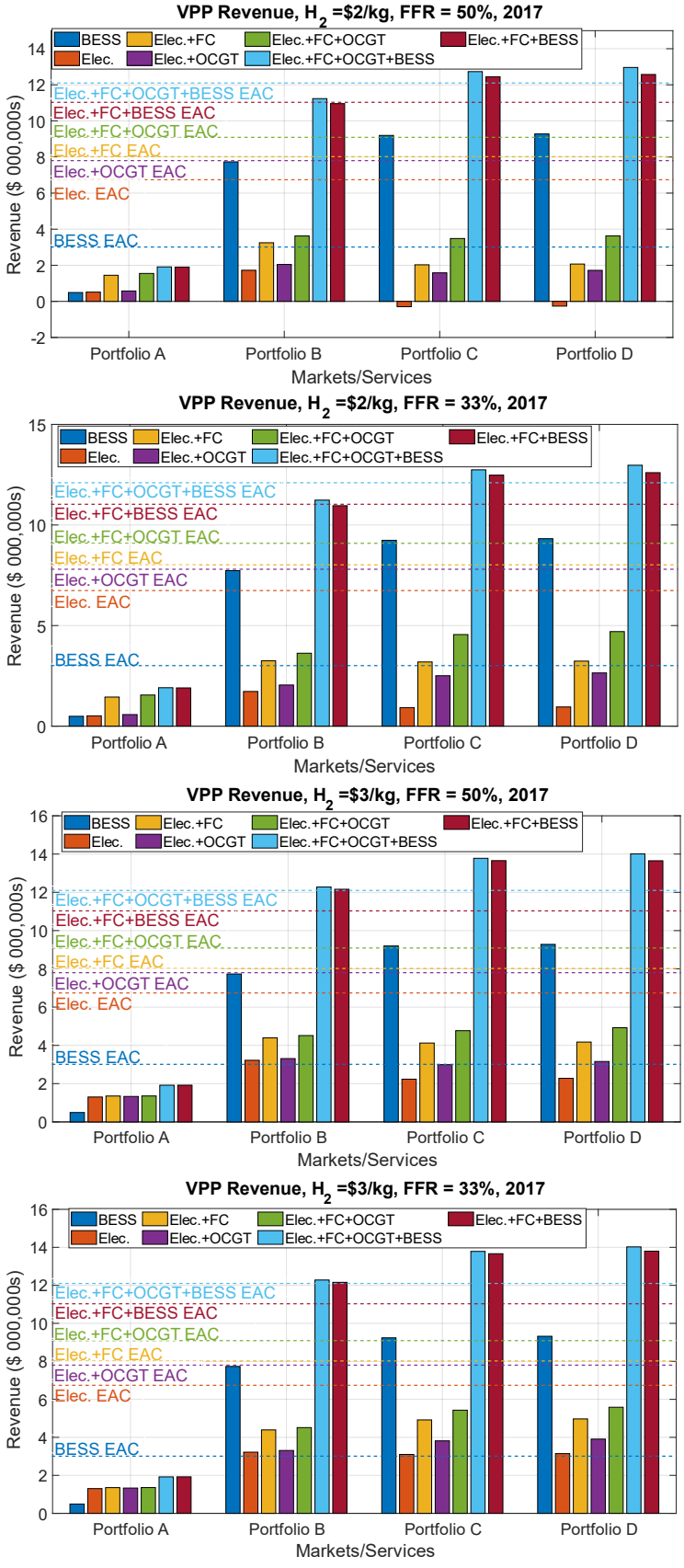

FIGURE 6.4: VPP revenues in 2017 for 50% and 33% contractual FFR provision and hydrogen prices of $2/kg or $3/kg.

Considering 2017 with a hydrogen price of \$3/kg in *Case 2A* the electrolyser capacity factor is 20.3%. In 2017, only 13.4% of price intervals are below the price threshold necessary to sell hydrogen at a profit. The reason in *Case 2A* that the electrolyser capacity factory is higher than this is due to the contractual arrangement that the electrolyser has with the RES to buy energy that would otherwise be curtailed. This contract leads to an additional \$1.05 million of hydrogen revenue in 2017 with a hydrogen price of \$3/kg. Participation in FCAS also leads to an increase in electrolyser capacity factor of 10.9% in 2016 and 25.1% in 2017, more than doubling the amount of hydrogen generated and sold in 2017. This shows how multi-market participation directly unlocks significant additional economically viable hydrogen generation.

6.3.2 Sensitivity to Magnitude of Contractual FFR

The only service that may causes a reduction in VPP revenue in these case studies is FFR. This is because this is a contractual arrangement rather than a market where a VPP can respond to price signals when deciding whether to participate. The VPP configuration that is worst affected by this is *Case 2* (only an electrolyser). This is because an electrolyser providing FFR must act as a load at the required magnitude (so that it can be reduce its load if required to provide the net increase in power output). During these periods of FFR provision the electrolyser is very limited in how it can respond to the wholesale energy market prices (as explained in Figure 6.2 and Section 6.2.4), thus exposing itself to possible high wholesale energy prices.

From Table 6.5 it is seen that in 2017 more FFR provision is requested from the VPP than in 2016 (due to the higher PV export in 2017). This, along with the higher wholesale energy price, is why in 2017 providing FFR in *Cases 2-5* costs the VPP more revenue than in 2016, and in some cases it costs the VPP more than the \$1,506,000 contract price (indicating that the contract has been valued too low for 50% FFR provision). It is noted that the VPP in Case 1 (BESS only) is largely unaffected by the changes in FFR magnitude due to its ability to provide FFR from a 0 MW operating point.

Year	50% FFR Provision		33% FFR Provision	
	FFR Provided (MWh)	**Equivalent Price ($/MWh)**	**FFR Provided (MWh)**	**Equivalent Price ($/MWh)**
2016	52,273	28.8	34,503	43.6
2017	74,714	20.2	49,336	30.5

TABLE 6.5: Amount of FFR being provided by the VPP and equivalent per MWh price in 2016 and 2017

6.3.3 Sensitivity to Hydrogen Price

Examining the revenues for different VPP configurations when the hydrogen price is $2/kg in Figure 6.3 in Figure 6.4 it is seen that the revenue of *Cases 2-5* are below their respective EAC. *Case 6* in 2016 is also below its EAC. A reason *Cases 6C, 6D, 7C, 7D* in 2017 have revenues greater than the required EAC is because the high FCAS prices allow the BESS to generate very high revenues, compensating for the poor performance of the hydrogen-based resources. The average wholesale energy prices in 2016 and 2017 are $80.59/MWh and $105.33/MWh respectively. These energy prices are too high most of the time for the electrolyser to be able to profitably generate hydrogen to be sold, or utilised by the fuel cell and hydrogen-OCGT for flexibility. Additionally, the current initial investment cost of a PEM electrolyser is too high for a $2/kg hydrogen price to be viable. For the electrolyser and storage system proposed here, if the electrolyser operates with an 85% capacity factor each year, $1.58 from each kg of hydrogen produced would be needed to match the EAC. This only leaves $0.42/kg of hydrogen to cover energy procurement costs, which is far below equivalent wholesale energy prices.

When the hydrogen price is changed to $3/kg there is a large change of hydrogen-based VPP revenues. In 2016 *Cases 2D-5D* are much closer to their EAC. This is true in 2017, although to a lesser extent. It is noted that the average wholesale energy price in 2017 is the highest recorded in the last 8 years, having a major effect on the viability of hydrogen creation.

An additional benefit of increasing the hydrogen price is that it allocates more value to the hydrogen produced when the hydrogen-based VPPs are providing FFR services. For hydrogen priced at $3/kg and FFR requirement of 33% all the VPP configurations manage to generate net revenue from providing FFR compensated at $1,506,000/year.

	Average Price ($/MWh)							
Market	**2013**	**2014**	**2015**	**2016**	**2017**	**2018**	**2019**	**2020**
Wholesale Energy	71.68	48.13	49.58	80.59	105.33	99.89	98.93	43.49
Fast Raise FCAS	0.93	1.42	2.28	5.37	12.67	11.38	9.87	24.99
Slow Raise FCAS	0.61	0.88	1.94	3.25	5.89	8.06	6.84	20.75
Delayed Raise FCAS	1.11	1.67	2.61	3.09	8.30	15.74	2.67	12.59
Fast Lower FCAS	1.43	0.43	1.85	0.45	0.42	0.19	9.64	8.75
Slow Lower FCAS	3.43	0.38	1.73	0.23	0.04	0.41	12.56	15.52
Delayed Lower FCAS	0.94	0.99	2.07	0.70	0.23	0.47	1.53	16.87

TABLE 6.6: Average electrical market prices in 2013-2020 in South Australia

6.3.4 Sensitivity to Energy and FCAS Prices

The revenue that a VPP can generate in a year is highly dependent on the wholesale energy and FCAS market prices that year. If economic analysis was conducted on 2016 or 2017 data individually, very different outcomes would be achieved. To further consider the effects of changing wholesale energy and FCAS prices, as well as trends within these markets, case studies are run utilising the market prices from 2013-2020, which are summarised in Table 6.6. Informed by the findings in Figure 6.3 and Figure 6.4 these further studies will only consider hydrogen priced at $3/kg and the FFR requirement for the VPP at 33% (where the contract value of $1,506,000 is deemed sufficient). These studies will look at all seven VPP configurations, but will only consider each configuration participating in all markets and services (i.e. *Cases 1D-7D*), as it has been established that multi-market participation increases VPP revenue.

Figure 6.5 shows that BESS revenue is almost entirely from FCAS markets, whereas the hydrogen-based VPPs have a more variable revenue mix and are more effected by changes in wholesale energy price. *Cases 2-7* in 2013 all generate revenue less than the EAC due to the combination of high energy prices and low FCAS prices. In general, a high average wholesale energy price causes *Cases 2-5* to accrue less revenue. Even though 2019 has a high average wholesale energy price, the high FCAS prices allows the VPPs to still make a profit. The significantly higher FCAS prices in 2020 leads to much higher revenue in all configurations. If wholesale energy prices fall in the coming years due to increased RES integration, and FCAS prices continue to rise in line with the trend seen in Table 6.4, then the profits of hydrogen-based VPPs will continue to increase.

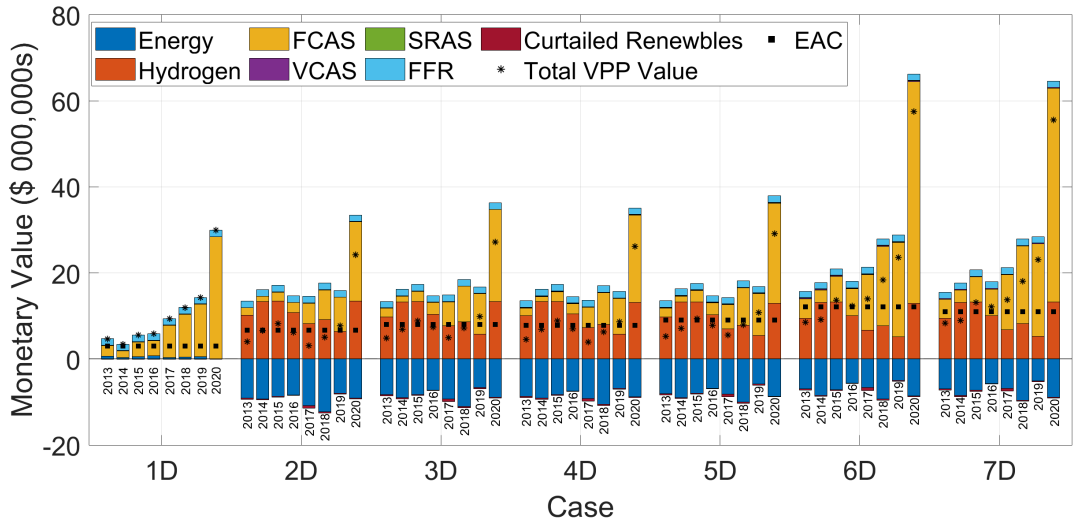

FIGURE 6.5: VPP revenue for 2013-2020 in *Cases 1D-7D* with hydrogen price of $3/kg and FFR requirement of 33% of PV generation.

VCAS and SRAS with the assumed pricing generate much less revenue compared with the other markets and services, which is why they are difficult to see in Figure 6.5. VCAS revenue varies from approximately $58,000 - $157,000 per year depending on the year and VPP configuration. SRAS, when it is provided, is worth $103,000 per year.

6.3.4.1 Hydrogen Sold in each Case and Year

To assess the amount of hydrogen that is sold each year, it is compared to the maximum possible sale (i.e. if the electrolyser was on at maximum power constantly over the whole year) which is referred to here as the VPP's hydrogen capacity factor. Table 6.7 shows the hydrogen capacity factors of each hydrogen-based VPP configuration (with a full market/service portfolio) for 2013-2020, as well as a "Business as Usual" (BaU) case. The (BaU) case considers only an electrolyser and the energy pricing throughout the year. It is assumed that the electrolyser operates at full capacity when the energy price is below the threshold where it can sell hydrogen for a profit at $3/kg.

Table 6.7 shows that using the VPP to participate in markets/services not only opens additional revenue streams for the VPP, but it also allows the VPP to generate and sell more hydrogen than it would be able to do if it were not providing services. By comparing (BaU) and *Case 2D* (in both cases the VPP only contains an electrolyser), the additional hydrogen generated while providing services in *Case 2D* is worth almost $3M/year on average. Even when the hydrogen is being consumed via the fuel cell and

	VPP Hydrogen Capacity Factor (%)						
Year	**BaU**	**2D**	**3D**	**4D**	**5D**	**6D**	**7D**
2013	57.8	67.9	65.2	66.9	64.8	62.9	63.0
2014	82.9	89.3	88.4	89.0	88.2	87.6	87.7
2015	86.7	90.0	89.0	89.2	88.7	88.3	88.4
2016	56.6	71.8	69.2	69.9	68.3	67.0	67.1
2017	13.4	55.2	51.2	48.6	46.8	44.9	45.4
2018	15.2	61.0	57.9	53.4	52.1	51.2	54.5
2019	22.2	42.9	38.8	38.5	36.2	34.6	35.3
2020	76.2	89.7	88.5	87.2	86.2	86.0	88.1
Average	**51.4**	**71.0**	**68.5**	**67.8**	**66.4**	**65.3**	**66.2**

TABLE 6.7: VPP capacity factor (considering hydrogen sold) for 2013-2020 *Cases 2D-7D* and a business as usual (BaU) case

hydrogen-OCGT to provide flexibility to the electrical network, the average hydrogen capacity factor of the VPP is still significantly higher.

6.3.5 Benefits to the Wider Network

The integration of a VPP can have wider network benefits, especially if the network is operating close to design limits (i.e., a congested network due to high RES export). These benefits can only be properly assessed by using an optimisation that models the electrical network, such as in this case study.

6.3.5.1 Curtailed RES

A benefit of the VPP being located in a congested area of the network is the ability of the VPP to utilise renewable energy that would previously have been curtailed. As an example, in the 2017 (BaU) case, 17% of the 156,820 MWh of energy generated by the wind farm at node 18 would be curtailed due to line thermal limits. In 2017 *Case 6D* this amount is reduced to only 4.1% of the wind farm energy being curtailed. The energy that would otherwise have been curtailed is now bought by the VPP and absorbed to create hydrogen or charge the BESS. If all of the power bought from the wind farm was converted into hydrogen it would create over 525,000 kg of green hydrogen over

2017. Using an operational model that captures the local electrical network allows this interaction to be considered.

6.3.5.2 Easing of Network Congestion

One of the additional benefits of having an electrolyser provide FFR is that when the electrolyser is absorbing energy to be able to provide FFR, it may act to relieve congestion in the wider network. This in turn can allow generators to export more energy and accrue higher revenue. In the case studies this additional export capability predominately effects the OCGTs at nodes 13 and 15. The easing of congestion that the hydrogen-based VPPs deliver when providing FFR is worth on average $2.3M/year between 2013-2020 to the generators in the network. In this work there is no mechanism for the VPP to access any of this additional value. However, agreements could be made to have part of these funds be used to supplement the FFR payment that the VPP receives from the PV generators, leading to additional VPP revenue.

6.3.6 Value Metrics

To assess the economic viability of the proposed VPP configurations over their lifetimes, two value metrics are used – Net Present Value (NPV) and Discounted Payback Period (DPP). NPV represents the difference between the expected revenues of a project (converted into "today's money" by using a discount rate) and the amount of initial investment required. In this way NPV captures the total value of the project. The NPV of each option is calculated using (6.2), where d is the discount rate of 7% and n is the lifetime of the VPP in years. The VPP includes resources with 20–40 year lifetimes. So, a conservative estimate for VPP lifetime of 20 years is considered for this analysis.

$$NPV = -CAPEX + \sum_{t=1}^{n} \frac{YearlyIncome - OPEX}{(1+d)^t} \tag{6.2}$$

$$DPP = \ln\left(\frac{1}{1 - \frac{CAPEX \times d}{YearlyIncome}}\right) \div \ln(1+d) \tag{6.3}$$

Another indicator that can be used to consider the economic viability of investment in a project such as this is the DPP on the investment, which can be determined by (6.3).

Case	Average Yearly Revenue	NPV	DPP
1D	$10,630,463	$80,707,072	3.20 years
2D	$8,167,473	$12,721,257	13.55 years
3D	$9,669,348	$15,014,878	13.60 years
4D	$9,039,243	$8,121,955	15.98 years
5D	$10,368,671	$8,588,670	16.26 years
6D	$19,657,388	$75,081,266	8.40 years
7D	$19,143,685	$83,473,934	7.34 years

TABLE 6.8: The average yearly revenue (from 2013 - 2020) of each VPP configuration with a full portfolio of markets/services, and their associated NPV and DPP

The DPP determines how long it would take to recoup the initial investment cost of a project while also incorporating a discount rate to recognize the changing value of money over time. The NPV and DPP for each VPP configuration with comprehensive portfolios is shown in Table 6.8. It should be noted that the calculations used assume the average yearly revenue shown in Table 6.8 is the VPP yearly income each year over the lifetime of the VPP.

Firstly, in all the VPP configurations the DPP is less than the assumed 20-year lifetime of the VPP. The NPV is also positive in all cases, indicating that any of these VPP configurations would be an economically viable venture. Secondly, whilst inclusion of the hydrogen-OCGT acts to increase the average yearly revenue (comparing *Case 2D* and *Case 4D*), it reduces the NPV of the VPP, and increases the DPP. This indicates that the extra value that the hydrogen-OCGT is providing the VPP is not significant enough to offset the required investment. This could be attributed to the fact that the OCGT lifetime is 40 years, but in this analysis it is assume that all resources in the VPP have a 20 year lifespan. Inclusion of the fuel cell increases the NPV of the VPP (comparing *Case 2D* and *Case 3D*), however it also increases the DPP, although not significantly. So on balance, it seems the fuel cell adds value to the investment. The results in Table 6.8 indicate that the solution with the shortest DPP is to install a BESS only. However, the VPP configuration with the highest NPV is an electrolyser, a fuel cell, hydrogen storage and a BESS. The DPP for this configuration is longer than for the BESS alone, but it is still well below the VPP lifetime. Additionally, this VPP has

greater flexibility to adapt to changing markets and services, including hydrogen related ones.

6.4 Key Remarks

Participating in multiple markets and services unlocks additional revenue streams for a VPP, without which it would not be an economically viable project. If contractual services are properly reimbursed, adding additional markets and services to a VPP portfolio increases VPP revenue. The modelling of the network in the analysis of VPP revenue generation is also important. It is shown that the network can both restrict VPP operation, and also provide additional revenue streams (in the form of curtailed RES energy in this case study). The pricing of wholesale energy in the Australian market, and the initial investment costs of resources, is currently too high to allow hydrogen to be sold at \$2/kg. However, with a comprehensive portfolio, generating and selling hydrogen at \$3/kg is an economically viable prospect for a hydrogen-based VPP. In fact, for hydrogen-based VPPs, participating in multiple markets acts to increase the maximum value of wholesale energy below which the VPP can profitably create hydrogen. This is turn allows the VPP the create more hydrogen. It is also important to analyse potential VPP operation over a number of years to determine an accurate value for VPP yearly revenue, as market prices vary greatly between years. The largest hurdle to a VPP's ability to sell hydrogen at \$2/kg is the current investment cost of the technology. However, as these technologies mature, investment costs will reduce and future multi-energy VPPs will be well placed to generate this low-cost hydrogen, especially if there is a reduction in wholesale energy prices or increase in FCAS prices.

Chapter 7

Conclusion

7.1 Answering the Research Questions

This thesis has met its primary aim to develop a comprehensive optimisation-based operational framework to allow a multi-energy VPP operator to utilise its operational flexibility to participate in multiple markets and services while considering uncertainty.

The framework has the capability to consider participation in multiple market and provision of multiple services. This framework is implemented in case studies to demonstrate that a VPP can simultaneously participate in markets and contractual services by assigning flexibility to each. The multi-market participation is key to long-term VPP profitability, but for contractual services it is important to ensure that they are monetised correctly to maintain VPP profitability. This framework can help inform VPP operators what the magnitude of that monetisation should be.

Incorporating a multi-energy node formulation into the framework enables the framework to capture the flexibility in the interchange between energy vectors. The application of the framework in case studies demonstrates multi-energy interactions to be an effective source of flexibility to participate in markets and provide services. It is also evident that proper utilisation of this multi-energy flexibility in the case of electricity and hydrogen can effectively reduce the economic threshold for profitable hydrogen production. The coupling of multi-energy flexibility and multi-market participation is important as it can fundamentally change the operation of multi-energy resources.

The combination of decomposing the framework into three optimisations with the utilisation of scenario-based optimisation and receding horizon control has allowed the framework to capture uncertainty in a tractable way. Case studies have highlighted the importance of the receding horizon control to maintain VPP profitability in a market with short bidding windows. Likewise it has been shown empirically that the scenario-based approach (and more specifically the robust restriction of the high-level optimisation provided in Appendix A) provides feasible solutions without being overly conservative.

The adaptable nature of the framework allows it to be used in a range of settings and by entities other than VPPs. A case study is provided that shows how a distribution system operator (DSO) could use this framework to allocate network capacity to DER in the network, and then VPPs/aggregators could also use the framework to optimise the operation of their DER under these constraints. It has also been shown that the framework is applicable for long-term techno-economic evaluations for business case assessments.

7.2 Addressing the Research Objectives

The objectives that are identified in Section 1.5.2 have been accomplished. Firstly, the formulation and operation of an optimisation-based VPP operational framework has been provided in Chapter 3. This framework allows participation in multiple markets, and in the case studies these have included wholesale energy, six contingency FCAS, and hydrogen markets. Provision of network and contractual services has also been included in the formulation. In the case studies these have included FFR, inertia, local network support, and reactive power services. The framework models network power flows and voltages using either a detailed linearisation, or second order cone relaxation depending on the level of accuracy required. This approach has been shown to effectively capture the power flow equations and has provided insights into constraints and opportunities for VPP operation in a network. The interactions between multiple energy vectors are considered through a multi-energy node formulation, in the case studies the focus has been placed on the electricity-hydrogen interaction. The framework uses a combination of scenario-based optimisation and receding horizon control to allow a VPP operator to mitigate the effects of uncertainty. For the high-level optimisation, a robust restriction has also been proposed in Appendix A to provide increased certainty of real-world

constraint satisfaction. Due to the approach taken to divide the framework into three linked optimisations, the framework is a tractable tool for markets with close to real time bidding windows.

The second objective is satisfied through the case studies conducted in Chapters 4 - 6 where the efficacy of the framework overall, and of each of the attributes laid out in Objective 1 is proved. It is shown that the framework allows a VPP to prioritise its participation in markets depending on prices, and shows that participation in multiple markets and services greatly supplements VPP revenue. The modelling of network power flows is shown to be sufficiently accurate, and measures have been proposed to increase that accuracy, and to provide verification of the accuracy. This modelling unlocks additional services such as local network support and contracts with curtailed RES. A number of case studies have examined the multi-energy flexibility available from coupling electricity and hydrogen. It is shown that leveraging this flexibility can be advantageous for the electrical network, and that considering it within a comprehensive framework provides insight into how the cost of generating hydrogen could be reduced. The method proposed to mitigate the effects of uncertainty is effective in ensuring that services can be provided under uncertainty, but it is also not too onerous compared to operation with perfect forecasts. The receding horizon control is shown to be effective in adapting to uncertainty, even when events occur which were not forecast. It is also highlighted that without a framework that can tractably optimise VPP operation considering short bidding windows, a VPP's revenue would be drastically reduced, again highlighting the significance of the framework methodology. This framework has been shown to be tractable for the case studies in this work, and so in less onerous market conditions is likely to be tractable for larger problems.

The third objective is demonstrated in Chapters 4 and 6. In Chapter 4 it is not only shown that a DSO could use this operational framework to allocate network flexibility to VPPs within its network (with various fairness paradigms), but also that each of these VPPs could then use this framework in determining their operation and market participation. The additional constraints for specific fairness paradigms or flexible network resources can easily be added. In Chapter 6 it is shown that the proposed framework can be adapted and utilised to provide long term techno-economic assessment of VPPs for business cases. The importance of participation in multiple markets and services is further conveyed. It is also shown that network modelling is of great importance to fully

understand the impact of the network on VPP operation, as well as possible additional markets/services to supplement VPP revenue. In both of these chapters it is shown that there is value in being able to use the optimisations in the framework individually as well as collectively.

7.3 Contributions of the Thesis

The first contribution of this thesis is the extensive review of the existing operational frameworks and methodologies for VPPs. It is identified that frameworks that considered both power flows and uncertainty are rare, and there are none that also consider multiple energy vectors. This can be attributed to the increased computational burden introduced by coupling these aspects. This review determines the gap in previous works which this thesis fills, namely a VPP operational framework with the six key attributes from Section 1.5.2.

The formulation and methodology of the proposed optimisation-based operational framework is a key contribution of this work. The novel features of this framework are that it couples the ability to participate in multiple markets, the ability to provide services, the modelling of power flows in the network, the modelling of multiple energy vectors, the consideration of uncertainty, and the ability to operate over short bidding windows. Such a comprehensive operational framework has not previously been proposed. The participation of multiple markets and provision of services is encoded through use of appropriate constraints and cost functions. Power flow is modelled using a detailed linearisation and a second order cone convex relaxation to balance tractability and accuracy. Multiple energy vectors are catered for through the use of a multi-energy node formulation. The effects of uncertainty are mitigated through the coupling of scenario-based optimisations and receding horizon control. A robust restriction of the scheduling optimisation is also exhibited in Appendix A to provide additional robustness to the problem. The overall framework is decomposed into three linked optimisations to help ensure problem tractability. Further contributions can be found in the implementation of this framework in various studies.

Chapter 4 demonstrates the capability of the framework to consider a wide range of markets and services including: energy, six contingency FCAS markets, FFR, inertia,

local network support and upstream reactive power support. The effectiveness of the robust restriction for the high-level optimisation to provide a feasible schedule is shown, as is the capability of the receding horizon control to adjust to uncertainties (both foreseen and unforeseen). The short optimisation time steps and receding horizon control have a significant impact on VPP revenue when compared with a VPP only matching day-ahead bids. The second order cone relaxation of the power flow equations is revealed to be effective at maintaining network limits.

Additionally, it is shown in Chapter 5 how the multi-energy flexibility of a electricity-hydrogen VPP can be quantified and translated into participation in multiple markets and services. This participation is effectively prioritised based on market prices, operating costs, and conversion losses between energy vectors. Using this framework, which considers multiple markets and energy vectors, reveals that the operation of multi-energy resources fundamentally changes when participating in multiple markets. Operation that previously would not occur, because it reduces the conversion efficiency between energy vectors, is now seen because it also maximises available flexibility, and therefore market participation. The ability of a VPP to utilise multi-energy flexibility to provide long-term contractual local network support is indicated. For the majority of the time the VPP utilises reactive power control to provide this service, limiting the constraints on VPP active power operation, and by extension VPP participation in active power markets. On rare occasions (usually during extreme events) the VPP must also use active power curtailment to provide this service, resulting in a more significant (but still limited) financial impact on VPP revenue. This demonstrates the importance of modelling network power flows that include reactive power.

This work also offers contribution by exhibiting the versatility of the application of the proposed framework. In Chapter 4 the framework is utilised by multiple entities in a network. The framework is effectively used by a DSO as well as multiple VPPs in one network. The method of network allocation used by the DSO is shown to be effective in maintaining the distribution network within allowable limits, whilst applying different fairness paradigms to the DER in the network. The flexibility of the framework allows the modelling of multiple network configurations, fairness paradigms, and DER operating schemes (reactive and/or active power control) which demonstrates the complex relationship between the financial and technical aspects of capacity allocation. The versatility of the framework is also evident in Chapter 6 where long-term techno-economic

analysis is conducted to support business case development for a multi-energy VPP. The long-term profitability of the VPP is shown to be heavily reliant on its ability to participate in multiple markets and services. The market prices also have a large impact on the revenue of an electricity-hydrogen VPP, as well as the valuation of contractual services that the VPP provides. By using a framework that explicitly models power flows in the network, this techno-economic analysis is able to consider the effects of network congestion. This allows the VPP to enter a contractual relationship with local RES to purchase their power that would otherwise be curtailed. It also reveals interactions between contractual FFR and network congestion which leads to the VPP providing valuable easing of network congestion worth millions of dollars each year. Therefore, it is apparent that a less comprehensive framework would miss many of these interactions, resulting in an inaccurate business case assessment.

7.4 Key Remarks

The comprehensive optimisation-based multi-energy operational framework and the case studies communicated in this thesis provide valuable insight to many actors in an electrical network. Each of the six aspects identified for a comprehensive framework are seen to be of great utility. In particular, the value of multi-market participation and provision of services encapsulated in the framework highlights how a VPP can increase its revenue generating capability. It could also be informative for network and market operators in understanding the capability of VPPs to participate in these mechanisms and assist in the secure and reliable operation of the electrical network. The understanding of a VPP's capability to provide network services, and the method by which these VPPs can be profitable will be useful in the move toward future networks with high penetrations of DER. In addition, the benefits of a holistic view of multi-energy integration are shown through electricity-hydrogen case studies. Hydrogen has been identified as an important fuel source in the future, and the technical and economic advantages of using the flexibility of hydrogen-based resources in the electrical network have been shown. Enabling hydrogen-based resources to participate in multiple markets will be important in driving down the cost of hydrogen production from RES. The business case techno-economic analysis conducted for VPPs could encourage investors to explore in more detail the potential value-stacking of revenue streams as well as the impacts of the

network constraints on VPP profitability. Understanding the many avenues of income available to a VPP will make them more economically attractive. More investment in flexible resources with proper operation could increase DER capability to provide network services, which could assist in maintaining future power system reliability. The versatility of the framework allows it to provide insights and utility to other network actors, as is demonstrated for a DSO determining DER capacity allocation. This issue is one that is currently being consider in a number of real world projects, and this type of analysis could help inform these projects and others.

7.5 Future Work

The presented framework could be expanded in the following ways. Peer-to-peer trading mechanisms have been receiving increasing interest as a possible method to economically benefit DER owners while assisting with network reliability. However, there are still a number of challenges associated with peer-to-peer trading [173]. The inclusions of peer-to-peer trading capability into this framework could allow further exploration of some of the technical challenges and opportunities of peer-to-peer trading.

In this work direct network capacity allocation by the DSO was considered. However, the SOC formulation of the power flow in the network allows the consideration of distribution local marginal pricing for active and reactive power as well as losses and network congestion through the use of dual variables [74]. Including these considerations into the framework could provide additional mechanisms for maintaining local network reliability and economic efficiency.

Another possible avenue of development that could be considered is including the provision for price-maker operation of the VPP (i.e., providing price/power pairs to a market operator). The interactions between multiple markets will then become even more complex, and will require in depth investigation.

A different avenue of enquiry could be to expand the framework to model the flow of other energy vectors, such as modelling electricity and gas flow [174], or electricity and gas and heat flow [175]. This could help capture in more detail the limitations of multi-energy flexibility due to operational constraints in other energy vectors. However, this comes with issues of additional computational complexity, although the gas flow

equations can also be relaxed to form SOC constraints [176]. For more accurate modelling of low voltage networks, a development of the framework to model unbalanced three-phase power flow could be considered. However, this modelling also brings with it significant computational burden that would need to be addressed. That being said, one possible avenue of investigation could be the SOC approach applied to unbalanced three-phase networks proposed in [177]. Although, this work relies on some restrictive assumptions, and requires preliminary load flow problems to be solved to obtain parameters for the optimisation. Another promising avenue to address this problem is through the use of Sequential Linear Programming, which has been shown to be highly effective in modelling distribution networks while maintaining tractability [178].

In conclusion, utilising a comprehensive operating framework such as the one proposed in this work can help unlock the flexibility of DER to assist in the economically efficient and reliable operation of a future grid. The insights offered in this work can help market operators, network operators, aggregators, and DER owners to better understand the technical and economic aspects of DER aggregation and network integration.

Appendix A

A Robust Restriction of the High-Level Optimisation

The following is a proof for the construction of a robust restriction of the high-level optimisation, reproduced from the author's paper *Co-optimizing Virtual Power Plant Services Under Uncertainty: A Robust Scheduling and Receding Horizon Dispatch Approach* [153].

The original high-level optimisation problem takes the following form:

$$\min_{y,(x_s)_{s\in[1:S^{HL}]}} \sum_{s=1}^{S^{\mathrm{HL}}} \pi_s J(x_s, y) \tag{A.1}$$

subject to:

$$K\epsilon_s = Cx_s + h, \;\; s \in \left[1 : S^{\mathrm{HL}}\right], \tag{A.2}$$

$$Ax_s + By \leq \overline{f}, \;\; s \in \left[1 : S^{\mathrm{HL}}\right], \tag{A.3}$$

$$Dx_s + E\epsilon_s \leq \overline{g}, s \in \left[1 : S^{\mathrm{HL}}\right], \tag{A.4}$$

where x_s denotes the vector of decision variables that can depend on the scenario $s \in \left[1 : S^{\mathrm{HL}}\right]$ corresponding to the high-level realisation, ϵ_s of the uncertain parameters (i.e., market prices, load demand, and available renewable generation), and y is the set of decision variables that are constant across scenarios (i.e., $\zeta_k(t), \;\; \forall k \in \Psi^K, t \in [1 : T^{\mathrm{HL}}]$). Assuming there are not redundant equality constraints, CC^T is non-singular.

The following problem is a restriction, but of much smaller and more manageable size:

$$\min_{y,z} \sum_{s=1}^{S^{\mathrm{HL}}} \pi_s J\left(C^R(K\epsilon_s - h) + z, y\right) \tag{A.5}$$

subject to

$$Az + By \leq \overline{\phi} - \hat{f}, \tag{A.6}$$

$$Dz \leq \overline{\gamma} - \hat{g}, \tag{A.7}$$

$$Cz = 0, \tag{A.8}$$

where $C^R = C^T(CC^T)^{-1}$, $\overline{\phi} = \overline{f} + AC^Rh$, $\overline{\gamma} = \overline{g} + DC^Rh$, $f_s = AC^RK\epsilon_s$, $g_s = \left(E + DC^RK\right)\epsilon_s$, for $s \in \left[1 : S^{\mathrm{HL}}\right]$, and

$$\hat{f} = \left[\max\left\{\mathrm{row}_i(f_s),\ \ s \in \left[1 : S^{\mathrm{HL}}\right]\right\}\right]_{i\in[1:n_f]'} \tag{A.9}$$

$$\hat{g} = \left[\max\left\{\mathrm{row}_i(g_s),\ \ s \in \left[1 : S^{\mathrm{HL}}\right]\right\}\right]_{i\in[1:n_g]'} \tag{A.10}$$

where $n_f = \dim\left(\overline{f}\right)$, $n_g = \dim\left(\overline{g}\right)$ and $[a_i]_{i\in[1:n]}$ denotes the vector $[a_i, \ldots, a_n]^T$. If the pair (y, z) satisfies the (A.6) - (A.8), then the pair

$$\left(y\left(x_s\right)_{s\in[1:S^{\mathrm{HL}}]}\right) = \left(y, \left(C^R\left(K\epsilon_s - h\right) + z\right)_{s\in[1:S^{\mathrm{HL}}]}\right) \tag{A.11}$$

satisfies (A.2) - (A.4). Note that f_s and g_s only depend on the realization ϵ_s of the uncertain parameters for the given scenario $s \in \left[1 : S^{\mathrm{HL}}\right]$; i.e., $\hat{f}$ and $\hat{g}$ are effectively problem data, to be determined before solving the optimisation problem. The same applies to the terms $C^R\left(K\epsilon_s - h\right)$ in (A.5). Importantly, the constraints in (A.6) - (A.8) retain the sparsity structure of the original constraints in (A.2) - (A.4).

To see that the optimisation problem in (A.5) - (A.8) is a restriction of the problem in (A.1) - (A.4), consider the following. First note that the equality constraint in (A.2) does not specify a unique x_s for a given ϵ_s. The equality constraint in (A.2) holds with

$$x_s = C^R\left(K\epsilon_s - h\right) + C^{\perp}w_s, \ \ s \in \left[1 : S^{\mathrm{HL}}\right] \tag{A.12}$$

for every w_s, where $C^{\perp}$ is a matrix with a range equal to the kernel of C. Introduce the variable z_s, and the constraint

$$Cz_s = 0, \quad s \in \left[1 : S^{\mathrm{HL}}\right]. \tag{A.13}$$

Then for every feasible z_s, there exists w_s such that $z_s = C^{\perp} w_s$, and this is unique because $C^{\perp}$ is full column rank. Given (A.12) and (A.13), the inequality constraints in (A.3) and (A.4) can be expressed as:

$$Az_s + By \leq \overline{\phi} - f_s, \quad s \in \left[1 : S^{\mathrm{HL}}\right], \tag{A.14}$$

$$Dz_s \leq \overline{\gamma} - g_s, \quad s \in \left[1 : S^{\mathrm{HL}}\right]. \tag{A.15}$$

Observe the $\overline{\phi} - f_s \geq \overline{\phi} - \hat{f}$, and $\overline{\gamma} - g_s \geq \overline{\gamma} - \hat{g}$ for $s \in \left[1 : S^{\mathrm{HL}}\right]$. As such, if there exists a z and y such that (A.3) and (A.4) hold, then (A.14) and (A.15) hold with $z_s = z$ for every $s \in \left[1 : S^{\mathrm{HL}}\right]$. Therefore, the original problem has a feasible solution via (A.11).

Note that the optimisation problem in (A.5) - (A.8) is a much smaller problem than the original one when S^{HL} is large, as it is reduced in size by a factor of S^{HL}. This smaller problem is a restriction on the original problem, requiring the flexibility corresponding to w_s in the relationship between x_s and ϵ_s to be constant across scenarios. However, x_s is still scenario dependent as shown in (A.11).

Appendix B

Resource Modelling Examples

This appendix is used to provide examples of how the resource modelling (B.1) can be used to model specific resources.

$$\overline{E}_k^{\text{elec}} \left(x_{k,s}(t+1) - x_{k,s}(t)\right) = \left(\eta_k^{\text{d}} P_{k,s}^{\text{d}}(t) - \frac{P_{k,s}^{\text{g}}(t)}{\eta_k^{\text{g}}} + \xi_{k,s,t} - \omega_{k,s}(t) - \nu_k\right) \Delta t, \quad \forall k \in \Psi^K \tag{B.1}$$

B.1 Battery Energy Storage System

To model a battery energy storage system (BESS) using (B.1), set $\xi_{k,s,t} = 0$ and $\omega_{k,s}(t) = 0$ as there is not external generation resource or demand, and therefore there can be no curtailment. This implies that the BESS operation is governed by

$$\overline{E}_k^{\text{elec}} \left(x_{k,s}(t+1) - x_{k,s}(t)\right) = \left(\eta_k^{\text{d}} P_{k,s}^{\text{d}}(t) - \frac{P_{k,s}^{\text{g}}(t)}{\eta_k^{\text{g}}} - \nu_k\right) \Delta t \tag{B.2}$$

B.2 Renewable Energy Source

To model a renewable energy source (RES) using (B.1), $\overline{E}_k^{\text{elec}} = 0$ and $\nu_k = 0$ (as an RES has no electrical energy storage), and $P_{k,s}^{\text{d}}(t) = 0$ (as RES is generator only). Therefore the operation of a RES is governed by

$$P_{k,s}^{\text{g}}(t) = \eta_k^{\text{g}} \left(\xi_{k,s,t} - \omega_{k,s}(t)\right). \tag{B.3}$$

However, the value of $\xi_{k,s,t}$ will vary over time, dependent on the availability of the RES. There may also be curtailment limits, or cost associated with curtailment of RES depending on the arrangement with the RES owners.

B.2.1 Wind Turbine

The power that a wind turbine can generate varies with the speed of the wind that flows past the turbine. Generally, the wind speed to power conversion of a wind farm can be modelled as:

$$P = \begin{cases} 0, & v^{\text{cut-in}} \geq v \\ \frac{\pi}{2} r^2 v^3 \rho \eta, & v^{\text{rated}} \geq v \geq v^{\text{cut-in}} \\ \frac{\pi}{2} r^2 {v^{\text{rated}}}^3 \rho \eta, & v^{\text{cut-out}} \geq v \geq v^{\text{rated}} \\ 0, & v \geq v^{\text{cut-out}} \end{cases} \tag{B.4}$$

where r is the radius of the circle swept by the turbine, v is the speed of the wind blowing past of turbine, ρ is the air density, and η is the conversion efficiency. $v^{\text{cut-in}}$ is the wind speed at which the turbine can begin to generate power. v^{rated} is the rated wind speed of the wind turbine associated with the rated power output of the turbine. $v^{\text{cut-out}}$ is the wind speed at which the wind turbine cannot continue to generate power in case of damage to the wind turbine.

This then means that (assuming the air density is constant) $\xi_{k,s,t}$ for a wind turbine can be considered as:

$$\xi_{k,s,t} = \begin{cases} 0, & v^{\text{cut-in}} \geq v_{s,t} \\ \frac{\pi}{2} r^2 v_{s,t}^3 \rho, & v^{\text{rated}} \geq v_{s,t} \geq v^{\text{cut-in}} \\ \frac{\pi}{2} r^2 {v^{\text{rated}}}^3 \rho, & v^{\text{cut-out}} \geq v_{s,t} \geq v^{\text{rated}} \\ 0, & v_{s,t} \geq v^{\text{cut-out}}. \end{cases} \tag{B.5}$$

If the VPP operator has a more detailed power curve for the wind farm, then this can be used to map the wind speed to the associated value of $\xi_{k,s,t}$.

B.2.2 PV

The power that PV can generate varies with the intensity of the solar irradiance to which it is exposed. The power generated by a PV can be modelled as:

$$P = \eta I A(1 - 0.005(T^{\text{amb}} - 25)) \tag{B.6}$$

where I is the solar irradiance, A is the array area, η is the conversion efficiency, and T^{amb} is the ambient temperature.

This means that (assuming constant ambient temperature) $\xi_{k,s,t}$ for a PV can be considered as:

$$\xi_{k,s,t} = I_{s,t} A(1 - 0.005(T^{\text{amb}} - 25)) \tag{B.7}$$

If the VPP operator has a more detailed power curve for the PV, then this can be used to map solar irradiance to the associated value of $\xi_{k,s,t}$.

B.3 OCGT

To model an OCGT using (B.1), $\overline{E}_k^{\text{elec}} = 0$ and $\nu_k = 0$ (as an OCGT has no electrical energy storage), and $P_{k,s}^{\text{d}}(t) = 0$ (as a OCGT is generator only). Therefore, the OCGT operation is governed by

$$P_{k,s}^{\text{g}}(t) = \eta_k^{\text{g}} \left(\xi_{k,s,t} - \omega_{k,s}(t)\right) \tag{B.8}$$

where $\xi_{k,s,t}$ is the available fuel and $\omega_{k,s}(t)$ is the fuel that is not utilised i.e., curtailed. Assuming that there is sufficient fuel to power the OCGT, then $\xi_{k,s,t}$ can be set arbitrarily so that it does not constrain OCGT power generation (i.e., $\xi_{k,s,t} = \frac{\overline{P}_k^{\text{g}}}{\eta_k^{\text{g}}}$). Likewise $\omega_{k,s}(t)$ would be unconstrained, and have no associated cost.

B.4 Curtailable Load

To model a curtailable load using (B.1), $\overline{E}_k^{\text{elec}} = 0$ and $\nu_k = 0$ (as a curtailable load has no electrical energy storage), and $P_{k,s}^{\text{g}}(t) = 0$ (as a curtailable load is a load only).

Therefore, the operation of a curtailable load is governed by:

$$\eta_k^{\mathrm{d}} P_{k,s}^{\mathrm{d}}(t) = -\left(\xi_{k,s,t} - \omega_{k,s}(t)\right). \tag{B.9}$$

In this equation $\xi_{k,s,t} \leq 0$ is the baseline demand and $\omega_{k,s}(t) \leq 0$ is the amount of load that is curtailed.

B.5 Multi-Energy Resources

$$\overline{E}_i^e \left(x_{i,s}^e(t+1) - x_{i,s}^e(t)\right) = \left(\sum_{k \in \Psi_{i,e}^K} \left(\eta_k^{\mathrm{d},e} P_{k,s}^{\mathrm{d}}(t) - \frac{P_{k,s}^{\mathrm{g}}(t)}{\eta_k^{\mathrm{g},e}}\right) + \xi_{i,s,t}^e - \omega_{i,s}^e(t) - \nu_i^e\right) \Delta t - E_{i,s}^{e,\exp}(t), \quad \forall i \in \Psi^N, \forall e \in \Psi^{\text{non-elec}} \tag{B.10}$$

It is also important to illustrate how the electrical resource modelling in (B.1) can be used in conjunction with (B.10) and how this can also be flexibly applied to numerous resources.

B.5.1 Electrolyser

Let us assume that there is an electrolyser at node i. The electrolyser converters electrical energy into hydrogen, so we consider $e = \mathrm{H2}$ as the secondary energy vector. In a purely electrical sense (assuming a constant efficiency), an electrolyser will operate as a curtailable load, and therefore its electrical operation is determined by (B.9). The value of $\xi_{k,s,t} = \frac{\overline{P}_k^{\mathrm{d}}}{\eta_k^{\mathrm{d}}}$ can be used in this case. The hydrogen operation of the electrolyser is constrained by the multi-energy node constraint (B.11).

$$\overline{E}_i^{\mathrm{H2}} \left(x_{i,s}^{\mathrm{H2}}(t+1) - x_{i,s}^{\mathrm{H2}}(t)\right) = \left(\eta_k^{\mathrm{d,H2}} P_{k,s}^{\mathrm{d}}(t) + \xi_{i,s,t}^{\mathrm{H2}} - \omega_{i,s}^{\mathrm{H2}}(t) - \nu_i^{\mathrm{H2}}\right) \Delta t - E_{i,s}^{\mathrm{H2,exp}}(t) \tag{B.11}$$

An electrolyser that only operates in the electricity and hydrogen energy vectors means that $\eta_k^{\mathrm{d,H2}} = \eta_k^{\mathrm{d}}$. (B.11) ensures that there is sufficient storage at node i for the electrolyser to operate, and that the hydrogen exported/imported and the hydrogen demand is balanced by the hydrogen created by the electrolyser. Now the operation of the electrolyser is constrained both by its electrical operation in (B.9) and its hydrogen operation in (B.11).

B.5.1.1 Additional Fuel Cell

Assuming a constant efficiency, a fuel cell can be modelled electrically as a dispatchable generator as in (B.8). The multi-energy node formulation of node i with both an electrolyser and a fuel cell is:

$$\overline{E}_i^{\mathrm{H2}} \left(x_{i,s}^{\mathrm{H2}}(t+1) - x_{i,s}^{\mathrm{H2}}(t)\right) = \left(\eta_{\mathrm{EL}}^{\mathrm{d,H2}} P_{\mathrm{EL},s}^{\mathrm{d}}(t) - \frac{P_{\mathrm{FC},s}^{\mathrm{g}}(t)}{\eta_{\mathrm{FC}}^{\mathrm{d,H2}}} + \xi_{i,s,t}^{\mathrm{H2}} - \omega_{i,s}^{\mathrm{H2}}(t) - \nu_i^{\mathrm{H2}}\right)\Delta t - E_{i,s}^{\mathrm{H2,exp}}(t) \quad \text{(B.12)}$$

B.5.2 Co-Generation Plant

A co-generation plant (CHP) burns gas to create electricity and also to generate heat. The electrical operation of the CHP can be modelled in the same way as other dispatchable generation, such as the OCGT in (B.8). However, because there is a CHP operating at node i, the heat energy vector ($e = \mathrm{ht}$) at node i must also be modelled

$$\overline{E}_i^{\mathrm{ht}} \left(x_{i,s}^{\mathrm{ht}}(t+1) - x_{i,s}^{\mathrm{ht}}(t)\right) = \left(\left(-\frac{P_{k,s}^{\mathrm{g}}(t)}{\eta_k^{\mathrm{g,ht}}}\right) + \xi_{i,s,t}^{\mathrm{ht}} - \omega_{i,s}^{\mathrm{ht}}(t) - \nu_i^{\mathrm{ht}}\right)\Delta t - E_{i,s}^{\mathrm{ht,exp}}(t), \quad \text{(B.13)}$$

In the case of a CHP the gas-to-electricity conversion efficiency η_k^{g} is not the same as the gas-to-heat conversion efficiency $\eta_k^{\mathrm{g,g2h}}$. The term $\eta_k^{\mathrm{g,ht}} = \frac{\eta_k^{\mathrm{g,g2h}}}{\eta_k^{\mathrm{g}}}$ relates the electrical power output to the heat power output. If there is no thermal energy storage at node i ($\overline{E}_i^{\mathrm{ht}} = 0$, $\nu_i^{\mathrm{ht}} = 0$) then the heat generated by the CHP must be balanced by heat demand at the node (minus curtailment) and any heat exported/imported.

Bibliography

[1] United Nations Framework Convention of Climate Change, 2015.

[2] H. Ritchie and M. Roser. Co_2 and greenhouse gas emissions. *Our World in Data*, 2020. URL https://ourworldindata.org/co2-and-other-greenhouse-gas-emissions.

[3] International Renewable Energy Agency (IRENA). *Renewable Energy and Climate Pledges: Five Years After the Paris Agreement*. 2019. URL https://www.irena.org/publications/2020/Dec/Renewable-energy-and-climate-pledges.

[4] International Renewable Energy Agency (IRENA). *Renewable Capacity Statistics 2021*. 2021. URL https://www.irena.org/publications/2021/March/Renewable-Capacity-Statistics-2021.

[5] *Australian Government Clean Energy Regulator*, 2021. URL http://www.cleanenergyregulator.gov.au/RET/Forms-and-resources/Postcode-data-for-small-scale-installations#Smallscale-installations-by-installation-year.

[6] Australian Energy Market Operator (AEMO). *Minimum operational demand thresholds in South Australia*. 2020. URL https://www.aemo.com.au/-/media/Files/Electricity/NEM/Planning_and_Forecasting/SA_Advisory/2020/Minimum-Operational-Demand-Thresholds-in-South-Australia-Review.

[7] Knowledge Sourcing Intelligence LLP. *Global Combined Heat and Power (CHP) Market - Forecasts from 2020 to 2025*. 2020. URL https://www.researchandmarkets.com/reports/5174330/global-combined-heat-and-power-chp-market?utm_source=GNOM&utm_medium=PressRelease&utm_code=kgw8qg&utm_campaign=1469471+-+The+

Worldwide+Combined+Heat+and+Power+Industry+is+Expected+to+Grow+at+a+CAGR+of+14.37%25+Between+2019+and+2025&utm_exec=jamu273prd.

[8] M. Jesper, F. Schlosser, F. Pag, T. G. Walmsley, B. Schmitt, and K. Vajen. Large-scale heat pumps: Uptake and performance modelling of market-available devices. *Renewable and Sustainable Energy Reviews*, 137:110646, 2021. ISSN 1364-0321. doi: 10.1016/j.rser.2020.110646.

[9] V.M. Zavala, D. Skow, T. Celinski, and P. Dickinson. *Techno-Economic Evaluation of a Next-Generation Building Energy Management System.* U.S. Department of Energy, 2011.

[10] Energy storage. *International Energy Agency (IEA)*, 2020. URL https://www.iea.org/reports/energy-storage.

[11] N. P. Brandon and Z. Kurban. Clean energy and the hydrogen economy. *Philosophical Transactions of the Royal Society A: Mathematical, Physical and Engineering Sciences*, 375(2098):20160400, 2017. ISSN 1364-503X. doi: 10.1098/rsta.2016.0400.

[12] Global ev outlook 2020. *International Energy Agency (IEA)*, 2020. URL https://www.iea.org/reports/global-ev-outlook-2020.

[13] J. P. Holguin, D. C. Rodriguez, and G. Ramos. Reverse power flow (RPF) detection and impact on protection coordination of distribution systems. *IEEE Transactions on Industry Applications*, 56(3):2393–2401, 2020. ISSN 0093-9994. doi: 10.1109/tia.2020.2969640.

[14] P. J. Baruah, N. Eyre, M. Qadrdan, M. Chaudry, S. Blainey, J.W. Hall, N. Jenkins, and M. Tran. Energy system impacts from heat and transport electrification. *Proceedings of the Institution of Civil Engineers - Energy*, 167(3):139–151, 2014. ISSN 1751-4223. doi: 10.1680/ener.14.00008.

[15] Australian Energy Market Operator (AEMO). *Market Insights and WA Market Operations.* Quarterly Energy Dynamics Q4 2020. 2021. URL https://aemo.com.au/-/media/files/major-publications/qed/2020/qed-q4-2020.pdf?la=en.

[16] Australian Energy Market Operator (AEMO). *Regulation FCAS Changes.* 2019. URL https://aemo.com.au/-/media/Files/Electricity/NEM/Security_and_

Reliability/Ancillary_Services/Frequency-and-time-error-reports/Regulation-FCAS-factsheet.pdf.

[17] Australian Energy Market Operator (AEMO). *Renewable Integration Study Stage 1 - Appendix B:Frequency control.* 2020. URL https://www.aemo.com.au/-/media/files/major-publications/ris/2020/ris-stage-1-appendix-b.pdf?la=en.

[18] Australian Energy Market Operator (AEMO). *Five-minute settlement and global settlement: 5MS Bidding Service Go-live Plan.* 2021. URL https://aemo.com.au/-/media/files/electricity/nem/5ms/readiness-workstream/2021/final-5ms-bidding-service-go-live-plan.pdf?la=en&hash=33349C960C71571E0BB803F98A7315F4.

[19] Australian Energy Market Operator (AEMO). Guide to ancillary services in the national electricity market. Report, 2015. URL https://www.aemo.com.au/-/media/Files/PDF/Guide-to-Ancillary-Services-in-the-National-Electricity-Market.ashx.

[20] Australian Energy Market Operator (AEMO). *Power System Requirements.* 2020. URL https://aemo.com.au/-/media/files/electricity/nem/security_and_reliability/power-system-requirements.pdf?la=en.

[21] Australian Energy Market Operator (AEMO). 2019 network support and control ancillary services (NSCAS) report. Technical report, 2019. URL https://aemo.com.au/-/media/files/electricity/nem/planning_and_forecasting/isp/2019/2019_nscas_report.pdf?la=en.

[22] CIGRE Study Committee C2 System operation and control. Power system restoration – world practices & future trends. *CIGRE Science & Engineering*, (14):6, 2019.

[23] Australian Energy Market Operator (AEMO). SRAS guideline: System restart ancillary services incorporating boundaries of electrical sub networks. Technical report, 2020. URL https://aemo.com.au/-/media/files/electricity/nem/security_and_reliability/ancillary_services/sras/sras-guideline-2020.pdf?la=en.

[24] Australian Energy Market Commission (AEMC). *Frequency Control Rule Changes*. Directions Paper. 2020. URL https://www.aemc.gov.au/sites/default/files/2020-12/Frequency%20control%20rule%20changes%20-%20Directions%20paper%20-%20December%202020.pdf.

[25] C. Christiansen and N. Hillmann. Feasibility of fast frequency response obligations of new generators. Report, AECOM Australia Pty Ltd, 2017. URL https://www.aemc.gov.au/sites/default/files/content/661d5402-3ce5-4775-bb8a-9965f6d93a94/AECOM-Report-Feasibility-of-FFR-Obligations-of-New-Generators.pdf.

[26] Australian Energy Market Operator (AEMO). 2020 system strength and inertia report. Technical report, 2020. URL https://www.aemo.com.au/-/media/files/electricity/nem/planning_and_forecasting/Operability/2020/2020-System-Strength-and-Inertia-Report.

[27] Australian Energy Market Operator (AEMO). *Inertia Requirements & Shortfall*. Inertia Requirements Methodology. 2018. URL https://www.aemo.com.au/-/media/Files/Electricity/NEM/Security_and_Reliability/System-Security-Market-Frameworks-Review/2018/Inertia_Requirements_Methodology_PUBLISHED.pdf.

[28] Australian Renewable Energy Agency (ARENA). AEMO and ARENA demand response trial to provide 200 megawatts of emergency reserves for extreme peaks. *AEMO-ARENA Demand Response*, Oct 2017. URL https://arena.gov.au/assets/2017/10/ARENA-AEMO-Media-Release-Demand-Response-pilot-programs-deliver-200-megawatts-to-manage-extreme-peaks-Wed-11-Oct-2017.pdf.

[29] Aurecon. *Large-Scale Battery Storage Knowledge Sharing Report*. 2019. URL https://arena.gov.au/assets/2019/11/large-scale-battery-storage-knowledge-sharing-report.pdf.

[30] Newport Consortium. *Coordination of Distributed Energy Resources; International System Architecture Insights for Future Market Design*. 2018. URL https://www.aemo.com.au/-/media/Files/Electricity/NEM/DER/2019/OEN/Newport-Intl-Review-of-DER-Coordination-for-AEMO-final-report.pdf.

[31] H. Gerard, E. Rivero, and J. Vanschoenwinkel. *TSO-DSO Interaction and Acquisition of Ancillary Services from Distribution*, pages 7–23. Springer International Publishing, Cham, 2020. ISBN 978-3-030-29203-4. doi: 10.1007/978-3-030-29203-4_2.

[32] A. Ulbig and G. Andersson. Analyzing operational flexibility of electric power systems. In *2014 Power Systems Computation Conference*, pages 1–8. doi: 10.1109/PSCC.2014.7038383.

[33] International Hydropower Association (IHA). Hydropower status report: Sector trends and insights. Technical report, 2020. URL `https://hydropower-assets.s3.eu-west-2.amazonaws.com/publications-docs/2020_hydropower_status_report.pdf`.

[34] S. Nelmes. Liquid air energy storage. *University of Warwick*, 2017. URL `https://warwick.ac.uk/fac/sci/eng/research/grouplist/electricalpower/images/newsnevents/hies2017/presentations/hies2017_highview.pdf`.

[35] G. Papaefthymiou, K. Grave, and K. Dragoon. Flexibility Options in Electricity Systems. Technical Report POWDE14426, ECOFYS, Berlin, March 2014. URL `https://www.ourenergypolicy.org/wp-content/uploads/2014/06/Ecofys.pdf`.

[36] J.I Pérez-Díaz, G. Cavazzini, F. Blázquez, C. Platero, J. Fraile-Ardanuy, J.A Sánchez, and M. Chazarra. Technological developments for pumped-hydro energy storage. Technical report, 2014. URL `https://eera-es.eu/wp-content/uploads/2016/06/Technological-Developments-for-Pumped-Hydro-Energy-Storage_EERA-report-2014.pdf`.

[37] Highview Power. *Highview Power: Plants.* URL `https://highviewpower.com/plants/`.

[38] C. Kaldemeyer, C. Boysen, and I. Tuschy. Compressed air energy storage in the german energy system – status quo & perspectives. *Energy Procedia*, 99:298–313, 2016. ISSN 1876-6102. doi: 10.1016/j.egypro.2016.10.120.

[39] Australian Energy Market Operator (AEMO). Initial operation of the hornsdale power reserve battery energy storage system. Report, April

2018 . URL https://aemo.com.au/-/media/Files/Media_Centre/2018/Initial-operation-of-the-Hornsdale-Power-Reserve.pdf.

[40] Dominion Energy. Bath county pumped storage station, 2020. URL https://www.dominionenergy.com/projects-and-facilities/hydroelectric-power-facilities-and-projects/bath-county-pumped-storage-station.

[41] C. Daley and E. Chan. *Big Batteries - big issues!* energybyte, 2021. URL https://energybyte.com.au/big-batteries-big-issues/.

[42] Deloitte. Assessing the flexibility of coal-fired power plants for the integration of renewable energy in germany. Technical report, 2019. URL https://www2.deloitte.com/content/dam/Deloitte/fr/Documents/financial-advisory/economicadvisory/deloitte_assessing-flexibility-coal-fired-power-plants.pdf.

[43] International Renewable Energy Agency (IRENA). *Flexibility in Conventional Power Plants: Innovation Landscape Brief*. 2019. URL https://www.irena.org/-/media/Files/IRENA/Agency/Publication/2019/Sep/IRENA_Flexibility_in_CPPs_2019.pdf?la=en&hash=AF60106EA083E492638D8FA9ADF7FD099259F5A1.

[44] C. Loutan, P. Klauer, S. Chowdhury, S. Hall, M. Morjaria, V. Chadliev, N. Milam, C. Milan, and V. Gevorgian. Demonstration of essential reliability service by a 300-MW solar photovoltaic power plant. Technical Report NREL/TP-5D00-67799. URL https://www.nrel.gov/docs/fy17osti/67799.pdf.

[45] E. Demirok, P. C. González, K. H. B. Frederiksen, D. Sera, P. Rodriguez, and R. Teodorescu. Local reactive power control methods for overvoltage prevention of distributed solar inverters in low-voltage grids. *IEEE Journal of Photovoltaics*, 1(2):174–182, 2011. ISSN 2156-3381. doi: 10.1109/jphotov.2011.2174821.

[46] International Renewable Energy Agency (IRENA). *Green Hydrogen: A guide to policy making*. 2020. URL https://www.irena.org/-/media/Files/IRENA/Agency/Publication/2020/Nov/IRENA_Green_hydrogen_policy_2020.pdf.

[47] S. Bruce, M. Temminghoff, J. Hayward, E. Schmidt, C. Munnings, D. Palfreyman, and P. Hartley. National hydrogen roadmap. Report, CSIRO, 2018. URL https://www.csiro.au/en/work-with-us/services/consultancy-strategic-advice-services/csiro-futures/futures-reports/hydrogen-roadmap.

[48] J. Eichman, K. Harrison, and M. Peters. *Novel Electrolyzer Applications: Providing More Than Just Hydrogen*. 2014. URL https://www.nrel.gov/docs/fy14osti/61758.pdf.

[49] Siemens Energy. *Silyzer 300: The next paradigm in PEM electrolysis*. URL https://assets.siemens-energy.com/siemens/assets/api/uuid:17cdfbd8-13bd-4327-9b26-383e4754bee3/datasheet-final1.pdf.

[50] K. Nikiforow, J. Pennanen, J. Ihonen, S. Uski, and P. Koski. Power ramp rate capabilities of a 5kW proton exchange membrane fuel cell system with discrete ejector control. *Journal of Power Sources*, 381:30–37, 2018. ISSN 0378-7753. doi: 10.1016/j.jpowsour.2018.01.090. URL https://dx.doi.org/10.1016/j.jpowsour.2018.01.090.

[51] M. A. Pellow, C. J. M. Emmott, C. J. Barnhart, and S. M. Benson. Hydrogen or batteries for grid storage? a net energy analysis. *Energy & Environmental Science*, 8(7):1938–1952, 2015. ISSN 1754-5692. doi: 10.1039/c4ee04041d. URL https://dx.doi.org/10.1039/c4ee04041d.

[52] M. Kauw, R. M.J. Benders, and C. Visser. Green methanol from hydrogen and carbon dioxide using geothermal energy and/or hydropower in iceland or excess renewable electricity in germany. *Energy*, 90:208–217, 2015. ISSN 0360-5442. doi: 10.1016/j.energy.2015.06.002.

[53] Australian Renewable Energy Agency (ARENA). *Hydrogen potential for local gas networks in SA and Victoria*. Media Release. URL https://arena.gov.au/assets/2020/02/ARENA-Media-Release_AGN-Hydrogen-Blending-Feasibility-Studies-21022020.pdf.

[54] Government of South Australia. *Renewables South Australia*, 2019. URL http://www.renewablessa.sa.gov.

au/topic/hydrogen/hydrogen-projects-south-australia/neoen-australia-hydrogen-super-hub.

[55] Australian Renewable Energy Agency (ARENA). Powering regional and remote australia with renewable hydrogen. 2020. URL https://arena.gov.au/news/powering-regional-and-remote-australia-with-renewable-hydrogen.

[56] Australian Renewable Energy Agency (ARENA). ATCO hydrogen microgrid. 2018. URL https://arena.gov.au/projects/atco-hydrogen-microgrid/.

[57] N. Good, E. Karangelos, A. Navarro-Espinosa, and P. Mancarella. Optimization under uncertainty of thermal storage-based flexible demand response with quantification of residential users' discomfort. *IEEE Transactions on Smart Grid*, 6(5): 2333–2342, 2015. ISSN 1949-3053. doi: 10.1109/tsg.2015.2399974.

[58] M. Giuntoli and D. Poli. Optimized thermal and electrical scheduling of a large scale virtual power plant in the presence of energy storages. *IEEE Transactions on Smart Grid*, 4(2):942–955, 2013. ISSN 1949-3053. doi: 10.1109/TSG.2012.2227513.

[59] C. Kieny, B. Berseneff, N. Hadjsaid, Y. Besanger, and J. Maire. On the concept and the interest of virtual power plant: Some results from the european project fenix. In *2009 IEEE Power & Energy Society General Meeting*, pages 1–6. ISBN 1932-5517. doi: 10.1109/PES.2009.5275526.

[60] B. Tavares and F. J. Soares. An innovative approach for distribution network reinforcement planning: Using DER flexibility to minimize investment under uncertainty. *Electric Power Systems Research*, 183:106272, 2020. ISSN 0378-7796. doi: 10.1016/j.epsr.2020.106272.

[61] S. Burger, J. P. Chaves-Ávila, C. Batlle, and I. J. Pérez-Arriaga. The value of aggregators in electricity systems. *MIT Center for Energy and Environmental Policy Research*, 2016. URL https://energy.mit.edu/wp-content/uploads/2016/01/CEEPR_WP_2016-001.pdf.

[62] M. Brenna, M. C. Falvo, F. Foiadelli, L. Martirano, and D. Poli. From virtual power plant (VPP) to sustainable energy microsystem (SEM): An opportunity for buildings energy management. In *2015 IEEE Industry Applications Society Annual Meeting*, pages 1–8. doi: 10.1109/IAS.2015.7356799.

[63] Australian Energy Market Operator (AEMO). *Knowledge Sharing Report #3*. AEMO Virtual Power Plant Demonstrations. 2021. URL https://aemo.com.au/-/media/files/initiatives/der/2021/vpp-demonstrations-knowledge-sharing-report-3.pdf?la=en.

[64] Australian Energy Market Commission (AEMC). *National Electricity Amendment (Wholesale Demand Response Mechanism) Rule 2020*. Draft Rule Determination. 2020. URL https://www.aemc.gov.au/sites/default/files/documents/wholesale_demand_response_mechanism_-_second_draft_determination.pdf.

[65] Sa virtual power plant. *Energy Locals*, 2022. URL https://energylocals.com.au/savpp.

[66] Customers reap rewards through agl virtual power plant. *AGL*, 2019. URL https://www.agl.com.au/about-agl/media-centre/asx-and-media-releases/2019/june/customers-reap-rewards-through-agl-virtual-power-plant.

[67] Virtual power plant. *ShineHub*, 2022. URL https://shinehub.com.au/virtual-power-plant/.

[68] P. Mancarella. MES (multi-energy systems): An overview of concepts and evaluation models. *Energy*, 65:1–17, 2014. ISSN 0360-5442. doi: 10.1016/j.energy.2013.10.041.

[69] G. Chicco, S. Riaz, A. Mazza, and P. Mancarella. Flexibility from distributed multienergy systems. *Proceedings of the IEEE*, pages 1–22, 2020. ISSN 1558-2256. doi: 10.1109/JPROC.2020.2986378.

[70] S. Riaz and P. Mancarella. On feasibility and flexibility operating regions of virtual power plants and TSO/DSO interfaces. In *2019 IEEE Milan PowerTech*, pages 1–6. doi: 10.1109/PTC.2019.8810638.

[71] E. K. P. Chong and S. H. Zak. *An Introduction to Optimization*. John Wiley & Sons, Incorporated, New Jersey, 2013.

[72] S. Boyd and L. Vandenberghe. *Convex Optimization*. Cambridge University Press, Cambridge, 2004. URL https://www.cambridge.org/core/books/convex-optimization/17D2FAA54F641A2F62C7CCD01DFA97C4.

[73] W. Forst and D. Hoffmann. *Optimization Theory and Practice*. Springer New York, New York, NY, 2010. ISBN 978-0-387-78977-4. doi: 10.1007/978-0-387-78977-4_2.

[74] J. A. Taylor. *Convex Optimization of Power Systems*. Cambridge University Press, 2015. doi: 10.1017/CBO9781139924672.

[75] F. A. Potra and S. J. Wright. Interior-point methods. *Journal of Computational and Applied Mathematics*, 124(1-2):281–302, 2000. ISSN 0377-0427. doi: 10.1016/s0377-0427(00)00433-7.

[76] B. S. Gomes De Almeida and V. C. Leite. *Particle Swarm Optimization: A Powerful Technique for Solving Engineering Problems*. 2019. doi: 10.5772/intechopen.89633.

[77] K. Sastry, D. Goldberg, and G. Kendall. *Genetic Algorithms*, pages 97–125. Springer US, Boston, MA, 2005. ISBN 978-0-387-28356-2. doi: 10.1007/0-387-28356-0_4.

[78] L. Wolsey. *Branch and Bound*. Integer Programming. John Wiley & Sons, Ltd, 2020. ISBN 9781119606475. doi: https://doi.org/10.1002/9781119606475.ch7.

[79] L. Wolsey. *Cutting Plane Algorithms*. Integer Programming. John Wiley & Sons, Ltd, 2020. ISBN 9781119606475. doi: https://doi.org/10.1002/9781119606475.ch8.

[80] W. Melo, M. Fampa, and F. Raupp. An overview of MINLP algorithms and their implementation in muriqui optimizer. *Annals of Operations Research*, 286(1-2): 217–241, 2020. ISSN 0254-5330. doi: 10.1007/s10479-018-2872-5.

[81] J. Frédéric Bonnans. *Convex and Stochastic Optimization*. Universitext, 2019. doi: 10.1007/978-3-030-14977-2_6.

[82] K. Marti. *Stochastic Optimization Methods*. 2015. doi: 10.1007/978-3-662-46214-0_1.

[83] A. Ben-Tal, L. El Ghaoui, and A. Nemirovski. *Robust Optimization*. Princeton University Press, Princeton, UNITED STATES, 2009. ISBN 9781400831050. URL `http://ebookcentral.proquest.com/lib/unimelb/detail.action?docID=457706`.

[84] H. Zhou, Z. Li, J. H. Zheng, Q. H. Wu, and H. Zhang. Robust scheduling of integrated electricity and heating system hedging heating network uncertainties. *IEEE Transactions on Smart Grid*, 11(2):1543–1555, 2020. ISSN 1949-3053. doi: 10.1109/tsg.2019.2940031.

[85] Liwei Ju, Rui Zhao, Qinliang Tan, Yan Lu, Qingkun Tan, and Wei Wang. A multi-objective robust scheduling model and solution algorithm for a novel virtual power plant connected with power-to-gas and gas storage tank considering uncertainty and demand response. *Applied Energy*, 250:1336–1355, 2019. ISSN 0306-2619. doi: https://doi.org/10.1016/j.apenergy.2019.05.027. URL `http://www.sciencedirect.com/science/article/pii/S0306261919308803`.

[86] J. Yi, P. F. Lyons, P. J. Davison, P. Wang, and P. C. Taylor. Robust scheduling scheme for energy storage to facilitate high penetration of renewables. *IEEE Transactions on Sustainable Energy*, 7(2):797–807, 2016. ISSN 1949-3029. doi: 10.1109/TSTE.2015.2498622.

[87] W. Van, R. Zorgati, R. Henrion, and A. Mller. *Chance Constrained Programming and Its Applications to Energy Management*. 2011. doi: 10.5772/15438.

[88] R. Tempo, G. Calafiore, and F. Dabbene. *Scenario Approach to Probabilistic Design*, pages 165–179. Springer London, London, 2013. ISBN 978-1-4471-4610-0. doi: 10.1007/978-1-4471-4610-0_12.

[89] G. C. Calafiore and M. C. Campi. The scenario approach to robust control design. *IEEE Transactions on Automatic Control*, 51(5):742–753, 2006. ISSN 1558-2523. doi: 10.1109/TAC.2006.875041.

[90] T. Alamo, R. Tempo, A. Luque, and D.R Ramirez. Randomized methods for design of uncertain systems: Sample complexity and sequential algorithms. *Automatica*, 52:160–172, 2015.

[91] M. Vrakopoulou, B. Li, and J. L. Mathieu. Chance constrained reserve scheduling using uncertain controllable loads part i: Formulation and scenario-based analysis. *IEEE Transactions on Smart Grid*, 10(2):1608–1617, 2019. ISSN 1949-3053. doi: 10.1109/tsg.2017.2773627.

[92] C. Suazo-Martinez, E. Pereira-Bonvallet, R. Palma-Behnke, and X. P. Zhang. Impacts of energy storage on short term operation planning under centralized

spot markets. *IEEE Transactions on Smart Grid*, 5(2):1110–1118, 2014. ISSN 1949-3053. doi: 10.1109/tsg.2013.2281828.

[93] S. Talari, M. Yazdaninejad, and M. R. Haghifam. Stochastic-based scheduling of the microgrid operation including wind turbines, photovoltaic cells, energy storages and responsive loads. *IET Generation, Transmission & Distribution*, 9(12):1498–1509, 2015.

[94] J. Toubeau, Z. De Grève, and F. Vallée. Medium-term multimarket optimization for virtual power plants: A stochastic-based decision environment. *IEEE Transactions on Power Systems*, 33(2):1399–1410, 2018.

[95] J. Mattingley, Y. Wang, and S. Boyd. Code generation for receding horizon control. In *2010 IEEE International Symposium on Computer-Aided Control System Design*, pages 985–992, 2010. doi: 10.1109/CACSD.2010.5612665.

[96] S. Han, S. Hee Han, and W. H. Kwon. *Introduction.* Receding Horizon Control: Model Predictive Control for State Models. Springer London, London, 2005. ISBN 978-1-84628-017-7. doi: 10.1007/1-84628-017-6_1. URL `https://doi.org/10.1007/1-84628-017-6_1`.

[97] G. Grimm, M. J. Messina, S. E. Tuna, and A. R. Teel. Nominally robust model predictive control with state constraints. *IEEE Transactions on Automatic Control*, 52(10):1856–1870, 2007. doi: 10.1109/TAC.2007.906187.

[98] A. Vesey. *The Virtual Utility.* The Virtual Utility: Accounting, Technology & Competitive Aspects of the Emerging Industry. Springer US, Boston, MA, 1997. ISBN 978-1-4615-6167-5. doi: 10.1007/978-1-4615-6167-5_3.

[99] K. Dielmann and A. van der Velden. Virtual power plants (VPP) - a new perspective for energy generation? In *Proceedings of the 9th International Scientific and Practical Conference of Students, Post-graduates Modern Techniques and Technologies*, pages 18–20, 2003. doi: 10.1109/SPCMTT.2003.1438108.

[100] R. Caldon, A.R. Patria, and R. Turri. Optimisation algorithm for a virtual power plant operation. In *39th International Universities Power Engineering Conference, 2004. UPEC 2004.*, volume 3, pages 1058–1062 vol. 2, 2004.

[101] N. Ruiz, I. Cobelo, and J. Oyarzabal. A direct load control model for virtual power plant management. *IEEE Transactions on Power Systems*, 24(2):959–966, 2009.

[102] D. Pudjianto, C. Ramsay, and G. Strbac. Virtual power plant and system integration of distributed energy resources. *IET Renewable Power Generation*, 1(1): 10–16, 2007.

[103] A. Mnatsakanyan and S. W. Kennedy. A novel demand response model with an application for a virtual power plant. *IEEE Transactions on Smart Grid*, 6(1): 230–237, 2015.

[104] E. Dall'Anese, S. V. Dhople, and G. B. Giannakis. Optimal dispatch of photovoltaic inverters in residential distribution systems. *IEEE Transactions on Sustainable Energy*, 5(2):487–497, 2014.

[105] R. Moreno, R. Moreira, and G. Strbac. A MILP model for optimising multi-service portfolios of distributed energy storage. *Applied Energy*, 137:554–566, 2015. ISSN 0306-2619. doi: https://doi.org/10.1016/j.apenergy.2014.08.080.

[106] H. Wang, S. Riaz, and P. Mancarella. Integrated techno-economic modeling, flexibility analysis, and business case assessment of an urban virtual power plant with multi-market co-optimization. *Applied Energy*, 259:114142, 2020.

[107] E. A. Martínez Ceseña, N. Good, A. L. A. Syrri, and P. Mancarella. Techno-economic and business case assessment of multi-energy microgrids with co-optimization of energy, reserve and reliability services. *Applied Energy*, 210:896–913, 2018. ISSN 0306-2619. doi: https://doi.org/10.1016/j.apenergy.2017.08.131.

[108] D. Koraki and K. Strunz. Wind and solar power integration in electricity markets and distribution networks through service-centric virtual power plants. *IEEE Transactions on Power Systems*, 33(1):473–485, 2018.

[109] A. Baringo and L. Baringo. A stochastic adaptive robust optimization approach for the offering strategy of a virtual power plant. *IEEE Transactions on Power Systems*, 32(5):3492–3504, 2017. ISSN 0885-8950. doi: 10.1109/TPWRS.2016.2633546.

[110] F. Bignucolo, R. Caldon, V. Prandoni, S. Spelta, and M. Vezzola. The voltage control on MV distribution networks with aggregated DG units (VPP). In *Proceedings*

of the 41st International Universities Power Engineering Conference, volume 1, pages 187–192, 2006. doi: 10.1109/UPEC.2006.367741.

[111] D. Zarrilli, A. Vicino, and P. Mancarella. Sharing energy resources in distribution networks: An initial investigation through OPF studies. In *2016 IEEE Innovative Smart Grid Technologies - Asia (ISGT-Asia)*, pages 306–311. doi: 10.1109/ISGT-Asia.2016.7796403.

[112] E. Mashhour and S. M. Moghaddas-Tafreshi. Bidding strategy of virtual power plant for participating in energy and spinning reserve markets - part i: Problem formulation. *IEEE Transactions on Power Systems*, 26(2):949–956, 2011. ISSN 0885-8950. doi: 10.1109/TPWRS.2010.2070884.

[113] E. Mashhour and S. M. Moghaddas-Tafreshi. Bidding strategy of virtual power plant for participating in energy and spinning reserve markets - part ii: Numerical analysis. *IEEE Transactions on Power Systems*, 26(2):957–964, 2011. ISSN 0885-8950. doi: 10.1109/TPWRS.2010.2070883.

[114] G. Mohy-Ud-Din, K. M. Muttaqi, and D. Sutanto. Transactive energy-based planning framework for VPPs in a co-optimised day-ahead and real-time energy market with ancillary services. *IET Generation, Transmission & Distribution*, 13(11): 2024–2035, 2019. ISSN 1751-8687. doi: 10.1049/iet-gtd.2018.5831.

[115] E. A. Bakirtzis, P. N. Biskas, D. P. Labridis, and A. G. Bakirtzis. Multiple time resolution unit commitment for short-term operations scheduling under high renewable penetration. *IEEE Transactions on Power Systems*, 29(1):149–159, 2014.

[116] A. Saint-Pierre and P. Mancarella. Active distribution system management: A dual-horizon scheduling framework for DSO/TSO interface under uncertainty. *IEEE Transactions on Smart Grid*, 8(5):2186–2197, 2017. ISSN 1949-3053. doi: 10.1109/TSG.2016.2518084.

[117] H. Fu, Z. Wu, X. P. Zhang, and J. Brandt. Contributing to DSO's energy-reserve pool: A chance-constrained two-stage μ VPP bidding strategy. *IEEE Power and Energy Technology Systems Journal*, 4(4):94–105, 2017. ISSN 2332-7707. doi: 10.1109/jpets.2017.2749256.

[118] Z. Wu, P. Zeng, X. P. Zhang, and Q. Zhou. A solution to the chance-constrained two-stage stochastic program for unit commitment with wind energy integration.

IEEE Transactions on Power Systems, 31(6):4185–4196, 2016. ISSN 0885-8950. doi: 10.1109/tpwrs.2015.2513395.

[119] M. Vahedipour-Dahraie, H. Rashidizadeh-Kermani, M. Shafie-Khah, and J. P. S. Catalão. Risk-averse optimal energy and reserve scheduling for virtual power plants incorporating demand response programs. *IEEE Transactions on Smart Grid*, 12 (2):1405–1415, 2021. doi: 10.1109/TSG.2020.3026971.

[120] M. Peik-Herfeh, H. Seifi, and M. K. Sheikh-El-Eslami. Decision making of a virtual power plant under uncertainties for bidding in a day-ahead market using point estimate method. *International Journal of Electrical Power & Energy Systems*, 44 (1):88–98, 2013.

[121] F. Luo, Z. Y. Dong, K. Meng, J. Qiu, J. Yang, and K. P. Wong. Short-term operational planning framework for virtual power plants with high renewable penetrations. *IET Renewable Power Generation*, 10(5):623–633, 2016.

[122] L. Ju, Z. Tan, J. Yuan, Q. Tan, H. Li, and F. Dong. A bi-level stochastic scheduling optimization model for a virtual power plant connected to a wind–photovoltaic–energy storage system considering the uncertainty and demand response. *Applied Energy*, 171:184–199, 2016. ISSN 0306-2619. doi: https://doi.org/10.1016/j.apenergy.2016.03.020.

[123] M. Rahimiyan and L. Baringo. Strategic bidding for a virtual power plant in the day-ahead and real-time markets: A price-taker robust optimization approach. *IEEE Transactions on Power Systems*, 31(4):2676–2687, 2016.

[124] H. Zhao, B. Wang, Z. Pan, H. Sun, Q. Guo, and Y. Xue. Aggregating additional flexibility from quick-start devices for multi-energy virtual power plants. *IEEE Transactions on Sustainable Energy*, 12(1):646–658, 2021. doi: 10.1109/TSTE.2020.3014959.

[125] T. Capuder and P. Mancarella. Assessing the benefits of coordinated operation of aggregated distributed multi-energy generation. In *2016 Power Systems Computation Conference (PSCC)*, pages 1–7, 2016. doi: 10.1109/PSCC.2016.7540829.

[126] McKinsay & Company. Hydrogen insights: A perspective on hydrogen investment, market development and cost competitiveness. Report, February

2021. URL `https://hydrogencouncil.com/wp-content/uploads/2021/02/Hydrogen-Insights-2021.pdf`.

[127] P. Ge, Q. Hu, Q. Wu, X. Dou, Z. Wu, and Y. Ding. Increasing operational flexibility of integrated energy systems by introducing power to hydrogen. *IET Renewable Power Generation*, 14(3):372–380, 2020. ISSN 1752-1416. doi: 10.1049/iet-rpg.2019.0663.

[128] N. A. El-Taweel, H. Khani, and H. E. Z. Farag. Hydrogen storage optimal scheduling for fuel supply and capacity–based demand response program under dynamic hydrogen pricing. *IEEE Transactions on Smart Grid*, 10(4):4531–4542, 2019. ISSN 1949-3053. doi: 10.1109/TSG.2018.2863247.

[129] S. H. Low. Convex relaxation of optimal power flow part i: Formulations and equivalence. *IEEE Transactions on Control of Network Systems*, 1(1):15–27, 2014. ISSN 2325-5870. doi: 10.1109/TCNS.2014.2309732.

[130] N. Li, L. Chen, and S. H. Low. Exact convex relaxation of OPF for radial networks using branch flow model. In *2012 IEEE Third International Conference on Smart Grid Communications (SmartGridComm)*, pages 7–12. doi: 10.1109/SmartGridComm.2012.6485951.

[131] J. Yang, N. Zhang, C. Kang, and Q. Xia. A state-independent linear power flow model with accurate estimation of voltage magnitude. *IEEE Transactions on Power Systems*, 32(5):3607–3617, 2017.

[132] N. Alguacil and A. J. Conejo. Multiperiod optimal power flow using benders decomposition. *IEEE Transactions on Power Systems*, 15(1):196–201, 2000. ISSN 0885-8950. doi: 10.1109/59.852121.

[133] C. Coffrin, H. L. Hijazi, and P. Van Hentenryck. The QC relaxation: A theoretical and computational study on optimal power flow. *IEEE Transactions on Power Systems*, 31(4):3008–3018, 2016. ISSN 0885-8950. doi: 10.1109/TPWRS.2015.2463111.

[134] B. A. Robbins and A. D. Domínguez-García. Optimal reactive power dispatch for voltage regulation in unbalanced distribution systems. *IEEE Transactions on Power Systems*, 31(4):2903–2913, 2016. ISSN 0885-8950. doi: 10.1109/TPWRS.2015.2451519.

[135] L. Gan and S. H. Low. Convex relaxations and linear approximation for optimal power flow in multiphase radial networks. In *2014 Power Systems Computation Conference*, pages 1–9, 2014. doi: 10.1109/PSCC.2014.7038399.

[136] L. R. Araujo, D. R. R. Penido, S. Carneiro, and J. L. R. Pereira. A three-phase optimal power-flow algorithm to mitigate voltage unbalance. *IEEE Transactions on Power Delivery*, 28(4):2394–2402, 2013. doi: 10.1109/TPWRD.2013.2261095.

[137] A. J. Conejo and L. Baringo. *Power Flow*. Power System Operations. Springer International Publishing, Cham, 2018. ISBN 978-3-319-69407-8. doi: 10.1007/978-3-319-69407-8_4.

[138] J. Jahn. *Existence Theorems for Minimal Points*. Introduction to the Theory of Nonlinear Optimization. Springer, Berlin, 2007. ISBN 978-3-540-49379-2. doi: 10.1007/978-3-540-49379-2_2.

[139] Y. Gu, J. D. Mccalley, and M. Ni. Coordinating large-scale wind integration and transmission planning. *IEEE Transactions on Sustainable Energy*, 3(4):652–659, 2012. ISSN 1949-3029. doi: 10.1109/tste.2012.2204069.

[140] K. Van den Bergh, E. Delarue, and W. D'haeseleer. DC power flow in unit commitment models. *Ku Leuven Energy Institute*, 2014. URL `https://www.mech.kuleuven.be/en/tme/research/energy_environment/Pdf/wpen2014-12.pdf`.

[141] S. H. Low. Convex relaxation of optimal power flow: A tutorial. In *2013 IREP Symposium Bulk Power System Dynamics and Control - IX Optimization, Security and Control of the Emerging Power Grid*, pages 1–15. doi: 10.1109/IREP.2013.6629391.

[142] S. H. Low. Convex relaxation of optimal power flow part ii: Exactness. *IEEE Transactions on Control of Network Systems*, 1(2):177–189, 2014. doi: 10.1109/TCNS.2014.2323634.

[143] L. Vandenberghe and S. Boyd. Semidefinite programming. *SIAM Review*, 38(1):49–95, 1996. ISSN 00361445. URL `http://www.jstor.org.ezp.lib.unimelb.edu.au/stable/2132974`.

[144] X. Bai, H. Wei, K. Fujisawa, and Y. Wang. Semidefinite programming for optimal power flow problems. *International Journal of Electrical Power & Energy Systems*,

30(6):383–392, 2008. ISSN 0142-0615. doi: https://doi.org/10.1016/j.ijepes.2007.12.003.

[145] R.A. Jabr. Radial distribution load flow using conic programming. *IEEE Transactions on Power Systems*, 21(3):1458–1459, 2006. ISSN 0885-8950. doi: 10.1109/tpwrs.2006.879234.

[146] M. Farivar and S. H. Low. Branch flow model: Relaxations and convexification: Part i. *IEEE Transactions on Power Systems*, 28(3):2554–2564, 2013.

[147] M. Farivar, R. Neal, C. Clarke, and S. Low. Optimal inverter VAR control in distribution systems with high PV penetration. In *2012 IEEE Power and Energy Society General Meeting*, pages 1–7, 2012. doi: 10.1109/PESGM.2012.6345736.

[148] C. Lee, C. Liu, S. Mehrotra, and Z. Bie. Robust distribution network reconfiguration. *IEEE Transactions on Smart Grid*, 6(2):836–842, 2015. doi: 10.1109/TSG.2014.2375160.

[149] H. M. Khodr, J. Martinez-Crespo, M. A. Matos, and J. Pereira. Distribution systems reconfiguration based on opf using benders decomposition. *IEEE Transactions on Power Delivery*, 24(4):2166–2176, 2009. doi: 10.1109/TPWRD.2009.2027510.

[150] S. Garatti and M. Campi. Modulating robustness in control design: Principles and algorithms. *Control Systems, IEEE*, 33:36–51, 2013. doi: 10.1109/MCS.2012.2234964.

[151] A. Shapiro, T. Homem-de Mello, and J. Kim. Conditioning of convex piecewise linear stochastic programs. *Mathematical Programming*, 94(1):1–19, 2002. ISSN 1436-4646. doi: 10.1007/s10107-002-0313-2.

[152] Australian Energy Market Commission (AEMC). *National Electricity Amendment (Fast Frequency Response Market Ancillary Service) Rule 2021*. Draft Rule Determination. URL `https://www.aemc.gov.au/sites/default/files/2021-04/FFR%20market%20ancillary%20services%20-%20Draft%20Determination_22APR2021.pdf`.

[153] J. Naughton, H. Wang, M. Cantoni, and P. Mancarella. Co-optimizing virtual power plant services under uncertainty: A robust scheduling and receding horizon

dispatch approach. *IEEE Transactions on Power Systems*, 36(5):3960–3972, 2021. doi: 10.1109/TPWRS.2021.3062582.

[154] Australian Energy Market Operator (AEMO). NEMWEB, 2018. URL `http://www.nemweb.com.au/`.

[155] SA Power Networks. Resource library, 2018. URL `https://www.sapowernetworks.com.au/resource-library/`.

[156] Bureau of Meteorology (BOM). About one minute solar data, 2018. URL `http://www.bom.gov.au/climate/data/oneminsolar/about-IDCJAC0022.shtml`.

[157] G. M. Masters. *Renewable and Efficient Electric Power Systems*. John Wiley & Sons, Incorporated, New York, UNITED STATES, 2013. ISBN 9781118633502. URL `http://ebookcentral.proquest.com/lib/unimelb/detail.action?docID=1207615`.

[158] Y. Lv, L. Guan, Z. Tang, and Q. Zhao. A probability model of PV for the middle-term to long-term power system analysis and its application. *Energy Procedia*, 103: 28–33, 2016. ISSN 1876-6102. doi: https://doi.org/10.1016/j.egypro.2016.11.244.

[159] T. Li, M. Shahidehpour, and Z. Li. Risk-constrained bidding strategy with stochastic unit commitment. *IEEE Transactions on Power Systems*, 22(1):449–458, 2007. ISSN 1558-0679. doi: 10.1109/TPWRS.2006.887894.

[160] J. Löfberg. Yalmip : A toolbox for modelling and optimization in matlab. In *In Proceedings of the CACSD Conference*.

[161] LLC Gurobi Optimization. Gurobi optimizer reference manual, 2021. URL `http://www.gurobi.com`.

[162] L. Lafayette, G. Sauter, L. Vu, and B. Meade. Spartan performance and flexibility: An HPC-cloud chimera. In *OpenStack Summit*.

[163] R. D. Zimmerman, C. E. Murillo-Sanchez, and R. J. Thomas. MATPOWER: Steady-state operations, planning, and analysis tools for power systems research and education. *IEEE Transactions on Power Systems*, 26(1):12–19, 2011.

[164] C. Long, J. Wu, L. Thomas, and N. Jenkins. Optimal operation of soft open points in medium voltage electrical distribution networks with distributed generation.

Applied Energy, 184:427–437, 2016. ISSN 0306-2619. doi: https://doi.org/10.1016/j.apenergy.2016.10.031.

[165] J. Naughton, H. Wang, S. Riaz, M. Cantoni, and P. Mancarella. Optimization of multi-energy virtual power plants for providing multiple market and local network services. *Electric Power Systems Research*, 189:106775, 2020. ISSN 0378-7796. doi: 10.1016/j.epsr.2020.106775.

[166] G. Matute, J.M. Yusta, and L.C. Correas. Techno-economic modelling of water electrolysers in the range of several mw to provide grid services while generating hydrogen for different applications: A case study in spain applied to mobility with fcevs. *International Journal of Hydrogen Energy*, 44(33):17431–17442, 2019. ISSN 0360-3199. doi: https://doi.org/10.1016/j.ijhydene.2019.05.092. URL `https://www.sciencedirect.com/science/article/pii/S0360319919319482`.

[167] Fabian Scheepers, Markus Stähler, Andrea Stähler, Edward Rauls, Martin Müller, Marcelo Carmo, and Werner Lehnert. Temperature optimization for improving polymer electrolyte membrane-water electrolysis system efficiency. *Applied Energy*, 283:116270, 2021. ISSN 0306-2619. doi: https://doi.org/10.1016/j.apenergy.2020.116270. URL `https://www.sciencedirect.com/science/article/pii/S0306261920316603`.

[168] P. Mancarella and G. Chicco. Real-time demand response from energy shifting in distributed multi-generation. *IEEE Transactions on Smart Grid*, 4(4):1928–1938, 2013. ISSN 1949-3061. doi: 10.1109/TSG.2013.2258413.

[169] T.S. Brinsmead, P. Graham, J. Hayward, E.L. Ratnam, and L Reedman. Future energy trends: An assessment of the economic viability, potential uptake and impacts of electrical energy storage on the NEM 2015-2035. Report, 2015. URL `https://www.aemc.gov.au/sites/default/files/content/fa7a8ca4-5912-4fa9-8d51-2f291f7b9621/CSIRO-Future-Trends-Report.pdf`.

[170] Aurecon. 2019 costs and technical parameter review. Technical Report 506837, 2019. URL `https://www.aemo.com.au/-/media/Files/Electricity/NEM/Planning_and_Forecasting/Inputs-Assumptions-Methodologies/2019/Aurecon-2019-Cost-and-Technical-Parameters-Review-Draft-Report.PDF`.

[171] Australian Energy Market Operator (AEMO). Power system security guidelines. Technical Report SO OP 3715, 2019. URL https://aemo.com.au/-/media/files/electricity/nem/security_and_reliability/power_system_ops/procedures/so_op_3715-power-system-security-guidelines.pdf?la=en.

[172] Australian Energy Market Operator (AEMO). NMAS cost and quantities report 2019, 2021. URL https://aemo.com.au/-/media/files/electricity/nem/data/ancillary_services/2021/nmas-cost-and-quantities-report-2019-20.pdf?la=en.

[173] W. Tushar, T. K. Saha, C. Yuen, D. Smith, and H. V. Poor. Peer-to-peer trading in electricity networks: An overview. *IEEE Transactions on Smart Grid*, 11(4): 3185–3200, 2020. doi: 10.1109/TSG.2020.2969657.

[174] S. Mhanna, I. Saedi, and P. Mancarella. Iterative LP-based methods for the multiperiod optimal electricity and gas flow problem. *IEEE Transactions on Power Systems*, 2021. doi: 10.1109/TPWRS.2021.3092760.

[175] E. A. Martínez Ceseña, E. Loukarakis, N. Good, and P. Mancarella. Integrated electricity– heat–gas systems: Techno–economic modeling, optimization, and application to multienergy districts. *Proceedings of the IEEE*, 108(9):1392–1410, 2020. doi: 10.1109/JPROC.2020.2989382.

[176] F. Liu, Z. Bie, and X. Wang. Day-ahead dispatch of integrated electricity and natural gas system considering reserve scheduling and renewable uncertainties. *IEEE Transactions on Sustainable Energy*, 10(2):646–658, 2019. ISSN 1949-3029. doi: 10.1109/tste.2018.2843121.

[177] R.R. Jha and A. Dubey. Network-level optimization for unbalanced power distribution system: Approximation and relaxation. *IEEE Transactions on Power Systems*, 36(5):4126–4139, 2021. doi: 10.1109/TPWRS.2021.3066146.

[178] S. Mhanna and P. Mancarella. An exact sequential linear programming algorithm for the optimal power flow problem. *IEEE Transactions on Power Systems*, 37(1): 666–679, 2022. doi: 10.1109/TPWRS.2021.3097066.